Landscape Complexity and Vegetation Dynamics in Riding Mountain National Park, Canada

by

David John Walker

A thesis presented to the University of Manitoba in partial fulfillment of the requirements for a degree of Doctor of Philosophy in the Faculty of Graduate Studies.

Department of Botany
University of Manitoba
Winnipeg, Manitoba R3T 2N2

THE UNIVERSITY OF MANITOBA

FACULTY OF GRADUATE STUDIES

*****

COPYRIGHT PERMISSION PAGE

LANDSCAPE COMPLEXITY AND VEGETATION DYNAMICS IN RIDING MOUNTAIN NATIONAL PARK, CANADA

BY

David John Walker

A Thesis/Practicum submitted to the Faculty of Graduate Studies of The University of Manitoba in partial fulfillment of the requirements of the degree of

Doctor of Philosophy

Big fleas have little fleas upon their backs
to bite them,
and little fleas have lesser fleas, and *so ad*
infinitum

- Swift, Poems II.651 (1733)
Anticipating Statistical Self-similarity.

Acknowledgements

Committee and Funding

I would like to give a general thanks to the committee: Dr. Steve McCanny, Dr. Dave Barber, Dr. Bruce Ford and Dr. Stéphane McLachlan for the reading of the manuscript, and their valuable comments and challenging questions related to this research. Sincere thanks to my advisor Dr. N. Kenkel for giving me the opportunity and support in making this thesis possible.

This research was supported by a Heritage Canada (Parks Branch) research grant to N.C. Kenkel through the University of Manitoba Centre for Earth Observation Science (CEOS). Additional funding in the form of a Natural Sciences and Engineering Research Council of Canada (NSERC) individual operating grant to N. Kenkel is gratefully acknowledged.

Thanks to E. Mazur (Harvard University) for permission to use the 'black' silicon image in Chapter 8 (Figure 8.2a).

Family

I want to thank my kids Alexander and Elizabeth for their patience in waiting "just 5 more minutes" so I could finish typing out my thoughts. We can go outside and play now.

A special thanks to Sharon Inch for the occasional reality check, and to Camilo for always keeping things energized. And lastly, thanks to Mom and Dad for the perennial rhetorical question "Isn't it finished yet?"

Friends

I want to thank all the graduate students in the Kenkel lab who I've worked with and had the opportunity to learn from over the years. I especially want to thank Rod Lastra and Richard Caners for the many interesting discussions about this and that. It was fun.

Abstract

The primary focus of landscape ecology is the interrelationship between spatial pattern and processes within an ecosystem. It is through their mutual interaction that landscape structure and complexity are ultimately determined. Complexity, which includes both the horizontal and vertical arrangement of vegetation structure on the landscape, is an emergent property of dynamic systems. In the boreal forest, landscape complexity is a product of successional dynamics, physiography and environmental variability. The objective of this study was to examine spatial and temporal changes to landscape complexity in the boreal mixedwood of Riding Mountain National Park (RMNP), Canada. Using remotely sensed Landsat data and scale invariant fractal measures of spatial pattern, change in landscape complexity under natural and human induced fragmentation regimes was examined. The importance of structure as an emergent property of boreal canopies and its influence on landscape mapping using satellite data was addressed. It was found that landscape-level spatial pattern became increasingly entropic during succession. Old landscapes (120 years post-fire) were typified by a landscape matrix dominated by small scale patches and low spatial persistence. Physiography was also found to influence scale invariant landscape complexity. Landscapes typified by simple physiographies (well-drained, topographically simple sites) were characterized by a few dominant over-dispersed land-cover classes. Complex landscapes (variably drained, topographically complex sites), patches were under-dispersed and contagious, however complex gradients resulted in high pattern complexity (increased juxapositioning of landscape elements). It is suggested that the accumulation of small-scale disturbances over time and species turnover along complex environmental gradient affect high landscape complexity in the boreal forest. In contrast, human driven disturbance processes in the boreal forest resulted in lower spatial complexity over time. Fragmentation and habitat losses in the region surrounding RMNP were found to be high, with only half of the forest present in 1950 remaining in the 1990's. Scale-invariant spatial dispersion of forest fragments decreased between the 1950's and 1990's. Thus, the study area is becoming increasingly isolated from other natural forested areas within the region. In creating maps of land cover for these analyses, it was found that structural composition of the canopy was often more important than floristics in determining

spectral reflectance in Landsat data. A rule-based optimization procedure using multivariate analysis was developed to maximize the relationship between vegetation on the ground and spectral reflectance. Because of the high degree of spatial complexity in these systems, an alternative approach to map accuracy assessment utilizing multiple discriminant analysis (MDA) was developed. It was found that closed conifer stands composed of different softwood species were not easily discriminated during classification because of identical spectral signatures at the stand-level. It is suggested that the highly structured architecture and conical form of conifer stands results in the anechoic interception and absorption of light. This light interception strategy may have adaptive advantages in regions where sun angle is low, or where cloud cover is high, such as in the boreal forest and montane environments. The results of these investigations into landscape pattern suggest that ecosystem dynamics in the boreal forest produce scale-invariant landscape complexity.

Table of Contents

List of Tables

List of Figures

Chapter 1

Literature Review

1.1 Introduction

The primary focus of landscape ecology is on the interrelationship between spatial pattern and processes within the ecosystem (Turner 1989). It is through their mutual interaction that landscape structure and complexity are ultimately determined (Bonan and Shugart 1989). For instance, disturbance processes such as crownfire affect a mosaic pattern on the landscape, and yet the extent and intensity of crownfire is also the expression of underlying topographic pattern (Turner and Romme 1994). The study of this reciprocal linkage between structure and function is the essential distinction between landscape ecology and traditional ecology. Landscape ecology is also a central theme in conservation biology (Forman 1995; Wiens 1997) because habitats are spatially structured, influencing organism perception and behavior (With 1994a; Haddad 1999; With and King 2000). When these landscapes become modified by agricultural or forestry development, higher level population dynamics and community structure can be altered (Bayne and Hobson 1998; Beier and Noss 1998). Changes in landscape patterns may compromise ecological integrity by interfering with processes necessary for population persistence and the maintenance of genetic diversity (Keymer et al. 2000; With and King 2000). Landscape ecology specifically addresses the configuration of habitat and its influence on ecosystem functioning, through the development of principles and methods to measure and understand spatial heterogeneity in the environment (Forman 1995; Wiens 1995).

By definition, the focus of landscape ecology is the study of landscapes, yet there is no one accepted definition for the term "landscape." Landscapes can have the traditional meaning of a unit of area at a 'human scale' of several thousand hectares (e.g. a drainage basin) or can be as small as a lichen thallus (Shorrocks et al. 1991). Common to all definitions is the requirement for heterogeneity and the interactions among multiple 'elements' whether these are defined as individuals, patches, communities or adjacent ecosystems (Turner 1989; Wiens 1995). Studies examining the structural components of the landscape usually focus on land units of several to thousands of hectares, whereas those focusing on functional aspects of habitat use organism centric definitions of landscape (Tischendorf, and Fahrig. 2000). Functional approaches to defining landscapes consider the interaction between organisms and the environment. This requires the identification of elements in the habitat that represent important species resources, or the identification of

'important' species within a habitat (Turner 1989; Noss 1999). However, because organisms 'perceive' habitat at different scales depending on their resource requirements (With 1994a), landscapes defined in this way do not have an absolute size (Wiens 1995). Thus, comparisons among studies using functional definitions of the landscape are difficult to interpret or generalize (Debinski and Holt 2000; Tischendorf, and Fahrig. 2000). Despite the often species specific results of functional landscape studies, conservation and ecosystem management most often uses this approach (Turner 1989; Franklin 1993; Noss 1999).

The structural definition of the landscape has much in common with the anthropocentric meaning of the term, that is it corresponds with large land areas several kilometers in size (Turner 1989). Most often these areas are defined using geographic criteria such as the edge between adjacent drainage basins (e.g. Clark and Slusher 2000). Large land units can be divided into 'structural components' that together comprise a landscape mosaic (Wiens 1997). The fundamental unit of the mosaic is the 'patch,' usually identified as a land cover type that is relatively homogenous in both structure and composition (Forman 1995; Wiens 1995). Patches like landscapes can be defined in many different ways, for example, they might represent different forest 'stands' in a region (e.g. Cumming et al. 1996) or be demarcated by the boundary of tessellation tiles among individuals within a stand (e.g. Frelich et al. 1998). Despite the often divergent uses of the term 'patch,' it has become a critical component of gap dynamic models (Weins 1995). Most landscapes can be 'decomposed' into a variety of patches of different sizes. For instance, the components of landscape mosaics as identified by Forman and Godron (1986), consist of patches, matrix and corridors. While the terms differ, they are all patches, either recognized as such and viewed as 'imbedded' within the matrix, or large enough to be considered a matrix 'patch.' Patches are ultimately artificial, because at some scale (usually relevant to the system or organism studied) it must be decided whether land-cover is homogenous 'enough' to be considered a patch (Wiens 1997). Thus, current structural definitions of the landscape based on patchiness suffer from the same fundamental shortcoming as functional approaches: scale must ultimately be defined arbitrarily. Because environmental heterogeneity is a common component in both structural and functional definitions of the landscape, an alternative approach would be to consider measuring spatial heterogeneity directly (cf. Wiens 1997).

Recent concern about the impact of habitat fragmentation has spurred interest in quantifying spatial heterogeneity on the landscape (Hargis et al. 1998; Jaeger 2000).

However, many definitions and approaches to quantifying complexity have been suggested with little consensus among researchers (Wiens 1997; Hargis et al. 1998). A utilitarian definition of landscape complexity is the "complex patterns on the landscape resulting from the juxapositioning of numerous components of the abiotic and biotic environment" (Turner 1989). Thus the measurement of landscape complexity allows linkages to be developed between observed pattern and processes in the environment (De Cola 1994). In general, complex systems can be typified as being predictable over short intervals in time or space, but this predictability decays rapidly as the interval length increases (Schroeder 1991). In the boreal forest, landscape complexity is an emergent property of a system driven by multiscale disturbances and environmental heterogeneity (Bonan and Shugart 1989; Turner and Romme 1994). This system thus affords an opportunity to examine the role of spatial and temporal dynamics in determining overall landscape complexity.

1.2 Landscape Complexity and Dynamics of the Boreal Forest

Introduction

The boreal forest is one of the largest biomes in the world, occupying ca. 8% of the global continental land mass (McDonald et al. 1998). It is a disturbance driven ecosytem dominated by landscape level crown-fire (Sousa 1984). Intense and frequent disturbance results in relatively low plant diversity and a simple trophic structure (Ritchie 1956). Although fire occurs throughout the boreal forest, burn frequency and intensity vary widely (Heinselman 1973). In the absence of human intervention, fire cycles in North American upland boreal forests range from < 50 years in many areas (Hirsch 1991; Turner and Romme 1994; Johnson et al. 1999) to >200 years in poorly-drained bogs, swamps and marshes (Payette 1992). Post-fire patch structure and species composition reflects both crown fire disturbance history, physiography as well as small-scale disturbances and species interactions (Turner and Romme 1994; Frelich and Reich 1999; Bergeron 2000). These multiscale processes cumulatively result in a complex landscape mosaic of stands that vary in floristic composition, canopy structure and successional age (Frelich and Reich 1995; De Grandpré and Bergeron 1997). Thus the boreal forest is typified by high spatial heterogeneity despite having relatively low floristic diversity. Because traditional ecological theory is grounded in floristic and not spatial dynamics (Wiens 1997), landscape processes and pattern development remain poorly understood in this system (Bonan and Shugart 1989).

Succession Theory

While the focus of landscape ecology is on understanding pattern and process, traditional branches of ecology are concerned primarily with process, often with very little attention to structure and form (Wiens 1995). This bias is especially evident in the historical development of successional theory. Traditional Clementsian succession models typify communities as 'superorganisms' wherein species are thought to modify the environment to provide support for the next seral stage in vegetation development. 'Relay floristics' continues until a self-replacing 'climax' community is achieved and a static equilibrium determined by climate is established (Clements 1936). Each seral stage from initial establishment to climax is considered to be a discrete step that is well defined in terms of species composition (Collins et al. 1993). This forest succession model was first developed in temperate deciduous forests of North America, which are not subject to major canopy-killing catastrophic disturbances (Pickett et al. 1987). Thus, the model makes no provision for stochastic processes during community development. As such, it is a "rigid conceptualization" of vegetation dynamics requiring the assumption that ecosystems are closed and homogenous (Wiens 1997). While this paradigm is incompatible with vegetation dynamics in the boreal forest, it has had a strong influence on the development of many branches of formal ecological theory, most notably equilibrium models (Turner 1989; Wiens 1995).

Individualistic-based models of succession that focus on life-history adaptations have largely replaced the Clementsian paragidm in ecology (Pickett et al. 1987). Gleason's (1926) model views plant communities as populations of species that only co-occur because of similar growth requirements (Johnson 1979). Species replacements take place on an individual basis, as a response to environmental heterogeneity and site history (Pickett et al. 1987). Watt (1947) incorporated disturbance in the Gleasonian model by recognizing that vegetation mosaic patterns and cyclical community changes are dependent on species life history strategies. A more rigid formalization of Watts approach is the 'initial floristic composition' model (Egler 1954). In this model, the propagules first available following disturbance constrain all future site dynamics. Stochastic factors and differential species dispersability often determine propagule availability, resulting in complex spatial patterns in disturbance driven landscapes (Pickett et al. 1987). No single 'unique' climax is expected in the boreal forest because of the strong dependency on site history in determining successional trajectory (Cummings et al. 1996).

Vegetation dynamics in the boreal forest appears to follow the Eglerian model of succession (Cogbill 1985; Galipeau et al. 1997). In the boreal forest, stand composition within 50 years of a major fire matches that of the pre-disturbance landscape (Bergeron and Dubuc 1989). Successional trajectories on these landscapes are often divergent, with no clear indication of a climax state (Carleton and Maycock 1978). Advance regeneration and understory species associated with secondary phases of succession are often unable to survive long enough to recruit into the canopy (Zoladeski and Maycock 1990; Holling 1992; Morin 1994; Bergeron et al. 1995). In some cases, pioneer species replacement may not occur at all, resulting in stand decadence (Heinselman 1973; Cogbill 1985). Indeed, few boreal canopy species are completely capable of self-replacement in the absence of disturbance (Rowe 1961). Most boreal tree species are unable to tolerate the low light conditions of older growth stands or germinate on organic substrates (Bergeron 2000). Thus, stand dynamics and species replacements are largely constrained by seed source and site availability following disturbance (Pickett et al. 1987; Frelich and Reich 1995). Initial floristic composition, while providing an adequate description of the processes in early succession, provides little prediction for stand dynamics where active fire suppression is practised. In order to address the effects of fine-scale disturbance in the absence of crown fire, we need to develop spatially explicit models for the boreal forest.

Successional Dynamics in the Boreal Forest

Successional dynamics of the boreal forest vary considerably following continental, latitudinal and elevational changes in fire return cycles (Turner and Romme 1994). In regions with short-period fires, vegetation composition becomes dominated by species with pyric adaptations such as jack pine and aspen (Johnson et al. 1999). In areas where fire return cycles are long, secondary successional species such as balsam fir or eastern white cedar are often common (Bergeron 2000). Within a region, floristic composition and community structure are largely determined by physiography (i.e. landform, soils and drainage patterns), seed availability, herbivory (including insect defoliation, granivory, beaver flooding), as well as abioic disturbance processes (Turner and Romme 1994; DeGrandpré et al. 1993; Galipeau et al. 1997; Bergeron 2000).

1. Physiography

The role of physiography is often overlooked in most discussions of successional dynamics in boreal forest, (Frelich and Reich 1999). Physiography, which includes

topography (i.e. landform), soils and drainage patterns have significant influence on vegetation dynamics, through the alteration of disturbance regimes, soil development and species interactions (Foster and King 1986; Turner and Romme 1994). Gradients in soil moisture strongly influence species distributions (Bonan and Shugart 1989; Naiman et al. 1993; Helm and Collins 1997; Frelich et al. 1998), and in doing so affect the size, structure and diversity of forest patches (Foster and King 1986; Host et al. 1987). Along the surface-watertable interface, competitive interactions among species result in exclusion and strong patch persistence (Sjörs 1980; Czárán 1989; Palmer and Dixon 1990; Zobel et al. 1993). It has been found that large scale abiotic gradients can account for up to 21% of overall vegetation trends in a region (Jean and Bouchard 1993). If an environmental gradient exerts a strong selective pressure on organisms, high beta diversity and a patterned climax may result (Whittaker 1953). Vegetation complexity on these landscapes increasingly matches the complexity of underlying resource availability (Watt 1947; Host et al 1987; Ohmann and Spies 1998). Thus, the interaction between vegetation and physiography produce complex, interdigitated and ecotonal landscape patterns that reflect underlying environmental trends (Gosz 1993).

Landform also influences disturbance regime by altering fire return cycles (Turner and Romme 1994). For instance, flat uplands are often burned more extensively and frequently than areas of complex relief and thus tend to become dominated by large monodominant stands of fire adapted species (Carleton and Maycock 1978). In contrast, areas of complex relief may block the movement of fire and thus provide refugia for late successional species such as balsam fir and white cedar (Bergeron and Dubuc 1989; Turner and Romme 1994; Bergeron 2000). Landform can also play an indirect role in successional dynamics through beaver mediated changes to community structure following the flooding of lower slopes and local depressions (Naiman 1988; Donkor and Fryxell 1999). Despite the importance of landform in boreal forest dynamics, theory relating physiography with regional diversity and landscape complexity is lacking (Turner 1989; Frelich and Reich 1999) .

2. Disturbance

Landscape-level Crown Fire

Landscape level crownfire is the most important disturbance event in the boreal forest (Ritchie 1956; Heinselman 1973; Carleton and Maycock 1978; Payette 1992; Johnson et al. 1999). Fire influences site floristics and community composition over extensive areas (Dix

and Swan 1971; Hirsch 1991), and much of the heterogeneity in post-fire regeneration can be attributed to variation in fire intensity (DeGrandpré et al. 1993; Turner and Romme 1994). Boreal landscapes are a mosaic of communities adapted to fire cycles of varying duration (Carleton and Maycock 1978; Bergeron 2000), where a fire cycle is defined as "the time required to burn and area equal in size to the study area" (Johnson 1999). In much of the boreal forest, fire cycles are shorter than the life span of the dominant canopy species (Bergeron 2000), occurring approximately every 75 years in western Canada (Johnson et al. 1999; Weir et al. 2000). Although not all areas are burned within this period, few stands exceed an age of 250 years in the southern boreal forest. (Payette 1992). Under short fire cycles, species that reach reproductive age rapidly (e.g. jack pine), or that regenerate vegetatively following disturbance (e.g. trembling aspen) become dominant on the landscape (Weir et al. 2000). These species typically have relatively short life spans and require mineral substrates to germinate (Bergeron 2000). With the exception of white cedar and balsam fir almost all boreal tree species in the mixed wood have pyric adaptations requiring fire for perpetuation (Frelich and Reich 1995; Bergeron 2000). Because the structure and composition of most stands is dominated by these early successional species, some authors have suggested that "apparent succession is simply an expression of differential longevity" (Cogbill 1985). Indeed, fire cycles of <150 years will perpetuate a community composition dominated by post-fire early successional species (Payette 1992).

Scaling Properties of Disturbances

Traditionally, succession models in the boreal forest have focussed on landscape-level post-fire dynamics , however disturbance operates across many different scales (Bonan and Shugart 1989; Bergeron 2000). For instance, spruce budworm can have a substantial influence on the structure and vegetation dynamics of older stands by creating gaps of various sizes (Bergeron, et. al 1995). Much of the canopy cover in old growth stands can be attributed to these gap forming processes (Kneeshaw, and Bergeron. 1998). Furthermore, the intensity of these disturbances varies in both space and time (Sousa 1984). High intensity disturbances are large and infrequent, while a range of medium to small scale disturbances occur with greater frequency (Bonan and Shugart 1989). Because these disturbances are stochastic in location and extent, the resultant patch structure is complex (Jakubauskas 1997). Surprisingly little research has been done examining the relationship between the development of complexity on the landscape and the cumulative effects of small scale disturbances (Turner 1989; He and Mladenoff 1999). Frelich and Reich (1995a,b) incorporated spatial scale into a study of successional processes in the Boundary Waters

area of Minnesota. Their analysis of two upland stands (both on sandy substrates over granitic rock) suggested a successional sequence from uniform, even-aged stands of jack pine or trembling aspen to old-growth multi-aged stands of balsam fir, black spruce, paper birch and eastern white cedar. In the absence of fire, they hypothesized that fine-scale (10-30 m) canopy openings caused by wind, insects and disease, drive the successional process. These canopy openings are often colonized by one of the later-successional species, so that uniform canopies are gradually "chipped away" over time. As a result, stands deemed to be 'pure' at a fine scale are part of a more complex mosaic at a coarser scale. Results obtained from a boreal forest canopy simulation model (He and Mladenoff 1999) are similar; after 100 years, fine-grained successional processes cause gradual disaggregation of the canopy.

Large-scale crownfires ultimately 'reset' the effects of small scale disturbances in the boreal forest (Frelich and Reich 1995). The widespread adoption of crown fire suppression techniques has the potential to substantially alter the cycle of landscape pattern generation (Johnson et al. 1995; Baker 1992ab). In the past, repeated large-scale disturbance have favored species that are adapted to rapid dispersal, germination and growth on mineral substrates (Bergeron 2000). Few boreal species may be suited to a landscape paradigm dominated by small scale asynchronous gap processes (Baker 1992a; Frelich and Reich 1995). Suppression of large scale fire events may ultimately result in the fragmentation of forest stands and increased spatial heterogeneity (Baker 1992b). The role of these small scale disturbances and neighborhood processes have only recently been investigated (e.g. Frelich and Reich 1995; He and Mladenoff 1999). However, these studies use patch based approaches, which may not capture multiscale spatial heterogeneity of pattern on the landscape (Turner 1989; Loehle and Wein 1994; cf. Wiens 1997).

1.3 Agricultural Fragmentation of the Boreal Forest Landscape

Introduction

Until recently most species existed on 'naturally' fragmented but connected landscapes (Beier and Noss 1998). Natural fragmentation, as discussed previously, is the result of complex patterns of interaction between climate, topography, soils and natural disturbances (Turner 1989; Dearden and Rollins 1993; Johnson et al 1995; Holt et al 1995). Natural processes of patch formation result in a paradigm of locally homogenous interconnected patches imbedded in a dominant 'matrix' (Forman 1995). Often the matrix and imbedded patches share a similar species composition or structure (Franklin 1993; Beier and Noss 1998) and are characterized by "shallow ecological gradients" across habitat boundaries

(Lord and Norton 1990). As a result, habitat fragments on naturally formed patch mosaic landscapes generally maintain high connectivity (Keitt et al. 1997). Anthropogenic fragmentation by constrast often results in abrupt changes in habitat structure (Barrett and Peles 1994; Jaeger 2000). Transitions between the disturbed and undisturbed habitat can be so abrupt that the 'edge' acts as a boundary, limiting the movement of organisms (Haddad 1999).

Fragmentation in the Agroecosystem

Fragmentation in the agroecosystem is now recognized as a major threat to biodiversity (Barret and Peles 1994; Kruess and Tscharntke 1994). Conversion of natural landscapes for agricultural and forestry production, results in both animal and plant population decline (Grashof-Bokdam 1997; Bayne and Hobson 1998). However, studies of the effects of human caused fragmentation are often species specific and produce conflicting results (Wright and Hubble. 1983; Debinski and Holt 2000). Many studies of fragmentation are restricted to a narrow range of spatial scales using empirically derived indices (Sharpe et al. 1987; Hargis et al 1998; Tinker et al. 1998). The type and extent of human activities in the agricultural matrix, as well as patch size and habitat quality, are often ignored (Barret and Peles 1994; Namba et al 1999). For instance, remnant corridors on these landscapes are generally associated with riparian habitats, fencerows and windrows that may not provide adequate connectivity for some species (Fritz and Merriam 1994; Beier and Noss 1998). Furthermore, the developed agricultural matrix may impede movement for some species but not others (e.g. predators may be impacted more than herbivores, Barret and Peles 1994). This has serious implications for biodiversity within human impacted ecosystems because land clearing often bisects the landscape (Kruess and Tscharntke 1994; Jaeger 2000).

Agricultural land-use and development patterns are receiving greater attention because of potential impacts on global biodiversity with increased development in tropical countries (Skole and Tucker 1993; Jorge and Garcia 1997). Agricultural land-use significantly alters the geometry of landscape pattern following a predictable sequence of events. In both North America (based on historical reconstruction) and in the tropics (from satellite data), land clearing is initiated from parallel access roads and spreads outwards (Sharpe et al 1987; Turner 1990; Foster 1992; Lavorel et al. 1993; Skole and Tucker 1993; Jorge and Garcia 1997). This geometric pattern of land clearing is significant, because it results in the isolation and fragmentation of the landscape well before most of the natural habitat has been lost. Indeed, the rate of forest fragmentation and isolation can exceed the rate of actual forest

loss (i.e. total cover of fragments exceeds total habitat loss; Skole and Tucker 1993). This regular pattern of clearing follows the rectangular grid used to survey property boundaries (Foster 1992; Turner 1990) without considering natural vegetation and landform patterns (Sharpe et al 1987). Habitat is bisected within the grid, creating retangularized patches with low edge complexity (Krummel et al. 1987). Final cover of unaltered habitat on most developed landscape is usually less than 12%, concentrated along linear shelterbelts and in small woodlots (Sharpe et al. 1983; Foster 1992). Many studies of habitat fragmentation overlook the influence of patch geometry in addition to habitat losses in predicting changes to biodiversity (Keymer et al. 2000; Tischendorf and Fahrig 2000).

Corridors and Connectivity

Many parks exist as preserved fragments of a once larger biome 'imbedded' within the agricultural matrix. These reserves are often too small and isolated to support viable population of some species and require inter-reserve movements to maintain biodiversity (Frankel et al 1995; Cummings et al. 1996). If species survival depends on successful dispersal between reserves, individuals must cross the agricultural matrix. Because the agricultural matrix is often 'hostile' for many species (i.e. does not meet minimum habitat requirements), the dispersion of habitat patches on the landscape becomes increasingly important as habitat availability decreases (Gustafson and Gardiner 1996; Keymer et al. 2000). If suitable habitat patches ('stepping stones') cannot be located during foraging and dispersal, the energetic cost of movement may become too great, resulting in the isolation of populations (Andren 1994; Simberloff 1994; Diffendorfer et al. 1995; Collingham and Huntley 2000). The creation of habitat corridors has been suggested as a means to overcome local extirpations (Haddad 1999), but the cost of this approach may exceed benefits (Lord and Norton 1990). To demonstrate the efficacy of corridors it must be shown that they provide connectivity by facilitating movements that would otherwise not occur (Beier and Noss 1998).

Connectivity has been broadly defined as critical features of landscape structure that affect dispersal success for organisms moving among habitat patches (Taylor et al 1993). Tischendorf and Fahrig (2000) define two principal approaches to assessing connectivity: 1) Structural connectivity - where habitat contiguity is measured by an analysis of landscape pattern without reference to any particular species; 2) Functional connectivity - where species behavior and overall success in crossing the matrix are considered in assessing contiguity. Landscape level studies tend to focus on measuring structural rather than

functional connectivity because the latter is organism centric (Franklin 1993; Lord and Norton 1990). Furthermore, when the matrix is too 'hostile' to permit movement or is preferentially avoided by dispersing individuals, structural and functional connectivity are equivalent (Tischendorf and Fahrig 2000).

To study structural connectivity, the concept of percolating clusters has been advanced (Johnson et al 1992; Lavorel et al. 1993). A percolating cluster is a locally homogenous cover-type (e.g. habitat) where all elements are completely linked (With and King 1999). Fragmentation can be understood as a threshold phenomenon where the proportion and spatial arrangement of habitat results in the breakup of percolating clusters (With et al. 1997). For a random landscape, habitat cover exceeding 0.5928 (rook's adjacency rule; Keitt et al 1997) will generally resulting in a percolating cluster that spans the region (Lavorel et al. 1993). Using percolation models, movements of organisms on artificially fragmented landscapes have been investigated (With and King 1999). However application of these models to agricultural landscapes may be limited because habitat loss is well below the percolation threshold (Dytham 1995; With et al 1997) and the role of the matrix in dispersal is poorly understood (Barrett and Peles 1994; Keymer et al 2000). Furthermore, these models do not account for the geometric loss of habitat on the agricultural landscape. Fragmentation is often simulated as a stochastic process (e.g Collingham and Huntley 2000; Keymer et al. 2000; With and King 1999), even geometric fragmentation is simulated by the removal of random 'blocks' of habitat (e.g. Lavorel et al. 1993; but see Dytham 1995). A methodological approach to studying fragmentation on landscapes with highly geometric patterns of habitat loss is required for predicting movements between reserves in the agroecosystem.

1.4 Fractal Complexity: Methodological Approaches

Introduction

Until recently, the inherent hierarchical complexity of natural and human fragmentation patterns could not be readily quantified. In the late 60's and early 70's Benoit Mandelbrot recognized that a number of 'mathematical monstrosities': i.e. functions that defied logic in being both continuous but non-differentiable, could be readily adapted to modeling natural phenomenon (Voss 1988: 25; Peitgen et al 1992: 117). To characterize spatial or temporal phenomena that display these properties, Mandelbrot (1975) introduced the term 'fractal' (from the latin *fractus*, meaning 'broken'). Unlike more familiar Euclidean objects such as

points, lines and areas, which are 'smoothed' with magnification, fractals display ever increasing complexity. Thus fractal 'curves' have infinite length, as more detail is resolved with increasing scale. Furthermore, no one scale is unique; a fractal object magnified by any arbitrary amount appears similar to the original (Voss 1988: 22). This property of scale invariance with magnification is termed self-similarity or self-affinity (the latter applies to systems where invariance is manifest through non-uniform rescaling: Voss 1988: 44).

Mathematical fractal objects are scale independent and self-similar or self-affine across all scales, whereas natural systems often display 'statistical' self-similarity over a finite range of scales (Voss 1988: 30; Schroeder 1991:81). For instance, the perimeter of the fractal Koch 'snowflake' is perfectly self-similar with all parts appearing the same as the whole (Peitgen et al 1992:103). In contrast 'real' snowflakes are asymmetric with branches of the crystal structure forming at different rates and orientations. Furthermore, at the finest scale a snowflake resolves into individual molecules and atoms with their own inherent geometric properties (Schroeder 1991: 63). Nevertheless, over a limited range of spatial scales snowflake geometry does have regular and repeating properties: it is statistically self-similar. Theoretically, the range of statistical self-similarity in any natural object is bounded at by the physical extent of the object at the largest scale and ultimately by the quanta of matter making up its atoms at the smallest scale (Schroeder 1991: 63). Many natural objects are now recognized as having self-similar properties, and fractals have been used to describe the geometry of objects ranging from biological molecules to galaxies (**Figure 1.1**).

Fractal Dimension

The topology of Euclidean objects is simple: points, lines and areas each occupy a discrete whole number dimension. However, in fractal geometry dimension is viewed as a continuous function referred to as the Hausdorff dimension (Tsonis and Tsonis 1987). A fractal object has a Hausdorff dimension (denoted as 'D') that exceeds the topological dimension. For instance, the dimension of a brownian trace is greater than the topological dimension of a line ($1 \leq D \leq 2$), a fractal surface occupies a portion of a volume ($2 \leq D \leq 3$) and a fractal volume fills part of a hypervolume ($3 \leq D \leq 4$: Schroeder 1991:153). In this sense, D can be though of as an index measuring the extent to which an object is 'space filling ' (Mandelbrot 1983) and can be viewed as a relative measure of complexity (Normant

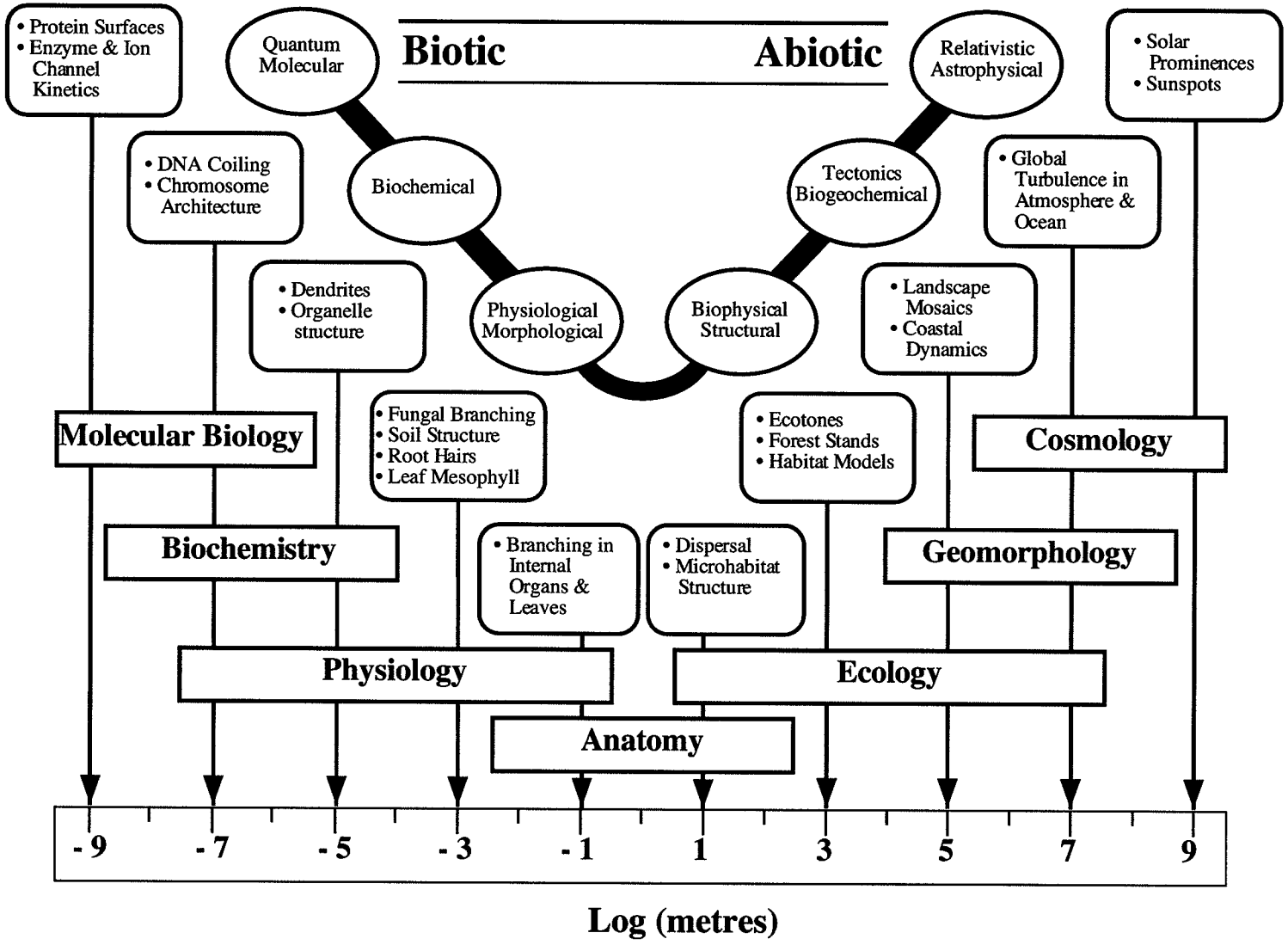

Figure 1.1: Fractal scaling has been demonstrated for a range of natural objects from molecular structures to large-scale patterns of galaxies in the Universe.

and Tricot 1993). With fractal geometry we recognize that *simple processes can generate complex patterns and that complex patterns can be quantified by means of a simple statistic* (Peitgen et al 1992: 117).

An example of a natural phenomenon with space filling properties is a coastline. From a high altitude only the largest features of a coastline are apparent. At lower altitudes smaller features such as peninsulas and bays become noticeable, until at the finest scale, water may be observed flowing around individual sand grains. Because of its space filling properties, the perceived length of the coastline increases as these finer scale features are recognized (Mandelbrot 1967). The total length L_δ measured using a set of N straight-line segments of length δ is dependent on spatial scale. For a highly convoluted coastline, as δ decreases an increasingly greater number of straight-line segments are required to circumscribe the fine scale features. The relationship between length and measuring scale is summarized by the power law:

$$L_\delta = K\delta^{1-D} \qquad \textbf{[Equation 1.1]}$$

where K is a constant. The fractal dimension ($1 \leq D \leq 2$) quantifies the degree of coastline complexity. This formulation of the fractal dimension is known as the 'compass dividers' method, which in practice is estimated from the corresponding slope of the log-log plot:

$$\log L_\delta = \log K + (1\text{-}D) \log \delta \qquad \textbf{[Equation 1.2]}$$

The estimation of the fractal dimension using the relationship between length and scale is known as the 'compass dividers' or simply the 'dividers' method approach (Mandelbrot 1983).

Estimating the Fractal Dimension

In this study, the fractal dimension was used as a statistic of landscape spatial complexity for both natural and human fragmented landscapes. A range of approaches were used in determining the value of D, reflecting differences in objectives and in the type of data analyzed. The purpose of this section is to discuss the theoretical basis of the methods selected in this study (for a review of other methods see: Voss 1988; Milne 1991). The primary consideration in choice of methodological approach was the 'nature' of the data

used in analysis. Raster imagery can consist of 'nominal' landscape classes (i.e. patch cover) or of some continuously varying property (e.g. surface elevation, or reflectance). While the compass dividers method can be used for both of these types of data (e.g. Mandelbrot 1983; Emerson et al. 1999), it requires the creation of 'artificial' boundaries. For raster imagery this can be particularly dangerous as often 'true' edges are imperfectly represented (Fisher 1997) or greatly simplified during vectorization (Bettinger et al. 1996). In this study, the compass dividers method was not used to measure landscape complexity. The approaches to landscape complexity analysis that were undertaken can be divided into two broad categories:

- Fractal complexity statistics designed to work with nominal, binary or point data (e.g. box count, cluster fractal dimension, probability density, multifractal spectrum).

- Fractal complexity statistics for continuously varying properties (e.g. surface persistence).

1. Complexity Statistics for Nominal, Binary or Point Data.

Box-Count (Cluster Fractal Dimension)

The box count approach is one of the most commonly used methods to obtain estimates of D for natural landscapes (Turcotte 1997). Unlike the dividers method, the box count will work with objects that are not spatially discrete, as is often the case with landscape patch patterns (Peitgen et al. 1992: 240; Hargis et al 1998.). Several variants have been developed for quantifying volumes (e.g. Milne 1988: 73), remote sensing 'surfaces' (e.g. De Cola 1989), as well as for one and two dimensional point patterns (e.g. Hastings and Sugihara 1993:44; Turcotte 1997). In the analysis of raster data (such as remotely sensed and GIS imagery), a regular grid of size $\delta \times \delta$ is placed over the image and the number (C) of 'occupied' grid cells is counted. This is repeated for a series of different values of δ. The power-law relationship is:

$$C = K \delta^{-D} \qquad \textbf{[Equation 1.3]}$$

The basic concept of grid counting underlies many of the fractal methods in this thesis (counts are used in estimating the cluster fractal dimension and in multifractal analysis). The box-counting method can be applied to one-dimensional sequences of 'points' to estimate the 'cluster' dimension with range $0 \leq D \leq 1$ (Turcotte 1997). This fractal approach to

clustering is based on the Cantor set (Smalley et al. 1987). In this study, the cluster fractal dimension was calculated for pixel sequences in GIS imagery. Instead of using a two-dimensional grid, a binary sequence of length L is examined, in which each pixel is coded as either 'on' (1) or 'off' (0). To determine the fractal dimension of the 'on' pixels, the sequence is divided into sections of length 'r' and the number of sections occupied by at least one 'on' pixel are counted. If the sequence is scale-invariant, the proportion P(r) of steps of length r that include at least one 'on' pixel scales as:

$$P(r) = r^{(1-D)} \qquad \textbf{[Equation 1.4]}$$

where the fractal dimension (D) is interpretable as an index of isolation (Smalley et al. 1987), ranging from 0 (isolated pixels) to 1 (maximally connected pixels). The linear portion of the log-log plot is used to determine the fractal dimension following:

$$\log P(r) = (1 - D) \log r \qquad \textbf{[Equation 1.5]}$$

As a fractal statistic of complexity the cluster dimension can be used to analyze any sequential spatio-temporal processes (Smalley et al. 1987). Alternative methods of calculating spatial statistics for point dispersions using lacunarity have been described (Turcotte 1997; Dale 2000).

Probability Density Function

Probability Density is an alternative method to measuring the degree to which patch structure become space filling (Hargis et al. 1998). This method was developed to analyze point pattern data (Voss 1988), but has been adapted for use in estimating the fractal dimension of raster imagery (e.g. Milne 1988). The basic algorithm uses a point centered sliding-box, that is counts are only made when the center is occupied. In image analysis this restricts the sliding box dimensions to odd integer values. The probability-density function ρ_L is obtained from square (L x L) sampling 'windows' successively placed over each 'on' pixel. Within each window, a count is made of the number (n) of 'on' pixels. Count

frequencies are then expressed as probabilities. For a given value of L, the first moment of the probability distribution is given by:

$$M(L) = \sum_{n=1}^{N(L)} n\rho L \qquad \textbf{[Equation 1.6]}$$

where $N(L) \leq L^2$, repeated using a range of values for L. Voss (1988: 66-67) shows that the following power law holds for fractal images:

$$M(L) = k\, L^D \qquad \textbf{[Equation 1.7]}$$

This spatial statistic is influenced by the total frequency of 'on' cells in an image. While this approach has been demonstrated to be able to measure increased levels of 'disturbance' in landscape simulations, it is less sensitive to patch configuration (Hargis et al. 1998). In ecology, this method has been used to examine the relationship between allometric herbivory and the fractal distribution of resources (Milne et al. 1992).

Multifractal Spectrum

Landscape pattern is often determined by a large number of generating processes operating at different scales (Loehle and Wein 1994; Scheuring and Riedi 1994). Landcover diversity and pattern in these systems cannot be summarized using a single fractal scaling coefficient but require a 'spectrum' of scaling statistics (Schroeder 1991: 194). Fractal objects which display scale dependencies are termed multifractals and have been observed in geophysical phenomena (Turcotte 1997: 113); landcover distributions (Loehle and Wein 1994; De Cola 1993) and in the locations of human populations (Appleby 1996). The multifractal 'spectrum' is simply a re-expression of generalized entropy (Rényi 1970), as a power-law relationship. The algorithm is similar to the box count introduced earlier. A grid of boxes of length δ is laid over the pattern of interest, and a count of the number of points in each of the N_δ occupied grid boxes is determined and expressed as a proportion:

$$p_i = n_i/N \qquad \textbf{[Equation 1.8]}$$

The generalized entropy (Rényi 1970) is defined as:

$$I_q(\delta) = \frac{1}{(1-q)} \log \sum_{i=1}^{N_\delta} p_i^q \qquad \textbf{[Equation 1.9]}$$

By varying q, an entire family of entropy functions is defined:

q	$I_q(\delta)$	*Name*	*Dimension*
0	$\log N_\delta$	log (box count)	box-count
→1	$-\Sigma p_i \log p_i$	Shannon entropy	information
2	$-\log \Sigma p_i^2$	log (Simpson index)	correlation

The generalized dimension D_q for the qth fractal moment is given by:

$$D_q = -\lim_{\delta \to 0} \left[I_q(\delta) / \log(\delta) \right] \qquad \textbf{[Equation 1.10]}$$

In practice, D_q is determined from the slope of the $I_q(\delta)$ vs. log δ plot (Appleby 1996). Values for q can range from $-\infty$ to $+\infty$ (Schroeder 1991). Numerically, values of $q < 0$ give more 'weight' to rare events, and the method becomes very sensitive to grid unit positioning and spatial resolution of the data (Appleby 1996). The function yields a monotonic negative slope except in instances where all classes are equifrequent (Schroeder 1991). For a 'classic' fractal object, D_q is a simple linear function of q (i.e. no additional information is obtained by examining higher moments). For multifractal objects, the relationship between D_q and q is non-linear.

2. Complexity Statistics for Continuous Data

Persistence

The previously discussed methods for estimating the fractal dimension of landscape patterns are primarily used for point processes or 'pixel' patches. Often the objective is to estimate fractal complexity for continuously varying sequences. While this can be determined indirectly using the compass dividers method (e.g. isarithm method: Emerson et al. 1999), there are more direct approaches available (Mandelbrot 1982). Spectral reflectance

in remotely sensed imagery (see § **1.5**) can be visualized as a continuous surface in three dimensions where each location (pixel) can be expressed as a grid coordinate (x and y) and a magnitude (z) value. A linear cross-section through this surface will yield a two dimensional sequence of reflectance values (a 'trace'). These sequences can be described using Fractional Brownian motion (fBm) models (Peters 1994: 53) to derive a scale invariant measure of path complexity (Polidori et al. 1991). Such models utilize a persistence parameter (H), originally developed as part of the rescaled range method (an affine transformation, Schroeder 1991: 141; Hurst 1951). Persistence refers to the degree of autocorrelation of adjacencies: for $H < 0.5$, a fractional Brownian motion trace is negatively correlated, whereas values are positively correlated for $H > 0.5$ (Sugihara and May 1990). In ecology, persistence has been applied in the study of landscape fragmentation using size frequency relations from binary imagery (Mandelbrot 1983; Hastings et al. 1982). A relation for determining the persistence parameter H for continuous spatial series (e.g. elevation profiles) is described in Polidori et al. (1991):

$$\log|e| = \log k + H \log \delta \qquad \textbf{[Equation 1.11]}$$

Where |e| for a surface is the mean absolute difference on the 'z-axis' (e.g. elevation) between all pairs of points a lag distance 'δ' apart. For a spatial sequence, persistence measures the degree to which a spatial property (e.g. elevation) diverges with distance (i.e. an 'indicator' of surface heterogeneity; Polidori 1991). For a topographic map, high persistence would be associated with smooth surface features (high spatial 'memory') whereas low persistence would result in a 'spikey' surface (low spatial 'memory'). Thus, there is a relationship between persistence in a spatial sequence and the complexity of the surface. An estimate of the fractal dimension of a surface ($2 \leq D \leq 3$) is obtained from the relation:

$$H = 3 - D \qquad \textbf{[Equation 1.12]}$$

Polidori et al. (1991) used this relation to assess the quality of raster digital elevation models for topographic surfaces. They found that interpolation artifacts were readily identified using a fractal analysis approach. Hastings et al. (1982) used the size class distribution of early and late successional patches in the Okefenokee Swamp. They found that the fractal dimension increased with stand age and interpreted the lower spatial persistence of early successional cypress patches as implying a lower temporal persistence. In modeling metapopulation dynamics, With and King (1999) suggested that low

persistence (i.e. highly fractal) landscapes may reduce dispersal success of some organisms. In their model, dispersal movements were constrained to single cell 'steps', the small patch size and frequent lacunae in the complex landscapes greatly slowed dispersal movements. In this study, persistence in Landsat reflectance related to heterogeneity in the biophysical properties of the canopy were investigated.

Bias in the Estimate of the Fractal Dimension

As a statistic of complexity, the fractal dimension represents a simplification of real world phenomenon into a single value (Normant and Tricot 1993; Turcotte 1997). Furthermore, when applied to natural objects the value is an estimate subject to sampling bias (Gautestad and Mysterud 1994). Although statistical self similarity may scale from the macroscopic to microscopic, the fractal estimate can only be as good as the range over which the measurements are recorded (Pruess 1995). Disregard for this basic fact has prompted some authors to dismiss certain methodological approaches (Normant and Tricot 1991), or to infer scale dependencies in fractal estimates where perhaps there are none (Kent and Wong 1982) or to erroneously conclude that patterns are not fractal (Turchin 1998). It is important to note that any fractal object once encoded in digital form for image analysis is no longer fractal but 'fraclidean.' Digital information is by its very nature discrete, and pixels represent a form of geometric simplification (Fisher 1997). Departure from a power-law relation at either the smallest or largest scales should be viewed with suspicion. In this study, fractal dimension values are used as relative indices of complexity and the fractal dimension was always calculated from the linear portion of the log-log plots.

1.5 Remote Sensing of the Boreal Forest

Introduction

To study the relationship between pattern and process on the landscape, spatially explicit landcover information is required. Landsat TM provides repeated coverage over large areas at a scale appropriate for the investigation of landscape complexity and is suited to the analysis of patterns and dynamics of natural and human impacted landscapes (Goward and Williams 1997). This technology been used to measure the biophysical structure of the canopy (e.g. Jakubauskas 1996a; Hall et al. 1995; Sampson 2001), landscape patterns arising from succession (e.g. Hall et al. 1991; Ranson and Williams 1992; Jakubauskas 1996b, 1997; Emerson et al. 1999), regional biodiversity (e.g. Rey-Benayas and Pope 1995;

Gould 2000), as well as in terrestrial mapping of vegetation types (e.g Bolstad and Lillesand 1992; Treitz and Howarth 2001).

The Landsat system of earth orbiting satellites was first launched in the early 1970's as part of the Earth Observational Satellite Series (EOSAT). Design and implementation of the sensor system was done in consultation with biologists, geographer and environmental scientists to ensure that the satellite would provide data that could be used in landscape monitoring (Wickland 1991; Goward and Williams 1997). Landsat-7 is the most recent addition to the series (Goward and Williams 1997), however in this study Landsat-5 data were used exclusively. Landsat-5 is a passive remote sensing platform that measures reflected incident sunlight from ground or cloud surfaces. The Thematic Mapping (TM) sensors operate at a ground resolution of 30 x 30 m, in six spectral bands (a seventh band samples in the infrared at a resolution of 80 x 80 m; Wickland 1991; ,Goward and Williams 1997). TM bands 1 to 3 sample in the visible spectrum, band 4 samples in the near-infrared, bands 5 and 7 sample in the mid-infrared portion of the spectrum (Moore and Bauer 1990; **Figure 1.2**).

There were two primary applications of Landsat data in this study:

1. The measurement of landscape complexity in the boreal forest using spatial statistics on band reflectance values as well as simplified imagery.

2. The mapping of the boreal forest using an optimized multivariate approach to improve classification accuracy.

Biophysical Components of Reflectance

In this study, measures of landscape complexity were determined from Landsat image reflectance values. In the interpretation of results, there is an assumed implicit relationship between the biophysical properties of the canopy (i.e. the 'real' ecological components of interest) and reflectance. In the following section the relationship between reflectance measured at-satellite and surface biophysical structure will be briefly discussed.

Landsat TM reflectance is a function of biophysical structure of within the canopy (Jakubauskas 1996a). Each band is treated as an independent spectral variable associated

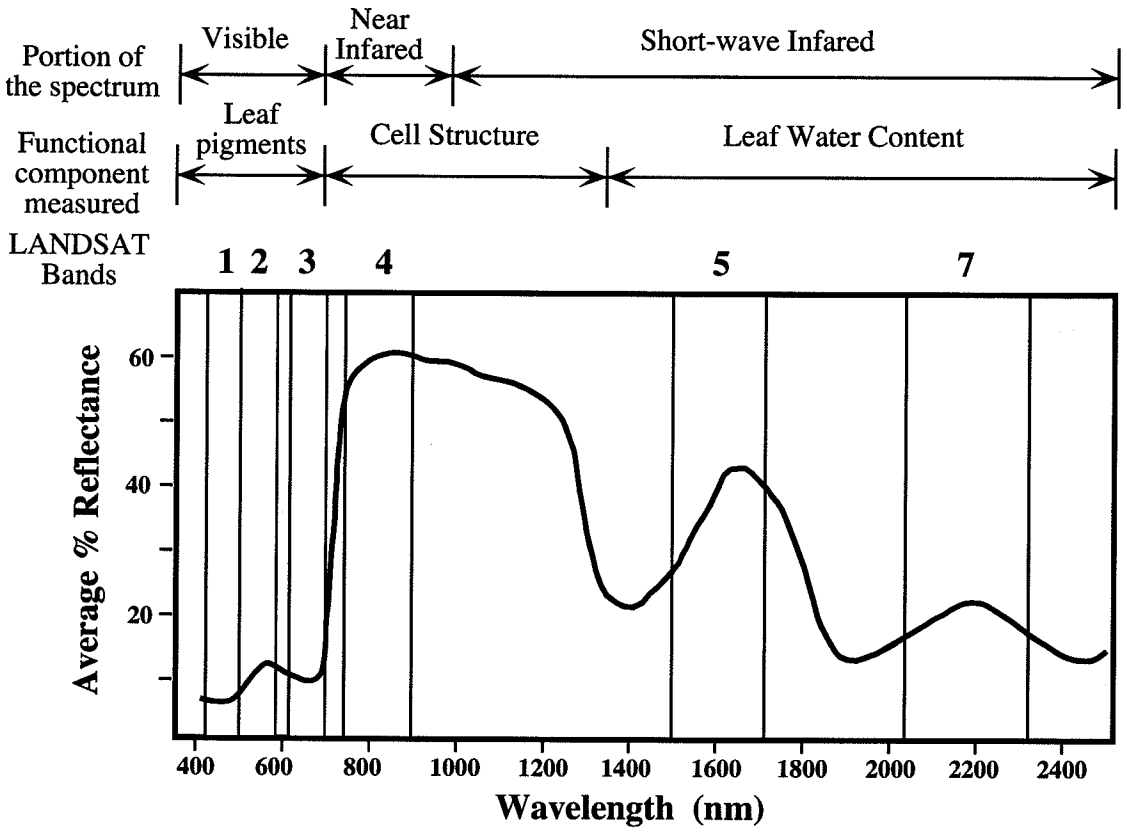

Figure 1.2: Average spectral reflectance for terrestrial surfaces and the associated Landsat 5 bands sampled.

with specific biophysical components (Colwell 1974; Hall et al. 1995) or combined with others to extract additional biophysical information (Chen 1996a.). However, significant correlation between bands exist such that only a subset provides unique information about canopy biophysics (Hall et al. 1995; Jakubauskas 1996a). In boreal mapping and the estimation of canopy biophysical properties Landsat bands 3, 4 and 5 are have been demonstrated to be the most optimal combination (Hall et al. 1995; Moore and Bauer 1990; Bolstad and Lillesand 1992). This study uses these three bands exclusively. The inferred biophysical components measured are:

1. Band 3 (PAR visible red, 0.63 μm-0.69μm)

In the visible portion of the spectrum, plant pigments absorb the majority of incident radiation resulting in high correlation among visible bands (e.g. r=.98) for most canopies (Jakubauskas 1996a). Much of the reflected visible light measured at-satellite is attributable to scattering from elements in the upper canopy (Ranson and Williams 1992). Band 3 reflectance is sensitive to the conditions of foliage within the canopy, decreasing with leaf maturation and increasing with leaf wilt (Myers 1983). For forests stands, reflectance in this band declines with age, associated with increase in live basal area and with canopy depth (Horler and Ahern 1986; Jakubauskas 1996a).

2. Band 4 (NIR near infrared, 0.76μm-0.90μm)

The internal structure of leaves determines the level of reflectance in the near infared, principally because of scattering from the surfaces of the cell walls in the spongy mesophyll (Myers 1983). Increased scattering occurs in band 4 as biomass accumulates within the canopy. Because very little incident radiation is absorbed in this region relative to band 3, reflectance between these bands is often expressed as a ratio to estimate productivity (Jordan 1969; Ranson and Williams 1992). Reflectance in this band can decrease significantly during leaf senescence, often resulting in the inversion of productivity estimates based on band ratios (Myers 1983). In forested systems, reflectance in band 4 decreases with the density of live trees, and increases as stands mature (Jakubauskas 1996a; Horler and Ahern 1986).

3. Band 5 (SWIR mid-infrared, 1.55μm-1.75μm)

Reflectance in the middle infared is controlled by vegetation moisture content (Myers 1983; Hall et al. 1995). Leaf area index (LAI), tissue moisture content and photosynthetic rate are highly correlated, thus often this band is used to infer the relative photosynthetic efficiency of a canopy (Ranson and Williams 1992; Jakubauskas 1996a). In forest canopies, band 5 reflectance declines with increasing biomass, and increases with leaf wilt (Myers 1983; Horler and Ahern 1986). In boreal and montane forests band 5 has been shown to correspond with different age classes, distinguishing young vs. old and closed vs. open stand types (Fiorella and Ripple 1993; Horler and Ahern 1986).

In Landsat TM imagery, 30 x 30 m is the finest scale for which ground reflectance is measured directly (excluding sub-pixel modeling, Richards 1993; Peddle et al. 1997). At that scale, a pixel usually contains several to many individuals (e.g. trees) representing multiple cover-types of varying composition and structure (Ranson and Williams 1992). Indeed, the measured reflectance for the vegetated landscape is a mixture of many different components (both biotic and abiotic) occurring at the sub-pixel level (**Table 1.1**; Colwell 1974). One of the biggest challenges in modeling canopy biophysical parameters is taking measurements taken for individual leaves and scaling them up to the level of the canopy (Hall et al. 1995). In conifers, radiant energy scattering is scale-dependent: measurements made at the canopy scale differ from those made at the leaf and branch scales (Chen 1996b; Colwell 1974; Norman and Jarvis 1975). For example, NIR reflectance declines significantly from the leaf-scale (50% reflectance), to the branch-scale (35% reflectance) to canopy-scale (18% reflectance; Williams 1991). In Hall et al. (1995), relationships were derived using end member fractions of sunlit crowns, sunlit background, and shadow to try to model the influence of these components on reflectance. They found that shadowing was especially important in the estimation of biomass density, average tree diameter, LAI and net primary productivity. While the discussion of mixture models is beyond the scope of this thesis, the scaling properties of conifers is particularly relevant for developing maps and productivity estimates for the boreal forest. These issues will be addressed in **Chapters 7** and **8**.

Landsat scenes also have scaling properties above the nominal resolution of 30 x 30 m. These scaling properties result in the spatial dependency of image elements within a scene, usually referred to as texture (Musick and Grover 1990). Textural features in satellite

Table 1.1: The biotic and abiotic components of pixel reflectance (compiled from Colwell 1974; Horler and Ahern 1986; Hall et al. 1995)

Biotic

Species Properties	*Canopy Structure*
a. Transmittance and Absorbtion by Leaves	a. Depth
b. Leaf shape, size and arrangement	b. Geometry and Architecture
c. Growth form, height and branching structure	c. Shading
d. Floristic composition	d. Arrangement of canopy types

Abiotic

Soil/Background Properties	*Landform Structure*
a. Soil Type	a. Slope and landform complexity
b. Moisture	b. Aspect
c. Water	c. Shading

data are most often measured using directional filtering approaches (e.g. Barber and LeDrew 1991; Cohen 1990) or by calculating local variance on imagery (e.g. Rey-Benayas and Pope 1995; Jakubauskas 1997; Gould 2000). Directional filtering using a grey-level co-occurency approach computes local information statistics within a window for which both an orientation and sampling distance must be specified. These metrics have been shown to differentiate the age of sea-ice for radar imagery, however the approach is sensitive to resolution (i.e. sampling distance: Barber and LeDrew 1991). To examine the influence of sampling scale on texture, semivariogram are often used (Cohen 1990; Trietz and Howarth 2000). This approach provides several statistics for quantifying local patterns of autocorrelation within a scene, often related to biophysical structure within the canopy (Sampson et al. 2001). One of the most common approaches for examining patterns of biodiversity and landscape complexity is to calculate local variance within a sampling window (Rey-Benayas and Pope 1995). For this method a regular grid or sliding window is placed over an image and the variance in reflectance (or vegetation index values) is calculated. Gould (2000) found that changes in local image variance could predict species richness in the arctic. He found that productivity and species richness was concentrated on the landscape, often in association with topographic variation and drainage patterns. In tropical systems, Rey-Benayas and Pope (1995) demonstrated that local variance could be used to predict several components of ecosystem diversity including Shannon's index. They concluded that image texture alone could predict species richness without requiring extensive ground sampling. In boreal coniferous forests, stand successional dynamics have been shown to influence texture. Jakubauskas (1997) computed local variance in a 3 x 3 pixel moving window and found that landscape complexity was dependent on stand age. The determination of landscape complexity in this study was also based on the measurement of spatial patterns in Landsat image reflectance. However, in this study texture measurements were made using scale-invariant fractal statistics (see § **1.4**).

Vegetation Indices: NDVI

Spatial patterns in ecosystem productivity are often examined using vegetation indices (Gould 2000). This approach has the advantage of combining the information content of one or more spectral bands into a single value that can be used to produce map classifications of 'desired' ecosystem attributes (Perry and Lautenschlager 1984). For example, Fiorella and Ripple (1993) developed a 'successional' index by taking the ratio of the Landsat mid-infrared bands, these were then used in forestry management applications. Some of these indices are based on empirically derived linear relationships such as the

tasseled-cap transformation (a PCA eigenvector; Hanson et al. 2001). However, the most commonly used indices are based on PAR and NIR reflectance (Myers 1983; Chen 1996a). In management applications these are used to predict primary productivity for extensive areas of the landscape. The basic assumption of this approach is that vegetation absorbs incident light in the PAR region of the spectrum but backscatters light in the NIR (Myers 1983). Jordan (1969) originally developed this measurement in tropical forest canopies. His 'simple ratio' (SR) vegetation index, is based on the relationship:

$$SR = NIR/PAR \qquad \textbf{[Equation 1.13]}$$

where the units of reflected PAR and NIR energy are in $W/m^2/ster/\mu m$.

It is important to note that all of his measurements were done underneath the canopy using a 'hand-held' spectrophotometer. In satellite applications, these values are obtained by measuring the at-sensor solar existence.

The SR ratio is unbounded and a modified version (NDVI) was developed for grasslands to 'normalize' the SR ratio to range between –1 and +1 (Rouse et al. 1973):

$$NDVI = \frac{NIR - PAR}{NIR + PAR} \qquad \textbf{[Equation 1.14]}$$

While negative values are uncommon, they have been observed for canopies where significant senescence of green biomass has occurred (e.g. fall and early winter: Blair and Baumgardner 1977).

NDVI has been applied across broad trends in vegetation conditions often with little critical evaluation. For instance, McDonald et al. (1998) used NDVI to characterize vegetation trends for montane sites with canopy cover ranging from 0% to 50%. They found a strong relationship between NDVI and cover over this range. In the same analysis, cover data from a boreal site that had 40% to 100% crown closure was added. NDVI for the boreal site did not trend with crown closure, however a single regression slope based on the full range (0% - 100%) was calculated. The application of ratio-indices to the boreal forest is problematic because they make simplifying assumptions about the structure of the canopy. In particular, most indices do not consider forward scattering of light and potential directionality in the estimated value (Leblanc et al. 1997) or scale effects. For instance, the

relationship between NIR and PAR in conifer canopies is known to 'invert' between the leaf and canopy scale (Ranson and William 1992). Despite these problems, NDVI is commonly used in image analysis to 'simplify' Landsat data into productivity classes prior to texture or other analyses (e.g. Rey-Benayas and Pope 1995; Jakubauskas 1997; Emerson et al. 1999; Gould 2000).

Image Simplification

For landscape spatial analyses that require binary or categorical data, a simplification of the three-band landsat scenes (24 bit pixels) is neccessary. Unsupervised classification is a 'neutral' data reduction strategy, since no *a priori* assumptions are made regarding the ground composition of the scene. Instead the classification group structure is based purely on spectral information (Richards 1993). The classification method used was non-hierarchical K-means clustering, in which an iterative algorithm is used to determine an optimal partitioning of variable space into 'K' non-overlapping groups (Lillesand and Kiefer 1994). The number of classes chosen must balance the need for retaining spatial information while simultaneously simplifying the imagery. Too many classes results in low frequencies within the classes, while too few classes can result in an image that is essentially 'filled' by one class.

Vegetation Mapping

1. Multivariate approaches to Landsat Analysis

Traditional graphical exploration of spectral classes in remotely sensed data is undertaken by examining combinations of bands in bivariate scatterplots (Richards 1993). These plots can be misleading because not all Landsat bands contribute equally to class discrimination (Lark 1995; Moore and Bauer 1990; Zhao and Maclean 2000). Indeed, while seven spectral bands are available for image classification only a subset provides significant class discrimination (Bolstad and Lillesand 1992; Horler and Ahern 1986; Shen et al. 1985).

One of the principal multivariate tools used in this study was multiple discriminant analysis. MDA was used to evaluate the separation of vegetation classes in spectral space prior to image classification and to test the accuracy of the final vegetation-map. Multiple discriminant analysis is often applied to remotely sensed imagery as a 'feature extraction' technique (Zhao and Maclean 2000). This method is constrained to optimally partition variance among *g a priori* defined groups, such that the between-group variance relative to the variance within groups is maximized (Legendre and Legendre 1998). In MDA group

discrimination is determined by comparing the within-groups pooled cross-products matrix **W** to the between-groups matrix **B**. This is accomplished by performing and eigenanalysis on the matrix product $\mathbf{W}^{-1}\mathbf{B}$ following:

$$(\mathbf{W}^{-1}\mathbf{B}-\mathbf{I}\lambda_i)k_i=0 \qquad \textbf{[Equation 1.15]}$$

where $\mathbf{k}_i$ is an eigenvector of discriminant weights, and λ_i is an eigenvalue. A maximum of t = MIN (g-1, p) eigenvalues are extracted. The eigenvalue λ_i is the ratio of the between-groups sum of squares to the within-groups sum of squares for the i^{th} discriminant axis. These eigenvalues measure the relative 'strength' of discrimination, but not the maximum amount of linear variance in the dataset as in PCA (Zhao and Maclean 2000). A *post hoc* transformation of the mean vectors is used to obtained scores for the objects along each discrimnant axis (Legendre and Legendre 1998). Plotting the object scores for the first two discriminant axes provides a useful visualization tool to assess the relative separation of classes within discriminant space (Peddle 1993). Structure coefficients (correlations) between the original variables and the discriminant axes can be used to infer the relative 'importance' of those variables in separating the classes (Zhao and Maclean 2000).

2. Map Agreement

To evaluate the agreement of the final map product with vegetation on the ground, additional data independent of the training set is required (Stehman 2001). From these data a confusion (error) matrix between class assignments on the map (rows) and class assignments in the reference set (columns) can be constructed (Congalton 1991). Classification accuracy for each class can be determined by dividing the diagonal elements of the matrix by the sum of each row and column (Congalton 1991). This generates two measures of accuracy for each class: "producers" accuracy (diagonal elements divided by each column total) and "users" accuracy (diagonal elements divided by the row totals). An overall measure of agreement can be obtained by dividing the sum of the diagonal by the matrix sum (Lark 1995; Richards 1996). A simplistic interpretation of this table would be that the diagonal elements represent correct classifications between the map and the reference sites, while off-diagonals indicate misclassifications. In reality, each cell in the matrix has a finite associated random error including the diagonal elements (Lark 1995). To correct for potential chance agreement between row and column values, the Kappa statistic (k-hat) is calculated (following Hudson 1987; Congalton 1991):

$$\hat{\kappa} = \frac{N\sum_{i=1}^{r} x_{ii} - \sum_{i=1}^{r} x_{i+}x_{+i}}{N^2 - \sum_{i=1}^{r} x_{i+}x_{+i}} \qquad \textbf{[Equation 1.16]}$$

One of the fundamental disadvantages of this method is the necessity of a classification of the test set. This can lead to potential errors because of difficulty in making class assignments in the field (Stehman and Czaplewski 1998). In this study a novel application of MDA was used to examine the agreement (verification step) for a vegetation map in the boreal forest. Using this approach, the vegetation class relationship determined in spectral space was used to partition a vegetation dataset collected within the mapped region. These data were then assessed to determine whether the vegetation map discriminated 'classes' on the ground.

3. Improving Map Agreement

Estimates of agreement for Landsat map classifications of the northern boreal forest vary widely (40% to 95%), with 85% generally considered to be acceptable for land management purposes (Bolstad and Lillesand 1992). Poor map performance in boreal regions is a consequence of spatial heterogeneity and the relative spectral similarity of boreal forest canopy-types (Moore and Bauer 1990; Shen et al. 1985). Among conifers spectral signature alone may not provide adequate class seperation (Trietz and Howarth 2000; Zhao and Maclean 2001). In many cases, these species must be 'pooled' into larger groups to increase overall accuracy (Moore and Bauer 1990). Several studies have used remotely sensed data in conjunction with ancillary surface data to improve image classification. The empirical relationships between soils, terrain and vegetation can be used to separate cover-types that occur under different environmental conditions (Peddle 1993; Treitz and Howarth 2000). Addition of terrain features normally improves conifer separation in lowland classes but has little influence on upland classes (Bolstad and Lillesand 1992). Alternatively, multitemporal imagery has been used to classify vegetation types based on seasonal changes in reflectance (Shen et al. 1985). To reduce the influence of spectral overlap on final accuracy, rule based algorithms can be used to help decide when classes need to be modified, merged or added (Treitz and Howarth 2000; Markon 1992; Franklin 1995; Peddle 1993). Image classification is a reciprocal training procedure where both the vegetation and spectral information ultimately determine map accuracy (Goodchild 1994). Spatial patterning of boreal forest communities reflects a complex continuum of floristic

associations, successional processes (e.g. disturbance, differential growth), and canopy structure (Hall et al. 1995; Frelich and Reich 1995; Cihlar et al. 1997). Mapping strategies must be optimized to adequately characterize the structural and spatial complexity of the boreal forest. In this study, a statistically rigorous multivariate approach is developed for analysis of remotely sensed imagery of the boreal forest.

1.5 Objectives

Purpose and Context

Landscape complexity in the boreal forest is an emergent property determined by interactions occurring over a range of scales. At the landscape scale, pattern is a function of climate, physiography and catastrophic disturbances (e.g. crown-fire), and patterns of post-fire colonization. At local scales, microtopography and disturbances such as herbivory, windthrows and lightning determine canopy structure. These processes result in a structurally complex landscape consisting of a mosaic of plant communities of varying age and composition. However, little is known about the development of landscape complexity or the long-term trajectory of change resulting from the superimposition of these processes. This knowledge is particularly critical for predicting the influence of forest management practices. For instance, active fire suppression alters the disturbance regime only at the broad-scale, potentially increasing the influence of local effects on landscape pattern development.

Fragmentation by agricultural development also influences the development of pattern on these landscapes. Human fragmentation presents major challenges for the conservation of biodiversity both through loss of habitat as well as by restricting movement of organisms to isolated wildlife reserves. In the study area, fragmentation is so severe that the boundaries of the nature reserves can be seen from space. However, little is known about the long-term effects of habitat fragmentation in these systems or its impact on landscape connectivity. The examination of past and current land-use practice is necessary to determine the future trajectory of landscape change.

Accurate vegetation maps are essential for managing boreal landscapes. For practical utility, maps must simplify floristic complexity on the landscape, while retaining ecologically meaningful information. Remote sensing provides spatially explicit information about landcover for large regions. However, mapping the boreal forest using remotely

sensed data is particularly challenging because of the high degree of spatial heterogeneity in the canopy requiring extensive ground information. To produce accurate maps, the relationship between reflectance and vegetation cover must be established using an adaptive map classification methodology. As these properties of the canopy change with time and space, it is imperative that multivariate methods be used in producing and assessing satellite classifications.

Alternative methods of mapping based on band-ratio indices such as NDVI are often used to measure ecosystem components of particular concern to land managers (e.g. ecosystem productivity). However, these indices make simplifying assumptions about the structure of the boreal canopy and how light interacts with vegetation. It is important to recognize that canopy species interactions with light have evolved over time. There is ample evidence that conifer species have unique emergent reflectance properties at the stand-level. The adaptive advantages of conifer architecture in light capture and its influence measurement of productivity in these systems needs to be examined.

Overview of Objectives

Landscape complexity is an emergent property of natural systems that must be quantified to better understand boreal ecosystem dynamics, the impact of fragmentation and to accurately map these systems. In this study, remote sensing technology and scale invariant spatial statistics based on fractals will be used to examine landscape complexity arising from temporal dynamics and spatial complexity. The impact of human fragmentation of the boreal landscapes will also be examined to determine the influence development on the dispersion of natural habitat patches. A mapping approach will be developed that uses spatial-spectral optimization to improve the classification of structurally complex landscapes. In addition, the adaptive significance of boreal conifer architecture and its influence on productivity estimates for these systems will be discussed. These different

aspects of landscape complexity in the boreal forest will be examined in the following questions:

I. How does landscape structure in the boreal forest change in space and time?

- How does the landscape change during succession and in response to topographic complexity?
- How does long-term vegetation dynamics influence the spatial persistence of the boreal canopy?

II. How do humans influence the development of landscape pattern?

- How does agriculture influence the extent and dispersion of forest patches?
- Does the dispersion of forest fragments change predictably in agricultural systems?

III. How does canopy structure influence our ability to model and map the boreal forest?

- What is an optimal method for classifying and mapping these systems?
- Is spectral reflectance an emergent property of boreal canopy structure?

Chapter 2

Study Area

2.1 Introduction

The study area, centred on Riding Mountain National Park (RMNP), incorporates 24,250 km^2 (50°11'-51°26' N, 99°06'-101°38' W) of southwest Manitoba (**Figure 2.1**). Initially established as a forest reserve, that area has had National Park status since 1930. The Park itself is 2,974 km^2 in size, extending about 115 km from east to west and 60 km from north to south at its greatest width (Parks Canada 1977)..RMNP and areas north of the Park are located in a southeastern extension of the Mixedwood Section (B18a) of the Boreal Forest Region (Rowe 1972; **Figure 2.2**). Areas south and east of the Park occur in the Aspen-Oak Region, while areas to the west occur in the Aspen Region. Much of the land surrounding RMNP has been modified by human activity, primarily through agricultural clearing. Current encroachment around the Park is so severe that the border is visible from space (Dearden and Rollins 1993). Corridors of natural vegetation (e.g. Grandview valley, **Figure 2.1**) no longer connect the Park with adjacent forest reserves, resulting in the Park being described as an ecological island in a "sea" of agriculture (Bailey 1968).

The most prominent physiographic feature of the study area is the Manitoba Escarpment. Originally named Fort Dauphin Mountain by Alexander Henry in 1799, the Escarpment was first referred to as the Riding Range in 1858 (**Figure 2.3**). The Escarpment rises approximately 430 m from the eastern Manitoba lowlands or first prairie level (mean elevation of 320 m) to the western Saskatchewan plain or second prairie level (mean elevation 610 m). Maximum elevations in the study area occur along hills of the Manitoba Escarpment (approximately 750 m). The Manitoba Lowlands and Lake Manitoba bound RMNP to the east. To the north a broad valley (Grandview valley) occupied by the Wilson and Valley Rivers separates the Park from Duck Mountain Provincial Forest. South of RMNP and to the west, the Assiniboine River valley and the Lac Du Prairie reservoir separates the Park from the rest of the Saskatchewan Plain (Bird 1961; Lang 1974). Five major vegetation types are characteristic of the study area: northern borealforest, aspen parkland, bur oak savannah, grassland, and eastern deciduous forest (Caners & Kenkel 1998). Factors such as post-glacial climate change, physiography, edaphic conditions, fire disturbance and herbivory have influenced the structure and development of natural vegetation in the region.

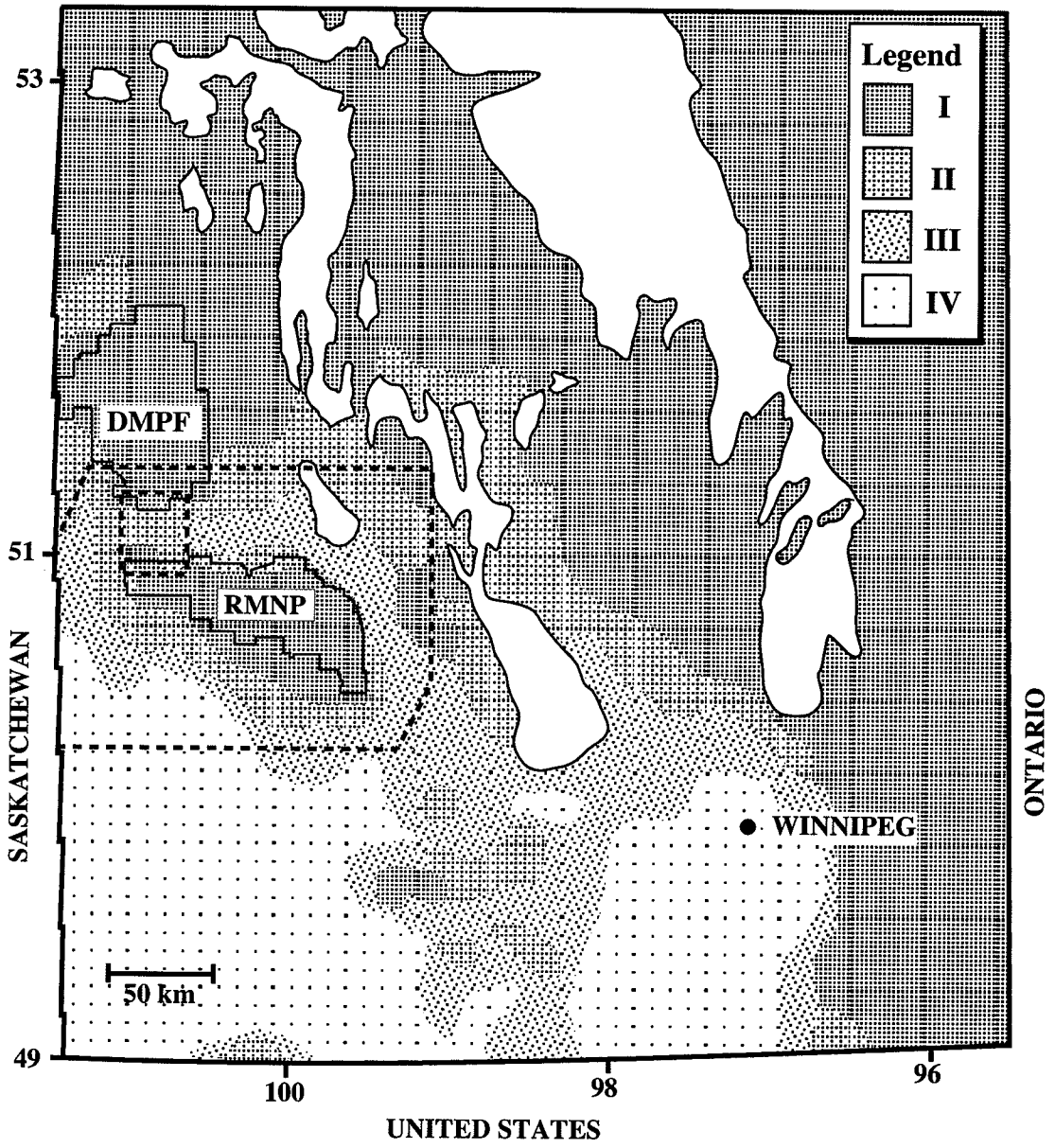

Figure 2.1: Map of Southwestern Manitoba indicating the location of RMNP and the study region (dashed line). Shadings indicate the dominant biomes for the region: (I) Boreal and mixed wood transition (white spruce and aspen); (II) Broadleaf forest with eastern deciduous elements (aspen, bur oak, elm and maple); (III) Aspen Parkland; (IV) Tall and mixed grass prairie. The Grandview Corridor is the historically contiguous belt of aspen parkland connecting RMNP with Duck Mt (inset dotted line, modified from Bird 1961).

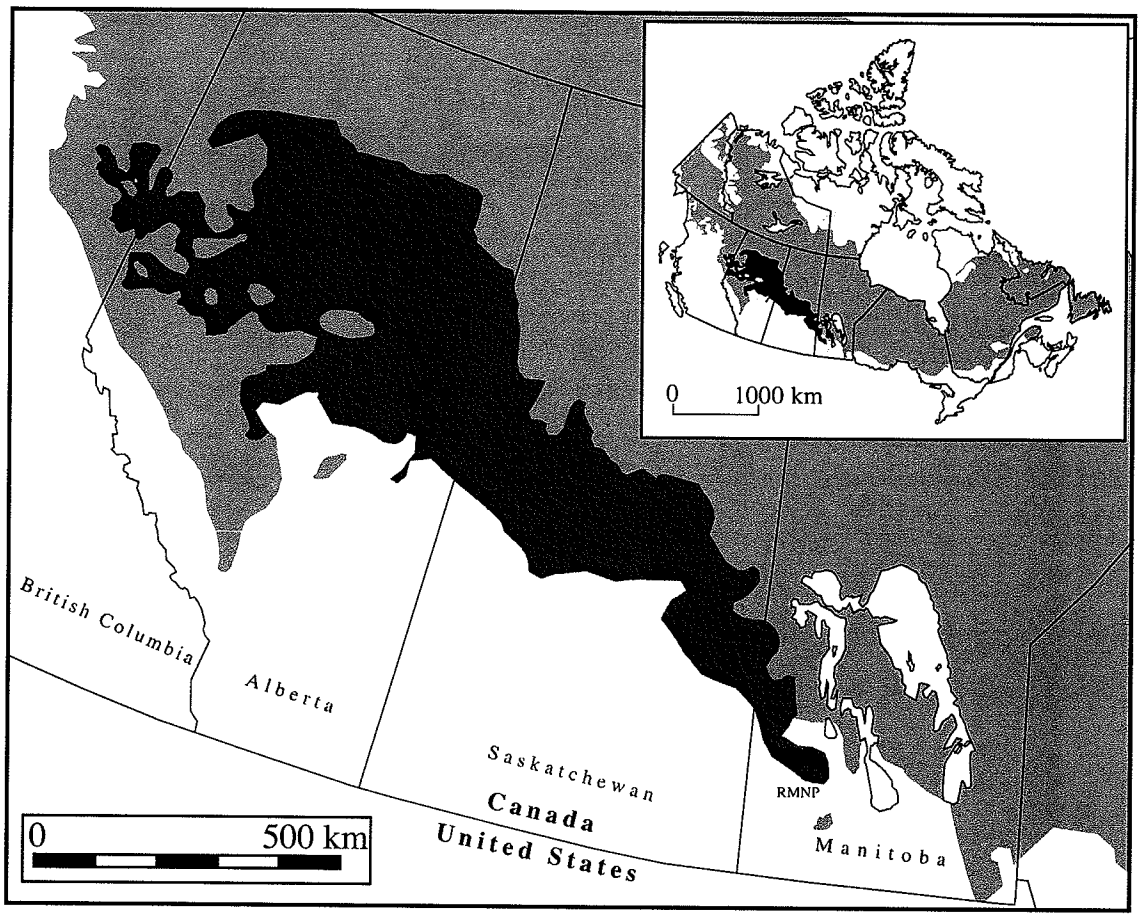

Figure 2.2: Distribution of the boreal forest in Canada (light grey, top inset) and the boreal mixedwood section (dark grey, main figure). The location of RMNP is indicated (bold dot, modified from Johnson 1992).

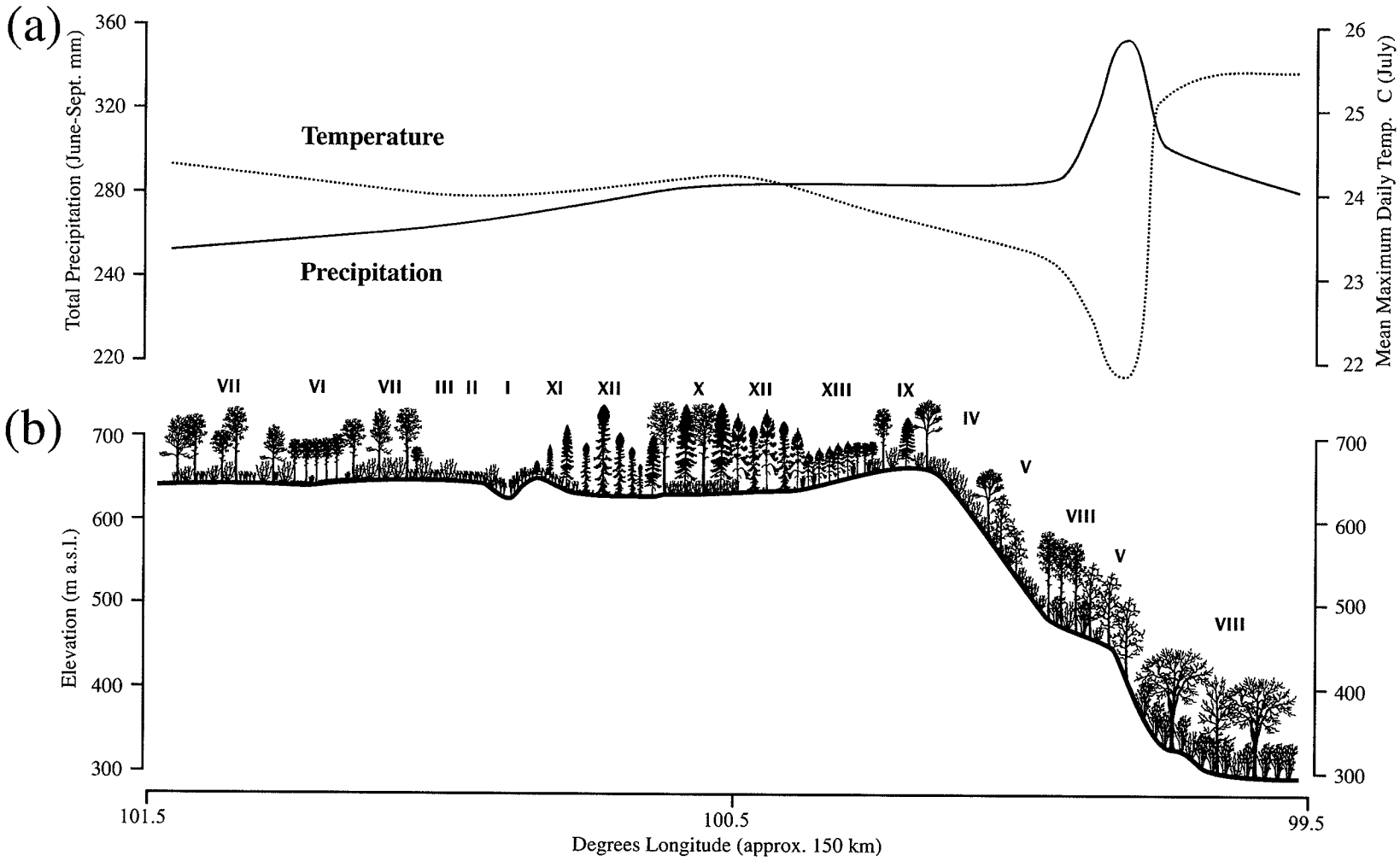

Figure 2.3: Cross-section (west to east) of the Manitoba escarpment in Riding Mountain National Park (approx. 150 km, 99.5 - 100.5). a) Climate normals, total precipitation (June-Sept, solid line) in mm and mean maximum daily temperature C (for July, dotted line) recorded at Environment Canada weather stations in the region (Canada 1979); b) Elevational profile across the Manitoba escarpment and the major vegetation association in RMNP (Roman numeral follow **Chapter 2 § 2.8**). The geographic ranges of vegetation associations in the Park follow trends in the climate and physiography.

2.2 Climate

The study area falls within the Humid Microthermal Climatic zone (Koopen-Geiger classification), which is characterized by a rain-snow climate of cold winters and warm summers (Waldron 1966). Marked differences in microclimatic conditions occur within the study area (**Figure 2.3**). Total summer precipitation decreases from higher to lower elevations along the Manitoba Escarpment, and summer maximum temperatures are lower on the Saskatchewan Plain (Ritchie 1964; Bailey 1968; Parks Canada 1977). Mean annual total precipitation for the study area ranges from 40-55 cm (Environment Canada 1990). June, July and August are the warmest and wettest months. The study area has a mean annual growing season of 160-180 days, and an average of 100-110 frost-free days (Weir 1983).

Summative climatic data (1966-1989) for the town of Wasagaming (50°39' N, 99°56' W) are presented in **Figure 2.4**. Total annual precipitation averages 51 cm, with 38 cm (about 75%) falling as rain. The mean annual temperature is minus 0.1°C, ranging from a mean of minus19.7°C in January to 16.5°C in July.

2.3 Physiography and Surficial Geology

Bedrock in the study area originated from silt deposits laid down by shallow Cretaceous seas between 136-65 million years ago (Lang 1974). This bedrock has been divided into six geological formations, the largest of which is the Riding Mountain formation. This formation, which is composed primarily of non-calcareous gray shales, covers most of southwest Manitoba including the Porcupine Hills, Duck Mountain, and Riding Mountain. The uplands of RMNP and adjacent areas consist of hummocky stagnation moraine deposits of calcareous glacial till (Ritchie 1964; Weir 1983).

The study area includes the rolling uplands of the Saskatchewan Plain, the Manitoba Plain and the Manitoba Escarpment. The Saskatchewan Plain is dominated by moderately calcareous glacial till derived from Mesozoic shales. Glaciofluvial morainic deposits occur along the Assiniboine River and near Lake Audy, Whitewater Lake, Clear Lake and Tilson Lake in RMNP. The Assiniboine, Little Saskatchewan and Birdtail River valleys are glacial spillways dominated by alluvial deposits. More coarse-textured alluvial deposits, including sand and gravel beach ridges from glacial Lake Aggasiz, occur along the base of the

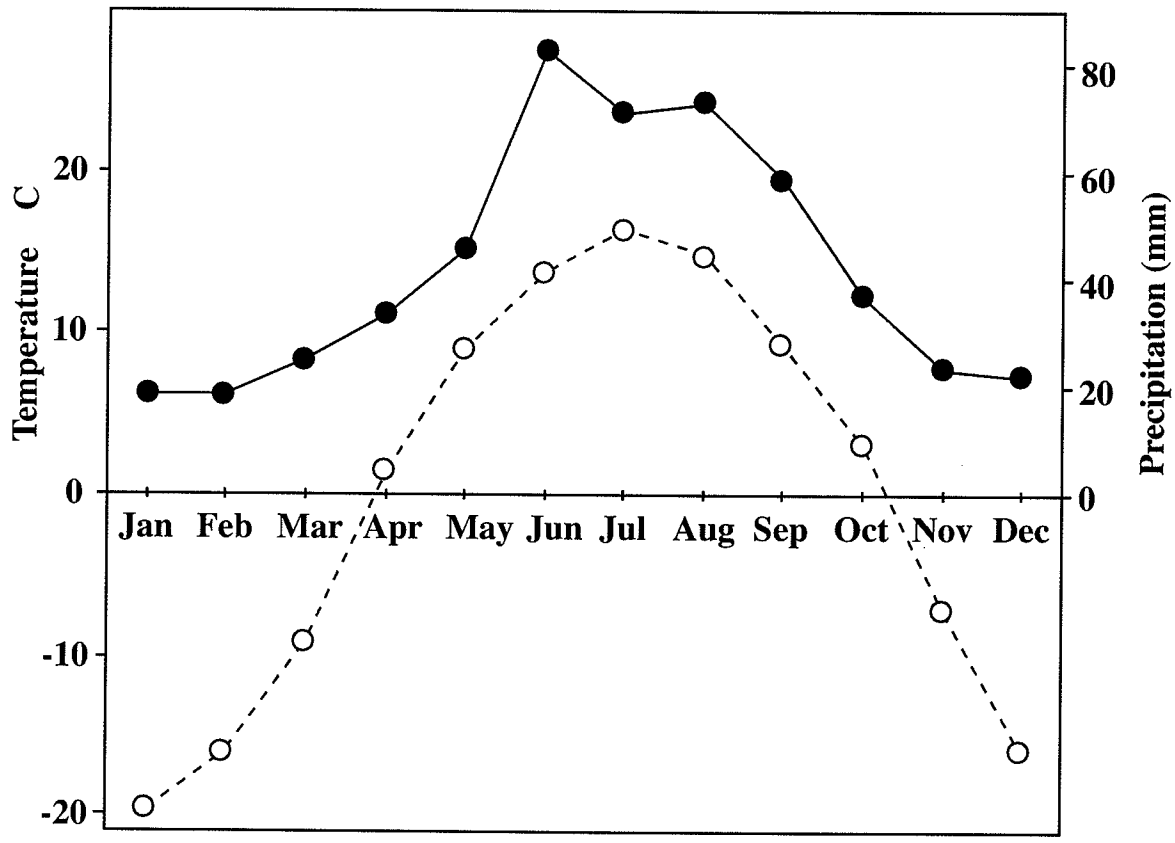

Figure 2.4: Annual Climate Normals for Riding Mountain National Park (Riding Mountain Weather Station, Canada 1979). Mean monthly precipitation (mm, solid lines and circles) and mean daily temperature (C, dotted line and hollow circles).

Manitoba Escarpment. The Manitoba Plain is dominated by highly calcareous glacial till derived from Paleozoic carbonate rock, as well as deep basin to nearshore glaciofluvial deposits (Weir 1983).

2.4 Soils

Luvisolic soils (Canadian System of Soil Classification, CSSC) predominate in Riding Mountain National Park and in the Duck Mountain Provincial Forest. These soils vary considerably in drainage, texture and nutrient status (Ritchie 1964). Areas surrounding RMNP are dominated by dark brown to black Chernozemic soils, although Luvic Gleysols of medium texture also occur (Weir 1983). Regosolic soils have formed on the alluvial fans and terraces at the base of the Escarpment. Shallow peat deposits occur in poorly-drained areas throughout the Park (Cody 1988).

2.5 Post-glacial History

The Manitoba flora and fauna were entirely eliminated during the last (Wisconsin) Ice Age. The ice sheet retreated from the Riding Mountain area about 12,500 years ago (Lang 1974). Fossil pollen records suggest that a spruce-dominated forest colonized the Riding Mountain area from the south, although a pioneer treeless phase probably existed immediately following glacial retreat (Ritchie 1969). Associated species included prairie sage (*Artemisia spp.*, Note: vascular plant scientific names follow Scoggan 1957), buffaloberry (*Shepherdia canadensis*), Cyperaceae, with some juniper (*Juniperus spp.*), ash (*Fraxinus spp.*), larch (*Larix laricina*), poplar (*Populus spp.*), pine (*Pinus spp.*), birch (*Betula spp.*) and alder (*Alnus spp.*, Ritchie 1985).

A warmer and drier climatic phase began about 10,000 years ago, resulting in a sharp decline in spruce forest within the study area. During the Hypsithermal or 'long drought' period that began about 7,500 years ago, drought-tolerant grasses, forbs and shrubs dominated the flora (Ritchie 1969). By about 6,500 years ago, bur oak (*Quercus macrocarpa*) and hazelnut (*Corylus cornuta*) appeared and the abundance of drought-tolerant species declined, indicating cooler and moister conditions (Ritchie 1985). About 3000 years ago, neoglacial cooling resulted in a dramatic change in the regional flora. The cooler, moister climate favoured the immigration of boreal forest elements into what is now Riding Mountain National Park (Ritchie 1969). Current evidence suggests that jack pine (*Pinus banksiana*) first arrived in the region about 2,500 years ago, likely from a western

refugium (Ritchie & Yarranton 1978). At about the same time, trembling aspen (*Populus tremuloides*), balsam poplar (*Populus balsamifera*), bur oak and white spruce (*Picea glauca*) began to invade into the grasslands south of Riding Mountain, forming the present-day aspen parkland (Bird 1961).

2.6 Disturbance History

Agricultural Settlement

Land in the Riding Mountain region was opened to European settlement in the 1880's (Lehr 1996). The Dominion Lands Act of 1872 determined property boundaries and settlement policies for the interior prairie region of Canada. The Act established a basic homestead size of 64.8 ha, and required that at least 12 ha of land be cleared within three years. Landowners were required to live on their property, which had the effect of suppressing the formation of towns. Settlement in the Grandview and Dauphin region was underway by 1885 (Dickson 1909), increasing dramatically following the publication of the Ukrainian "On Emigration" by Oleslow in 1895 and the extension of the Winnipeg Great Northern Railway Company line in 1899 (Goldrup 1992; Lehr 1996). By 1904, much of the available land in the region had been purchased, although most of the forests remained uncleared until after 1925. An accelerated period of forest clearing occurred after the Second World War following the introduction of the bulldozer (Bird 1961). During this period, the population more than tripled from approximately 15,000 at the turn of the century to 47,000 by the late 1940's (Stadel 1996). Since 1951, farming in the region has intensified as a result of increased mechanization. Extensive areas of upland forest have been cleared, leaving behind small forest refugia along rivers and wetlands and on unproductive land (Bird 1961; Stadel 1996). By the 1990's, much of the land surrounding RMNP had been cleared for agriculture. The major agricultural products are cereal and oil crops, and livestock. Over half of the land in production is seeded in wheat, although barley and canola are also important crops in the area (Carlyle 1996). Some of the most productive land in Manitoba occur within the study region: crop yields exceed 1.85 tonnes/ha southwest of RMNP, while yields of 1.55 - 1.85 tonnes/ha occur north of the Park (Weir 1983; Carlyle 1996).

Livestock

Substantial beef cattle production occurs within the study area, primarily on marginal land south and east of RMNP. Much of the forested land in these areas was converted to pastureland in the 1970's (Carlyle 1996). Cattle production in the eastern part of the study area (i.e. adjacent to Lakes Dauphin and Manitoba) is well above the provincial average, with up to 80% of farmed land in the region under pasture.

Cattle grazing was allowed within RMNP until 1970. Grazing peaked at over 4,500 head of cattle in 1919, but continued at relatively high levels (about 1,375 head) into the 1950's and 1960's (Trottier 1986). Cattle grazing led to the deterioration of many of the native fescue prairies within the Park (Blood 1966).

Logging Activity

Following European settlement, the Manitoba Escarpment forests were a critical source of timber for buildings, railway ties and firewood (Harrison 1934; Goldrup 1992). Historically, clearing on private land resulted in permanent conversion to agriculture, requiring increased extraction of wood products from the escarpment forests to meet demand (Evans 1923; Goldrup 1992). Recognition of the need to manage and conserve these forests resulted in the establishment of the Riding Mountain Forest Reserve in 1895 and the Duck Mountain Forest Reserve in 1906 (Bailey 1968; Goldrup 1992). An Order-in-Council in 1906 established cutting regulations for the Reserves, but illegal timber cutting continued in the region (Harrison 1934; Sentar 1992). After much debate, the Riding Mountain Forest Reserve was granted National Park status in 1930 and was officially opened to the public in 1933.

Peak logging activity in RMNP coincided with settlement and railway construction near the end of the 19th century (Bailey 1968). Milling operations were concentrated close to settlements along the base of the Manitoba Escarpment (Sentar 1992). Selective harvesting was commonly practiced, encouraged in part by the Dominion Lands Act which required that all merchantable trees > 25 cm at the base be taken (Weir and Johnson 1998). White spruce was the most heavily exploited species in the park, but jack pine, balsam fir (*Abies balsamea*), aspen, bur oak, green ash (*Fraxinus pennsylvanica*) and black spruce (*Picea mariana*) were also harvested (Bailey 1968). Sawmills operated within RMNP from the late 1880's until the mid-1940's, and logging continued within the Park boundaries into the mid-

1960's. Although there are no records documenting forest stands prior to the 1880's, there is some evidence that white spruce stands were once far more abundant (Dickson 1909). For example, in the western portion of the Park it was noted that "...the original forest type on the reserve was coniferous. It consisted principally of white spruce" (Evans 1923). The reduction in white spruce is attributable to the combined effects of logging in the 1880's and devastating fires at the turn of the century.

Fire

Fire plays a critical role in the perpetuation and health of northern ecosystems, including the boreal forest (Rowe 1961), prairie grassland (Anderson & Bailey 1980) and trembling aspen parkland (Bird 1961). Historically, wildfires were common in the prairie grasslands of southern Manitoba. These fires would occasionally burn into the forests of the plateau areas of RMNP (Trottier 1986). Fire suppression policies implemented at the turn of the century have greatly reduced the extent and frequency of burning within the study area (Bailey 1968; Hirsch 1991). There is some concern that fire suppression policies in boreal forests may promote fire-intolerant stands at the expense of pyric (fire-adapted) ones. Furthermore, fire suppression in prairie grasslands and aspen parkland may result in increased tree and shrub encroachment (Bailey 1968).

Fire has strongly influenced forest stand structure and development in RMNP (**Fig. 2.5**). The oldest forest stands occur on hygric sites, and in areas where physiographic features have provided fire protection. Fire scar and stand age data indicate that large fires occurred in 1822, 1853-1855, 1889-1891 and 1918-1919 (Rowe 1955). Fires were most prevalent during European settlement (1885-1889) frequently accompanying timber harvesting, and were often set by loggers and settlers burning hay meadows or clearing land (Tunstell 1940; Sentar 1992). Two catastrophic fires in the early 1890's burned over 70% of the area west of the Strathclair trail, "...not leaving even a spruce seed-tree over large tracts" (Dickson 1909; Evans 1923). Prior to these fires, the region was characterized by a number of white spruce stands "...of several square miles" in area (Dickson 1909). Most of the post-fire regeneration in the region has been to trembling aspen and balsam poplar. Jack pine stands in the southeastern portion of the Park have burned repeatedly over the last 120 years (Sentar 1992). While fire-fighting efforts since the 1930s have dramatically reduced the incidence and extent of forest fires (Sentar 1992), major fires occurred in 1940 (Whitewater Lake), 1961 (Gunn Lake) and 1980 (Rolling River). A number of small fires in the 1930's

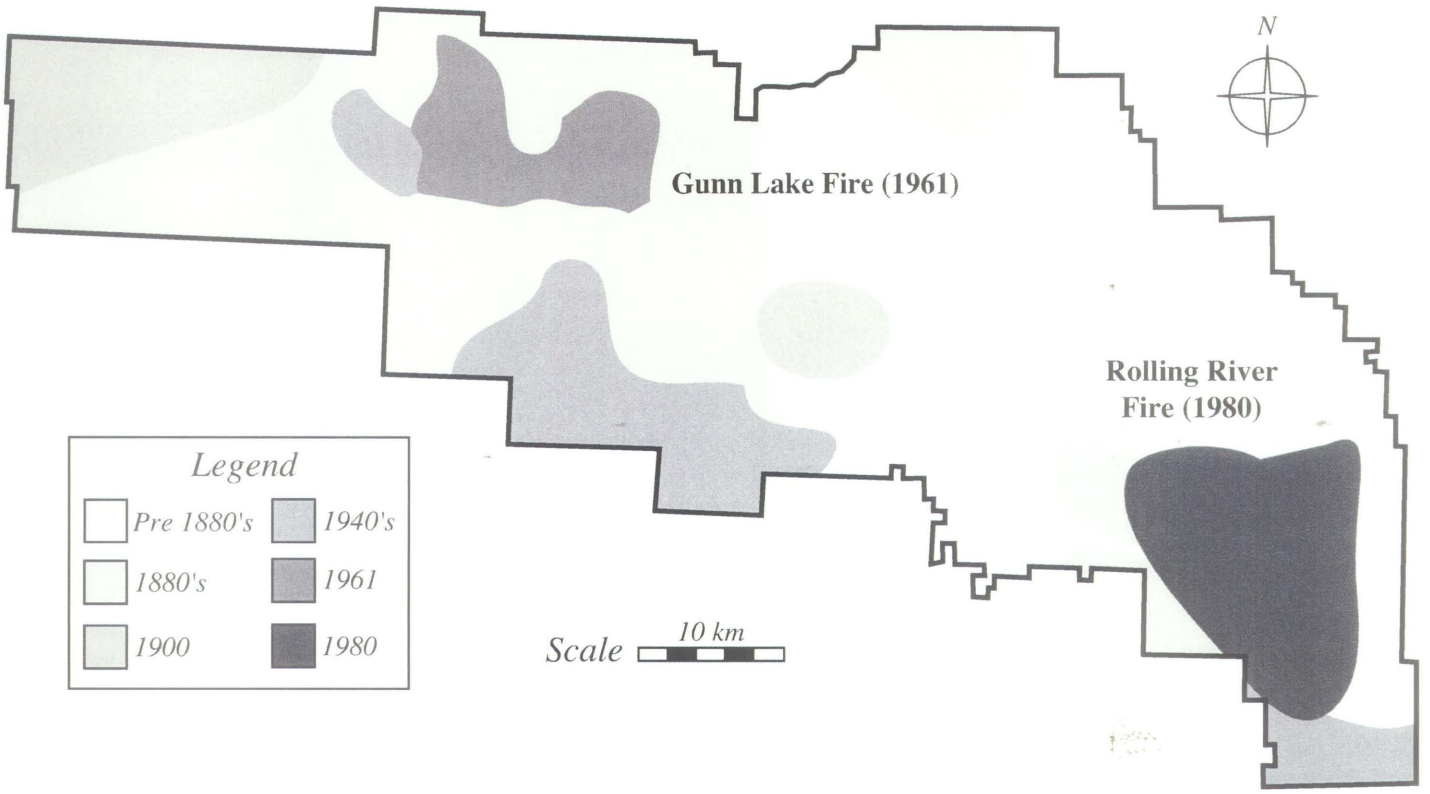

Figure 2.5: Locations of the major landscape-level crownfires in Riding Mountain National Park and the approximate year of occurance (modified from Sentar 1992).

and 1940's were thought to have been deliberately set by farmers (Bailey 1968; Ringstrom 1981).

Herbivory and Granivory

Large herbivores such as elk (*Cervus canadensis*, Note: mammal scientific names follow Banfield 1974), moose (*Alces alces*), and white-tailed deer (*Odocoileus virginianus*) selectively browse shrub species, as well as saplings and seedlings of a number of tree species (Caners & Kenkel 1998). Deer and elk show a strong preference for balsam fir while largely avoiding white and black spruce (Rowe 1955). In southern Manitoba, mountain maple (*Acer spicatum*), beaked hazelnut and trembling aspen are important components of moose diet (Trottier 1981). Beaked hazelnut is also an important browse of elk, white-tailed deer and hare (*Lepus spp.*). Hares feed on buds and smaller twigs of white spruce during the winter, and may kill saplings through repeated browsing (Rowe 1955). Voles (*Microtus spp.*) significantly reduce the amount of overwintering white spruce seed in medium to poor seed crop years, while red squirrels (*Tamiasciurus hudsonicus*) consume most of the seed crop except in heavy cone production years (Rowe 1955; Nienstaedt & Zasada 1990).

Beaver (*Castor canadensis*) plays a critical role in boreal forest ecosystem dynamics (Naiman 1988). Beaver damming results in the flooding of lowland forests and the killing of trees. The catchment basin accumulates organic matter and nutrients, and alters downstream hydrology (Shaw 1993). Beaver strongly select for trembling aspen, balsam poplar, and willows (*Salix spp.*) and so alter the forest structure and composition along the catchment basin.

2.7 Regional Vegetation

Parkland vegetation

Outside of RMNP, the dominant natural vegetation types are trembling aspen parkland (Bird 1961) and mixed-grass prairie (**Fig. 2.1**). The dominant graminoids of undisturbed mixed-grass prairie include june grass (*Koeleria cristata*), slender wheat grass (*Agropyron trachycaulum*) and western porcupine grass (*Stipa spartea* var. *curtiseta*). A number of forb species are also present, including the prairie crocus (*Anemone patens*), bastard toadflax (*Comandra umbellata*), three-flowered avens (*Geum triflorum*), northern bedstraw

(*Galium boreale*) and hoary puccoon (*Lithospermum canescens*). Common shrub species include snowberry (*Symphoricarpos occidentalis*), prickly rose (*Rosa acicularis*) and wolf-willow (*Elaeagnus commutata.*).

Gallery forests dominated by Manitoba maple (*Acer negundo*), green ash and american elm (*Ulmus americana*) occur along watercourses in aspen parkland (Bird 1961). Subcanopy elements in these forests include red-osier dogwood (*Cornus stolonifera*), sarsaparilla (*Aralia nudicaulis*) and chokecherry (*Prunus virginiana*). Numerous vines of eastern floristic affinity such as hops (*Humulus lupulus*), bittersweet (*Celastrus scandens*), virginia creeper (*Parthenocissus quinquefolia*) and carrionflower (*Smilax herbacea*) are frequently encountered. The herb-rich understory includes ostrich fern (*Matteuccia struthiopteris*), goldenrod (*Solidago* spp.), asters (*Aster* spp.) and wild mint (*Mentha arvensis*). In drier and more exposed areas along watercourses, bur oak, poison-ivy (*Rhus radicans*) and chokecherry often occur.

Upland boreal plain and escarpment vegetation

Riding Mountain National Park and Duck Mountain Provincial Forest are dominated by mixedwood boreal forest vegetation (Bailey 1968). Although vegetation composition differs somewhat in the two reserves, broad vegetation trends are similar. In RMNP, patterns in the distribution of vegetation communities correspond with changes in climate induced by the escarpment and with local edaphic gradients (**Figure 2.2**). In both reserves, higher elevations are conifer dominated in both pure and mixedwood stands. Moderately to well-drained upland areas are characterized by semi-open to closed stands of trembling aspen, balsam poplar and white spruce. Mixedwood stands of white birch and balsam fir are also encountered; they are more occasional in RMNP (located primarily in the northeast) and are common in Duck Mountain. Jack pine and/or black spruce, in both mature and fire-regenerating stands dominate sandy soils. In RMNP, these are found east of Clear Lake and in Duck Mountain adjacent to East Blue Lake. Black spruce stands with eastern larch are found in poorly-drained boggy lowlands throughout both reserves. Deciduous dominated communities are generally found in the western portion of RMNP and along the eastern escarpment adjacent to the Aspen-Oak region in both parks (Rowe 1956, 1972). Parkland vegetation is more commonly encountered in RMNP than Duck Mountain, thought to be the result of several recurrent fires within the region. In RMNP, bur oak 'savanna' occurs on steep, exposed slopes of the upper escarpment and on coarse-textured outwash deposits in the extreme north-east. These stands are very occasional in Duck Mountain, found

scattered on south-west facing slopes along the eastern escarpment. In the rich soils along the lower edge of the escarpment, eastern hardwood stands dominated by white elm (*Ulmus americana*), green ash (*Fraxinus pennsylvanica* var. *subintegrrima*) and Manitoba maple (*Acer negundo*) are common in RMNP. In Duck Mountain these stands are dominated by well developed trembling aspen and balsam poplar forests. Grasslands are a very minor component of both RMNP and Duck Mountain Provincial Forest, often occurring along river valleys, but also on excessively drained soils and post-burn sites. These communities consisti of both plains rough fescue (*Festuca halli*) and mixed-grass prairie elements. In Duck Mountain many of the grasslands along river valleys have been planted to white spruce (e.g. Shell River valley) and are now highly disturbed and degenerate.

2.8 Vegetation Association Descriptions

In this study, a series of vegetation association were established to represent the range of floristic variation in RMNP that could be identified using satellite imagery (**Chapter 7**). The vegetation association descriptions (color Plates) in the following pages correspond to those used in the Landsat map classification. For each association a brief description of the canopy dominants, distribution in RMNP, physiognomy and environment are given (roman numeral designations follow those used in **Chapter 7**).

Plate I. Wetland

Description

Non-forested wetlands, typically dominated by graminoids (grasses, sedges), found throughout the Park. Species common in this association are bluejoint grass (*Calamagrostis canadensis*) and/or sedges (*Carex spp.*) in wetmeadows and cattail (*Typha spp.*), or common reed (*Scirpus spp.*) in open water sytems. Flood-tolerant shrubs (e.g. willows) may also occur at low abundance.

Physiognomy

Graminoid or graminoid-like marshes with a relatively even canopy up to 2 m in height often in large monodominant species patches.

Environment

Seasonally to permanently flooded wetlands along or adjacent to water courses; may be the result of, or perpetuated by, beaver activity.

Variants

Two variants are recognized:

(a) Meadow marsh: seasonally to semi-permanently flooded areas, usually dominated by bluejoint grass and/or sedges; floodplains of small streams, beaver meadows, and lakeshores.

(b) Marsh: semi-permanently to permanently flooded areas, usually dominated by cattails and/or common reed; wave-washed lakeshores, sheltered bays and isolated basins.

Plate II. Grassland

Description

Open dry grasslands with few shrubs in species-rich communities dominated by graminoids and forbs. Grasslands have a restricted distribution within the Park occurring along river valleys and in regenerating post-burn areas (e.g. Rolling River). Common species include plains rough fescue (*Festuca hallii*), kentucky bluegrass (*Poa spp.*), june grass (*Koeleria cristata*), wheat grass (*Agropyron trachycaulum*) and rose (*Rosa spp.*)

Physiognomy

Low graminoid-forb vegetation with few low shrubs. Low 'bunchgrass hummocks' in plains rough fescue prairie. Patches contain mixed species composition, with a relatively even canopy 1 m in height.

Environment

Well to excessively drained sandy outwash material, or coarse glacial till. Grasslands are found along localized ridges in river valleys throughout the Park. In the western region of RMNP grasslands occur on raised deposits of glacial till.

Variants

Three variants are recognized:

(a) Plains Rough Fescue: the main climax grassland in the Park.

(b) Kentucky Bluegrass-Wheatgrass: deteriorated rough fescue grassland resulting from past disturbance (mainly overgrazing by cattle).

(c) Junegrass-Wheatgrass: a drier variant of the Kentucky bluegrass-wheatgrass type.

Plate III. Low Shrub Grassland

Description

Grasslands with a distinctive low shrub component; species-rich communities dominated by graminoids, forbs and low shrubs. In well-drained areas western snowberry (*Symphoricarpos albus*) and/or shrubby cinquefoil (*Potentilla fruticosa*) are the dominant shrub components. Along forest edges and depressions taller stature species such as hawthorn (*Crataegus spp.*) and chokecherry (*Prunus virginiana*) are common. In these moister sites, trembling aspen and/or white spruce may invade.

Physiognomy

Grasslands with moderate or high cover of low (generally < 1 m high) shrubs although patches of hawthorn > 1 m tall are common, resulting in an uneven canopy structure.

Environment

Well-drained sandy outwash material, or coarse-textured glacial till. Most commonly encountered in the western portions of the Park, often adjacent to open grasslands.

Variants

Two variants are recognized:

(a) Grassland/Low Shrubs: grasslands with low to moderate cover of western snowberry and/or shrubby cinquefoil.

(b) Grassland/Low Shrubs/Tall Shrubs: low shrub grasslands with low to moderate cover of taller (> 1 m) shrubs (e.g. hawthorn, willow, chokecherry).

Plate IV. Shrubland

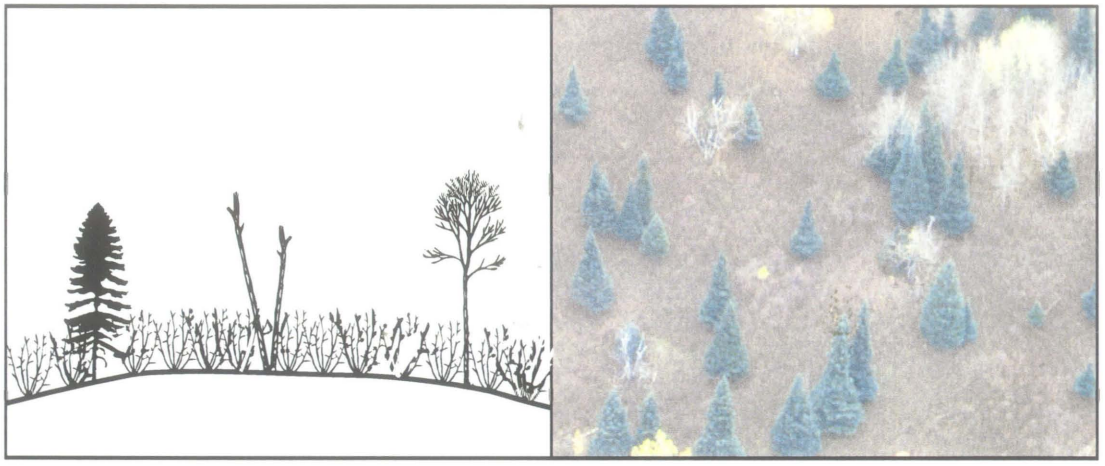

Description

Dense, tall shrublands usually dominated by beaked hazelnut (*Corylus cornuta*) and alder (*Alnus spp.*); in post-fire stands these are also mixed with dense regenerating trembling aspen (e.g. 1980 Rolling River fire). Mature trees occur at low density (e.g. trembling aspen, paper birch, white spruce). Located throughout the Park but most commonly found in the north-eastern and central region in areas that have not burned in over 120 years.

Physiognomy

Tall shrubland (2m in height); relatively uniform canopy but subject to heavy browsing.

Environment

Moderately to well drained till deposits, often in exposed areas (higher elevations) or on steep slopes along the Escarpment.

Variants

Three variants are recognized:

(a) Beaked Hazel Shrubland: generally found in well-drained upland areas. It may be maintained as a 'climax' vegetation type from heavy ungulate browsing and/or environmentally stressful conditions favouring shrubs over trees.

(b) Alder Shrubland: most commonly encountered in regenerating stands (e.g. Rolling River fire).

(c) Trembling Aspen Regeneration: occurs mainly in recently burned areas (e.g., the 1980 Rolling River fire); characterized by dense regeneration of trembling aspen, forming nearly pure stands.

Plate V. Bur Oak Forest

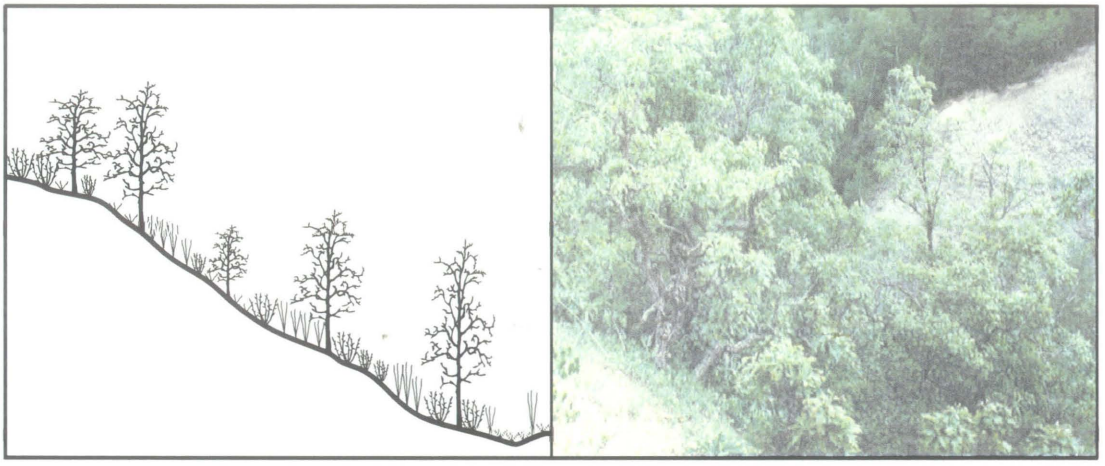

Description

Open to semi-closed 'savanna' forest dominated by bur oak (*Quercus macrocarpa*); minor components may include green ash (*Fraxinus pennsylvanica*), and Manitoba maple (*Acer negundo*) in richer soils. Understory is variable, in excessively drained sites grasses and forbs dominate. In moderate to well-drained areas shrub species such as snowberry (*Symphoricarpos occidentalis*), rose (*Rosa spp.*), beaked hazelnut (*Corylus cornuta*) and hawthorn (*Crataegus spp.*) are common. Poison ivy (*Rhus radicans*) is often a major understory component in oak stands. Oak forests are most often encountered on south facing portions of the Manitoba escarpment.

Physiognomy

Open forest stands, with an understory of low shrubs, graminoids and forbs. Oak regeneration varies from poor to good. Canopy height varies from 8 m on excessively drained sites to 20m on richer soils.

Environment

Well to excessively drained sand, glacial till or alluvium; eastern portions of the Park, along the Escarpment base.

Variants

Three variants are recognized:

(a) Sandy Ancient Beach Ridges: these occur along the Escarpment at the north end of the Park (near Highway 10); dominated by bur oak, green ash, Manitoba maple, and mountain-ash (*Sorbus americana*).

(b) South-Facing Shale Slopes: these steep, excessively-drained slopes occur along the Escarpment; open stands of bur oak, with poison ivy, beaked hazel, and a graminoid-forb understory.

(c) Alluvial Fans: alluvial fans occur in the north-eastern portion of the Park near the Escarpment base (e.g. Agassiz Ski Road, lower Ochre River); extensive semi-closed stands of bur oak, with an understory of low shrubs (e.g. rose, snowberry) and graminoids-forbs.

Plate VI. Low Canopy Deciduous Forest

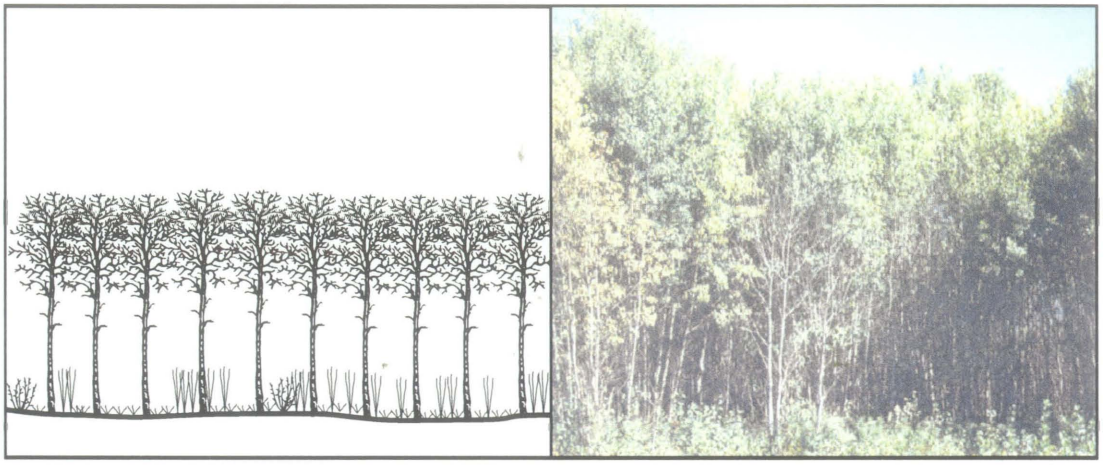

Description

Continuous low canopy (generally 10m high) forest dominated by high density trembling aspen (*Populus tremuloides*); minor components of balsam poplar (*Populus balsaminifera*). Shrubs are infrequent although tall willows with a forb understory. Rich and varied forb and grass dominated understory with few shrubs.

Physiognomy

Continuous low canopy trembling aspen forest; includes younger (< 50 years) post-burn stands (e.g. 1961 Gunn Lake fire area), and rarely stands on well-drained, nutrient-limited substrates in exposed areas.

Environment

Stands generally occur on poorly drained clay deposits which may experience seasonal flooding. Excessively dry sites that promote a similar low canopy physiognomy are a minor environmental variant in this association.

Variants

Four variants are recognized:

(a) Aspen-Forb: found in areas with extensive clay deposits and subject to seasonal flooding. May include small stands of balsam poplar.

(b) Regenerating Trembling Aspen: young, regenerating aspen stands, mainly in the 1961 Gunn Lake fire area; stands are dense and are beginning to undergo self-thinning.

(c) Upland Low Canopy Trembling Aspen: Dense aspen stands with a substantial forb component. Commonly associated with well-drained areas within the aspen parkland.

(d) Willow copse: Extensive patches of tall stature willow (8 to 10 m tall) with a substantial forb component, structurally similar to aspen stands within this class.

Plate VII. Aspen Parkland

Description

Semi-open to open stands of trembling aspen (*Populus tremuloides*) alternating with < 1 ha patches of shrubland and shrub dominated grasslands, forming a complex mosaic pattern at the landscape level. Balsam poplar (*Populus balsaminifera*) stands and small wetlands occur in poorly-drained areas. The aspen dominated 'phases' of Parkland class can differentiated from Low Canopy Deciduous (VI) by the presence of a discontinuous and taller stature canopy as well as increased shrub components. This complex forms the predominant vegetation association within the Park and is especially common in the western region.

Physiognomy

Mosaic of trembling aspen groves (often with a high shrub component), shrublands, shrubby grasslands, and wetlands. Canopy height varies from low stature (1 m) in small grass dominated patches, medium stature (2 m) in shrubby patches to tall (20 m) in aspen dominated canopies.

Environment

Moderately-drained glacial till; gently rolling topography. Extensive areas of parkland in the western portion of RMNP may be the result of a short fire return interval in the late 1800's.

Variants

High local variability; expect to encounter stands of trembling aspen or balsam poplar, meadow marshes, shrublands and shrubby grasslands. This class intergrades with several of the open canopy associations as aspen density declines.

Plate VIII. Eastern Deciduous Forest

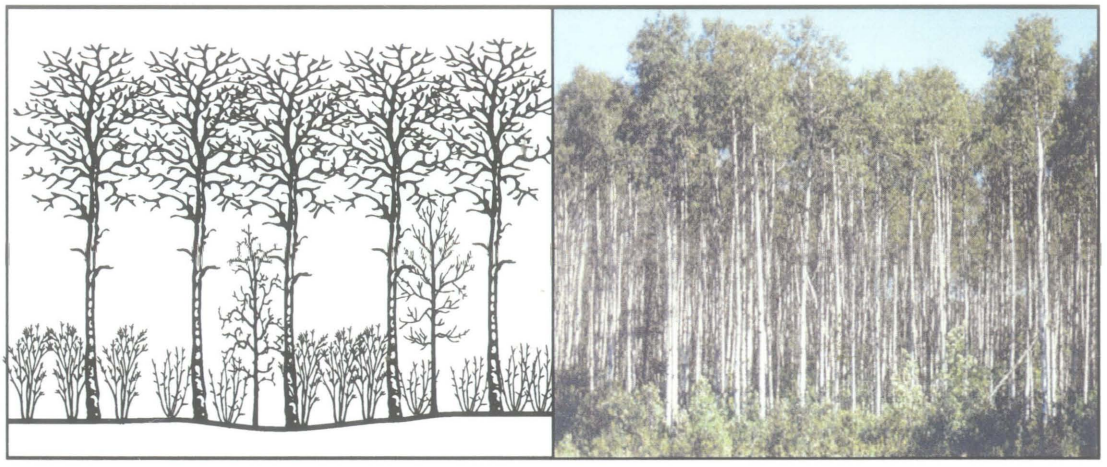

Description

High-canopy deciduous forest (30 m tall) with a tall shrub component and herb-rich understory. Tree species composition includes stands of pure mature trembling aspen (*Populus tremuloides*) on nutrient-rich sites, or mixed eastern deciduous forest containing green ash (*Fraxinus pennsylvanica*), elm (*Ulmus americana*), Manitoba maple (*Acer negundo*), paper birch (*Betula papyrifera*) and cottonwood (*Populus deltoides*). Tall shrubs are common and include mountain maple (*Acer spicatum*), beaked hazelnut (*Corylus cornuta*) and viburnum (*Viburnum spp.*). This association is normally encounter on the lower portions and at the base of the Manitoba Escarpment.

Physiognomy

Trembling aspen stands have a high canopy, and the subcanopy and sapling layers are poorly to moderately well-developed; tall shrubs (mainly beaked hazelnut) may be sparse to relatively common. Mixed hardwood forest stands show moderate to good regeneration in the subcanopy and sapling layers; tall shrubs (beaked hazelnut, mountain maple) are often common.

Environment

Moist, nutrient-rich loamy soils, often with a well-developed organic layer. Generally found at the base and lower slopes of the Escarpment, in the extreme eastern and north-eastern portions of the Park.

Variants

Two variants are recognized:

(a) Mature Trembling Aspen: tall trembling aspen with a herb-rich understory; some stands are being invaded by coniferous trees (white and black spruce), but aspen regeneration is poor. Paper birch may also be present.

(b) Mixed Eastern Deciduous: restricted to the base of the Escarpment, often in river and stream valleys. Rich, mixed-forest stands showing good regeneration. Many species show an eastern floristic affinity, and are at or near their north-west distribution limits in the Park.

Plate IX. Deciduous Canopy - Coniferous Subcanopy Forest

Description

Deciduous-dominated usually trembling aspen (*Populus tremuloides*) forest canopy with a well-developed subcanopy and sapling layer dominated by conifers (usually white or black spruce). Presence of mountain ash (*Sorbus americana*) indicative of old growth stands, is often present. Tall shrubs range from sparse to relatively common in the semi-closed stands. Understory is often herb-rich; feathermosses (*Hylocomnium splendens* and *Pleurozium schreberi*) may be common. These stands are most frequent at higher elevations in the central region and along the Manitoba escarpment.

Physiognomy

Physiognomy is highly variable within this group, ranging from tall trembling aspen stands forming a semi-continuous to gap dominated canopy, with a moderately dense conifer subcanopy to a discontinuous open canopy forested 'shrubland', with a highly variable stature conifer 'subcanopy' of varying density. The physiognomy of this class could be described by analogy as equivalent to'mixedwood' aspen parkland. It is important to note that gap formation is primarily the result of hardwood mortality, in these stands the majority of tallest stature living trees are often 'subcanopy' conifers (i.e. the term subcanopy is relative). Canopy depth ranges from 25 m to 2 m in gap dominated stands.

Environment

Moderately-drained glacial till, often associated with undulating topography; largely restricted to areas of the Park that have not been burned for at least 100 years; common along Highway 10.

Variants

Variation occurs at a small spatial scale; the subcanopy varies from relatively sparse to dense. This association intergrades with class X (Mixed Canopy Deciduous-Coniferous Forest) as canopy closure increases and with class IV (Shrubland) in gap dominated stands. Post-burn shrub and conifer regenerating stands (e.g. Rolling River) form a small component within this association.

Plate X. Mixed Canopy (Deciduous-Coniferous) Forest

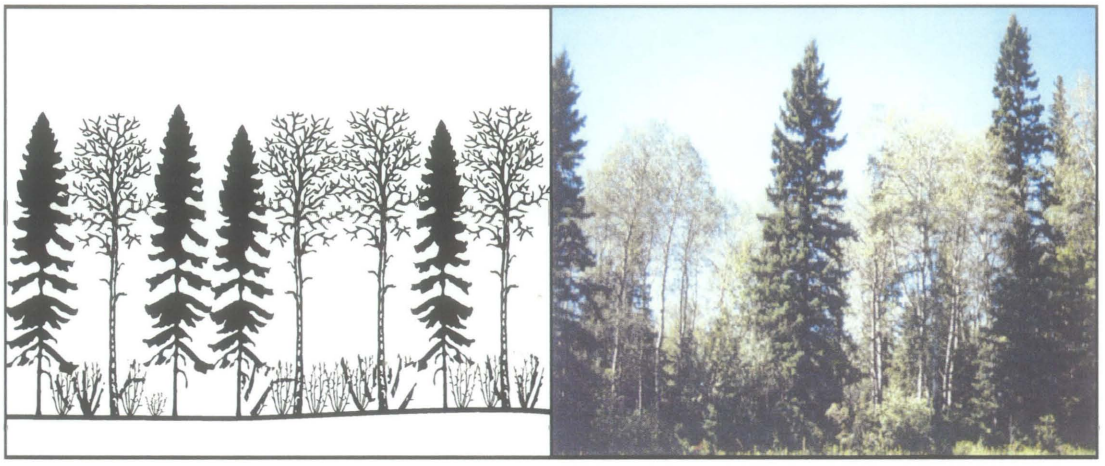

Description

Tall, closed mixed canopy forests, typically with trembling aspen (*Populus tremuloides*) and white spruce (*Picea glauca*) as codominants; black spruce (*Picea mariana*), paper birch (*Betula papyrifera*), balsam poplar (*Populus balsamifera*) and jack pine (*Pinus banksiana*) are occasional. Generally located at higher elevations in the central region of the park, but stands occur throughout.

Physiognomy

Mixed deciduous-coniferous canopy generally closed, sometimes with a subcanopy dominated by conifers. Tall shrubs are sparse to relatively common. Understory is often herb-rich; feathermosses may be common.

Environment

Moderately drained glacial till; often undulating topography. Usually at higher elevations in areas with lower annual temperatures and greater rainfall.

Variants

Variation in this type occurs at a small spatial scale; the forest canopy consists of a patchwork of deciduous and coniferous tree species. This association can be differentiated from Deciduous Canopy - Coniferous Subcanopy Forest (IX) by the high degree of canopy closure and the equal size/stature of the hard and softwood tree species. Post-burn shrub and conifer regenerating stands (e.g. Rolling River) form a small component within this association.

Plate XI. Open Canopy Coniferous Forest

Description

Conifer-dominated stands with < 30% canopy cover; includes semi-treed bogs and fens with black spruce (*Picea mariana*) and/or larch (*Larix laricina*), and sparsely-treed dry uplands with white spruce (*Picea glauca*). Encountered throughout the Park.

Physiognomy

Semi-treed stands, often associated with low shrubs and sedges (bogs, fens) or grassland (dry uplands). Canopy height is variable from 15 m under tree cover to 1 m in open phases.

Environment

Variable; poorly-drained organic substrates (bogs, fens), or well drained sandy outwash material or glacial till (dry uplands).

Variants

Two variants are recognized:

(a) Semi-Treed Bog (Fen): open forest stands dominated by black spruce and/or larch; black spruce often layers in these stands; low ericaceous shrubs are often abundant such as. leatherleaf (*Chamaedaphne calyculata*), bog laurel (*Kalmia polifolia*), bog rosemary (*Andromeda polifolia*); peat moss (*Sphagnum spp.*) and sedges (*Carex spp.*) are common; most common in and south of the Birdtail Valley, in the Gunn Lake area and in the south-east portion of the Park.

(b) Sparsely Treed Upland: open stands of white spruce on grasslands, generally on well-drained, coarse-textured soil (e.g. Deep Lake warden station area). This type might be described as a 'white spruce parkland' associated with sites where white spruce is encroaching on grasslands. Fire suppression might increase the abundance of this cover-type within the Park.

Plate XII. Closed Canopy Coniferous Forest

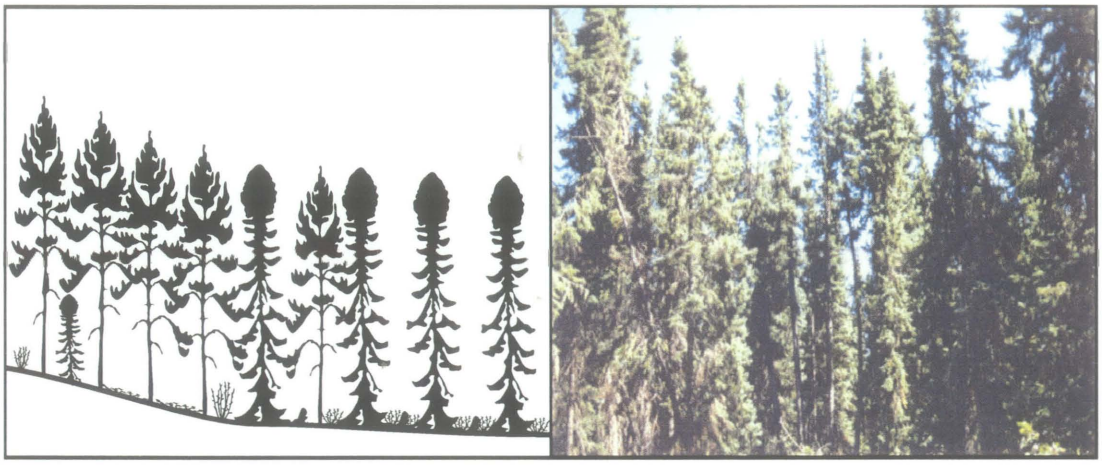

Description

Mature closed stands dominated by coniferous trees; generally pure stands of white spruce (*Picea glauca*), black spruce (*Picea mariana*), balsam fir (*Abies balsamea*) or jack pine (*Pinus banksiana*) mixed with black spruce. Deciduous tree species may form a minor component of the overstory especially in white spruce dominated stands. Understory is generally poorly developed with low shrubs and forbs in drier sites, feathermoss (*Hylocomnium splendens* and *Pleurozium schreberi*) in moist closed forest and sphagnum moss (*Sphagnum spp.*) in poorly drained stands. Conifers are found throughout the Park, however pure stands are generally localized on the landscape.

Physiognomy

Pure stands of moderate to complete canopy closure, or more commonly with a minor component of deciduous trees (especially in white spruce stands) and a forb understory, mosses are common (black spruce stands). Canopy height varies from 25 m in stands on moderately drained soils to 10 m in poorly drained bogs.

Environment

Variable environmental conditions depending on stand-type. Moderately drained glacial till (white spruce, balsam fir, jack pine) or poorly drained organic material (black spruce).

Variants

Four variants are recognized:

(a) Balsam Fir: these stands are restricted to the north-eastern portion of the Park, on north-facing slopes of the Escarpment where cooler, moister conditions prevail.

(b) White Spruce: mature stands of white spruce, mostly in infrequently burned areas east of Strathclair Road; may occur as pure stands, or more commonly with a minor component of deciduous trees.

(c) Black Spruce (Poorly Drained): closed black spruce stands; found mostly in the south-eastern portion of the Park, as well as in the western regions (e.g. upper Birdtail Creek, Gunn Lake area).

(d) Black Spruce - Jack Pine (Well Drained): these stands are restricted to the south-eastern portion of the Park, in the vicinity of the 1980 Rolling River fire. The mature (unburned) stands are dominated by black spruce, or are mixed black spruce - jack pine stands.

Plate XIII. Regenerating Coniferous Forest

Description

Dense, nearly pure to mixed, regenerating coniferous forest stands. In the 1980 Rolling River fire, jack pine (*Pinus banksiana*) or black spruce (*Picea mariana*) dominates most of these stands. Swamp birch (*Betula glandulosa*) is an important shrub component within the association. Regenerating stands of black or white spruce are found locally in other areas of the Park where natural disturbances (e.g. beaver activity) have occurred.

Physiognomy

Dense conifer canopy (generally < 3 m tall), with a sparse shrub and/or herb layer.

Environment

Generally moderately to well-drained glacial till and sandy soils or burned bog and wetlands where post-fire conifer establishment occurred, organic substrates occasional.

Variants

Three variants are recognized:

(a) 1980 Rolling River Fire: upland and some lowland sites with very dense jack pine regeneration; black spruce (occasionally larch) predominate in poorly-drained areas.

(b) Local Disturbances: small regenerating patches of black or white spruce, in recently disturbed sites (e.g. beaver activity).

(c) Swamp birch-conifer: a common component in the above two variants. The unique thick cuticle of this species and its presence in many post-fire regenerating sites used for map classification resulted in a 'sensitivity' to the abundance of this species in mapped polygons.

Chapter 3

Fractal analysis of spatio-temporal dynamics in boreal forest landscapes

Abstract. Remotely sensed data (LANDSAT) were used to investigate landscape-scale spatial and temporal dynamics in the boreal forests of Riding Mountain National Park, Canada. The analysis of temporal dynamics involved comparing the forest structure of regenerating post-fire sites (11 and 30 years old) to late-successional ones (> 95 years old), while the spatial analysis involved comparing sites of differing physiographic complexity (well-drained vs. impeded drainage). To facilitate the analysis, all images were simplified to K = 10 land-cover classes using K-means clustering. Fractal dimensions (computed using the probability-density function) were used to quantify landscape-scale spatial patterning. In addition, randomization tests (observed vs. randomized patterns) were used to compare spatio-temporal trends in landscape pattern. Without exception, observed landscapes were significantly more contagious (clumped) than random (maximally entropic) landscapes. The temporal analysis revealed that landscape-level patch structure becomes increasingly entropic during succession: regenerating (post-burn) sites showed greater spatial contagion than late-successional ones. Also, the equitability of land-cover classes declines as succession proceeds. In the spatial analysis, it was found that simple physiographies (well-drained sites) were characterized by a few dominant, overdispersed land-cover classes; less frequent classes showed high contagion. By contrast, sites of complex physiography (impeded drainage) had greater equitability of land-cover classes, and all classes had similar degrees of contagion. The implications of these findings in understanding ecosystem processes and management practices of boreal forests are briefly discussed.

3.1 Introduction

The boreal forest is subject to repeated large-scale disturbances such as crown fires, which produce vegetation patches of various successional ages on the landscape (Ritchie 1956; Rowe 1956; Dix and Swan 1971; De Grandpré et al. 1993). Natural fire cycles in the boreal forest range from less than 50 years to 200 years or more (Hirsch 1991; Payette 1992). In North America, large catastrophic burns are initially colonized by fire-adapted species such as jack pine and trembling aspen, producing localized uniform monocultures (Carleton and Maycock 1978). As these stands age, smaller-scale disturbances such as lightning ignitions (Granström 1993), windthrows (Dyer and Baird 1997), ungulate herbivory (Pickett et al.

1987), budworm infestations (Holling 1992; Morin 1994; Bergeron et al. 1995) and beaver flooding (Naiman 1988) gradually 'chip away' at the uniform early succession canopy (Frelich and Reich 1995). These smaller-scale gap disturbances are important in determining local successional pathways and biodiversity in boreal forests (Kenkel et al. 1997).

Underlying environmental gradients are also important in determining vegetation pattern, community composition and biodiversity (Watt 1947; Whittaker 1953; Noble and Slatyer 1980). Gradients in soil moisture are spatially complex over a wide range of scales (Smith and Huston 1989). In areas of impeded drainage, water movement and depth to water table are critical determinants of vegetation composition and patch dynamics (Mitsch and Gosselink 1993; Helm and Collins 1997). Intersection of the water table with an undulating topography creates a spatially complex ecotonal landscape (Gosz 1993). Such landscapes are characterized by discrete, oriented patches of vegetation that are sculpted by the movement and impoundment of water (Forman 1995).

Patchiness in boreal landscapes results in the exchange of species, energy and nutrients across ecotones and along interconnecting corridors. Disturbances and strong spatial gradients determine both the creation of new patches and the dynamics of existing patches (Dearden and Rollins 1993). Studies of the relationship between patch size and shape suggest that large contiguous habitat patches have a lower spontaneous extinction rate and are more biologically diverse (Frankel et al. 1995). In addition, biodiversity may decline when habitat patches are fragmented by natural or human disturbances (Dearden and Rollins 1993). Parks and ecological reserves, which are often preserved fragments of a once much larger landscape patch, are often too small to support viable populations of some species (Frankel et al. 1995; Glenn and Nudds 1989). An understanding of the role of natural fragmentation and spatial complexity is therefore critical to developing recommendations and protocols for habitat management at the landscape scale.

Fractal analysis is well-suited to the study of vegetation pattern, since fractals quantify spatial heterogeneity over multiple scales on the landscape (Lavorel et al. 1993; Loehle and Wein 1994: Kenkel and Walker 1996). The term 'fractal' (Mandelbrot 1983) was introduced to characterize scale-invariant phenomena, such as the repeating pattern of a forest canopy (Zeide 1991). Mathematical fractals are 'self-similar' in the sense that the

same basic structure is repeated over all spatial scales. The following power-law relationship holds for natural fractal objects:

$$L_\delta \propto \delta^{(1-D)} \qquad \textbf{[Equation 3.1]}$$

where L is the length of the object at measuring scale δ, and D is the fractal dimension (Mandelbrot 1983).

Fractal analysis of remotely-sensed images has been used to quantify landscape patterns (Lam 1990; De Cola 1989), to characterize the spatial structure in forest stands (Ravan and Roy 1997), and to model forest succession (Hall et al. 1991; Fiorella and Ripple 1993). Of the currently available technologies, LANDSAT is well-suited for terrestrial vegetation studies (Treitz et al. 1992; Wickland 1991), and is particularly useful in investigating landscape-level patterns and processes in boreal forest (Hall et al 1991). The LANDSAT-5 Thematic Mapper samples seven spectral bands at 30 x 30 m ground resolution (Richards 1993). Vegetation produces a distinctive reflectance spectrum that is a complex function of physiognomy, canopy surface complexity and species composition (Markon 1992; Thomson et al. 1985; Rencz 1985; Hall et al. 1991).

Spatial statistics in landscape ecology have been used mainly for descriptive purposes, and most studies have examined the effects of human-induced habitat fragmentation (e.g. Tinker et al 1998; Ravan and Roy 1997; Rignot et al 1997; Tang et al 1997; Miller et al 1996; Baskent and Jordan 1995; Krummel et al. 1987). In many studies, remotely-sensed images are simplified into a series of binary representations prior to analysis (Milne 1992; Loehle and Wein 1994). Wiens (1995) argues that concepts of spatial "complexity" must be modelled in terms of both spatial and temporal processes. He also notes that formal theories of landscape spatial patterning lag far behind their description. A consensus is emerging of a strong relationship between spatial pattern and vegetation dynamics (e.g. Jakubauskas 1997; Milne 1992; Hastings et al 1982; Frelich and Reich 1995), but specific hypotheses regarding spatio-temporal processes are still in the formative stages.

3.2 Objective

The objective of this chapter is to examine temporal changes in spatial dispersion of patches on boreal forest landscapes following fire, and to examine how spatial dispersion is affected by physiographic complexity. The following questions are addressed:

1. Does landscape-level patch dispersion in the boreal forest change following fire?
2. Does landscape physiography influence patch dispersion ?
3. Is patch dispersion on the boreal landscape fractal?

3.3 Study Area – See Chapter 2

3.4 Materials and Methods

Image Preprocessing

All landscape analyses were performed on a LANDSAT-5 image of RMNP acquired on August 3, 1991. This image was selected for its high atmospheric transmittance and minimal cloud cover. The three reflectance bands most useful in distinguishing vegetation in boreal ecosystems (Bolstad and Lillesand 1992) were used: band 3 (red, 0.63-0.69 μm); band 4 (near infrared, 0.76-0.90 μm); and band 5 (mid infrared, 1.55-1.75 μm). Some image preprocessing was performed by Radarsat International (Vancouver), including a standard radiometric correction to eliminate variability in sensor response ('destriping', Richards 1993), and a bit error reduction in the geometric registration of the scene. The final raster product conformed to the NAD27 grid system at a pixel resolution of 30 x 30 m. Each of the three LANDSAT bands were centred at 5631.3 km N by 403.4 km E. Prior to classifying the image, a dark order subtraction was used to correct for residual atmospheric effects (Chavez 1988). Band reflectance histograms from the image indicated that a path irradiance model of λ^{-4} (corresponding to a clear atmosphere dominated by Rayleigh scattering, Richards 1993) was appropriate. Additional subtraction constants were then determined from standard path radiance tables (Chavez 1988).

Site Selection

i) Temporal Analysis: Regenerating vs. Mature Sites.

Three square sites, 100 x 100 pixels (3 x 3 km) in size, were selected from each of two burned areas: (a) 1980 Rolling River fire, 11 years old; (b) 1961 Gunn Lake fire, 30 years old. Each burn site was paired ('matched') to a mature (> 95 year old) site (**Figure 3.1a, Table 3.1a**). The 'match' sites were carefully selected using several criteria: (a) spatial adjacency to burned sites; (b) matching topography and elevation; (c) matching soil texture and drainage patterns (data from Canada 1979). Careful matching ensured minimal confounding between inherent spatial variation and temporal variation in landscape patterns (i.e. changes related to stand age). All sites occurred on the Saskatchewan Plain.

ii) Spatial Analysis: Simple vs. Complex Physiographic Gradients.

Six square sites, 100 x 100 pixels (3 x 3 km) in size, were selected from areas characterized by spatially complex physiographic gradients. Each of these 'complex' sites was paired ('matched') to a site having a spatially 'simple' physiographic gradient (**Figure 3.1b, Table 3.1b**). Spatially 'complex' sites exhibited a ridge-swale topography and a stationary elevational profile indicative of restricted drainage, and had soils associated with a high water table (Canada 1979). Conversely, spatially 'simple' sites did not exhibit a ridge-swale topography, had a non-stationary (directional, sloping) elevation profile, and occurred on well-drained soils (Canada 1979). All selected sites had < 5% open water, to ensure that only terrestrial vegetation patterns were being compared. As in the temporal analysis, all sites occurred on the Saskatchewan Plain.

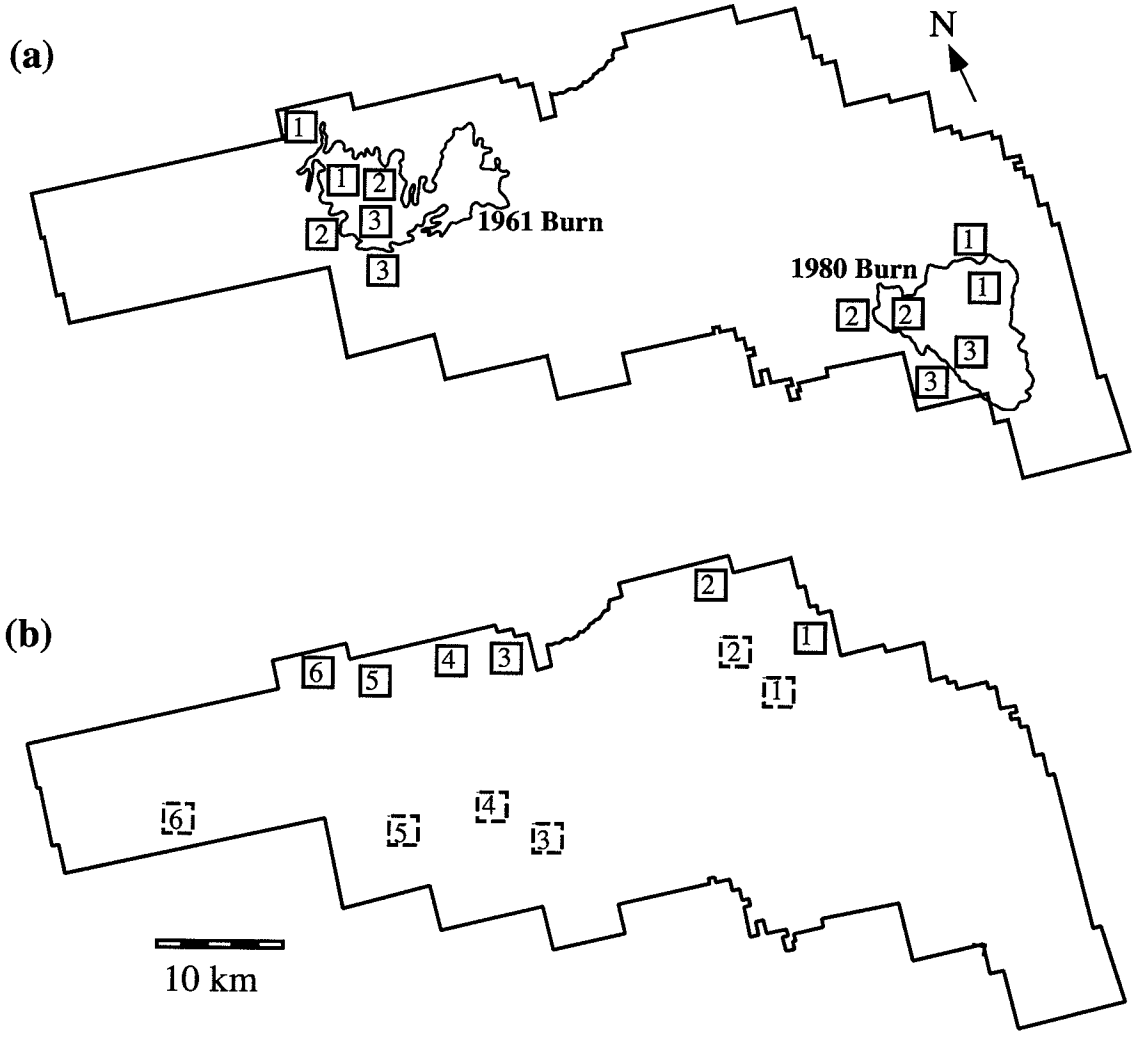

Figure 3.1: Locations of the 24 sample sites in Riding Mountain National Park: (a) 1961 and 1980 burn sites and their matches; (b) 'complex' physiography sites (dashed lines) and matched 'simple' physiography sites (solid lines).

Image Reduction

Because the landscape spatial analysis used in this study requires binary data, a simplification of the three-band LANDSAT scenes (24 bit pixels) was required. An unsupervised classification (Richards 1993) was used to reduce each three-band scene into a simplified image. Unsupervised classification is a 'neutral' data reduction strategy, since no prior assumptions are made regarding the floristic composition of pixels; instead, the classification group structure is based purely on spectral information (Richards 1993). The classification method used was non-hierarchical K-means clustering, in which an iterative algorithm is used to determine an optimal partitioning of variable space into K non-overlapping groups (Lillesand and Kiefer 1994). In this study, K = 10 'land-cover' classes were determined for each image; preliminary analyses indicated that ten groups produced an optimal image reduction for fractal analysis.

To ensure that each landscape comparison was treated identically during the image reduction (classification) phase, each site was paired with its match to create a single image (100 x 200 pixels in size). Unsupervised classifications were performed on these 'paired' images. There were a total of six paired images for the temporal analysis (3 in the 1980 burn, 3 in the 1961 burn), and six paired images for the spatial analysis (**Fig. 2**).

Data Analysis

i) Probability-Density Function

Although probabilty-density was originally developed for point processes (Voss 1988), it can be used to estimate the fractal dimension of a binary (black/white) pixel image (e.g. Milne 1991). This method has advantages over the area-perimeter fractal method (Hastings and Sugihara 1993) in that discrete habitat 'islands' are not required. The probability-density function is obtained by successively centering a square (L x L) sampling 'window' on each occupied (black) pixel of the binary image. The number of occupied pixels (n) is counted in

each sampling window. The frequencies of these counts are then expressed as probabilities:

$$\sum_{n=1}^{N(L)} \rho_L = 1 \qquad \textbf{[Equation 3.2]}$$

where $N(L) \leq L^2$. For a given value of L, the first moment of the probability distribution is:

$$M(L) = \sum_{n=1}^{N(L)} n\rho_L \qquad \textbf{[Equation 3.3]}$$

These computations are repeated for various values of L (L must be an odd number, since windows are centred on occupied pixels). Fractal images follow a power law relationship (Voss 1988: 66):

$$M(L) \propto L^D \qquad \textbf{[Equation 3.4]}$$

The fractal dimension D is thus determined as the log-log slope of the first moment M(L) as a function of L (Milne 1992: 47). Using this method, the fractal dimension has a theoretical range from 1 (minimal dispersion, maximal contagion) to 2 (maximal dispersion or entropy). In practice, the upper limit of D for random landscapes is a function of the frequency of occupied pixels, with the result that dominance and contagion are potentially confounded (cf. Milne 1988; Hargis et al. 1998). To overcome this problem, a randomization technique (Manly 1991) was used to establish a statistical 'baseline' for determining deviations of the observed probability density D-values from random. For each site (binary image), occupied pixels were spatially randomized (maintaining the same pixel frequency on the landscape) and the probability density D recomputed. This step was repeated 19 times per site, to generate expected D-values for spatially random (maximally entropic) landscapes.

For each of the 24 sites (**Figure 3.1**), probability density function D-values were determined separately for the four most frequent 'landscape classes' (96 analyses in total). For each of these 96 analyses, the probability density function was also determined for each of the 19 randomizations of the landscape (1824 randomizations in total). In all analyses, L ranged from 3 to 25 in steps of two (12 values in total). All log-log plots were linear (r^2 = 0.996 to 0.999, $p < 0.001$), indicating that the landscapes were statistically self-similar.

ii) Evenness

Changes in the relative frequency of the K = 10 land-cover classes was also determined for the spatial and temporal analyses. The Shannon-Weaver diversity index:

$$H = -\sum_{i=1}^{K} p_i \ln p_i \qquad \textbf{[Equation 3.5]}$$

measures the entropy of land-cover classes. The maximum value of H = ln K, which occurs when all land-cover classes are equally frequent ($f_1 = f_2 = ... = f_{10} = 0.1$). Hill (1973) suggested a measure of 'effective' richness, $N = e^H$, that has an upper limit of K. Evenness is simply a relativized measure of class equitability (upper limit = 1), computed as:

$$E = N/K \qquad \textbf{[Equation 3.6]}$$

The frequency of pixels in each land-cover class from the unsupervised classifications was used in the evenness calculations.

3.5 Results

Observed vs. Random Landscapes

Fractal dimension (D) values of the four most frequent land-cover classes in each of the 24 sites are summarized in **Figure 3.2**. Without exception, the observed landscapes had significantly greater spatially contagion (lower fractal dimension) than random landscapes of the same frequency. A nonlinear relationship exists between relative frequency and D for random landscapes: for frequencies > 40% the expected D = 2, but for frequencies of 25% this declines to D = 1.9. D-values drop precipitously for frequencies < 10%.

Two observed landscapes, and corresponding random landscapes of the same relative frequency, are illustrated in **Figure 3.3**. These examples are taken from the spatial analysis (i.e. comparison of simple vs. complex physiographic landscapes) discussed below. Note that the observed landscapes are considerably less spatially entropic (i.e. have greater spatial contagion) than their corresponding random landscapes.

Temporal Analysis

Comparisons of the 11 year old burns and their matched sites (> 95 years old) are summarized in **Figure 3.4a**. D-values for the burn sites were generally lower than those of the matches sites, and showed greater deviation from the randomly generated landscapes (**Figure 3.5a**). Similar results were obtained in the comparison of 30 year old burns and their matched sites, although trends were somewhat less clear (**Figure 3.4b**). Compared to early-successional (11 year old) sites, mid-successional (30 years old) sites are spatially more similar to late-successional sites (**Figure 3.5b**). Together, these results indicate that landscape-level patch structure in boreal forest becomes increasingly spatially entropic during succession: early successional (post-burn) sites are under-dispersed (i.e. greater spatial contagion) compared to late-successional ones.

Landscape evenness (unsupervised classifications, K = 10 land-cover classes) declined during succession, from 0.75 in early-succession (11 and 30 years old) to 0.63 for late-succession (> 95 year old) sites (**Table 3.1**). Land-cover class evenness was significantly greater in the 11 year old sites compared to late-succession matched sites (paired t-test, $t = 5.02$, $p = 0.038$). Similar results were obtained for the mid-succession (30 year old) sites ($t = 3.95$, $p = 0.059$). These results indicate that land-cover classes are more equitable in early-successional sites, but as succession proceeds sites become increasingly dominated by a few land-cover classes.

Spatial Analysis

The six physiographically 'simple' sites are located near the northern boundary of RMNP (**Figure 3.1**) on gentle north-facing slopes (mean slope = 2.17°). By contrast, the six physiographically 'complex' sites are located on gently rolling terrain (mean slope = 0.43°, **Table 3.1**). Topographical contour maps for representative 'simple' and 'complex' physiographic landscapes are illustrated in **Figure 3.3**. The simple physiographic landscape displays a strongly directional (south to north) drainage pattern, whereas more circuitous drainage patterns characterize the complex landscape.

For complex sites, approximately 75% of the total landscape cover was accounted for by the first four classes, while over 90% was accounted for in physiographically simple sites

(**Table 3.1**). For the two most frequent land-cover classes I and II, fractal dimensions (D) for simple sites were greater than those of complex sites. However, the reverse was generally true for the less frequent land-cover classes III and IV (**Figure 3.6**). Similarly, classes I and II of the simple sites deviated less from random landscapes, but classes III and IV showed a greater deviation (**Figure 3.7**). Landscape evenness was significantly lower in simple sites (0.36 vs. 0.76 for complex sites; $t = 11.03$, $p < 0.001$). These results indicate that simple physiographies are characterized by a few dominant, overdispersed land-cover classes, with the less frequent classes being highly under-dispersed (i.e. high contagion) on the landscape. By contrast, complex physiographies show greater equitability of land-cover classes, and classes have similar degrees of dispersion (deviation from random landscapes) irrespective of their absolute frequency (**Figure 3.7**).

Table 3.1: Summary of the physiographic variables and land-cover classes for the 24 study sites shown in Fig. 2. a) landscapes of different ages; b) landscapes with different physiographic complexity.

(a)

	Elevation (m)			Slope*	Class Frequency				Hill's
	Mean	Min	Max	(degrees)	I	II	III	IV	Evenness
11 Year									
1	720	685	749	.68	.248	.194	.141	.129	.71
2	657	646	678	.26	.257	.239	.103	.095	.76
3	666	644	686	.44	.287	.177	.132	.104	.76
>95 Year									
1	682	604	736	.85	.283	.245	.187	.144	.58
2	677	644	704	.63	.275	.262	.161	.105	.64
3	666	640	680	.26	.382	.277	.134	.061	.53
30 Year									
1	572	540	589	.44	.226	.190	.179	.125	.74
2	585	564	604	.44	.246	.209	.147	.141	.72
3	595	580	613	.26	.195	.171	.154	.142	.81
>95 Year									
1	564	526	581	.57	.294	.292	.140	.073	.62
2	598	548	615	.44	.337	.164	.162	.107	.68
3	614	581	634	.36	.263	.240	.112	.110	.72

(b)

	Elevation (m)			Slope*	Class Frequency				Hill's
	Mean	Min	Max	(degrees)	I	II	III	IV	Evenness
Complex									
1	684	643	722	.89	.187	.182	.146	.131	.77
2	698	663	734	.57	.237	.202	.194	.138	.71
3	600	592	617	.13	.213	.197	.136	.131	.83
4	604	592	615	.26	.183	.172	.140	.109	.74
5	622	593	638	.36	.248	.172	.169	.142	.82
6	626	598	664	.51	.270	.241	.122	.114	.69
Simple									
1	526	410	675	3.30	.407	.258	.170	.092	.46
2	496	363	669	4.22	.474	.392	.054	.033	.33
3	502	445	566	1.36	.492	.419	.035	.030	.30
4	535	472	589	1.78	.561	.365	.037	.017	.27
5	527	475	584	1.28	.434	.301	.086	.082	.43
6	539	496	575	1.06	.403	.327	.190	.052	.38

* Slope determined from plane of best fit using digital elevation data.

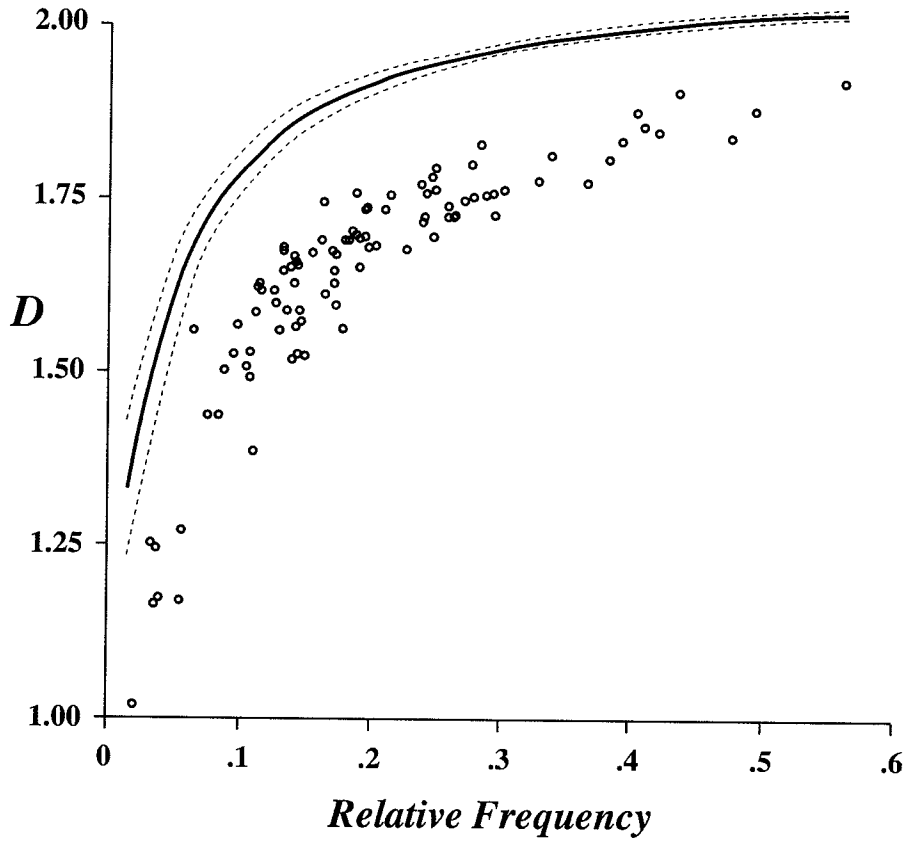

Figure 3.2: Probability density fractal dimension (D) as a function of relative class frequency. The confidence envelope for simulated random landscapes is shown (solid line = mean, dashed lines = upper and lower limits). Open circles are values from the 96 land-cover and site combinations used in this study (refer to text for details).

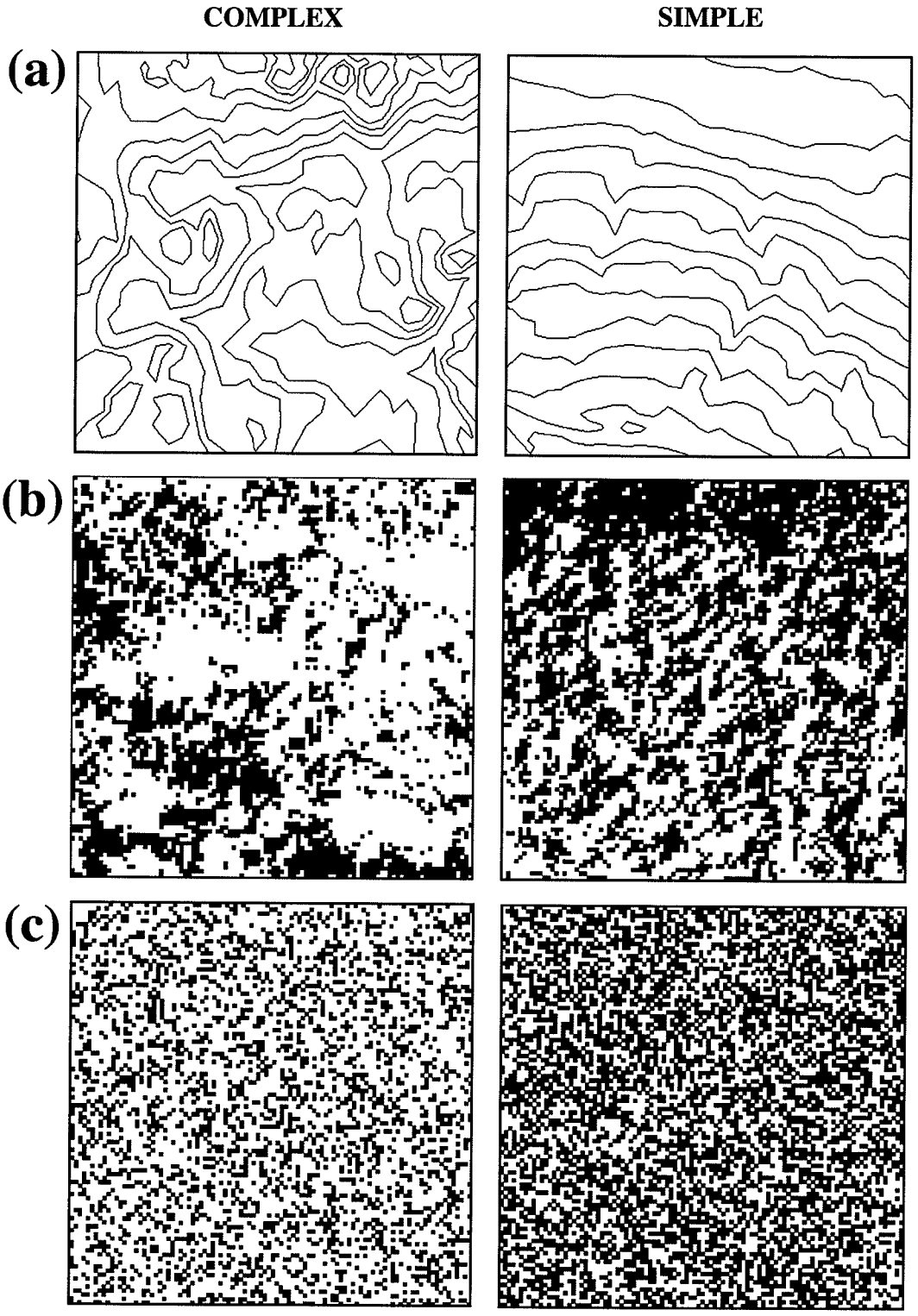

Figure 3.3: Examples of sites used in comparing complex and simple physiographies: (a) elevation contours; (b) patterns of the most frequent land-cover class: complex f = 0.3, D = 1.75, and simple f = 0.5, D = 1.83; (c) simulated random landscapes: f = 0.3, D = 1.89, and f = 0.5, D = 1.95.

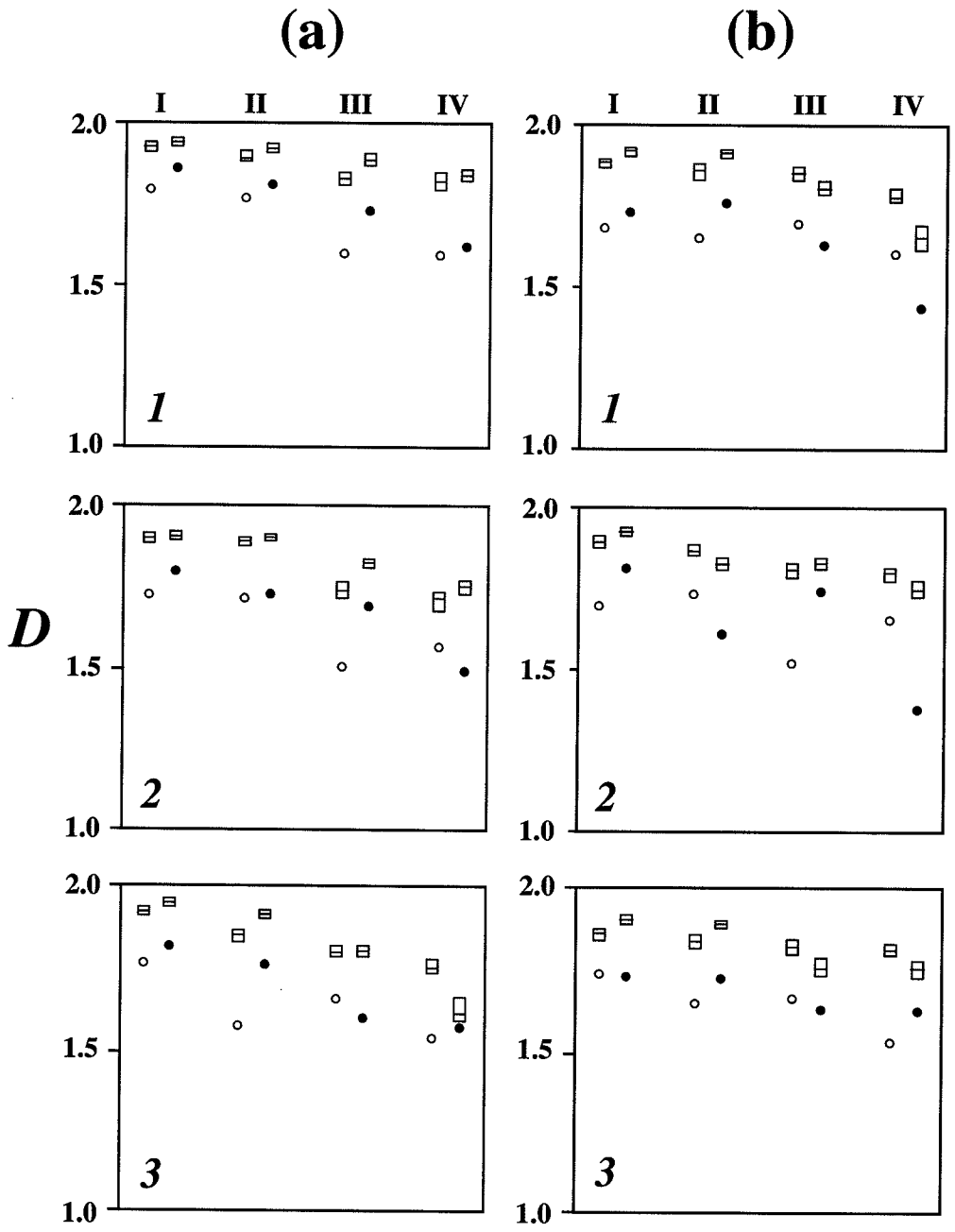

Figure 3.4: Temporal analysis for 11, 30 and 120 yr post-burn landscapes: observed probability-density function D-values (circles) and random expectation (boxes, showing mean and range) for the four most frequent land-cover classes I - IV: (a) 11-year old sites (open circles) and matched 120 year old mature sites (filled circles); (b) three 30-year old sites (open circles) and matched mature sites (filled circles).

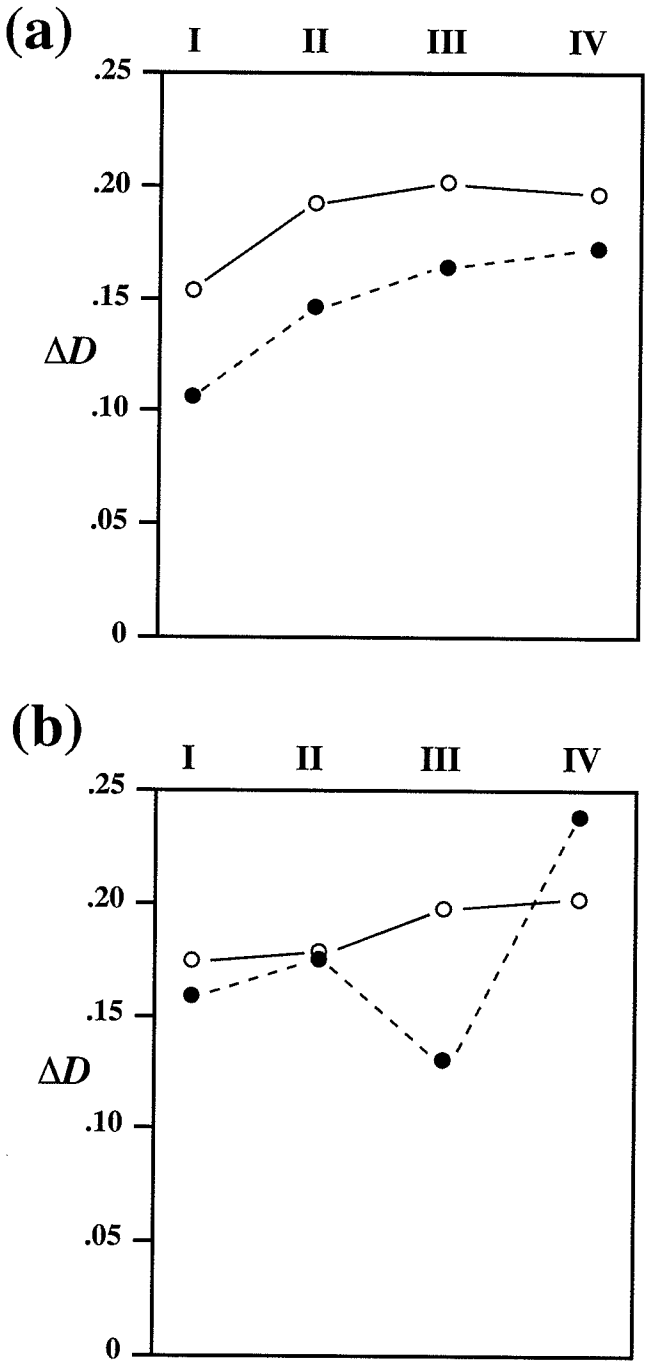

Figure 3.5: Temporal analysis, mean deviations of observed probability-density function D-values from random. (a) 11-year old sites (open circles) and matched mature sites (filled circles); (b) 30-year old sites (open circles) and matched mature sites (filled circles).

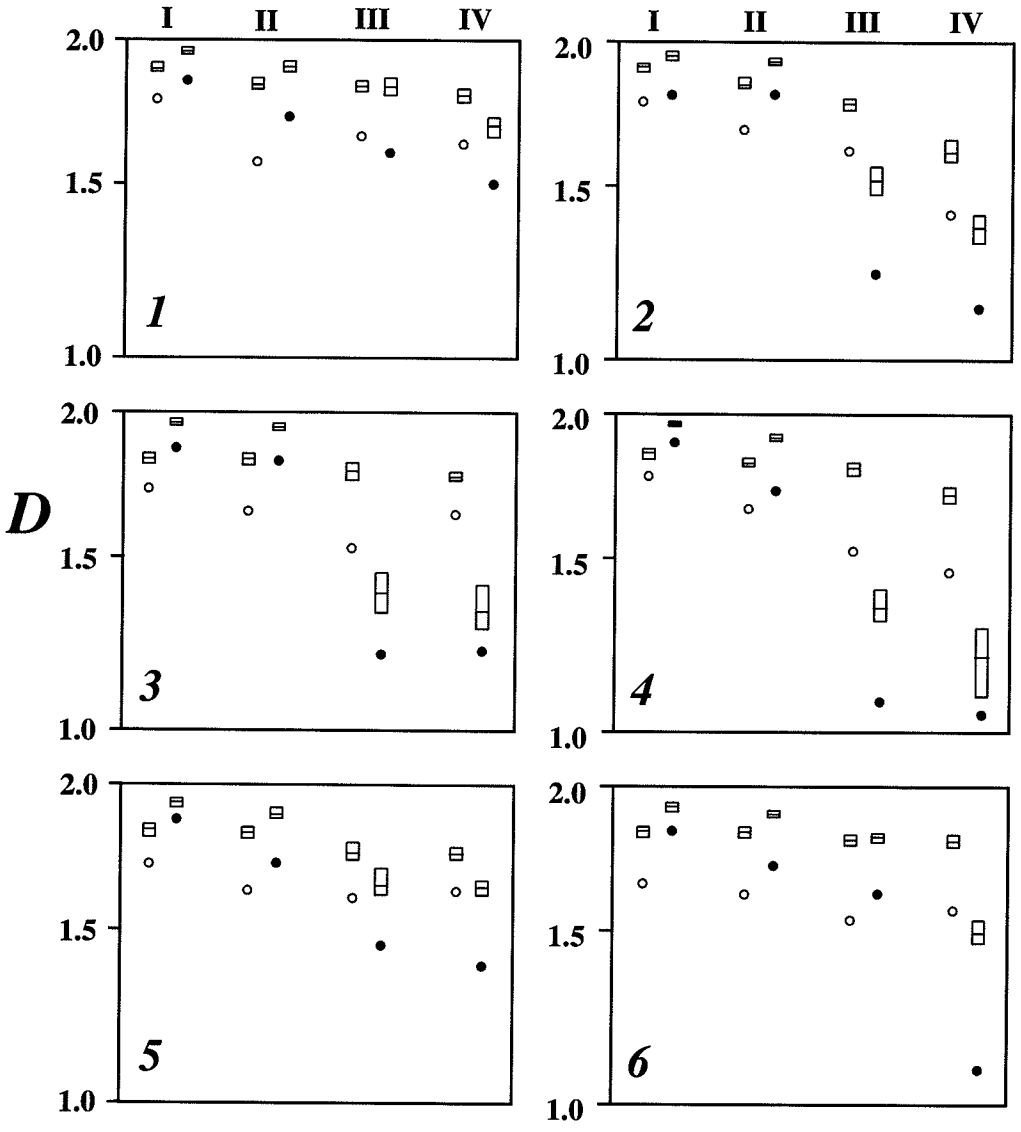

Figure 3.6: Spatial analysis: observed probability-density function D-values (circles) for simple (solid circles) and complex landscapes (open circles). Random expectation is indicated (boxes, showing mean and range) for the four most frequent land-cover classes (I - IV) in each of six sites.

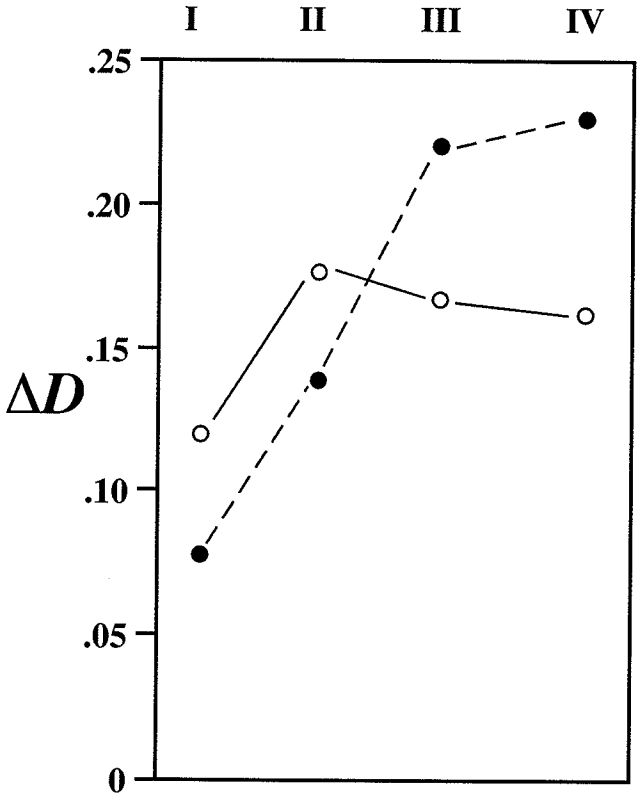

Figure 3.7: Spatial analysis, mean deviations of observed probability-density function from random for simple (solid circles) and complex landscapes (filled circles).

3.6 Discussion

The influential theory of vegetation dynamics proposed by Clements (1936) states that self-replacing 'climax' communities are characteristic of specific climatic zones. However, in disturbance-driven ecosystems such as the boreal forest (where catastrophic fire cycles are often < 100 yrs), the development of a Clementsian climax is not expected (Pickett et al. 1987; Horn 1976; Rowe 1961). These results demonstrate that late-successional stands, as well as physiographically simple landscapes, are spatially dominated by one or two land-cover classes. This should not be interpreted as a validation of Clements' climax model, since few boreal trees are able to regenerate beneath their own canopy as required of a Clementsian 'climax' species (Dix and Swan 1971). The dominance of trembling aspen in RMNP is attributable to the cumulative effects of past disturbances, the ability of the species to root sucker, and its persistence in the canopy of post-fire stands for 100 years or more (Heinselman 1973; Kneeshaw and Bergeron 1996). Rare land-cover classes in late-successional stands may be attributable to gap dynamic processes. Kneeshaw and Bergeron (1998) found that canopy gaps increase from 7% in early succession stands to 40% in old-growth (> 200 year old) boreal forests. Colonization of canopy gaps may reflect a lottery model, in which the first species to establish in a gap usurps the space to the exclusion of other species (Hurtt and Pacala 1995).

Temporal Dynamics

These results indicate that early successional sites are under-dispersed (greater contagion) relative to late-successional ones (cf. Frelich and Reich 1995), and that sites becomes increasingly dominated by a few land-cover classes as succession proceeds (cf. Tinker et al. 1998; Ravan and Roy 1997). These findings are consistent with a three-phase dynamic model of landscape-level structural succession:

1. Colonization Phase

Following a catastrophic fire, boreal forest sites are rapidly recolonized by invasive, opportunistic species (Shafi and Yarranton 1973). High diversity of land-cover classes in early succession is attributable to the combined effects of differential propagule availability (cf. Egler 1954), variation in fire severity, and environmental heterogeneity. In recently

disturbed habitats, limited propagule dispersal and differences in the colonization strategies of species result in complex patterns of establishment that promote high contagion of vegetation classes (Holt et al. 1995). In addition, pyric ecosystems are characterized by complex patterns of fire intensity that reflect physiographic variation on the landscape (Turner and Romme 1994; Kushla and Ripple 1997). Considerable variation in fire intensity was also noted in the study sites, from severe fires on well-drained uplands to much lighter fires in moist depressions. Together, these factors result in a floristic landscape that is characterized by discrete, early-successional vegetation patches of simple horizontal and vertical structure. No single land-cover class predominates at this stage of vegetation development.

2. Competition Phase

As succession proceeds, the increasing girth and stature of colonizing tree species has two important consequences at the landscape scale: (a) the development of a more variable and structurally heterogeneous vertical physiognomy; (b) the development of closed-canopy forest stands, leading to greater resource competition and the local extripation of opportunistic species assemblages. During the competition phase, species are 'sorted' along important environmental gradients (Czaran 1989), with some species assemblages being restricted to localized landscape patches where specific environmental conditions prevail (e.g. small wetlands in an upland landscape). Land-cover class evenness declines as fast-growing pioneer trees consolidate their dominance of the landscape (cf. Carleton and Maycock 1978). During this phase, the landscape consists of a matrix of one or two dominant land-cover classes, interspersed with localized environmentally distinct patches (e.g. wetlands), remnant unburned patches (De Grandpré et al 1993), and patches into which pioneer trees have not yet dispersed. As a result, the predominant land-cover classes become increasingly over-dispersed (more spatially entropic) on the landscape.

3. Gap Dynamic Phase

Once the pioneer trees have consolidated their dominance on the landscape, subsequent colonization is largely restricted to canopy gaps created by various small-scale disturbances (Galipeau et al. 1997). Restrictions imposed by dispersal mechanisms will limit the ability of late-successional species (e.g. white spruce, balsam fir) to dominate late-successional

stands. Small-scale canopy gaps gradually break up the contiguous forest canopy (cf. Frelich and Reich 1995), creating a distinctive 'peppering' effect in the predominant land-cover classes. These result in a further increase in spatial entropy at the landscape scale (Baker 1992a).

Spatial Dynamics

These results reveal that physiographically 'complex' sites have a greater equitability of land-cover classes than 'simple' ones. In addition, land-cover classes in 'complex' sites have similar degrees of dispersion on the landscape, whereas 'simple' sites are characterized by over-dispersed dominant land-cover classes and under-dispersed (strong contagion) subordinate classes. In 'complex' sites, dominance of a single land-cover class is precluded by the physiological constraints imposed on the system by strong environmental gradients (Host et al. 1987). Environmental heterogeneity, particularly variations in watertable depth in poorly drained landscapes, produces complex scale-dependent patterns of vegetation composition and physiognomy (Palmer and Dixon 1990; Sjörs 1980). As a result, high evenness of land-cover classes is expected in sites where strong and spatially complex environmental gradients prevail. In addition, the most common land-cover classes in 'complex' sites are more contagious than those in 'simple' sites (**Figure 3.6 and 3.7**); strong environmental gradients result in a highly 'ecotonal' landscape (Forman 1995).

The persistence of long-lived species, which it is argued, results in land-cover class dominance in physiognomically 'simple' sites, also enhances evenness and contagion in 'complex' sites. Mechanisms promoting spatial patchiness in physiographically 'complex' sites include: (a) interspecific competition: species become distributed along one or more environmental gradients in accordance to their adaptive physiologies (cf. Czaran 1989); (b) patch isolation: land-cover classes below a critical proportion on the landscape (the percolation threshold, $\approx$ 0.59) become disconnected, greatly diminishing propagule immigration (Lavorel et al. 1993; With and Crist 1995); (c) patch size: species richness may decline by up to 50% for each 10% reduction in optimal habitat (Hansson 1992; May 1975). Together, these mechanisms enhance the influence of long-lived species on the 'local' character of 'complex' landscapes.

To summarize, in complex physiographies (i.e. strong environmental gradients present) the physiological requirements of species assemblages closely match the spatial complexity of the environment, thus maintaining high biodiversity on the landscape (i.e. high evenness of land-cover classes) and a high degree of contagion or patchiness. By contrast, 'simple' physiographies become increasingly dominated by a few land-cover classes, with subordinate classes persisting only as small, highly contagious patches where suitable environmental conditions prevail (e.g. wetlands, areas of excessive drainage). During late succession, gap dynamic processes will "chip away" at the dominant land-cover classes (cf. Frelich and Reich 1995), producing a 'peppering' effect (increased spatial entropy) in simple physiographic landscapes.

It is hypothesized that early-successional and 'complex' physiographic landscapes are entropic *between* contagious patches, whereas late successional and 'simple' landscapes are characterized by high levels of entropy *within* patches (**Figure 3.3b**). During succession, there is a 'paradigm shift' from discrete, contagious patches toward 'peppered', highly entropic landscapes (Frelich and Reich 1995; Kenkel et al. 1997). As an analogy, consider changes in the entropy of a gaseous system. Initially, two gases are separated by a simple divider; this is analogous to a landscape in which propagule availability and dispersal are limited. When the divider is removed, the gases are free to disperse and eventually becoming completely intermixed. Analogously, forest stands becomes both a source and sink for dispersing propagules once reproductive age is achieved. Stochastic small-scale disturbances create gaps that are available for colonization, eventually creating a uniformly heterogeneous landscape (i.e. high within-patch entropy). This analogy can of course only be taken so far: the mixing of gases is completely stochastic, whereas in natural landscapes competition, physiological constraints and spatially-varying environmental conditions will maintain some degree of 'order' on the landscape (**Figure 3.3**). For example, strong environmental gradients will prevent the complete mixing of land-cover classes. Thus maximal landscape-scale between patch entropy is expected in early-successional stands on complex physiographic sites, whereas late succession stands on simple physiographic landscapes are expected to have the highest within patch entropy.

3.7 Conclusions

A boreal landscape is a complex mosaic of habitat patches, the spatial juxtaposition of which affects various ecological processes. The movements of species, energy and material between these patches are critical determinants of ecosystem function (Wiens et al. 1985). The population dynamics of both plant and animal species are affected by landscape complexity, since organisms perceive their environment at various spatial scales (Pulliam et al. 1992). These results indicate that natural landscapes are structurally complex, and that landscape patterning is highly dynamic in space and time. Management of natural habitats must therefore consider more than biodiversity; maintaining variation in landscape structural complexity is also of critical importance.

Chapter 4

Landscape complexity in space and time

Abstract. Landscape complexity in the boreal forest is a function of physiographic complexity (spatial processes) and post-fire successional (temporal) processes operating across scales. In this study, the role of succession and topographic complexity in determining the landscape pattern complexity of Riding Mountain National Park, Manitoba, Canada is examined. Landscape pattern complexity was assessed by using multifractal analysis to quantify landscape patterns from Landsat TM imagery. To determine whether complexity changes with age, "young" sites (post-fire stand ages = 11 and 30 years) were matched with adjacent "old" sites (post-fire stand ages > 95 years). The influence of physiography on landscape pattern complexity was examined by comparing sites having "simple" and "complex" physiographies (as determined by fractal surface analysis). The scaling properties of landscape complexity were determined by calculating the multifractal spectrum (D_q) for each site. Landscape complexity increases during early succession; multifractal profiles of 11 year old sites are lower than those of adjacent older stands. However, the multifractal profiles of 30 year old and adjacent older stands are indistinguishable, suggesting that change in landscape complexity occurs within 30 years following fire. Physiographically "complex" sites had consistently greater landscape complexity than adjacent "simple" sites. It is concluded that landscape complexity increases over time as successional proceeds, and in space along a gradient from "simple" to "complex" physiographies. It follows that landscape complexity is lowest in early-successional, physiographically "simple" sites and highest in late-successional, physiographically "complex" sites.

4.1 Introduction

Landscape pattern complexity of forested ecosystems is a function of both successional processes (post-disturbance colonization, and subsequent canopy development) and structural aspects of the underlying physiography (Frelich et al. 1998; Gosz 1993; Bonan and Shugart 1989). Catastrophic wildfire is the predominant large-scale disturbance in boreal forest ecosystems, with fire cycles ranging from less than 50 years to over 200 years (Hirsch 1991; Payette 1992). Post-fire colonization occurs as large, relatively uniform patches dominated by early-successional species

such as jack pine (*Pinus banksiana*) and trembling aspen (*Populus tremuloides*). These species are well adapted to regeneration following fire and form extensive, dense, uniform post-fire stands. As succession proceeds, various processes, including differential tree growth and the superimposition of smaller-scale stochastic disturbances, modify the canopy structural properties of these early-successional stands. Small-scale disturbances in boreal forest ecosystems include individual tree mortality resulting from lightning strikes (Granström 1993) and windthrow (Dyer and Baird 1997), spruce budworm infestations (Holling 1992), and beaver flooding (Naiman 1988). The cumulative effect of small-scale disturbances is to " chip away" at what was initially a relatively uniform canopy structure. The " gaps" created by these stochastic disturbances produce a forested landscape characterized by fine-scale patchiness. The creation of forest gaps also drives late-successional processes, favouring advanced regeneration of more shade-tolerant species and thus altering stand composition and structure (Frelich and Reich 1995; Kneeshaw and Bergeron 1998).

Physiography, which incorporates surficial topography and drainage, is also an important determinant of landscape complexity (Foster and King 1986). Gradients in soil moisture strongly influence species distributions (Bonan and Shugart 1989; Naiman et al. 1993; Helm and Collins 1997; Frelich et al. 1998), and in doing so affect the size, structure and diversity of forest patches (Foster and King 1986; Host et al. 1987). The interaction between vegetation and physiography produces complex, interdigitated and ecotonal landscape patterns that reflect underlying environmental trends (Gosz 1993).

The combined influence of post-disturbance dynamics (a temporal process) and physiography (a spatial process) on the landscape pattern complexity of forested ecosystems has received surprisingly little attention (but see Foster and King 1986; Frelich and Reich 1999). Studying the effect of spatio-temporal processes on landscape complexity requires examination of spatially-explicit data across many scales. Unfortunately, such data are very difficult to obtain using traditional ground-survey methods (Rey-Benayas and Pope 1995). Remote sensing is therefore the preferred technology for quantifying landscape complexity. Complexity of a remotely sensed image is normally assessed by examining the spatial patterns of spectral reflectance (De Cola 1994; Jakubauskas 1997). Pattern-based methods use the interdigitation and

juxtaposition of landscape elements (e.g. pixels or patches) to measure landscape complexity (Rey-Benayas and Pope 1995). In remotely-sensed images of forest landscapes, variations in canopy composition and structure produce complex patterns of pixel spectral reflectances that define the landscape "texture" (Colwell 1974; Ravan and Roy 1997). Jasubauskas (1997) used this approach to examine changes in landscape pattern across a successional sere, based on Landsat imagery. The changes observed were consistent with known successional trends at the stand level, suggesting a commonality across scales.

Although the influence of temporal (successional) and spatial (physiographic) processes on forest canopy structure has been examined at both stand and landscape scales, there is a lack of integration across scales. Fractal theory (Mandelbrot 1983) provides a scale-invariant approach to measuring landscape complexity. In "classic" fractal systems, pattern complexity is characterized as a single scaling exponent, the fractal dimension (D). However, it has been argued that landscapes cannot be characterized by a single scaling exponent, since a number of generating processes operating at different scales determine landscape complexity (Loehle and Wein 1994). Patterns resulting from multiple underlying processes are best studied using a multifractal approach (Scheuring and Riedi 1994). A multifractal system is characterized by a continuous "spectrum" of scaling exponents (Schroeder 1991). Many natural systems have multifractals characteristics, including geophysical phenomenon (Turcotte 1997), species patterns (Loehle and Wein 1994), and landscape patterns (De Cola 1994).

4.2 Objective

In this study, a multifractal analysis of remotely-sensed imagery (Landsat thematic mapper data) is performed to examine how spatial and temporal phenomena affect scale-invariant landscape complexity. Specifically, the role of successional change and

physiographic complexity in influencing landscape pattern is assessed by addressing the following questions:

1. Does landscape pattern complexity change predictably during succession?
2. To what extent is landscape pattern complexity influenced by underlying physiography?
3. How do spatial and temporal processes interact in determining scale-invariant landscape pattern complexity?

4.3 Study Area – See Chapter 2

4.4 Materials and Methods

Remote Sensing Data

A Landsat-5 image of RMNP acquired on August 3, 1991 is used in this study, and all landscape ages cited are expressed relative to this date. The image has high atmospheric transmittance and minimal cloud cover. The analyses utilized three spectral reflectance bands: band 3 (red, 0.63-0.69 μm), band 4 (near infrared, 0.76-0.90 μm), and band 5 (mid infrared, 1.55-1.75 μm). A standard radiometric correction (Radarsat International, Vancouver) was used to eliminate variability in sensor response. The final raster product conformed to the NAD27 grid system (Zone 14) at a pixel resolution of 30 x 30 m. Bands were centred at 5631.3 km N by 403.4 km E. A dark order subtraction based on a path irradiance model of λ^{-4} (corresponding to a clear atmosphere dominated by Rayleigh scattering, Richards 1993) was performed to correct for residual atmospheric effects (Chavez 1988).

An unsupervised K-means classification was performed on the three-band data to simplify the spectral image into ten discrete "classes" (Richards 1993). Unsupervised classification is a "neutral" strategy that makes no prior assumptions regarding ground-based floristic composition. The classes are therefore defined purely on the basis of pixel-based spectral reflectance data.

Topographic complexity of the study sites was measured using a digital elevation map (DEM) based on orthophotography of RMNP. Resolution of the DEM was 120 x 120 m, and elevation was recorded as metres above sea level.

Site Selection

1. "Young" vs. "Old"

Three square study sites (2.88 x 2.88 km, or 96 x 96 pixels) were selected from each of two recently burned areas: the 1980 Rolling River fire (11 years old), and the 1961 Gunn Lake fire (30 years old). Each "young" site was then paired (matched) with an "old" site, i.e. a region that has not burned for at least 95 years (**Figure 4.1a**). The "old" sites were selected using several criteria: (a) adjacency to "young" sites; (b) similar topography and elevation to "young" sites; (c) similar soil texture and drainage patterns to "young" sites (data from Canada 1979). All twelve study sites occur on the Saskatchewan Plain and have less than 5% open water.

2. "Simple" vs. "Complex"

Six square study sites (2.88 x 2.88 km, or 96 x 96 pixels) exhibiting a ridge-swale topography and a stationary elevational profile indicative of restricted drainage were. These are referred to as "complex" physiographic sites. Each "complex" site was paired (matched) with an adjacent site having a non-stationary (directional or sloping) elevation profile, and occurring on well-drained soils (Canada 1979). These are referred to as "simple" physiographic sites. All twelve study sites occur on the Saskatchewan Plain and have less than 5% open water. Example digital terrain maps of a "simple" and "complex" site pair are shown in **Figure 4.2**.

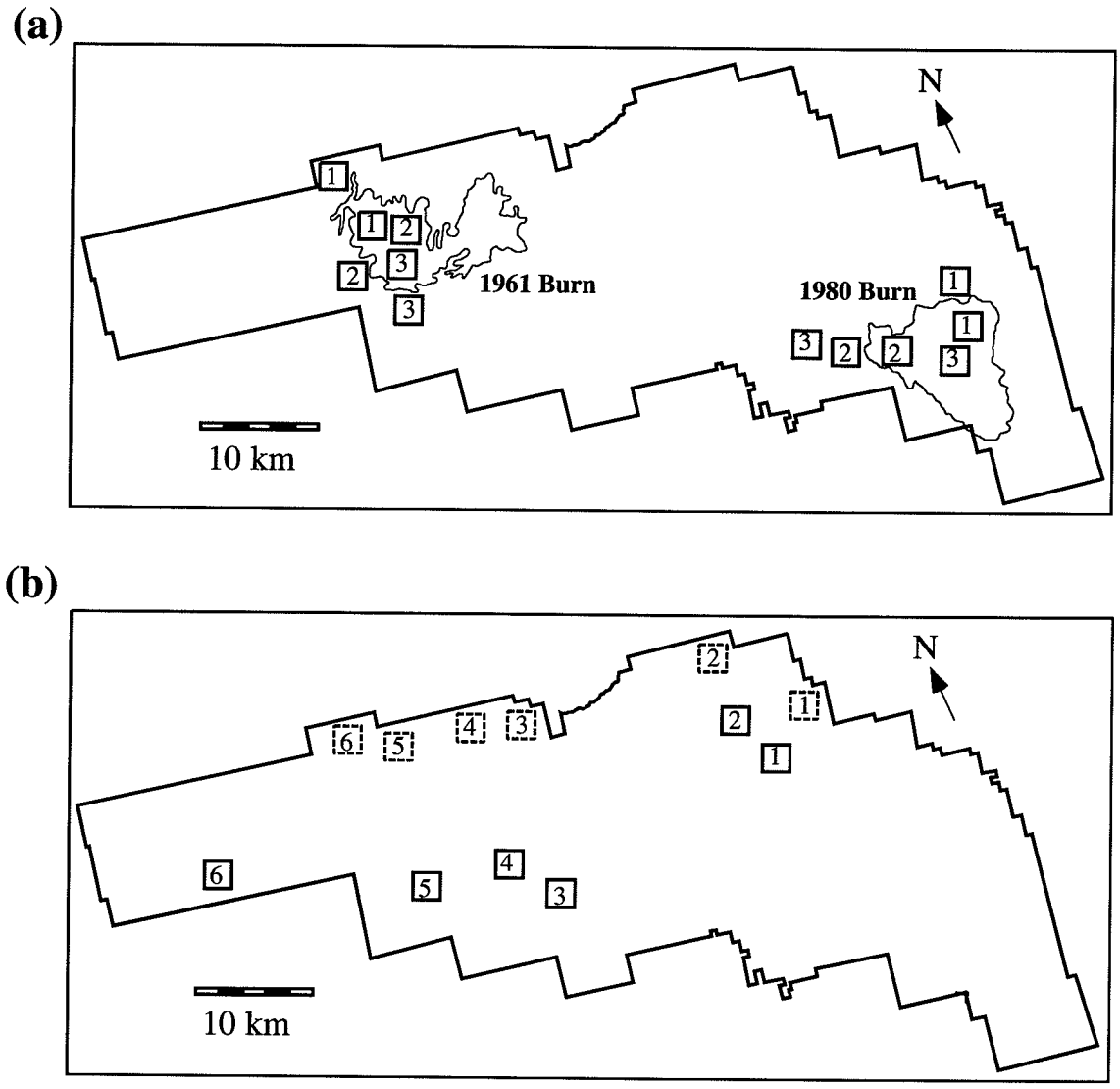

Figure 4.1: Locations of the 24 sample sites in Riding Mountain National Park: (a) "young" (11-30 year) sites mapped within the boundaries of the 1980 and 1961 burns and adjacent "old" (> 95 yr) sites; (b) "complex" (solid lines) and matching "simple" sites (broken lines).

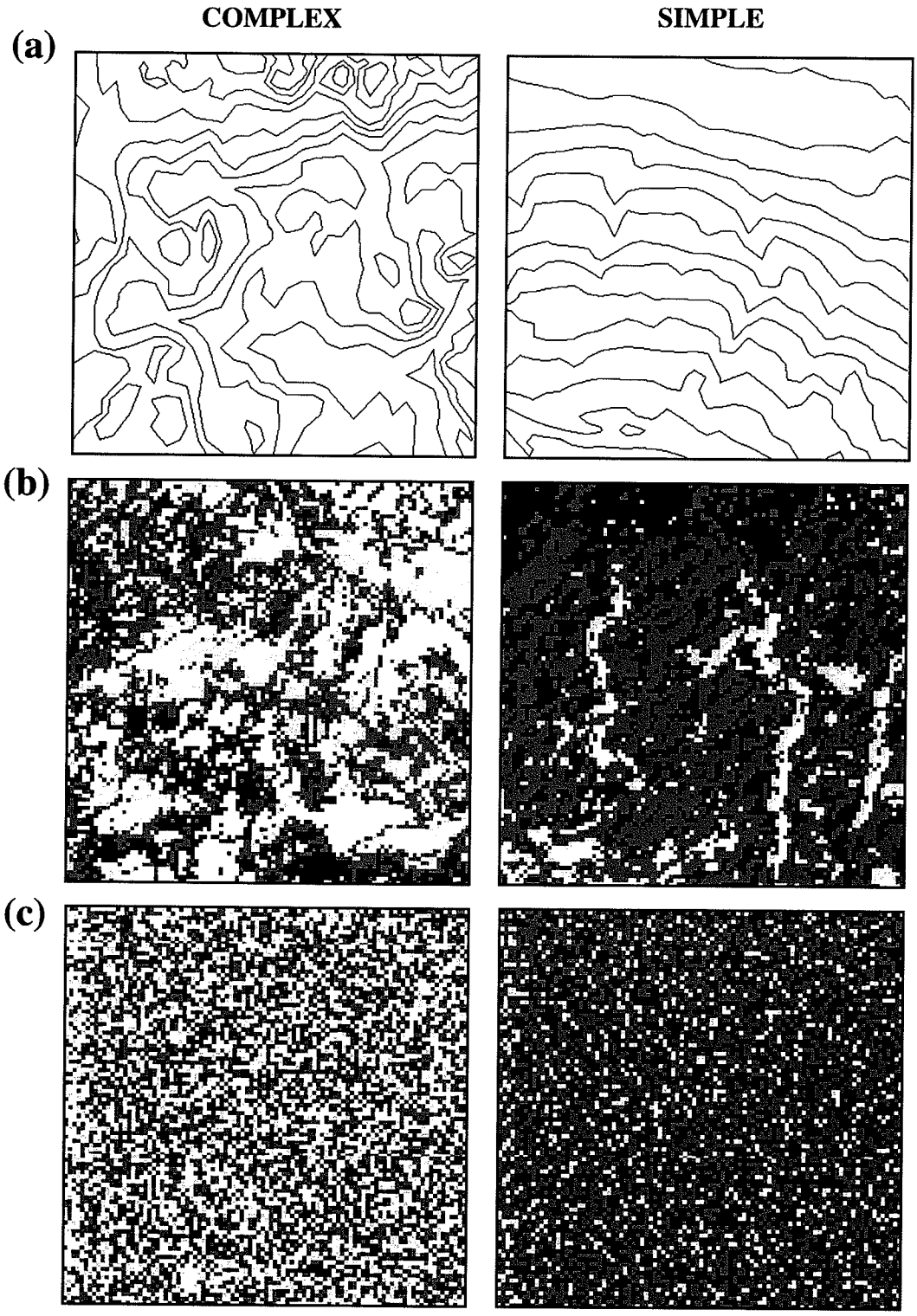

Figure 4.2: "Complex" site with a pair-matched "simple" site: (a) elevation contours; (b) patterns of the 3 most frequent land-cover classes (black and grey shades - the remaining 7 classes are combined as white); (c) random landscapes generated from

Data Analysis

1. Site Physiography

Physiographic complexity was determined for each site to ensure that "young" and "old" sites are not confounded by differences in physiography, and that landscape physiographic complexity is greater for "complex" sites compared to "simple" ones. For all 24 study sites, both slope and topographic variation (based on DEM data) are used as measures of physiographic complexity.

A principal component analysis (PCA) was performed on the DEM for each site to obtain a "plane of best fit". Site slope was then determined from the direction cosines of the principal axis. Slope values are compared across sites using paired t-tests.

To quantify topographic variation, a surface complexity analysis was performed on the DEM for each sample site using an algorithm described by Polidori et al. (1991). This method calculates a persistence exponent (η) for sequential values in a spatial (or temporal) series. Persistence measures the degree of autocorrelation of adjacencies in a series; if $\eta < 0.5$ the series is negatively autocorrelated, whereas $\eta > 0.5$ indicates positive autocorrelation. Persistence η is computed from the power-law relationship:

$$\log |e| = \log k + \eta \log d \qquad \textbf{[Equation 4.1]}$$

where $|e|$ is the mean absolute difference between values in a spatial series separated by lag distance d. The surface algorithm was implemented using a "rook" sampling technique. The fractal dimension (D) of the surface is calculated as:

$$D = 2 - \eta \qquad \textbf{[Equation 4.2]}$$

Fractal surface complexity values were compared across sites using paired t-tests.

2. Landscape Complexity

A multifractal analysis was used to measure landscape complexity for each of the 24 study sites. Each study site consists of a 96 x 96 grid of pixels, with each pixel

assigned to one of s = 10 "classes". To characterize the scaling properties of landscape pattern, study sites were gridded into square units of side length δ, ranging from δ = 2 (2 x 2 pixels, or 0.36 ha) to δ = 48 (48 x 48 pixels, or 207 ha) and using all whole number factors of 96. For a given side length δ, the "local diversity" H_i of the i^{th} unit is computed as Shannon's entropy:

$$H_i(\delta) = \sum_{k=1}^{s} (f_k/\delta^2) \ln (f_k/\delta^2) \qquad \textbf{[Equation 4.3]}$$

where f_k is the frequency of kth class in the ith unit. The relative entropy contributed by each unit to the entire site is then determined as:

$$p_i = H_i(\delta) / \sum_{i=1}^{(96/\delta)^2} H_i(\delta) \qquad \textbf{[Equation 4.4]}$$

Using these proportional values, the generalized entropy (q^{th} moment of a multifractal) is determined from the function (Renyi 1970; Scheuring and Riedi 1994):

$$I_q(\delta) = 1/(1-q) \log \sum_{i=1}^{N_\delta} p_i^q \qquad \textbf{[Equation 4.5]}$$

From this, the generalized dimension D_q for the q^{th} fractal moment is given by:

$$D_q = -\lim_{\delta \to 0} \left[\frac{I_q(\delta)}{\log(\delta)} \right] \qquad \textbf{[Equation 4.6]}$$

In practice, a plot of generalized entropy $I_q(\delta)$ against log δ is used to estimate D_q (Hentschel and Procaccia 1983). If a straight line is obtained over the range of δ, D_q is given by the negative of the gradient.

A "family" of generalized dimensions is obtained by varying q. By measuring dimension as a function of q, the multifractal nature of a spatial pattern is revealed (Scheuring and Riedi 1994). As the value of q increases, greater weight is given to grid units with high "local diversity" in calculating D_q. While q can in theory range from -∞

to $+\infty$ (Schroeder 1991), it is generally recommended that $0 \leq q \leq 3$ when analyzing statistical fractals (Appleby 1996). In this study, the multifractal spectrum of landscape complexity for each study site was characterized by plotting D_q against q, with q ranging from 0 to 3 in increments of 0.5. For "classic" fractal objects D_q is a simple linear function of q; no additional information is obtained by examining higher moments. For multifractal objects, D_q is a non-linear function of q (Schroeder 1991).

Landscape complexity is also a function of class frequency, since the number of possible adjacencies is determined by the frequency distribution of classes (Turner 1989). It is therefore important to determine the degree to which the observed landscape pattern deviates from a random one (Harvey et al. 1983). For each study site, random (null model) landscapes were generated by randomizing pixel positions while maintaining the observed class frequency distribution. Examples of observed and randomized study site landscapes are shown in **Figure 4.2b, c.** Randomized landscapes were analysed using the same multifractal method described above. A Monte Carlo proceedure (Manly 1991) was used to test the null hypothesis that the observed landscape patterns are statistically random. Specifically, the D_q profile for each site was compared with those obtained from100 randomized landscapes.

Multifractal response profiles (plot of D_q vs. q) are analogous to other continuous, highly autocorrelated processes in biology. Profile analysis (Morrison 1990) was used to test for differences in the profiles of "simple" and "complex" sites.

4.5 Results

Site Physiography

There were no significant differences in physiographic characteristics between "young" (11 - 30 years) and "old" (> 95 years) sites (**Table 4.1a**). Terrain slopes were similar (paired t = 0.46, P = 0.67) and ranged from 0.26° to 0.85°. Topographic fractal dimension ranged from D = 1.07 - 1.41, but differences between site pairs were not significant (paired t = 0.81, P = 0.46). Indicating successful site matching for topography for these sites.

As anticipated, significant differences were found between the physiography of "simple" and "complex" sites (**Table 4.1b**). The "simple" sites have a moderate terrain slope (mean = 2.16°), whereas "complex" sites are almost flat (mean = 0.45°; paired t = 3.67, P = 0.014). Topographic fractal dimension of "simple" sites is significantly lower than for "complex" sites (mean D = 1.09 vs. 1.34; paired t = 10.03, $P < 0.001$).

Landscape Complexity

Observed values of D_q for all sites approached the maximum value of the function (D → 2), indicating that boreal forests in RMNP have high landscape complexity at all successional stages (**Figures 4.3, 4.4**). However, the multifractal profiles of all sites deviated significantly from random (Monte Carlo confidence limits), indicating some degree of "spatial organization" at all successional stages. The multifractal profiles of all sites are broadly linear over the observed scale range (30 to 3000 m), suggesting that landscape complexity can be characterized using a single scaling exponent.

The earliest successional landscapes (Rolling River fire, 11 years) have lower landscape complexity than paired "old" sites (**Figure 4.3a**; $D_0 \approx 1.96$ for "young" sites, vs. $D_0 \approx 1.98$ for "old" sites). However, the multifractal profiles of 30-year old sites (Gunn Lake fire) and paired "old" sites are indistinguishable ($D_0 \approx 1.98$; **Figure 4.3b**). This indicates that changes in landscape complexity attributable to successional processes occur within the first few decades of stand development.

Sites characterized by greater physiographic complexity had higher landscape complexity than physiographically simple sites (**Figure 4.4**; $D_0 \approx 1.94$ for "simple" sites, vs. $D_0 \approx 1.98$ for "complex" sites). Profile analysis confirmed that these differences in landscape complexity are statistically significant (**Figure 4.4c**; t = 4.57, P = 0.001).

Table 4.1. Physiographic characteristics (terrain slope and topographic fractal dimension) for the 24 sample sites (site numbering follows **Figure 4.1**.): (a) "young" (11-30 year post-burn) and "old" (> 95 years) sites; (b) physiographically "simple" and "complex" sites.

(a)

	Young		Old	
Site	**Slope (degrees)**	**Surface Fractal**	**Slope (degrees)**	**Surface Fractal**
11 year				
1	.68	1.23	.85	1.41
2	.26	1.35	.63	1.23
3	.48	1.25	.67	1.24
Mean	*.47*	*1.28*	*.72*	*1.29*
30 year				
1	.44	1.14	.57	1.16
2	.44	1.07	.44	1.27
3	.26	1.31	.36	1.28
Mean	*.38*	*1.17*	*.46*	*1.24*

(b)

	Simple		Complex	
Site	**Slope (degrees)**	**Surface Fractal**	**Slope (degrees)**	**Surface Fractal**
1	3.30	1.03	.89	1.29
2	4.22	1.07	.57	1.30
3	1.36	1.11	.13	1.44
4	1.78	1.07	.26	1.22
5	1.28	1.04	.36	1.34
6	1.06	1.21	.51	1.47
Mean	*2.16*	*1.09*	*.45*	*1.34*

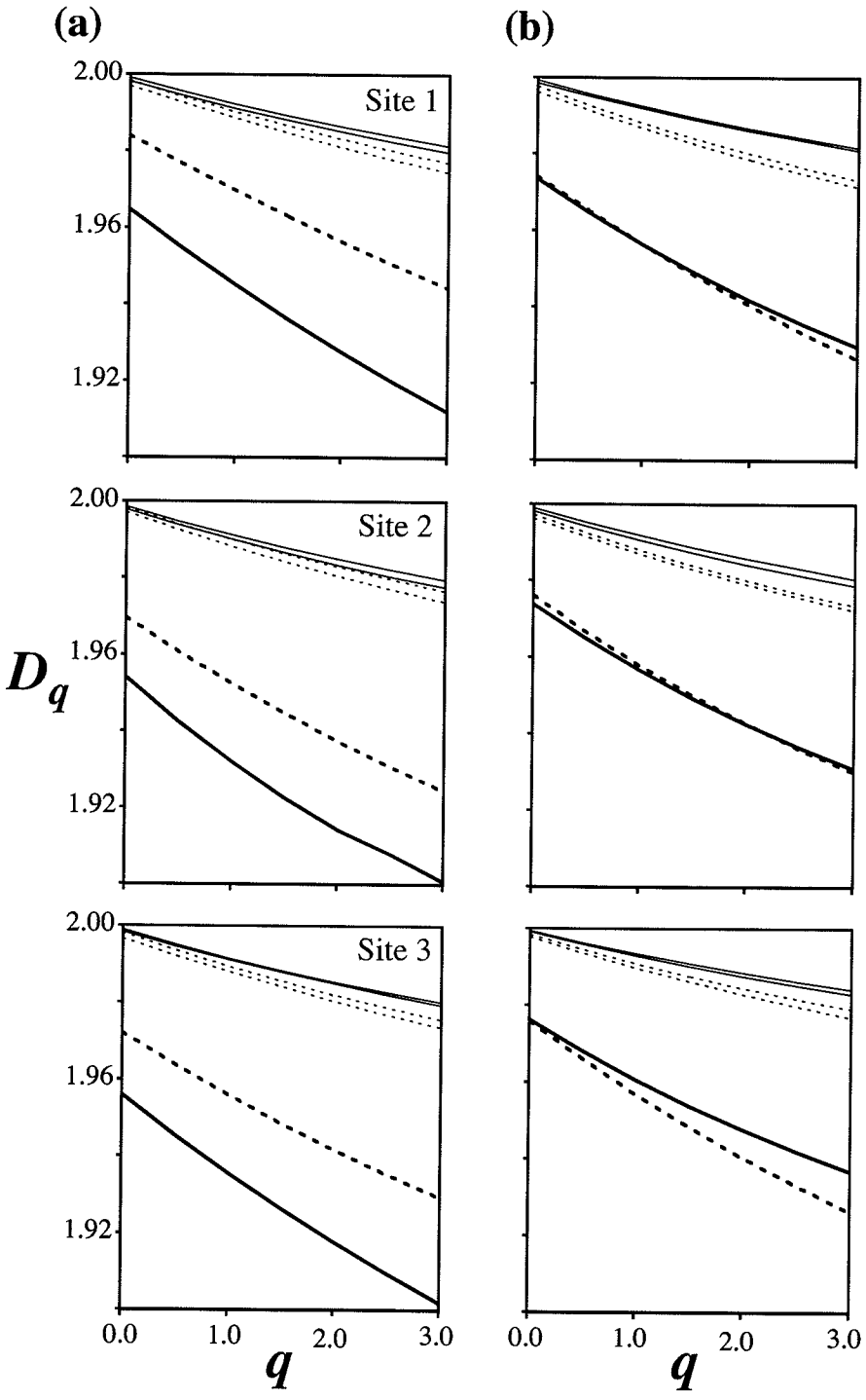

Figure 4.3: Multifractal profiles for "young" (solid thick lines) and "old" (broken thick lines) sites. (a) 11-year post-burn "young" sites and paired "old" sites; (b) 30-year post-burn "young" sites and paired "old" sites. Upper and lower bounds for the random landscapes are shown: "young" sites (solid fine lines) and "old" sites (broken fine lines).

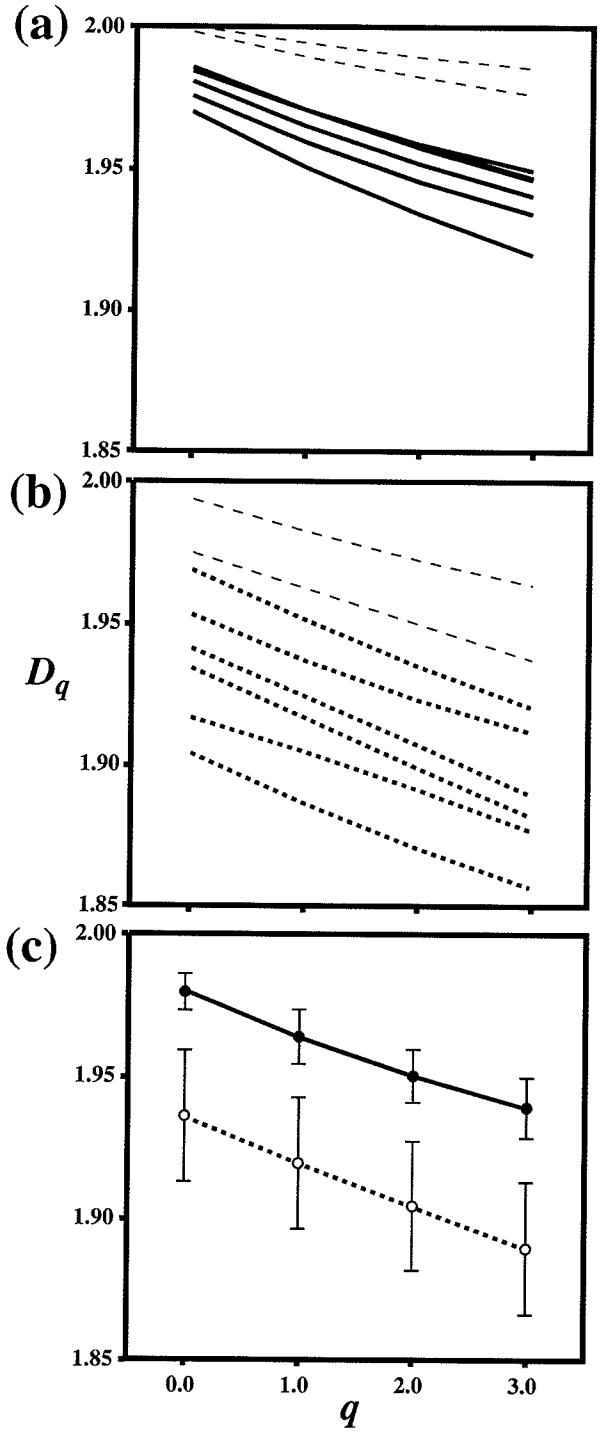

Figure 4.4: Multifractal profiles for "complex" and "simple" sites: (a) "complex" sites (solid thick lines) with the upper and lower bounds of the random landscapes (fine broken lines); (b) "simple" sites (broken thick lines) and envelops for the random landscapes (fine broken lines); (c) mean values for the "complex"sites (solid circles and thick line) and "simple" sites (open circles and broken thick line:), bars indicate the standard deviation.

4.6 Discussion

This study makes extensive use of simplified (through unsupervised classification) Landsat TM imagery to examine changes in landscape complexity in space and time. By using an unsupervised classification approach, spatial patterns can be characterized without having to resort to an *a priori* delineation of floristic groupings. Previous studies have generally relied on spatially explicit polygon mapping techniques, photographic interpretation, or supervised classification to delineate floristic groupings prior to spatial analysis (e.g. Hall et al. 1991; Frelich and Reich 1995; Ravan and Roy 1997). Such an approach is scale-specific and requires a detailed knowledge of vegetation classes on the ground. Furthermore, the interpretation of results is restricted to the vegetation classes specified. The delineation of vegetation classes is also problematic, as it necessarily results in oversimplification of inherently complex, heterogeneous landscapes (Bettinger et al. 1996).

In this study, multifractal analysis was to characterize spatio-temporal changes in landscape pattern complexity. A number of Landsat-based studies have used band-ratioing techniques to estimate biophysical parameters of forest stands along successional gradients (e.g. Fiorella and Ripple 1993). Such an approach ignores the complex spatio-structural patterns of spectral reflectance characteristic of forested landscapes. Structural properties of tree canopies (e.g. branching patterns, leaf arrangement and shadowing) are often more important than floristic composition in determining the reflectance properties of forested landscapes (Colwell 1974; Jakubauskas 1996a). Surface albedo is affected by the presence of small canopy gaps (Rowe 1993), and may be an expression of emergent properties of canopy architecture (Walker and Kenkel 2000). Local variations in canopy structure, even at the scale of a few metres, produce complex patterns of spectral reflectance in Landsat images (Jakubauskas 1997). A multifractal approach is thus well suited to detecting spatio-temporal changes in landscape complexity and structure (De Cola 1994).

It was found that landscape pattern complexity of "young" (11 year old) forest stands was lower than that of adjacent "old" (> 95 year old) stands. Spatially variation in fire intensity (Turner and Romme 1994) and rapid post-fire recolonization (Pickett et al. 1987; Walker and Kenkel 1998) result in "young" landscapes characterized by

compositionally and structurally homogeneous forest patches of relatively uniform size (Frelich and Reich 1995; **Figure 4.5**). Over time, these homogenous patches begin to "disaggregate" (He and Mladenoff 1999) as small (10-30 m in diameter) gaps accumulate and progressively "chip away" at the canopy (Frelich and Reich 1995). Both biotic and abiotic processes are involved in forest canopy "breakup". Abiotic processes such as windthrow and lightning damage are stochastic in origin and produce gaps ranging in size from a single large tree branch to an entire stand (Ganström 1993; Dyer and Baird 1997). Biotic processes such as insect damage, ungulate herbivory and beaver activity are also stochastic in nature and variable in spatial extent (Naiman 1988; Holling 1992). Biotic and abiotic disturbances accumulate on the landscape over time, with smaller-scaled events occurring more frequently than larger-scaled ones (He and Mladenoff 1999). The canopy gaps created by such disturbances favour the release of suppressed understory trees, driving succession and producing more diverse, multi-aged and structurally complex forest canopies (Pickett et al. 1987; Frelich and Reich 1995). In 200 year old boreal stands, canopy gap processes may account for over 40% of total forest cover (Kneeshaw and Bergeron 1998). On a Landsat image, these canopy gap processes result in spectral reflectance features that become progressively finer-grained and stochastic as stands age (Rey-Benayas and Pope 1995; Jakubassas 1997). Over time, canopy gap processes can produe landscape patterns that are entirely stochastic (De Cola 1994).

The results indicate that the time required for post-fire boreal landscapes to achieve a high level of spatial complexity is short; by 30 years post-fire, landscape complexity is not discernibly different from that of older (> 95 years) stands (**Figure 4.3**). By contrast, other researchers have concluded that more than a century of cumulative gap-disturbance events are required to appreciably alter landscape complexity (Frelich and Reich 1995; He and Mladenoff 1999). However, these studies specifically focussed on changes resulting from canopy gap formation (tree senescence); changes in the structural properties of the canopy prior to gap formation were not considered. In contrast, Landsat imagery is able to discern a broad range of biophysical components of canopy structure, not just the formation of gaps. Changes in canopy structural properties attributable to differential growth rates, self-thinning, shadowing and differences in leaf distribution and branching patterns all contribute to variation in spectral reflectance values (Colwell 1974; Rey-Benayas and Pope 1995; Jakubauskas

1996a). As a result, Landsat imagery is able to detect changes in landscape complexity long before canopy tree senescence and gap formation occur (Hall et al. 1991; Jakubauskas 1997).

In this study, physiographically "complex" sites were found to have greater landscape pattern complexity than "simple" ones. In RMNP, physiographic complexity is positively correlated with landscape-scale variation in soil moisture availability. It is this coupling of physiography and resource availability that determines landscape pattern complexity. The spatial pattern of "islands" created by "flooding" a fractal landscape reflects underlying surface complexity (Mandelbrot 1983: Chapter 28). Similarly, a complex physiographic landscape intersected by the water table produces heterogeneous patterns of soil moisture availability (**Figure 4.5**). Because competitive success is often determined by the relative availability of soil resources (Palmer and Dixon 1990; Zobel et al. 1993; Frelich and Reich 1998), vegetation (i.e. landscape) complexity will mimic physiographic complexity.

In the boreal forest, succession (temporal processes) and physiography (spatial processes) interact to determine scale-invariant landscape pattern complexity (**Figure 4.6**). The spatial complexity of early-successional "simple" landscapes is primarily a reflection of post-fire colonization patterns that produce relatively large and structurally homogenous forest patches. By contrast, "complex" physiographic landscapes have greater microsite variation, resulting in smaller, more structurally heterogeneous patches. Over time all landscapes develop greater canopy structure complexity, and accumulate stochastic disturbances that "chip away" at the forest patches. As these processes accumulate, the landscape takes on an increasingly finer-grained texture. In physiographically "simple" sites only one or a few landcover-types dominate. Gaps therefore create structural discontinuities in a relatively simple canopy. By contrast, in "complex" physiographic sites stochastic disturbance events accumulate on what was initially a more fine-grained landscape pattern. Thus this model predicts that landscape pattern complexity is lowest in early-successional "simple" sites and highest in late-successional "complex" sites (**Figure 4.6**).

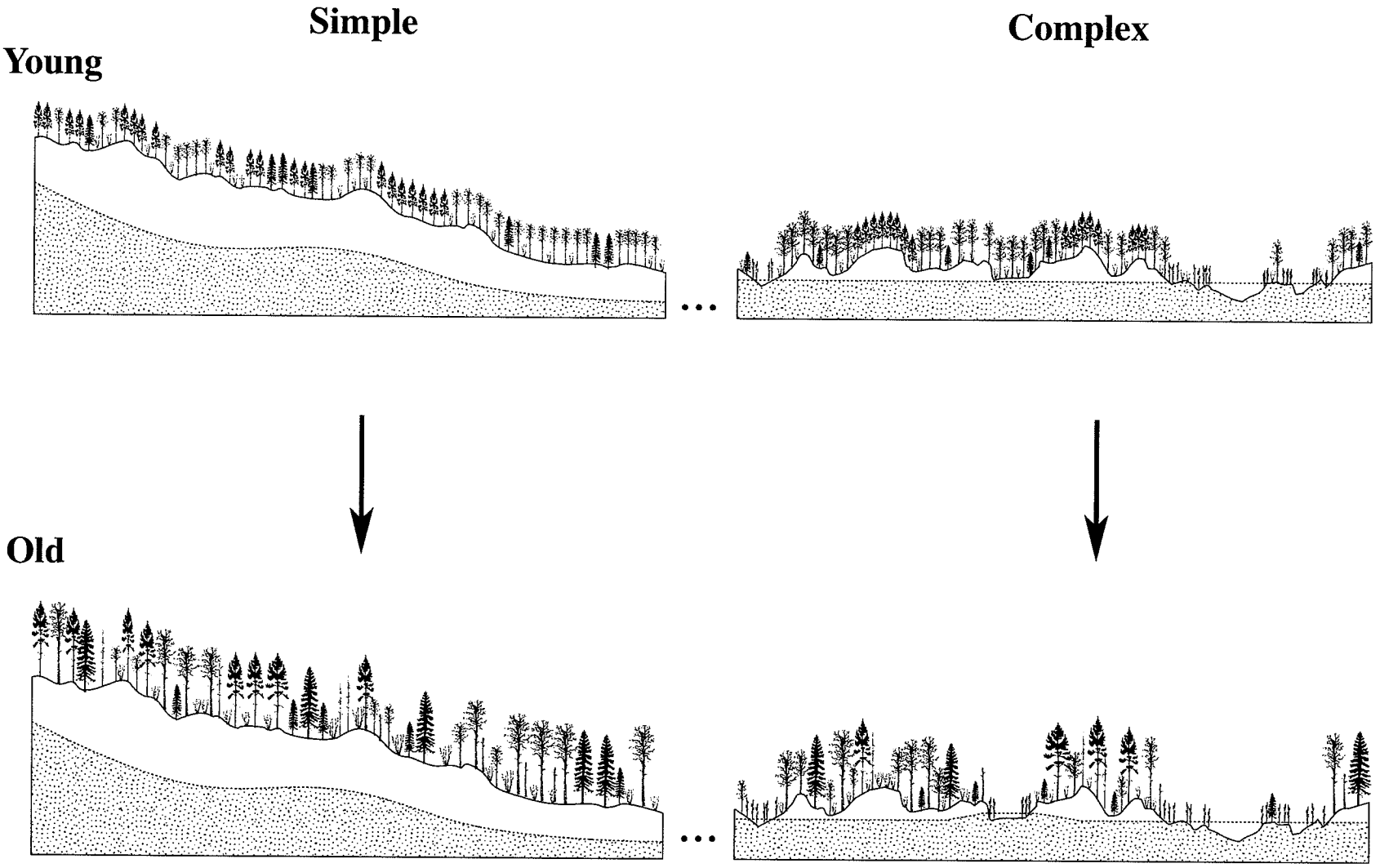

Figure 4.5: Landscape cross section showing change in canopy structure over time ("young" to "old" sites) and space ("complex" and "simple" sites). The upper limit of the watertable is indicated by a dotted line with a darker grey shade beneath.

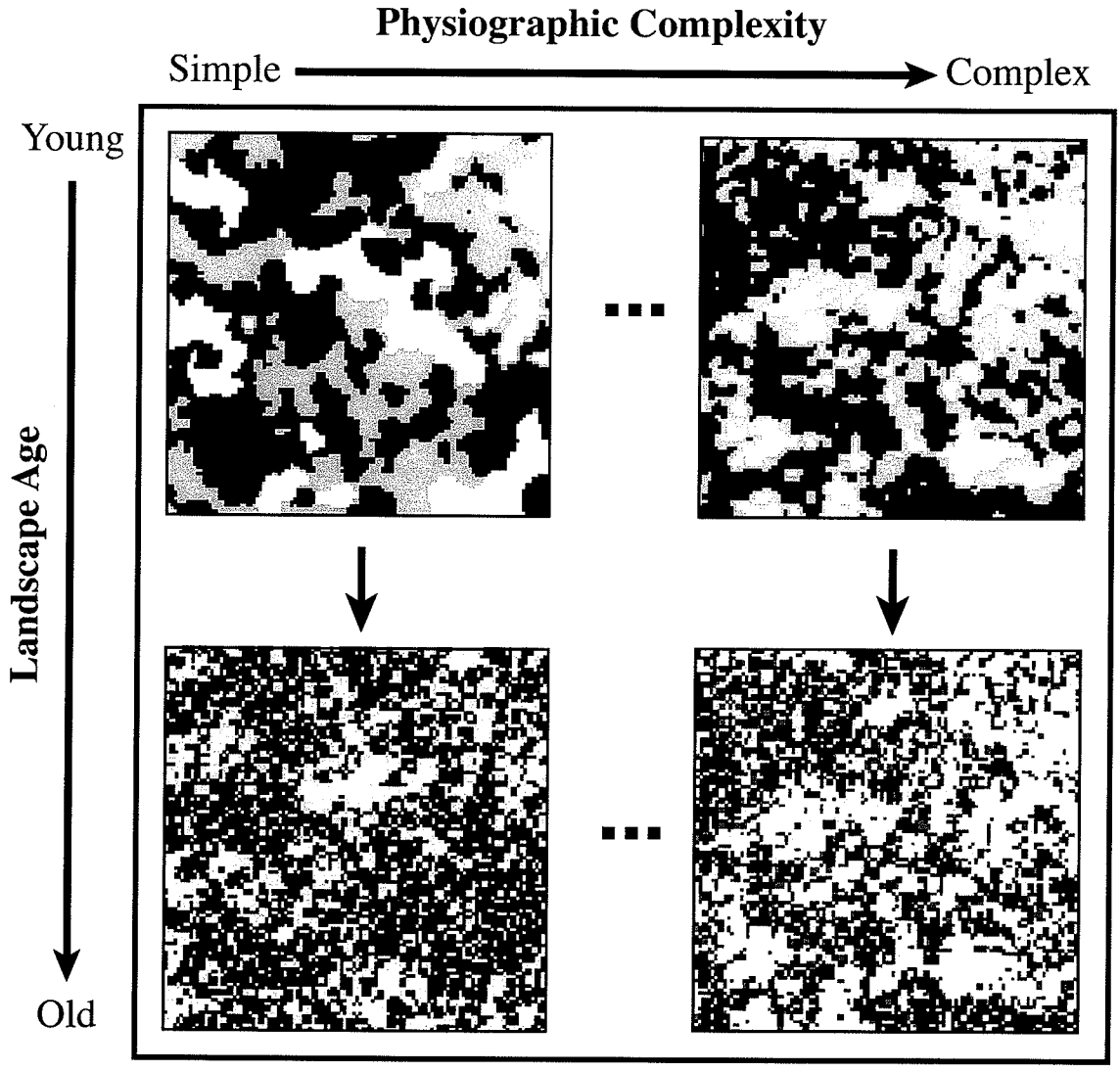

Figure 4.5: Landscape complexity resulting from canopy structural change in the boreal forest in space and time (see Fig. 6). Landscape complexity and patch heterogeneity is greatest for "old" physiographically "complex" sites.

4.7 Conclusion

The recognition that physiographic complexity strongly influences forest landscape complexity has potential application in predicting trends in biodiversity. Numerous models predict that complex fractal habitats will have greater overall species richness than simple ones (e.g. Scheuring 1991; Palmer 1992). Complex physiographic surfaces promote the "coexistence" of a larger number of habitats. Because landscape (and thus habitat) complexity is scale-invariant, complex landscapes are also expected to support a larger number of species. Recent research supports this view: complex landscapes have been shown to be more biologically diverse than simple ones (Zobel et al. 1993; Rey-Benayas and Pope 1995). The measurement of scale-invariant landscape pattern complexity may therefore have direct application to biodiversity and ecosystem monitoring studies.

Chapter 5

Landscape-Level Structural Dynamics of Boreal Forest Succession

Abstract Landscape-level structural complexity of boreal vegetation resulting from post-disturbance temporal dynamics was examined in Riding Mountain National Park, Canada. In this study, twenty-one ground sites (3 x 3 km in area) were selected from Landsat TM imagery (bands 3, 4, and 5) of the Park. To examine temporal change, the sites were stratified into age classes based on time since last major landscape-level crownfire. A method based on fractional brownian motion (using the Hurst exponent, H) was used to examine the spatial persistence of Landsat surface reflectance values in each of the three bands as well as a composite of the three. A randomization procedure was used to determine the expected value of H for a completely heterogeneous landscape. To account for the potentially confounding influence of topographic complexity, an analysis of spatial persistence was also performed on a digital elevation dataset (DEM) for the Park. A test of spatial autocorrelation (Moran's I) was also performed to ensure that the persistence values measured among the sampled landscapes were not spatially dependent. All 21 sites examined had Hurst (H) exponent less than 0.5, indicating anti-persistent spatial patterns. The observed values of H greatly exceeded random expectation, indicating that although these systems are anti-persistent they are not purely stochastic. It was found that H declined from younger to older landscapes ('composite:' mean H_{11yr}= 0.24; mean H_{120yr}= 0.14.). Landsat band 4 was most sensitive to landscape change over time and band 5 the least. An analysis of the physiographic complexity for the sites found no significant trend between the H values obtained from vegetation surface reflectance and topography (r=-.13). No evidence of between-site spatial autocorrelation was observed in H values calculated from vegetation surface reflectance (Moran's I = 0.203, Z = 1.345; p = 0.09), or for the DEM data (I = 0.066, Z = 0.615; p = 0.27). It is hypothesized that in the absence of large scale crown fires the boreal forest becomes increasingly spatially anti-persistent (i.e spatial entropy increases).

5.1 Introduction

Interest in spatial pattern and landscape dynamics within the boreal forest has increased in recent years because of concern over global climate change and the need for sustainable development within this ecosystem (Brown 2000; Sampson et al. 2001). Developing models

for both require a means to measure and predict canopy structural properties over extensive regions (Hall et al. 1991; Middleton et al. 1997). However, this is particularly challenging because the influence of multiscale stochastic disturbance on canopy structure is poorly understood (Frelich and Reich 1995b). The boreal forest is a disturbance driven ecosystem subject to catastrophic landscape-level crown fires with a return-cycle as short as every 50 years (Rowe 1956; Dix & Swan 1971; Hirsch 1991, Payette 1992). The frequent intense disturbances result in the development of a 'simple' community composition with few trophic levels (Sousa 1984; Franklin 1986). However, vegetation structural complexity within this ecosystem is highly variable, because of the repeated superimposition of new disturbances that vary in scale and intensity (Frelich and Reich 1995b; Cumming et al. 1996). Small scale stochastic disturbance events such as lightning strikes (Granström 1993), windthrows (Dyer and Baird 1997; van der Meer and Bongers 1996), ungulate herbivory (Pickette et al. 1987), budworm infestations (Holling 1992; Morin 1994; Bergeron et al. 1995) and Beaver flooding (Naiman 1988; Donkor and Fryxell 1999) are frequent on the landscape. The impact of these processes on landscape pattern is cumulative as the spatial heterogeneity resulting from these events can persist for up to a century in the absence of fire (De Grandpré et al 1993; Bergeron 2000). The wide-scale adoption of fire suppression techniques will likely have an important influence on landscape pattern in the boreal forest, but the long-term consequences of this management practice are not well understood (Baker 1992a; He and Mladenoff 1999).

Until recently, there has been surprisingly little research linking processes occurring at the local scale with landscape-level changes in spatial complexity. Studies that have been undertaken have used patch based simulations, neighborhood interactions (Frelich et al. 1998) or stand mapping as input for spatial analysis (Frelich and Reich 1995b; He & Mladenoff 1999). These approaches either simulate or require the presence of canopy gaps before change in pattern can be detected. However, significant change in canopy structure can take place without the formation of obvious gaps (van der Meer and Bongers 1996). In this context, the measurement of landscape complexity using a gap 'criterion' may be considered arbitrary (Bunnell and Huggard 1999). Other approaches recognize the continuous nature of structural complexity and attempt to determine the range over which biophysical parameters have predictable change (e.g. Cohen et al. 1990; Leduc et al. 1994; Baskent and Jordan 1995). The practical application of these approaches however, is severely limited by the availability of spatial databases at the regional scale (Sampson et al. 2001).

Spatially-explicit data covering large regions are difficult to obtain using ground-survey methods (Rey-Benayas and Pope 1995). Over the past three decades, remote sensing has become the preferred technology for quantifying landscape complexity (Ravan and Roy 1997). Satellite imagery contains distinctive reflectance spectra that are a function of canopy structural complexity and species composition (Colwell 1974; Rencz 1985; Hall et al. 1995; Sampson et al. 2001). Unlike the panchromatic aerial photography used in past studies (e.g. Frelich and Reich 1995b), satellite imagery samples several portions of the electromagnetic spectrum. Multiband data is especially valuable in examining the biophysical structure of vegetation, because the scattering of light by different canopy components is wavelength dependent (Rey-Benayas and Pope 1995). Reflectance in the visible-red portion of the spectrum (0.63-0.69 μm) is primarily determined by leaf pigmentation, which absorbs 90-94% of incident light (Myers 1983; Myneni et al 1992). Near-infrared reflectance (0.76-0.90 μm) is considered to be principally influenced by physical structure within the canopy and increases as phytomass increases (Ranson and Williams 1992; Chen 1996a). In forests, near-infrared reflectance is associated with the development of multiple canopy layers (Horler and Ahern 1986; Jakubauskas 1996a). At longer wavelengths (1.55-1.75 μm) the strong absorptive properties of water in plant tissues reduces spectral reflectance (Myers 1983; Hall et al 1995). By examining trends over several portions of the solar spectrum, valuable insight into the biophysical structure of canopies may be gained (Rey-Benayas and Pope 1995).

Reflectance resulting from light interaction with the canopy is measured within individual pixel elements. However, it is the spatial arrangement of multiple pixels that determines landscape complexity (Colwell 1974; Baskent and Jordan 1995). This is because ecosystem processes (e.g. disturbance) influences the juxtapositioning and interdigitation of light scattering components within and among stands, thus increasing the spatial heterogeneity in reflectance values (Jakubauskas 1997). For instance, the formation of small canopy gaps often results in alternating patterns of high and low surface albedo (Rowe 1993). Spatial co-occurrences in digital imagery are considered to be 'textural' features (Peddle and Franklin 1991; Richards 1993) for which number of landscape statistics have been developed (Curran 1988; O'Neill et al 1988; Musick and Grover 1990; Leduc et al. 1994). These statistics have been primarily used to quantify landscape changes caused by human driven fragmentation (e.g. Miller et al. 1996; Rignot et al. 1997; Tang et al. 1997; Tinker et al. 1998). However, few studies have examined textural changes in remotely sensed imagery resulting from natural vegetation dynamics (but see Jakubauskas 1997). The measurement

of spatial dependencies in Landsat data provide an important source of information for the examination of temporal dynamics of boreal forest canopies.

5.2 Objective

The role of small scale disturbances and neighborhood processes in affecting pattern, although demonstrated at the local scale (Frelich and Reich 1995a; Conroy and Noon 1996), has only recently been quantitatively examined at the landscape level (Mladenoff et al 1993; Rey-Benayas and Pope 1995). In this chapter change in canopy structural complexity resulting from temporal dynamics in the boreal forest is examined. A measure of the spatial persistence of pattern in Landsat TM surface reflectance is used to examine scale invariant landscape complexity. Specifically the following questions are addressed:

i) Does canopy structural complexity have scale invariant properties?

ii) Does canopy structural complexity change predictably during succession?

5.3 Study Area – See Chapter 2

5.4 Material and Methods.

Remote Sensing Data

The analysis of landscape complexity in RMNP was based on LANDSAT 5 imagery (ground resolution 30 x 30 m) acquired on August 13, 1991. For this study three spectral bands were chosen: band 3 (0.63 - 0.69 μm), band 4, (0.76 - 0.90 μm) and band 5 (1.55 - 1.75 μm). Each band was centred at 5,631,290 m N by 403,373 m E on the UTM North American Datum 1927 (NAD27) grid system. Image preprocessing calibrations were applied to eliminate the effects of variability in sensor response and atmospheric distortion (Richards 1993). A bulk atmospheric correction was applied to each band using the improved dark order subtraction technique as described in Chavez (1988). A path radiance model of λ^{-4} was selected, corresponding to a clear atmosphere dominated by Rayleigh scattering (Richards 1993).

Site Selection

Twenty-one 3 x 3 km (100 x 100 pixels) sites were selected from the Landsat image using a stratified random approach (**Figure 5.1**). Strata were defined on the basis of landscape 'age', which was determined from ground data collected in 1992 and 1993, and forest fire records dating back 120 years (Sentar 1992). Areas subjected to landscape level fires during six different time periods were located. Sites for which no historical fires were recorded were considered to have a landscape age greater than 120 years. Within each of these age strata, sample location was determined randomly. Sites with evidence of repeated disturbance (e.g. multiple fires), variable local relief (excessive topographic complexity) and poor drainage (e.g. lakes, marshes) were avoided to ensure comparability. Once sites were located, the reflectance in bands Landsat bands 3, 4., and 5 were saved for further analysis (see below).

Surface reflectance properties and landscape complexity are also a function of underlying topographic complexity (Walker and Kenkel 2001). Although areas of excessive topographic variability were avoided during site selection, separate analyses were performed to ensure that temporal change in landscape complexity had not been confounded with topography variability. The topographic variability for each site selected on the Landsat imagery was obtained from a digital elevation model (DEM) of RMNP with a pixel resolution of 120 x 120 m. Using the UTM locations for the sample sites, the appropriate location on the DEM was determined and the elevation data in m a.s.l. was saved for further analysis (see below).

Canopy structural complexity

Spectral reflectance in remotely sensed imagery can be visualized as a continuous surface in three dimensions where each location (pixel) can be expressed as a grid coordinate (x and y) and a magnitude (z) value. A linear cross-section through this surface will yield a two dimensional sequence of reflectance values, or 'trace'. These sequences can be described using Fractional Brownian motion (fBm) models (Peters 1994: 53) to derive a scale invariant measure of path complexity (Polidori et al. 1991). Such models utilize a persistence parameter (H), originally developed as part of the rescaled range method (Hurst 1951), an affine transformation (Schroeder 1991: 141). Persistence refers to the degree of autocorrelation of adjacencies: for $H < 0.5$, a fractional Brownian motion trace is negatively

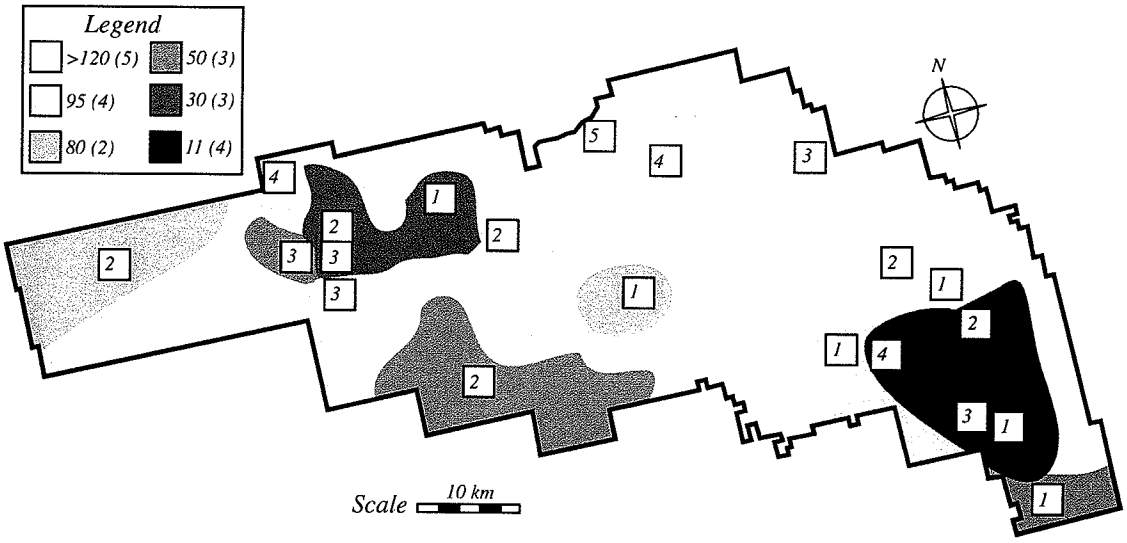

Figure 5.1: Map of RMNP showing locations of the six age strata (crownfire patches indicated in shades of grey) and the locations of the site selected for the analysis (21 in total). The number of sites sampled in each age group is indicated on the legend.

correlated, whereas values are positively correlated for H > 0.5 (Sugihara and May 1990). In ecology, persistence has been applied in the study of landscape fragmentation using size frequency relations from binary imagery (Hastings et al. 1982; Mandelbrot 1983). In this study, a relation for continuous spatial series described in Polidori et al. (1991) was used to determine the persistence parameter H:

$$\log|e| = \log k + H\log\delta \qquad \textbf{[Equation 5.1]}$$

Where |e| for a surface is the mean absolute difference on the 'z-axis' (e.g. elevation) between all pairs of points a lag distance 'δ' apart.

In this study, canopy structural complexity was calculated from Landsat TM reflectance in bands 3, 4, 5 as well as from a 'composite' of the three bands. For each of the three Landsat bands, the values for |e| were calculated following **Equation 5.1** (i.e. as the mean *difference* in pixel reflectance at lag δ). For the composite analysis the three spectral bands were combined to calculate a value for |e| using a 'multivariate' approach. This was accomplish by first standardizing the Landsat bands to unit variance to eliminate magnitude effects (Yakoya et al. 1989). From these standardized values the *distance* 'Δ' was calculated between pairs of points $z_b(x,y)$ and $z_b(x + \delta x, y + \delta y)$ spatially separated by lag δ as:

$$\Delta = \sqrt{\sum_{b=3,4,5}\left[z_b(x+x\delta, y+y\delta) - z_b(x,y)\right]^2} \qquad \textbf{[Equation 5.2]}$$

where $z_b(x,y)$ is the reflectance for band 'b' in units of digital number at the pixel coordinate (x,y). Following **Equation 5.1** the log of the mean values for Δ were plotted against the log of the lag distance (i.e. mean Δ = |e| in **Equation 5.1**). The purpose of developing a composite image was to examine whether the trends in persistence for individual bands corresponded with coordinated changes effecting the all of the bands.

In this study the lag values chosen for δ ranged from .06 to 3 km. The landscapes were sampled using both horizontal and vertical pair-wise lag distances (rook's sampling rule). A toroidal correction was implemented when either the horizontal or vertical lag 'δ' exceeded the edge of the image. To determine if the landscape complexity values observed in the study differed from random expectation, H was calculated for randomized landscapes (following Manly 1991).

Topographic complexity

To measure the topographic complexity for each study site, the relation described in **Equation 5.1** was used. For this analysis the z-axis values were determined from the DEM of RMNP and using lag values chosen between .12 and 3 km. The DEM was sampled using a rook's rule, however for these data a torroidal correction was not implemented (the topographic surface profiles were non-stationary).

Test of spatial independence

The limited areal extent and tendency of crown fires to be aggregated on the landscape (e.g. frequent fires in eastern portions of the Park) constrained site choice. To ensure that the values for H obtained in this study were spatially independent, Moran's I (Upton and Fingleton 1985 p. 170) was used to test for positive autocorrelation. In calculating this statistic, the inverse squared distances between the sites (measured from the centre of each using UTM coordinates) were compared with the H values obtained from the Landsat composite image. Because this test is for positive spatial autocorrelation, the p-values were one-tailed.

5.5 Results

Typical landscapes examined in this study are shown (**Figure 5.2**), ordered by increasing age since last major forest fire. Landscape texture is noticeably 'grainy' and 'speckled' for all age classes from the youngest (recently burned) landscape (**Figure 5.2a**) to the oldest (120 years post-fire) landscape (**Figure 5.2c**). The young landscapes appear to have a coarser 'grained' texture, while older landscapes have a finer scale 'speckled' appearance. The evident visible complexity in image texture corresponds with the measured spatial persistence for these landscapes (**Figure 5.3a-d**). For all of the 21 sites examined in this study the values obtained for H were less than 0.5, indicating a complex spatially anti-persistent pattern. Landscape pattern was not entirely stochastic as the observed values of H greatly exceed the maximum value obtained for the randomized landscapes (H for the random simulations was usually $<< .05$).

Persistence declined with time since the last landscape-level crownfire for the sites examined in this study (**Figure 5.3**). Reflectance in all Landsat bands became increasingly anti-persistent with landscape age from 11 to 120 years post-fire (**Table 5.1**). All

regressions were significant, with band 4 (near-infrared) showing the greatest decline with time (slope=-.0011) and band 5 (mid-infrared) the least (slope=-.0007). The combined spectral reflectance (composite) of all three bands showed similar trends, indicating a coordinated change in persistence involving several components of canopy biophysical structure. These results suggest that in the absence of crown fire, boreal forest landscapes develop increasingly anti-persistent spatial patterns and increase in complexity.

Unlike spectral reflectance patterns, surface topography within the sample sites was found to be highly spatially persistent: H calculated from the digital elevation data exceeds .5 (range=.62 to .98). No statistical trend between landscape age and topographic complexity was observed (**Table 5.1**), indicating that these were not confounded. A regression analysis of landscape complexity (H for the 'composite' imagery) against topographic complexity was also not significant (r^2=-.13). In this study, changes in landscape complexity cannot be attributed to differences in topographic complexity among the sample sites.

No systematic trend was observed among the geographic locations of the sample sites and the persistence values measured. Tests of among-site autocorrelation using Moran's I were not significant with respect to landscape complexity ($I = 0.203$, $Z = 1.345$; $p = 0.09$), or topographic complexity ($I = 0.066$, $Z = 0.615$; $p = 0.27$). Thus, the observed trends in landscape and topographic complexity are not the result of autocorrelation among the locations sampled in the study.

Table 5.1: Landscape age and mean persistence (± std. error) for Landsat TM bands 3, 4, 5 and the composite of the three. The mean persistence for site topographic complexity is also given. Landscape age is determined as years since the last major crownfire and expressed relative to the date of the Landsat imagery (Aug., 1991). Slopes for the regression relation between persistence and time are indicated.

Landscape age	**Band 3**	**Band 4**	**Band 5**	**Composite**	**DEM**
11	.20 (±.016)	.31 (±.020)	.26 (±.021)	.24 (±.018)	.70 (±.019)
30	.23 (±.011)	.26 (±.015)	.26 (±.018)	.24 (±.011)	.76 (±.080)
50	.18 (±.006)	.23 (±.021)	.23 (±.023)	.21 (±.012)	.69 (±.040)
80	.14 (±.017)	.19 (±.006)	.19 (±.012)	.17 (±.011)	.72 (±.089)
95	.19 (±.022)	.20 (±.017)	.21 (±.012)	.19 (±.013)	.76 (±.037)
120	.10 (±.015)	.18 (±.019)	.18 (±.017)	.14 (±.013)	.81 (±.075)
Slope	-0.0008	-0.0011	-0.0007	-0.0009	0.0008
P-value	0.0007	<.0001	<.0001	<.0001	0.18

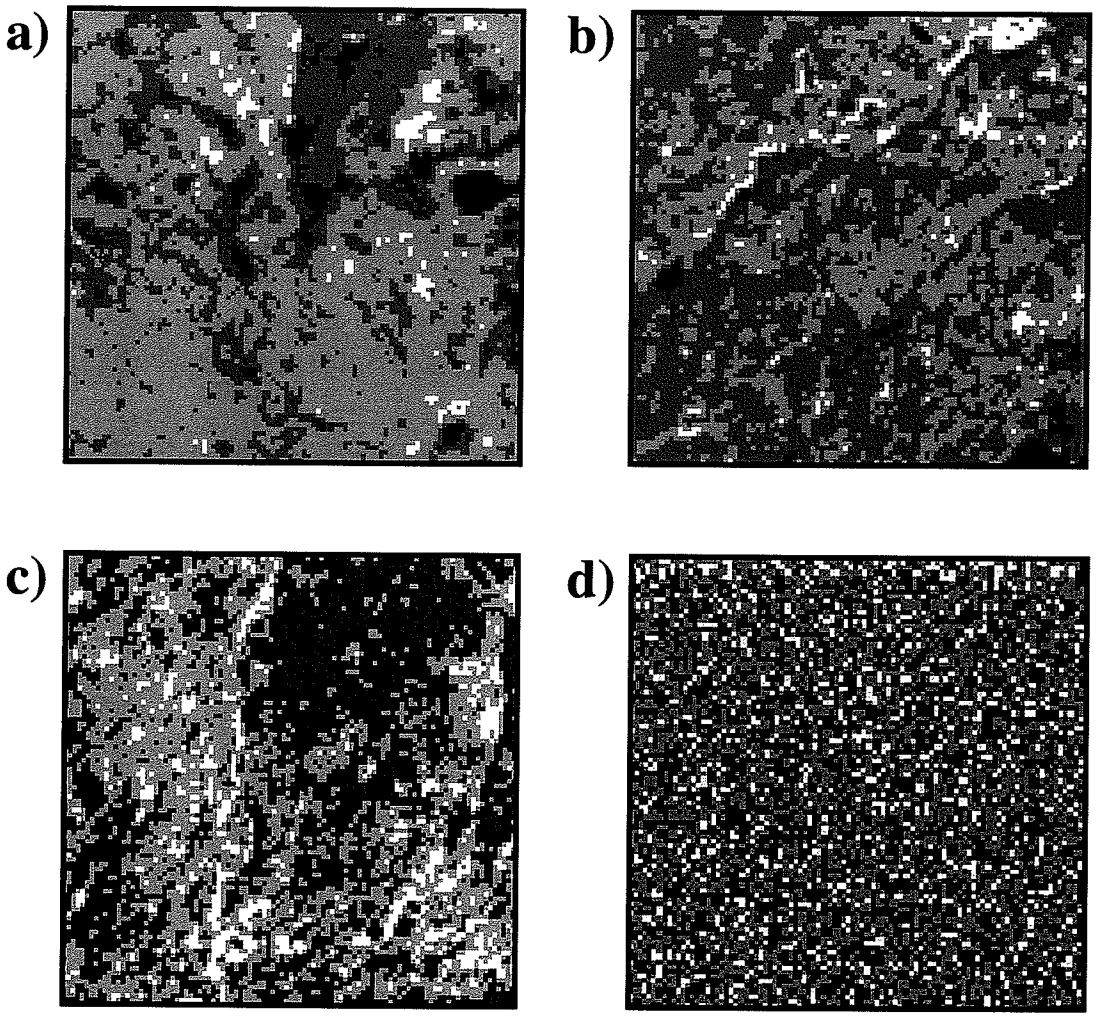

Figure 5.2: Four representative landscapes analyzed in the study: a) 11 year burn site; b) 50 year site; c) > 120 year site; d) a random landscape. Note: the full range of Landsat pixel reflectance (8 bit values) was reduced to 4 shades of grey for print reproduction.

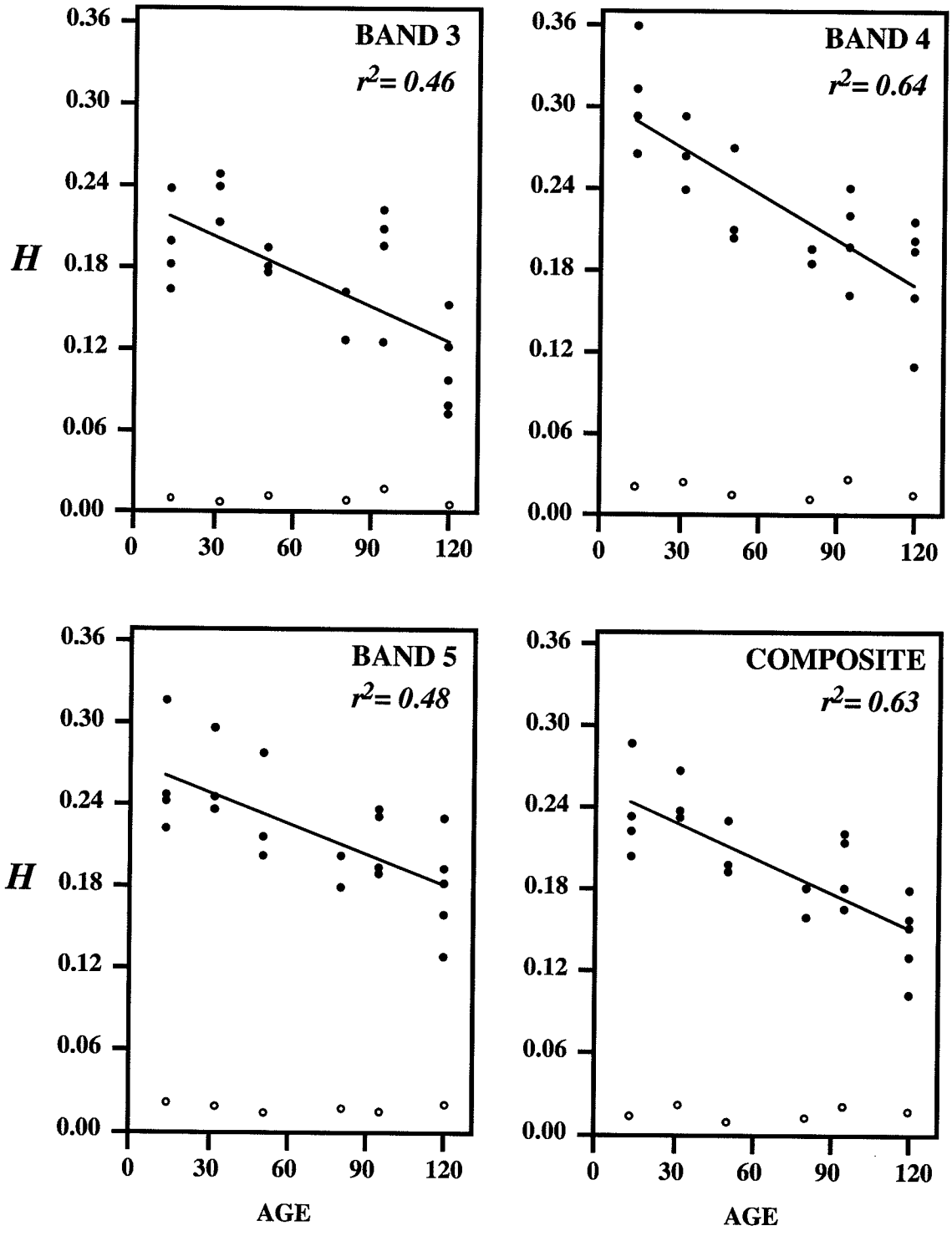

Figure 5.3: Graphs showing the decline in persistence (H) of surface reflectance measured for Landsat bands 3,4 and 5, and the composite.

5.6 Discussion

Most studies of spatial pattern in the boreal forest are based on spatially explicit mapping techniques, supervised classification approaches or polygon smoothing prior to spatial analysis (Ravan & Roy 1997; He & Mladenoff 1999). However, these approaches can result in the inadvertent simplification of heterogeneous areas (Bettinger et al. 1996; Jelinsky and Wu 1996). Furthermore, fine-scale disturbances may not result in the creation of a visible gap and thus be completely missed using ocular texture classification (e.g. Frelich and Reich 1995b). Comparison of the results from classification studies is also problematic: terms such as 'patch' and 'mosaic' are often based on different scale specific criteria (Bunnell and Huggard 1999). Indeed, the definition of 'patch' used in the analysis of pattern varies from the total cover in 'blocks' (e.g. Frelich and Reich 1995b), shape and size of tessellation tiles (e.g. Frelich et al. 1998), to 'units' of similar stand floristic composition (e.g. Cumming et al. 1996). Vagueness in the use of terminology represents a significant "conceptual limitation" of these approaches (Bunnell and Huggard 1999). In this study, spatial persistence was measured directly on the 'raw' digital numbers of a Landsat scene avoiding the necessity of image classification.

In this study, persistence was quantified from a spatial series (i.e. Landsat reflectance data) and temporal change was determined by repeating this measure on landscapes differing in age. Previously, persistence has been applied to temporal series data directly (e.g. Nile river flows, Hurst 1951; change in stock value, Peters 1994). In this context, it has the interpretation of the degree of 'divergence' within a system over time and in a general sense it predicts the direction in which a system will trend to the future (Schroeder 1991:131). High persistence ($H \rightarrow 1$) implies the continuity of a trend through time (high system 'memory' or autocorrelation), while low persistence ($H \rightarrow 0$) indicates lack of continuity (low temporal 'memory' or autocorrelation). In a spatial context, persistence measures the degree to which a spatial property (e.g. elevation) diverges with distance (i.e. an 'indicator' of surface complexity, Polidori 1991). For a topographic map, high persistence would be associated with smooth surface features (high spatial 'memory') whereas low persistence would result in a 'spikey' surface (low spatial 'memory'). It was found that spatial persistence in Landsat reflectance was low for all landscapes examined in this study, this suggests that the boreal canopy represents a complex 'spikey' surface (i.e. canopy structure is spatially complex).

The spatial antipersistence observed in Landsat spectral reflectance was likely the result of gross changes in the biophysical structure of the canopy. Traditionally, surface reflectance has been interpreted as the product of floristic composition (Wickland 1991; Markon 1992; Treitz et al. 1992). However, given the relatively low floristic diversity of the boreal forest, "structure and density would be expected to have a greater effect on reflectance characteristics than species composition" (Franklin 1986). Indeed, reflectance from boreal landscapes is a function of multiple biophysical components such as soil, trunks, branches, leaves and the shadows cast by these structures (Colwell 1974; Jakubauskas 1996a). In this study, all of the bands sampled showed a corresponding decrease in persistence with landscape age with each band measuring a different biophysical aspect of the canopy. Absorption in band 3 is a function of chlorophyll content in leaves, thus change in reflectance can be the result of leaf senescence (Myers 1983), needle age (Middleton et al 1997) and differences in foliar density in the canopy (Franklin 1986).

The decrease in band 3 persistence with landscape age may indicate that canopy productivity becomes more antipersistent as stands mature. Band 4 is sensitive to changes in the arrangement of canopy elements such as branches, leaves and stems (Horler and Ahern 1986), as well as biomass density and depth (Horler and Ahern 1986; Rey-Benayas and Pope 1995; Chen 1996a). Persistence in band 4 showed the greatest change with landscape age, possibly the result of canopy break-up during succession. The biophysical components related to band 5 include overall canopy height, leaf area index (LAI), standing dead biomass and total biomass (Horler and Ahern 1986; Jakubauskas 1996a). The development of an uneven canopy structure on the older landscapes in the study area might account for the decline observed in band 5 persistence. When persistence was calculated in the composite analysis, the trends obtained closely matched those for the individual bands. This likely indicates a 'coordinated response' among the bands (i.e. gross changes in biophysical structure influencing reflectance in all bands). An example of such a response would be changes in albedo and shadowing resulting from canopy gaps (Rowe 1993). In this case, the change in biophysical structure (i.e. the gap), results in a 'shadow' that reduces reflectance in all bands (i.e. a coordinated response across bands). Canopy disturbances in the study area, which usually result in partial senescence or damage, would be another example of a process generating a coordinated response in Landsat image reflectance.

It is suggested that disturbance processes and species response to those disturbances (including colonization patterns, differential growth and self-thinning) drive the changes in

persistence observed. It was found that all landscapes regardless of age were antipersistent (i.e. H was in the range: $0.5 \geq H \geq 0$). For early post-burn landscapes this may be a reflection of the stochastic aspects of fire intensity and post-fire vegetation establishment (Turner and Romme 1994; Hurtt and Pacala 1995; Jakubauskas 1997). Fires rarely burn an entire area and often leave small patches of forest especially on topographically complex landscapes, or where small lakes can act as barriers (Turner and Romme 1994). Within the 11 year old burn (Rolling River fire), patches of mature trees are often encountered despite the high intensity of that fire. At the landscape-level these patches result in antipersistence because they represent a substantial 'divergence' from the biophysical structure of post-fire vegetation. Chance establishments are also common in the boreal forest, especially where fire frequency is high, because it favors seedbank ephemerals and species capable of rapid dispersal (De Grandpré et al. 1993). Because of post-disturbance seedsource availability in the Rolling River fire area, jack pine can be periodically found colonizing organic soils, an atypical growth substrate for the species. These same factors have been cited in other studies to explain heterogeneity in Landsat surface reflectance for post-burn sites (Jakubauskas 1996b).

Following initial site colonization, it was found that landscape complexity increased (i.e. persistence declined) consistently with age. This implies that the large scale mosaic patterns resulting from landscape-level fire (Sousa 1984; Turner and Romme 1994), very rapidly begin to develop small-scale divergent canopy structural properties. It has been suggested that as the landscape ages patches begin to "disaggregate" (He and Mladenoff 1999) as fine-scale (10-30 m) gaps caused by wind, insect and disease begin to "chip away" at the canopy (Frelich and Reich 1995b). In old boreal stands canopy gaps may account for over 40% of total forest cover (Kneeshaw and Bergeron 1998). Although gap formation is important in determining landscape complexity, gaps alone do not account for the trends in persistence observed in this study. Significant landscape change resulting from canopy gaps usually takes a century to develop (Frelich and Reich 1995a; He and Mladenoff 1999) whereas change in this study was already apparent at 30 years. This is because fine-scale stochastic disturbances, self thinning and differential growth can dramatically influence surface reflectance without creating a visible gap or visible change in patch structure. Indeed, 35% of fallen trees and 40% of damaged trees in a stand may not contribute to gap formation at all (van der Meer and Bongers 1996). This represents a significant change in canopy structure not visible using traditional photographic and mapping approaches. Persistence as measured using Landsat is able to detect these small-scale changes, providing information regarding landscape complexity that would otherwise

be unavailable (Rey-Banayas and Pope 1995). The results of this study suggest that dynamic processes in the boreal forest canopy are continuous and cumulative, affecting change long before visible gaps appear.

A conceptual model of the mechanisms determining spatial persistence in the boreal forest is presented (**Figure 5.4**). In the boreal forest, intense landscape level fires followed by post fire propagule dispersal result in the establishment of large uniform patches (Sousa 1984; Pickett et al 1987; Turner and Romme 1994). However, post-fire vegetation spatial pattern is somewhat anti-persistent, reflecting the stochastic aspects of chance establishment and propagule availability. Within a very short time period, small scale stochastic processes begin to change the post-fire landscape pattern (Hall et al. 1991; Frelich and Reich 1995a). Many of these small scale disturbance (e.g. branch and individual treefall) may not create gaps, instead only local patterns of stem and branch densities are altered (van der Meer and Bongers 1996). After 30 years (**Figure 5.4b**), intrinsic factors such as self-thinning (Kenkel 1986) and differential growth rates, as well as extrinsic disturbances such as lightning strikes (Ganström 1993) and windthrows (Dyer and Baird 1997; Tang et al. 1997), begin to alter canopy patch structure. These gaps accumulate comprising 7% of forested canopy at 40 years of age to 40% for sites older than 200 years (Kneeshaw & Bergeron 1998). Differential seed availability, advance regeneration, herbivory, and pathogens may result in species replacements in area occupied by the gap (Heinselman 1973; DeGrandpré et al. 1993; Galipeau et al. 1997). As the landscape accumulates a hierarchy of disturbance effects, its spatial pattern becomes more anti-persistent (**Figure 5.4c**) and progressively 'chipped away' (Frelich and Reich 1995a,b). As the system ages, it becomes dominated by spatially asynchronous stand dynamics (Johnson et al. 1995).

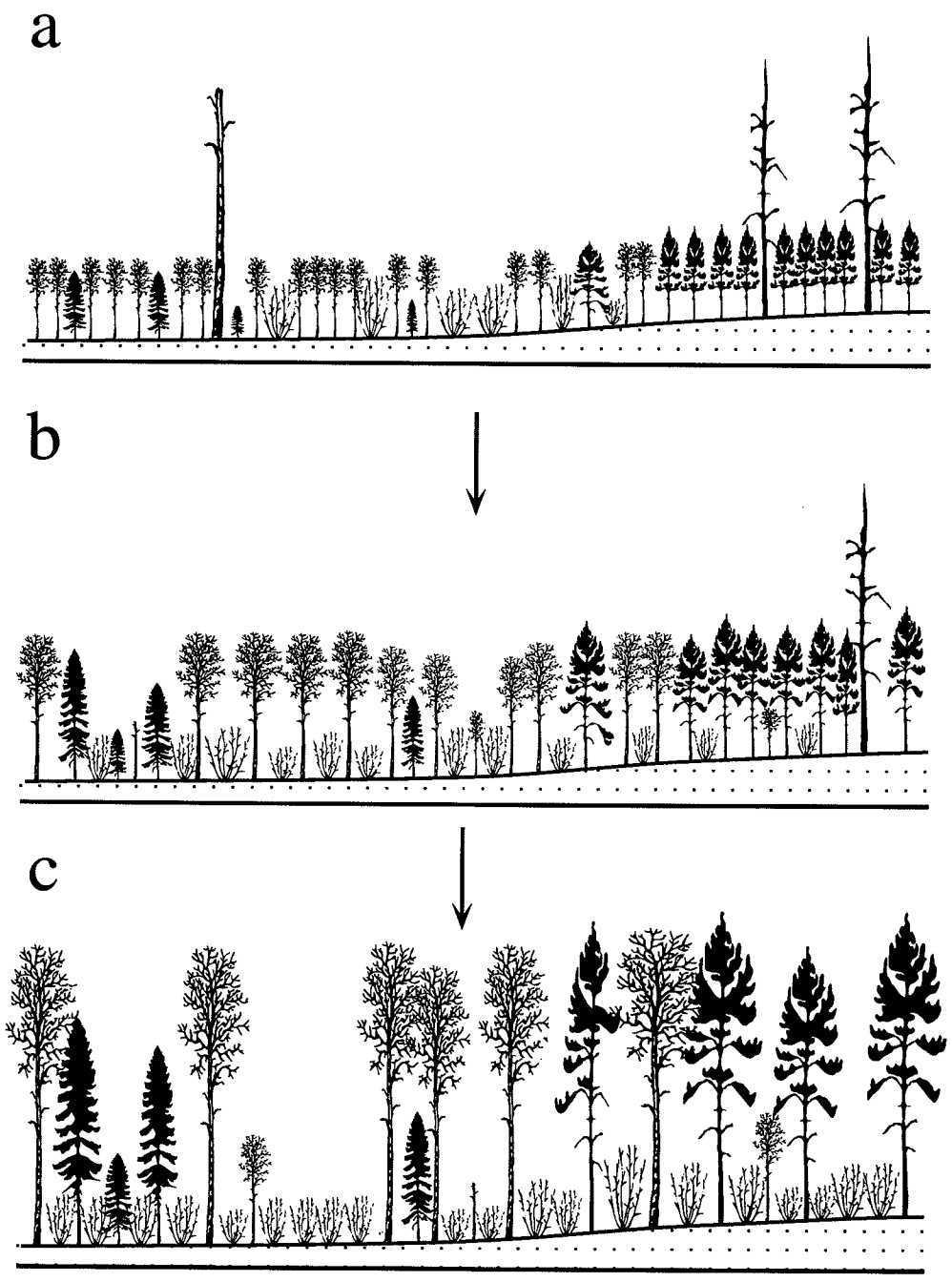

Figure 5.4: Illustrative model showing the break-up of the boreal canopy over time: a) 10 years, initial post-fire colonization in uniform patches with some chance establishment and species mixing; b) 50 years, mortality (from self-thinning and disturbance) and differential growth result in change canopy structure without forming gaps; c) 120 years, the development of a gap dominated canopy with high spatial anti-persistence with patches that differ in floristic composition and structure.

5.7 Conclusion

As stands age, the accumulation of independent stochastic disturbances results in the loss of shared 'memory' at the landscape-level. Canopy properties such as primary productivity, tree age, size structure and density become spatially asynchronous. This has implications for forest management: suppression of large scale fire events may result in the fragmentation of forest stands and increased spatial heterogeneity (Baker 1992b). While some authors link increased complexity with higher biodiversity (e.g. Sugihara and May 1990; Sheuring 1991; Rey-Benayas and Pope 1995), others make the distinction between moderate levels of landscape complexity and complete antipersistence (i.e. $H \rightarrow 1$ vs. $H = 1$; DeCola 1994; With and King 1999). In their view, complexity must have some predictable structure to provide appropriate habitat for organisms. In the absence of some level of persistence, organisms cannot develop a 'global' perception of the environment to forage and disperse effectively. Indeed, simulation studies have indicated that under certain circumstances, systems may become so spatially antipersistent that metapopulations become threatened (With and King 1999). While crown fire has often been cast in a negative light, it is important to recognize the critical role that it plays in determining canopy structure and spatial persistence in the boreal forest. In the absence of crown fire, landscapes dominated by completely asychronous stand dynamics will be a challenge for forest and wildlife management (Cumming et al. 1996).

Chapter 6

Forest Fragmentation and Habitat Loss Following European Settlement in the Riding Mountain Region of Manitoba

Abstract. Human-driven fragmentation of the landscape presents major challenges for conservation. Agricultural fragmentation reduces biodiversity through loss of habitat extent and through restricting movement of individuals to isolated patches or wildlife reserves. In this study, topographic maps and remotely sensed data (LANDSAT) were used to investigate change in forest habitat extent and pattern over three time periods (1950's 1970's and 1991) in the area surrounding Riding Mountain National Park (RMNP) Manitoba, Canada. The impact of agricultural development in a corridor (Grandview Corridor) that historically provided connectivity with Duck Mt. Forest Reserve was also examined. A random transect sampling approach was developed to examine the dispersion of fragmented forest habitat in the region. To assess the loss of connectivity and isolation of habitat along each transect, the fractal 'cluster dimension' was calculated. It was found that forest loss surround RMNP was extensive during the 40 years examined, only half of the forest present in the 1950's remained by the early 1990's. The areas most impacted were to the north and east of RMNP, especially in the Grandview Corridor. Fractal analysis of the landscape pattern indicated that the park is becoming increasingly isolated on the landscape. It was found that intensive agricultural development resulted in fractal patterns of habitat dispersion that were lower in 1991 than in the 1950's. Human patterns of fragmentation in the region ultimately reflected the geometric simplicity of the land survey system, and not natural community patterns.

6.1 Introduction

The relationship between biodiversity and patch size and shape has been well studied (Wright and Hubbell 1983; Frankel et al 1995; Hamazaki 1996). Regions with large contiguous habitat patches have a lower spontaneous extinction rate and are biologically diverse (Debinski and Holt 2000). The global impact of human activities such as farming, forestry and urban development has resulted in fragmentation of natural habitat and is a major threat to biodiversity (Dearden and Rollins 1993; Bayne and Hobson 1998; Barret and Peles 1994; Kruess and Tscharntke 1994). Agricultural development threatens the viability of wildlife populations by both reducing the extent of existing habitat and isolating

the remaining fragments (Skole and Tucker 1993). Isolation limits population dispersal and interactions on these landscapes, resulting in genetic drift (Wauters et al. 1994), reduced competitive ability (Dytham 1995), and disruptions in predator-prey interactions (Kruess and Tscharntke 1994). When regional habitat loss becomes too extensive, the increased energetic cost of foraging and dispersal can result in local extirpation (Andren 1994; Simberloff 1994; Diffendorfer et al. 1995; Collingham and Huntley 2000). Wildlife reserves in regions with intensive agricultural development are often themselves small and isolated habitat 'islands' unable to support viable populations of some species (Frankel et al 1995).

The extent to which agricultural land-use alters landscape pattern has recently been examined in studies combining multitemporal remotely sensed data and GIS analysis (Foster 1992; Turner 1990; Sharpe et al 1987; Skole and Tucker 1993; Jorge and Garcia 1997; Lavorel 1993). Common to all of these studies, is the regular pattern imposed on the landscape by the rectangular grid used to survey property boundaries (Foster 1992; Turner 1990). Because these survey systems were developed without considering natural vegetation and landform patterns, habitat patches are arbitrarily bisected resulting in the rapid loss of habitat contiguity (Sharpe et al 1987). The isolation of forest patches is further accelerated by clearing that often spreads outwards from parallel surveyed transects (Skole and Tucker 1993; Jorge and Garcia 1997). This geometric pattern of development severs the landscape and isolates habitat at an early stage of land clearing, often well before most of the natural habitat has been lost (Foster 1992). These studies suggest that both the pattern of development as well as loss of habitat extent is important in determining the degree of fragmentation and loss of connectivity on agricultural landscapes .

The geometric pattern of habitat loss presents a challenge for measuring and modeling corridor connectivity. Most landscape level studies examining the impact of fragmentation on habitat corridors focus on physical adjacency or 'structural connectivity' among patches, often using a percolation approach (Tischendorf and Fahrig 2000). In a percolating system, connectivity exists when at least one habitat patch (percolating cluster) completely spans the landscape (With and King 1999). For landscapes where both the initial pattern and patch losses are anisotropic, connectivity is lost when habitat extent is reduced below the percolation threshold of 0.59 (With et al. 1997; Lavorel et al. 1993). While percolation models have been suggested as a tool for conservation planning (With and King 1999), they are not readily applicable to landscapes with geometric patterns of habitat loss (Tischendorf and Fahrig 2000). Indeed, the influence of patch geometry on connectivity is not well

understood (Lavorel et al 1993) and alternative methods to assessing isolation and connectivity have been recommended (Tischendorf and Fahrig 2000; Lord and Norton 1990).

Recent studies have begun to consider the relationships between connectivity, pattern and scale (Keitt et al. 1997; With and Crist 1995; Lavorel et al 1994; Milne et al. 1992). For moving organisms, detection of pattern is scale-dependent: smaller species 'perceive' the environment differently than large organisms (With 1994a; Johnson et al 1992) and will alter dispersal and foraging movements accordingly (With and Crist 1995). Thus, connectivity has spatio-temporal properties that are not restricted to a single scale (Lord and Norton 1990; Keymer et al 2000). The scaling properties of habitat patches are critical in predicting species response to landscape fragmentation (With 1994b). Fractal mathematics (Mandelbrot 1983), provides a tool that can be used to quantify and describe the scaling properties of habitat fragmentation in disturbed landscapes (Hastings et al. 1982; With 1994b). Several studies have used fractal measures to examine patch complexity on agricultural landscapes (Krummel et al. 1987; Sharpe et al 1987; Leduc et al. 1994). While these studies suggest that agricultural development reduces the complexity of individual habitat patches, little research has been done examining how these changes effect habitat pattern and connectivity along wildlife corridors.

6.2 Objective

In this chapter, historical changes to the spatial extent and dispersion of forest fragments are examined for the agricultural landscape surrounding Riding Mountain National Park. A combination of topographic data and remotely sensed Landsat imagery was used to develop a multitemporal GIS database covering three time periods (1950's, 1970's and 1991). From these data, forest fragmentation and loss of habitat extent were measured at the regional scale and subsampled within a corridor (Grandview corridor) that links the Park with adjacent protected forests. A random transect sampling approach was developed to examine fractal patterns of habitat patch dispersion and isolation surrounding the Park. In assessing the impact of agricultural development in the Riding Mountain region, the following questions are addressed:

1. How has the spatial extent of forest habitat changed in the region?

2. Is the dispersion of forest habitat patches on agricultural landscapes fractal?

3. Does the spatial dispersion of forest patches change in a predictable way as habitat fragmentation increases on agricultural landscapes?

6.3 Study Area – See Chapter 2

6.4 Materials and Methods

Image Processing

Fragmentation and loss of forested land in the Riding Mountain region was determined over three time periods: 1) the 1950's (based on 1954-57 photogrametry); 2) the 1970's (based on 1971-74 photogrametry); 3) the 1990's (from a 1991 Landsat image). For the first two time periods (1950's and 1970's) initial forest-habitat maps were obtained by digitizing and combining 1:250,000 scale and 1:50,000 topographic maps (Government of Canada, National Topographic System). These maps distinguish between forested (coded green) and non-forested regions at the landscape level. Forest cover on the topographic maps was carefully checked using aerial photographs and was found to be accurate, however it was noted that forest patches less than 2 ha were not mapped. Most of these small patches were planted shelterbelts around farms and were not included in this study.

The forest-habitat map for the 1990's was produced from Landsat imagery using bands 3 (red: 0.63-0.69 μm), 4 (near infrared: 0.76-0.90 μm), and 5 (mid infrared: 1.55-1.75 μm). Image preprocessing by Radarsat International included radiometric correction to eliminate variability in sensor response ('destriping'; Richards 1993), and a bit error reduction. To correct for residual atmospheric effects a dark order subtraction based on a path irradiance model of λ^{-4} was performed (Chavez 1988). Image classification involved the selection of 24 ground-verified training areas representing three forest vegetation classes (deciduous, coniferous, and mixed forest). A supervised classification of the image was performed using a maximum likelihood classifier (Richards 1993). Classification accuracy (by training site resubstitution) was over 95%. As a final step, isolated forest fragments less than approximately 2 ha in extent (25 pixels) were removed to ensure that the Landsat forest map was comparable to the topographic maps.

The final raster maps were input into the GIS package GRASS 4.0, registered to the NAD27 grid system (Zone 14) and centred at 5630.7 km N by 401.7 km E. Each GIS

database layer was 140 km by 185 km in size with a pixel resolution of 30 x 30 m (**Figure 2.1**). In the area historically occupied by the Grandview Corridor, a subset of the imagery 36 x 27 km in size was selected. The lower edge was oriented along the north-west boundary of RMNP and the upper along the southern boundary of Duck Mt. Prov. Forest. The Grandview corridor subset imagery was centred at 5668.3 km N by 366.5 km E (**Figure 2.1**).

Change in Forest Extent

To examine the change in the extent of forest cover at the regional scale, the study area was stratified into 4 non-overlapping components defined by the main compass directions (N, E, S, W). The strata were created by dividing the imagery from each corner (SW to NE; NW to SE) to form four triangular areas. For example, the 'south' strata is a triangle with its apex centered in Riding Mountain National Park and its base oriented with the southern edge of the study region. This stratification was undertaken since the four compass 'edges' of the Riding Mountain National Park region differ in their physiography, vegetation and disturbance history. In the Grandview Corridor, change in the extent of forest cover was measured over the entire subarea. For both the region and corridor imagery the forest in reserve areas (i.e. RMNP and Duck Mt. Prov. Forest) was masked-out such that only 'unprotected' forest on the agricultural landscape was examined.

Change in Dispersion of Forest Fragments

To assess the fragmentation of forest habitat, a transect sampling protocol was used (see Shiyomi and Yamamura 1993; Leduc et al 1994). Transects 30 m wide (i.e. 1 pixel width) were generated by linking a random 'starting' point within RMNP to a random 'exit' point chosen along the edge of the imagery. Length varied as only the contiguous portions of transects within the agricultural landscape were analyzed. Forest inside of the reserves were not included in the sampled transects. Each transect 'exiting' RMNP was terminated when either: (1) it intersected a waterbody; (2) it intersected the boundary of the Duck Mt. Reserve; or (3) it reached the edge of the GIS layer. At the regional scale, the transects were stratified by main compass direction (N, E, S, W) based on the location of the exit points. For the regional scale, one hundred transects were selected for each of the strata on the 1950's layer (400 transects) and then revisited in subsequent time periods (400 x 3 = 1,200 transects). These transects varied in length from 15 to 130 km (mean length 52 km). In the Grandview Corridor, one hundred transects were chosen on the 1950's layer and then

revisited in each of the subsequent time periods (100 x 3 = 300 total transects). Transect lengths varied from 25 to 35 km in the Grandview corridor (mean length 30 km).

Forest fragmentation along the transects was assessed by measuring three parameters: (1) proportion of forest cover (calculated as the total number of forested pixels along a transect divided by the length of the transect in pixels); (2) mean forest patch intercept length (determined by counting the number of consecutive adjacent pixels in each patch and then calculating the mean); (3) the cluster fractal dimension.

The cluster fractal dimension approach for measuring isolation/clustering is based on the Cantor set (Smalley et al. 1987; Turcotte 1997 p. 100). Consider a binary sequence (pixel transect) of length L, in which each pixel is coded as either forested (Black=1) or non-forested (White=0: **Figure 6.1**). If forest patches on the landscape are scale-invariant, the proportion P(r) of steps of length r that include at least one forested pixel scales as:

$$P(r) = r^{(1-D)} \qquad \textbf{[Equation 6.1]}$$

where the fractal dimension (D) is interpretable as the "strength of clustering" (Smalley et al. 1987), ranging from D=0 (highly clustered and isolated) to D=1 (unclustered; Turcotte 1997 p.103.). The cluster fractal dimension is determined from the slope of the power-law relation:

$$\log P(r) = (1 - D) \log r \qquad \textbf{[Equation 6.2]}$$

In this study, the linear range of r-values retained for calculation of the slope corresponded to a scale between 0.1 km - 2 km on the landscape. All regression slopes were statistically significant ($r^2 = .98$ for most transects).

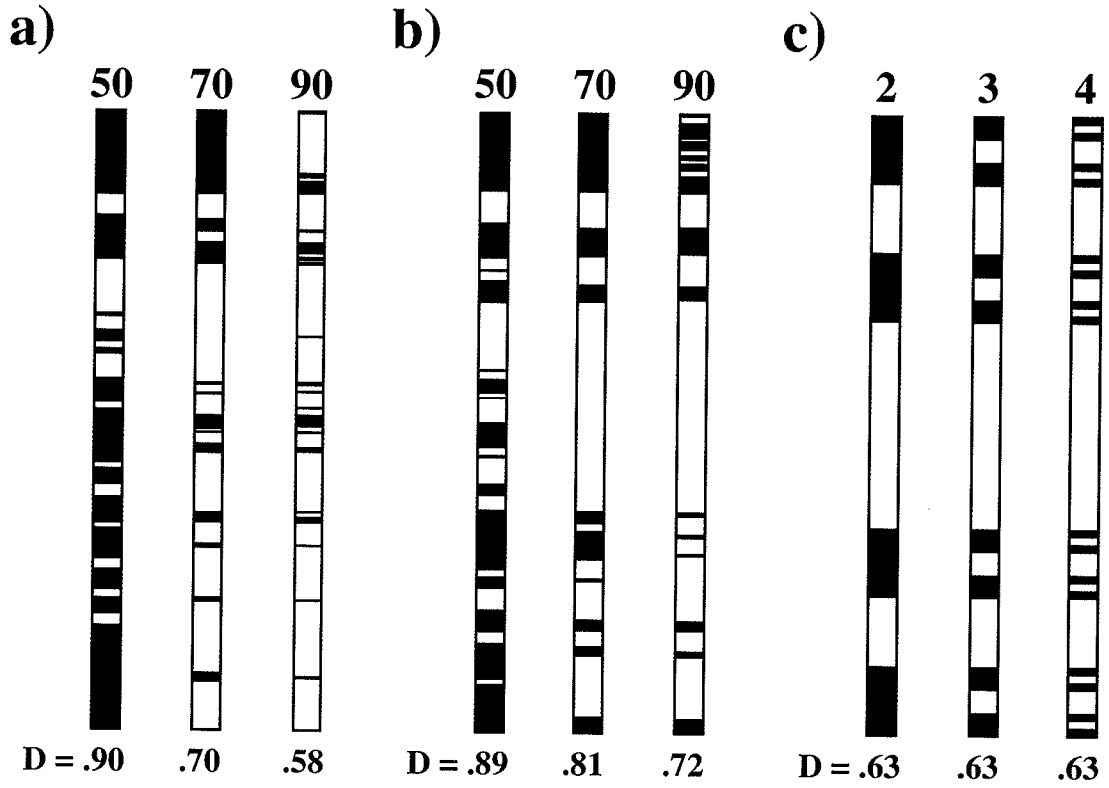

Figure 6.1: Forest fragmentation along random transects compared with a Cantor point process (black pixels). a & b) examples of matched random transects (i.e. same transect revisited in the 1950's, 1970's and 1991) from the corridor between RMNP and Duck Mt. (black pixels represent forest); c) First 3 iterations of a regular Cantor fractal process. The cluster fractal dimension for the dispersion of "black" pixels is given beneath each "transect."

Landscape metrics often overestimate the degree of clustering when class frequency is low, even when pattern is completely random (Gustafson and Parker 1992). The theoretical maximum for the cluster fractal dimension is D=1 (a random pattern) however, in practice the upper limit of D is a function of frequency (Milne 1988; Hargis et al. 1998). Because the proportion of habitat along the transects changed over time, it need to be established that estimates of D were not confounded by class frequency. This was done by comparing the estimates of D with those generated by a randomization procedure (*sensu* Manly 1991). For each transect the class frequency was kept constant while the locations of forest habitat pixels was randomized. The mean cluster fractal dimension was then calculated from these 'null landscape' transects and then compared with the observed fractal dimensions.

A randomization approach was also used to test for differences in the transect parameters across the three time intervals (following Manly 1991: 64). Each randomization involved reassigning the observed parameter value for a transect (e.g. mean intercept length along a transect in 1950) to one of the three time intervals ('treatments'). After randomization was completed, the between-treatment sum of squares was calculated. Observed between-treatment sum of squares exceeding the maximum value from 5000 randomizations were deemed to be statistically significant.

6.5 Results

Change in Extent of Forest Habitat

The extent of forest habitat in the region surrounding RMNP declined over the forty year period examined in this study (**Figure 6.2a-c.**). Even in the earliest time period, much of the forest had been cleared for agriculture (25% forested in 1950: **Table 6.1**). The proportion of forest remaining in the 1950's varied substantially over the region. To the north of RMNP almost half of the original forest remained (43%) while to the south 92% of the land base was already cleared (a small fraction remained adjacent to the Assiniboine river valley). Between the 1950's and 1970's, increased forest clearing took place over much of the region. Most of the forest loss over this period resulted from the attrition of existing patches (loss of habitat around edges of a patch), although the removal of large forested blocks is evident to the north of RMNP. Habitat loss continued into the 1990's, with the clearing of several large areas. Most noticeable was the loss of forest along the Assiniboine River valley to the west and south of the Park following the completion of the Shellmouth Dam. Agricultural clearing for pastureland to the north and east of RMNP resulted in substantial

forest losses in areas where crop productivity was traditionally low. By 1991 only half of the area forested in the 1950's remained. Indeed, over the period examined in this study the only area where reforestation was observed occurred along the Birdtail River valley to the south of RMNP (compare bottom middle **Figure 6.2a** with **6.2b**).

Similar trends in forest losses were observed for the Grandview Corridor over the three time intervals (**Figure 6.3**). In the 1950's for a nearly contiguous forest corridor existed between Riding Mountain and Duck Mountain (44% forest cover, **Table 6.1**). By the 1970's, forest habitat had declined to 23%. This was largely the result of clearing in the centre of the corridor adjacent to the main highways and rail lines. By 1991 only 14% of the corridor remained forested, much of this occurring along the Valley river. Recent losses along the border of Duck Mountain Provincial Forest are mainly attributable to logging to provide pastureland (top left of 1990's image). In general, it was found that forest closest to the reserves was more likely to be retained over time. Along the border of RMNP very little forest has been lost over the last 40 years (64.7% of the border had adjacent forest in 1950 and 57.8 % in 1991). Agricultural development was more intense towards the center of the Grandview Valley, effectively bisecting the landscape.

Change in dispersion of forest habitat

Over the forty year period, forest habitat along transects exiting RMNP declined. (**Table 6.1**). Forest habitat varied throughout the region. In the 1950's one third of the transects to north and east of the Park had a forest cover greater than 40%, while transects in the south had the least (**Figure 6.4**). In the 1950's the proportion of forest per transect was highest in the Grandview Corridor, with most sample transects exceeding 50% cover. Between the 1950's and 1970's a rapid shift in the proportion forest along the transects is evident. When these transects were revisted in the 1970's, nearly all of the sampled transect had a cover of less than 50%. These trend continued into the 1990's, consistent with the those observed for the loss of forest extent (**Table 6.1**). Randomization tests indicated that these changes were significant: observed between-treatment sums of squares exceeded the maximum value from the random distribution (**Table 6.2**).

Patch intercept lengths along the transects also declined over the forty years examined in the study. Mean forest intercept length in the region surrounding the Park was 1.02 km in the 1950's but by 1991 it was 0.42 km (**Table 6.1**). A similar pattern is observed for the Grandview Corridor where mean patch intercept length declined by two thirds between the

1950's and 1991. Both attrition along patch edges as well as the bisection of existing forest habitat resulted in the decline in mean patch 'size.' Randomization tests indicated that these changes were significant: observed between-treatment sums of squares exceeded the range of the random values. The corresponding cumulative frequency plots summarize these trends (**Figure 6.5**). The general shape of the curve and the location of the sill indicates that the probability of encountering smaller patches is greater in 1991 (sill ≈ 2 km) than the 1970's (sill ≈ 5 km) and 1950's (sill ≈ 9 km). The sharpest decline in mean patch intercept length occurred in the Grandview Corridor (10 km in 1950's down to 2 km in the 1990's).

Patch dispersion along the transects became increasingly clustered between the 1950's and 1991 (**Table 6.1**). The mean cluster fractal dimension for the entire region declined (D = 0.81 in 1950's, 0.76 in 1970's, 0.65 in 1990's), and a similar trend was observed for all transects exiting RMNP (**Figure 6.6**). The patch dispersion in the Grandview Corridor was most impacted by agricultural development (D = 0.87 in the 1950's declining to 0.69 by 1991). Fractal clustering on the landscape was not a function of random association among pixels: the observed values of D were less than those calculated for the null landscapes. Indeed, the difference in the cluster dimension between the actual transects and the randomized transects increased over time, indicative of non-random clustering. Change in proportion of habitat was therefore not confounding estimates of the cluster fractal dimension. A randomization test of the differences across the time periods indicated that the changes observed were significant (**Table 6.2**).

Table 6.1: Habitat loss and fragmentation summary statistics for the region surrounding RMNP (blocked by principal compass direction) and for the Grandview corridor. Percent loss of forest habitat aerial extent surrounding RMNP and means for the transect parameters measured (±std.err.).

	Forest Extent	**Transect Parameters**		
	Percent Forested	***Proportion Forest/Transect***	***Forest Intercept (km)***	***Cluster Dimension***
1950				
N	27	.30 (.015)	1.074 (.052)	.808 (.008)
E	43	.40 (.015)	.917 (.038)	.818 (.008)
S	8	.18 (.011)	1.142 (.042)	.810 (.007)
W	21	.23 (.010)	.925 (.043)	.802 (.005)
Total	25	.28 (.008)	1.015 (.023)	.810 (.070)
1970				
N	20	.21 (.011)	.813 (.045)	.766 (.010)
E	33	.31 (.013)	.789 (.038)	.777 (.009)
S	7	.16 (.008)	.831 (.042)	.760 (.009)
W	17	.17 (.007)	.597 (.027)	.756 (.007)
Total	19	.21 (.006)	.757 (.020)	.762 (.090)
1990				
N	13	.15 (.009)	.491 (.022)	.663 (.012)
E	26	.22 (.011)	.414 (.017)	.687 (.012)
S	5	.13 (.007)	.423 (.017)	.642 (.012)
W	8	.10 (.006)	.348 (.021)	.615 (.010)
Total	13	.15 (.005)	.419 (.010)	.651 (.117)
Corridor				
1950	44	.49 (.013)	1.284 (.039)	.870 (.004)
1970	23	.25 (.011)	.861 (.035)	.804 (.009)
1990	14	.16 (.007)	.474 (.017)	.694 (.010)

Table 6.2: Observed between-treatment sum of squares compared with random expectation for the three transect variables (mean and maximum values for 5000 randomizations).

	Prop. Forest			***Patch Intercept***			***Cluster Fractal***		
	Random		***Obs.***	***Random***		***Obs.***	***Random***		***Obs.***
	Mean	*Max.*		*Mean*	*Max.*		*Mean*	*Max.*	
North	.16	.30	1.13	2262.15	4232.72	18984.22	.14	.23	1.12
East	.20	.59	1.56	1853.34	3175.31	15202.94	.12	.23	.89
South	.08	.14	.17	760.73	1470.45	28835.83	.15	.30	1.49
West	.08	.16	.76	1590.40	2929.48	18653.13	.15	.28	1.89
Corridor	.39	.86	5.80	2152.12	4826.59	36432.56	.11	.22	1.59

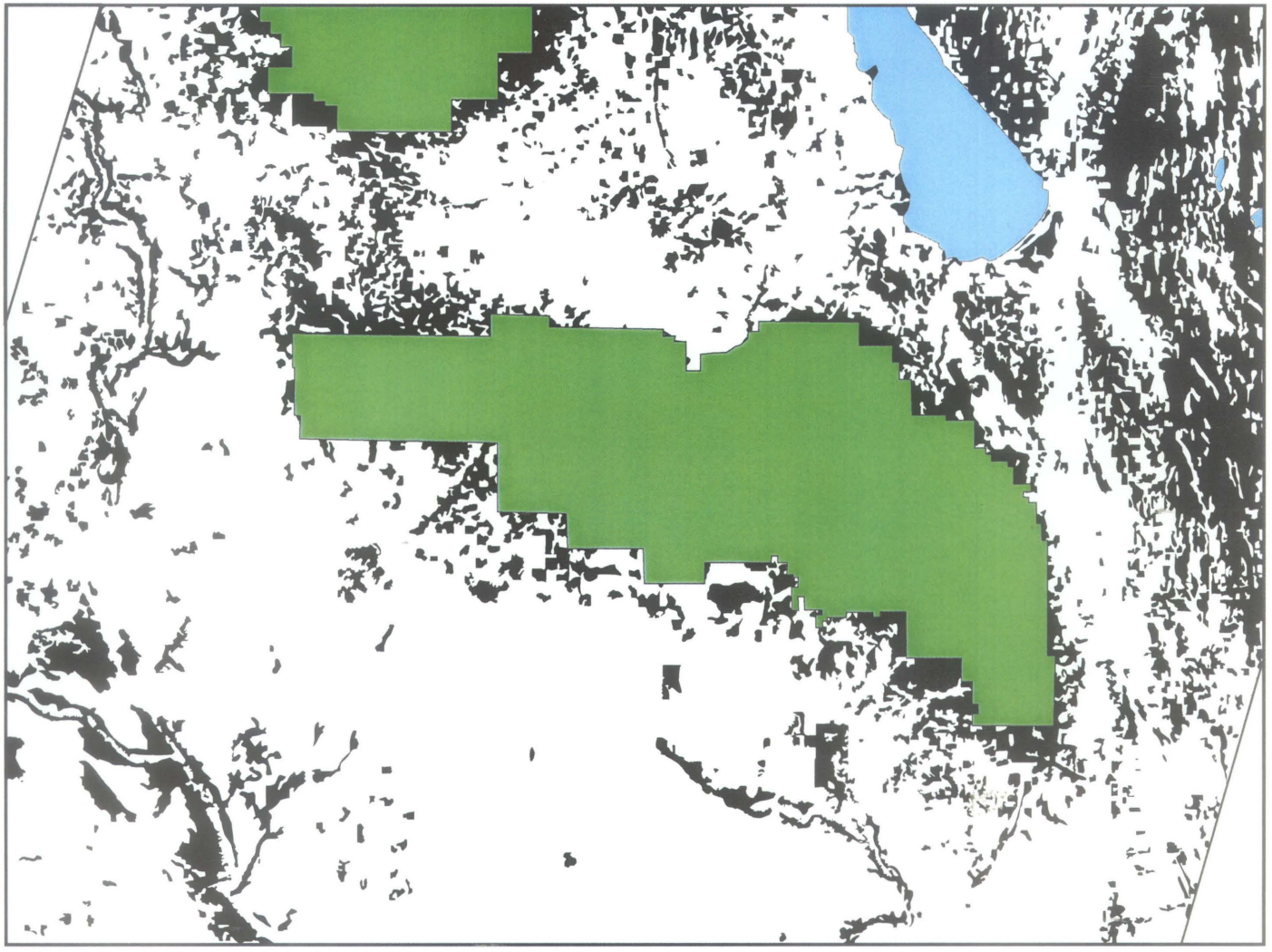

Figure 6.2a: 1950's map of forest habitat extent (black areas) in the region surrounding RMNP. Areas cleared for agricultural development are white; lakes and forest reserves are grey.

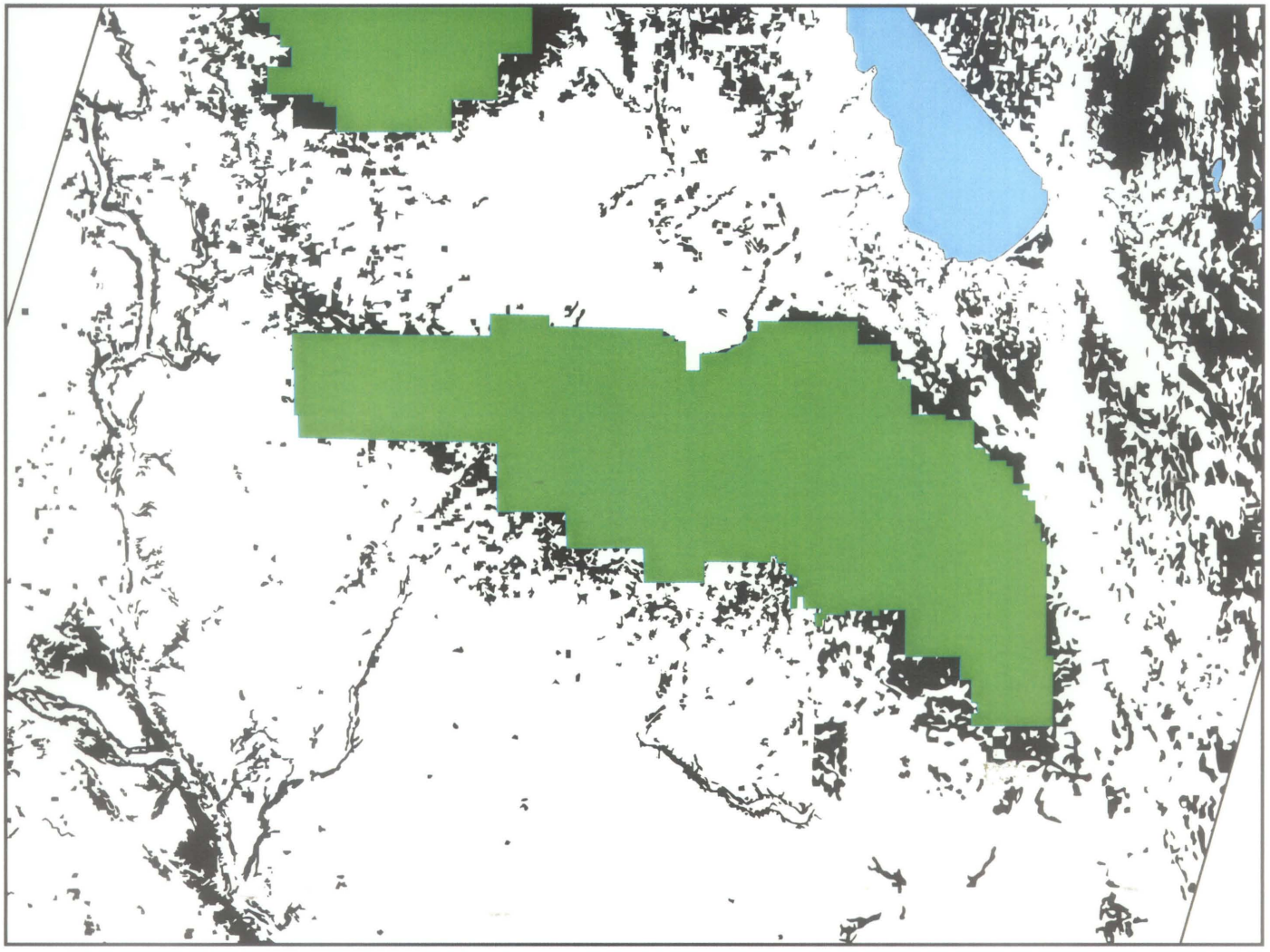

Figure 6.2b: 1970's map of forest habitat extent (black areas) in the region surrounding RMNP. Areas cleared for agricultural development are white; lakes and forest reserves are grey.

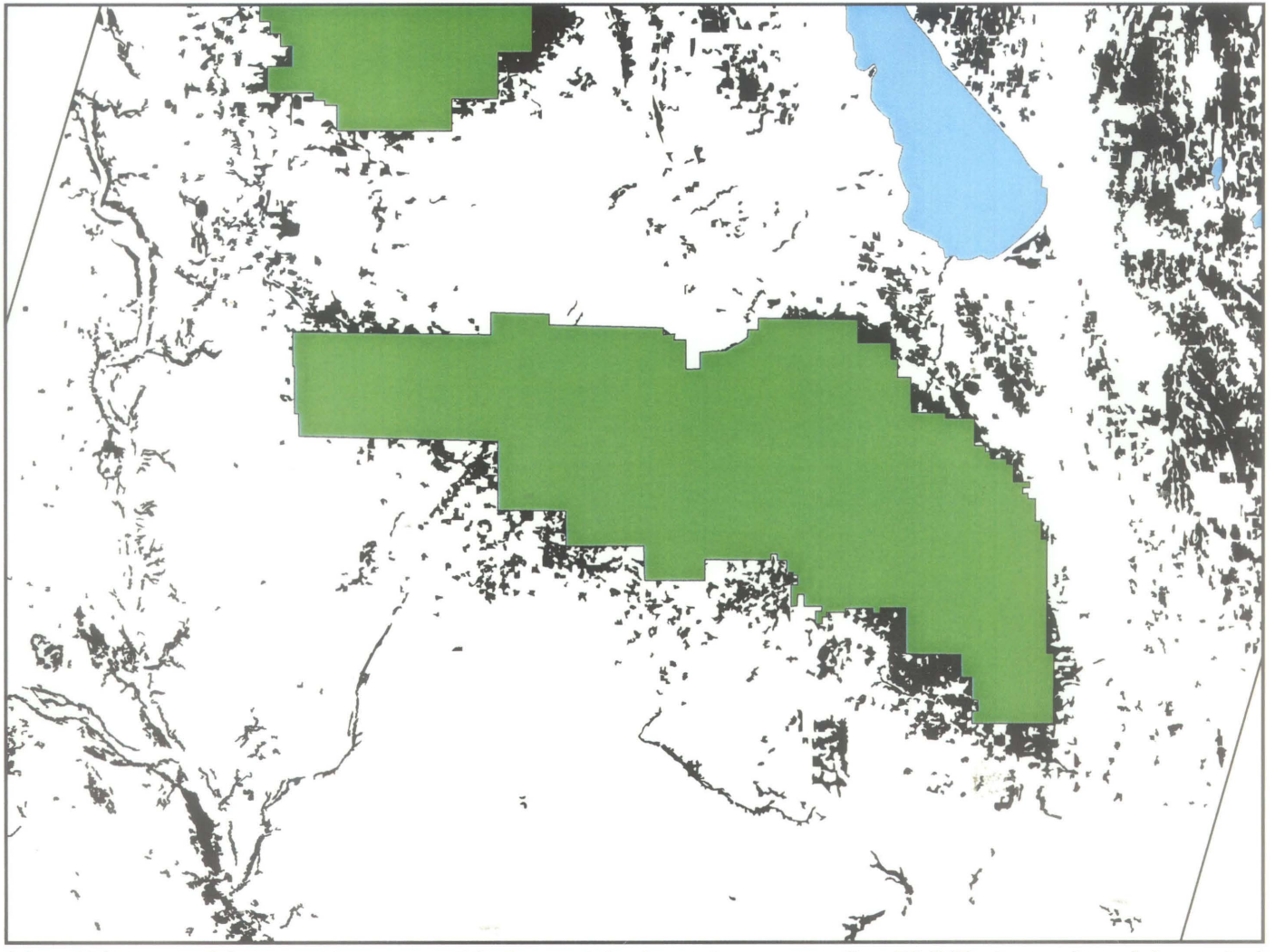

Figure 6.2c: 1991 map of forest habitat extent (black areas) in the region surrounding RMNP. Areas cleared for agricultural development are white; lakes and forest reserves are grey.

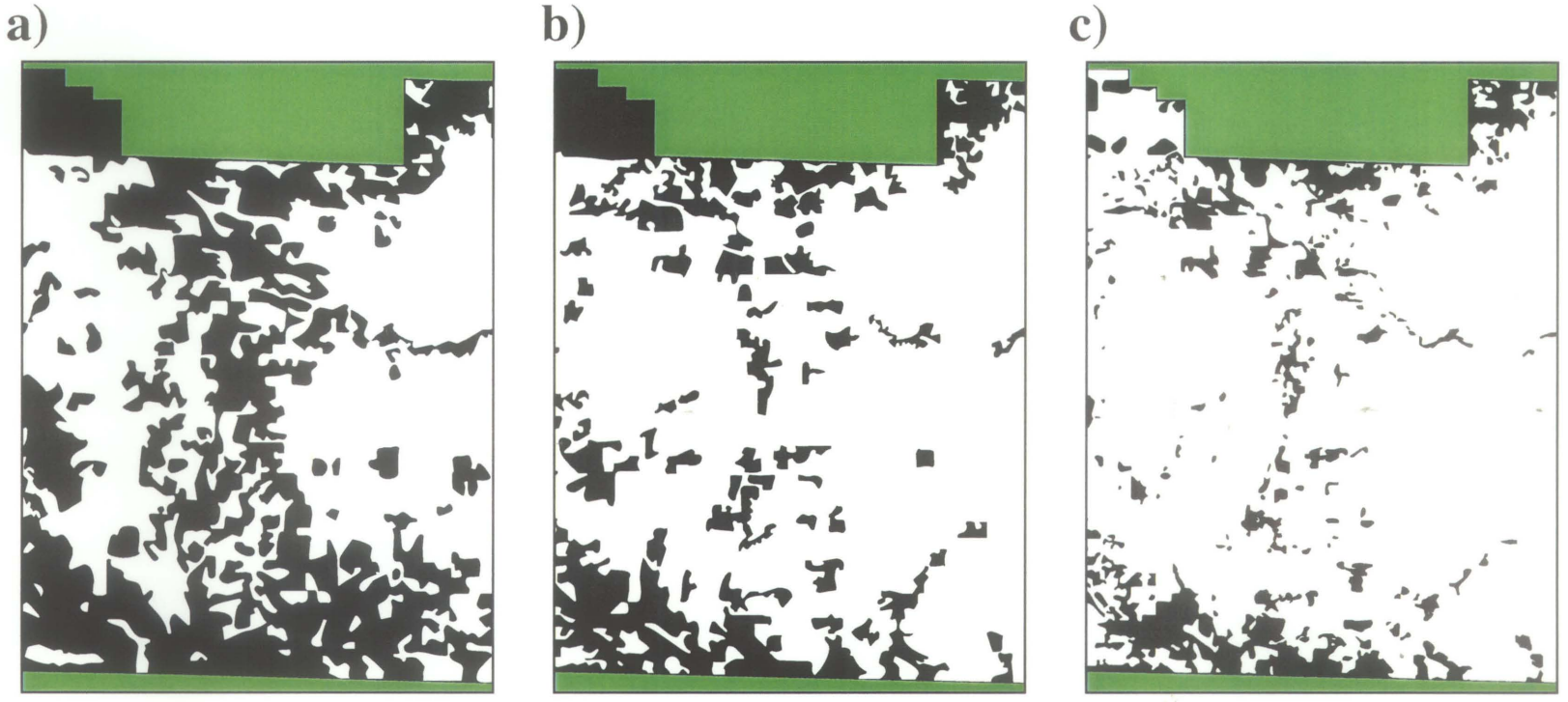

Figure 6.3: Maps showing loss of forest extent (black areas) between RMNP and Duck Mt. for: a) 1950's; b) 1970's and c) 1991. Areas with agricultural development are white and forest reserves are grey.

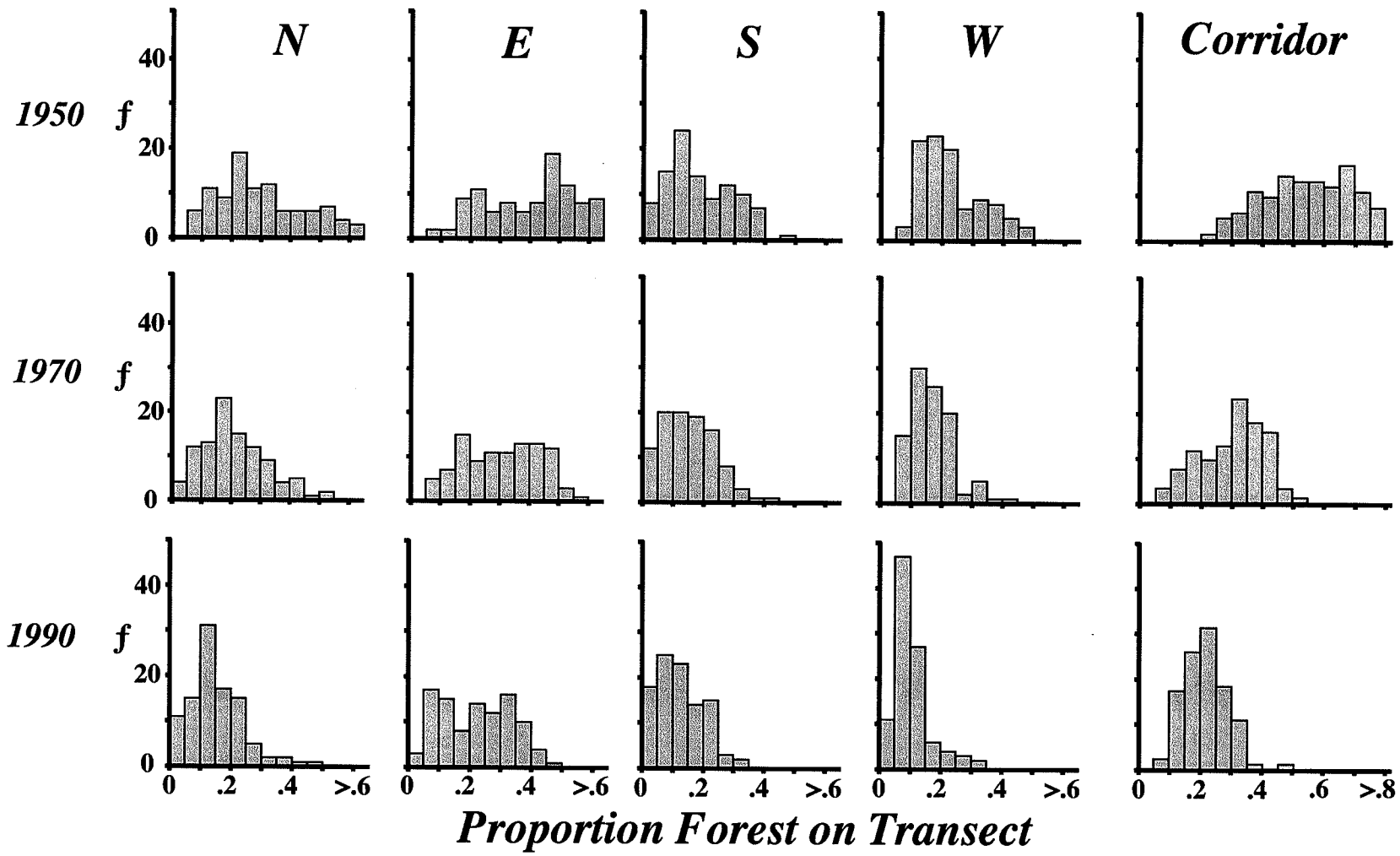

Figure 6.4: Frequency histograms giving the proportion of forested habitat along random transects in the region surrounding RMNP stratified by principal compass direction (N, E, S, W) and in the Grandview corridor.

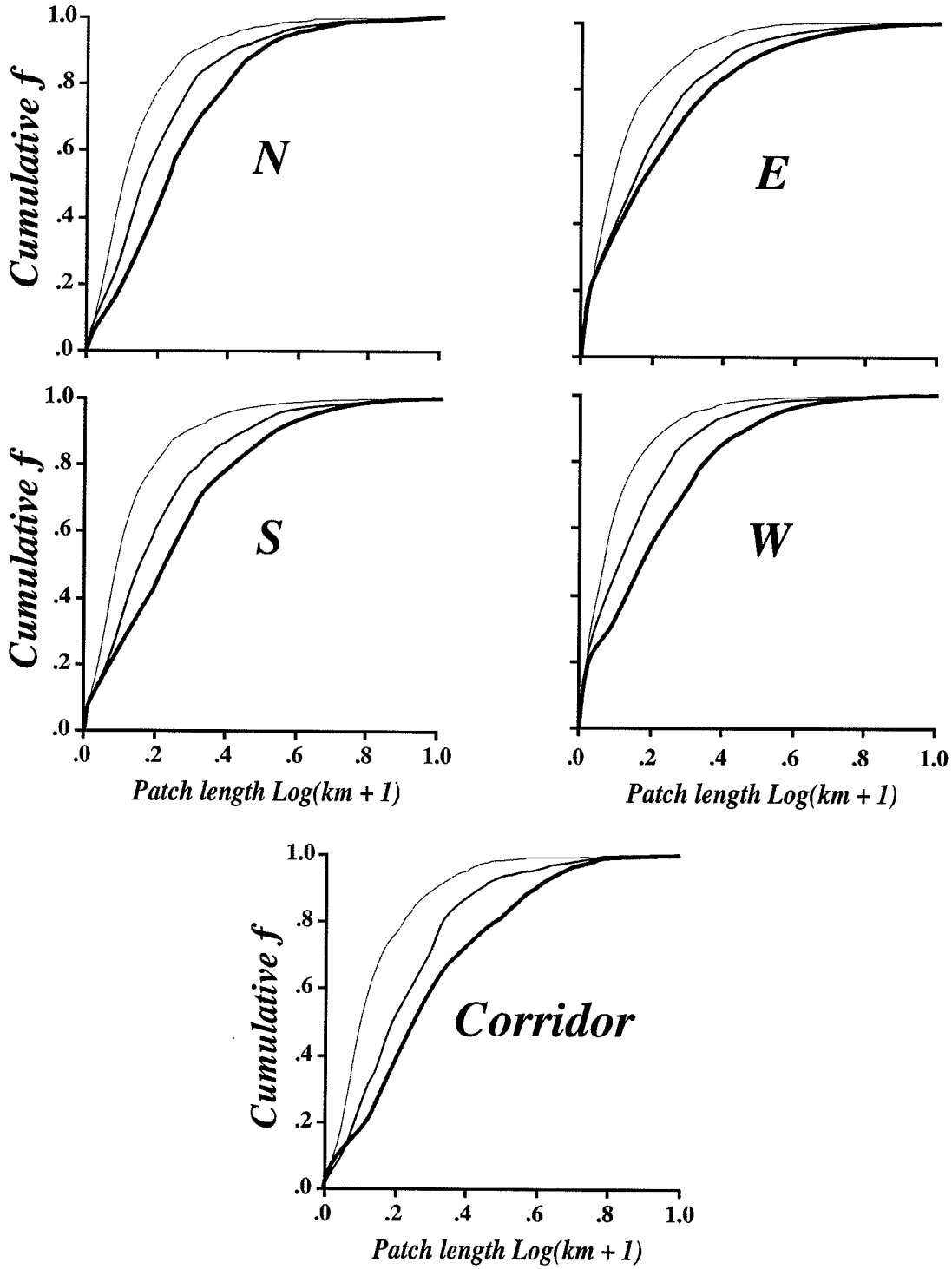

Figure 6.5: Cumulative frequency against log forest intercept length (km +1) for the random transects in the region surrounding RMNP and in the Grandview corridor. Time periods are indicated by line thickness: 1950's (thick); 1970's (medium) and 1991 (thin). Transect results are blocked by principal compass direction and a pooled frequency plot is presented.

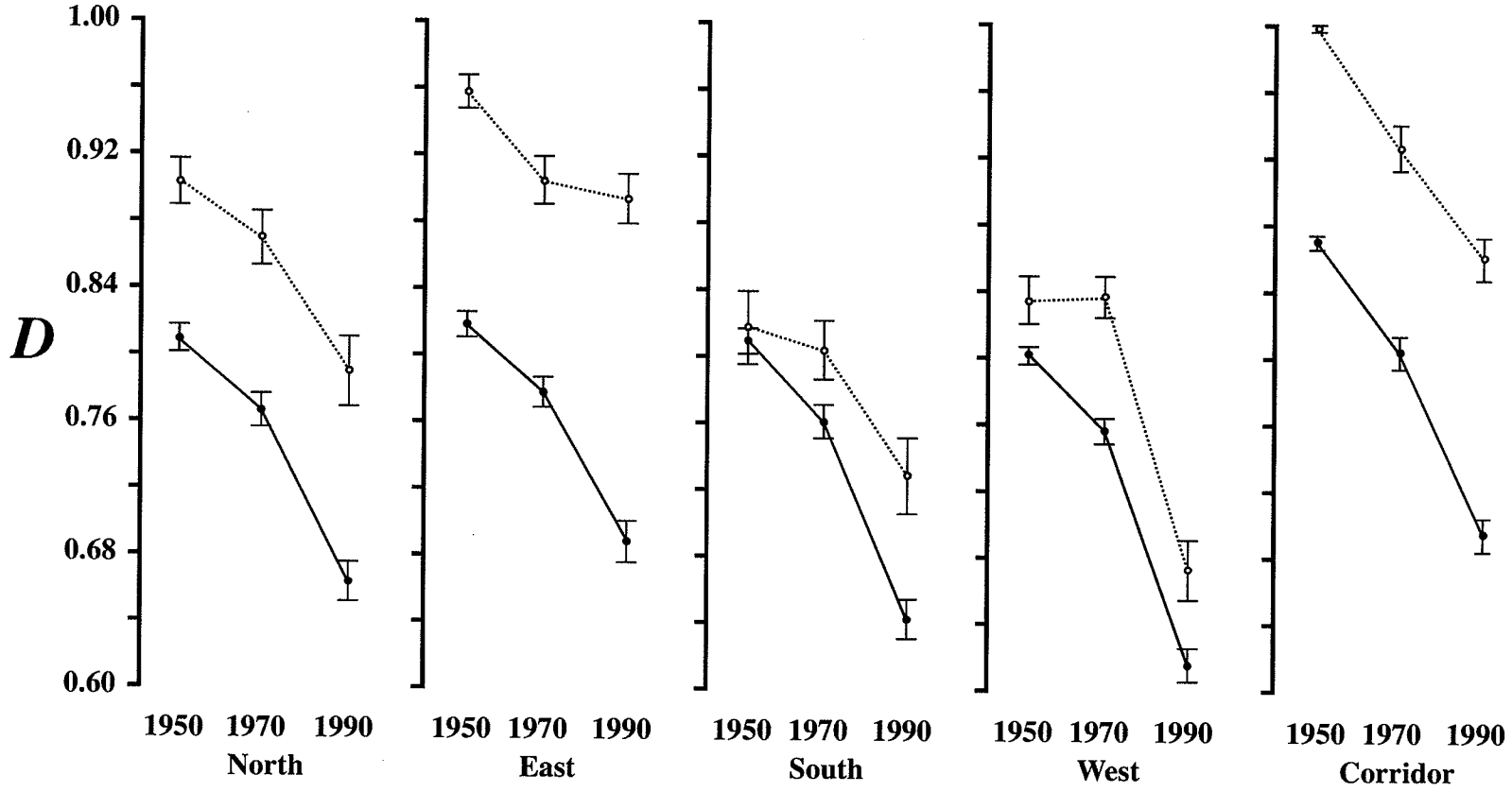

Figure 6.6: Mean cluster fractal dimension for the random transects in the region surrounding RMNP and in the Grandview corridor (filled circles, solid lines) and the randomized transects (dashed line, open circle). Standard deviation is also shown (bars).

6.6 Discussion

Assessing Habitat Loss in the Agroecosystem using GIS

Significant forest habitat loss and fragmentation in the Riding Mountain region occurred over the 40 year period examined. However, reconstruction of historical change in habitat cover using GIS requires the use of multiple data sources (e.g. satellite vs. topographical maps) which can potentially confound the results (Bettinger et al 1996; Jelinski and Wu 1996). For instance, topographic maps are produced using interpreted photogrammetric imagery and are initially stored as vector data, whereas satellite sensors sample reflected solar radiance along predetermined rasterized scan lines (Richards 1993; Fisher 1997). These distinct sampling approaches can result in statistically significant differences in ground cover classification (Bettinger et al. 1996), often refered to as the Modifiable Areal Unit Problem (MAUP: Jelinski and Wu 1996). Data representation can also have important consequences for patch shape: vector imagery retains smooth boundaries between adjacent classes (Bettinger et al 1996), while satellite sensors 'blur' any sub-pixel edges (Fisher 1997).

In this study a number of steps were taken to ensure that the changes measured were the result of historical landscape fragmentation dynamics and not differences between data sources. To facilitate comparisons across GIS layers, these data were converted to a single raster format and registered to a common datum. By performing this step, the long-term fate of individual landscape patches could be followed, which is often not possible with historical data (Turner 1990). These layers were then examined against aerial photographic sources from their respective time periods and found to match closely. While vector to raster conversion can affect changes in patch shape and size (Bettinger et al. 1996), overall patch shape was similar between the topographic and satellite data layers. To avoid potential bias however, edge or shape based measures of spatial complexity such as perimeter-area were not used in this study (e.g. Krummel et al 1987; Jorge and Garica 1997).

Change in Forest Extent

Before settlement by Europeans the landscape along the Manitoba escarpment was contiguous with the boreal forest in the north and the aspen parkland and grasslands to the south (Bird 1961). However, current encroachment of farmland to the edge of RMNP is so severe that much of the boundary of RMNP is visible from space (Dearden and Rollins

1993) and structural connectivity with other wild areas has been completely severed (**Figure 6.1c**). These patterns of forest loss are similar to those observed in the literature. Deforestation from agricultural clearing in Brazil resulted in rapid isolation and spatial concentration of undisturbed habitat during land development (Skole and Tucker 1993). There, large forest stands became isolated and surrounded by highly fragmented edge dominated patches within 10 years of initial clearing. Similar patterns of land use have been reconstructed in eastern North America (Foster 1992). In Massachusetts, peak logging and clearing occurred adjacent to roadways, rapidly leading to the removal of all but 25% of the original forest. Indeed, the rate at which forest is fragmented can often exceed the loss of forest extent (Skole and Tucker 1993). In this study, it was found that forest losses were concentrated in areas easily accessed by roads, resulting in habitat fragmentation. Once access roads or railways bisect the natural landscape, a paradigm shift takes place: structural connectivity is almost immediately lost and remaining natural habitat becomes fragmented. The impact of this process is especially evident in the Grandview Corridor, nearly all of the forest adjacent to the main highway and railway system is now developed for agriculture.

In the Riding Mountain region, clearing for grain crops resulted in rapid loss of natural habitat during the period of high immigration during the late 1800's to early 1900's (Carlyle 1996). This conversion of forest cover to agricultural land continued until well after the 1950's, especially in the rich river valleys to the north and southwest of the Park. In this area, farming is almost exclusively field crops with yields well above provincial average (Weir 1983; Carlyle 1996). Forest losses east of RMNP were likely the result of increased livestock production. Poor drainage limited the rate of initial agricultural clearing in this area, however the establishment of new community pasturelands has recently accelerated forest loss (80% of the farmed land base east of RMNP is now in pastureland, Carlyle 1996). It has been found that the order and timing of land development is often associated with soil productivity. Clearing for crop production generally begins on rich soils followed by development for livestock in poor soils (Turner 1990; Sharpe et al 1987). In the Riding Mountain region, the combined effects of grain and livestock production has resulted in a small percentage of remaining forest habitat (13%) in woodlots and riparian refugia.

Forest patches consistently retained in the study area were almost always directly adjacent to rivers. Primary woodlands are often associated with poorly drained soils where agricultural development is not possible (Foster 1992; Turner 1990). In the study area, little forest clearing has taken place along the larger flood plains and steep embankments of the upper Assiniboine, the Shell and Valley Rivers. Some of the largest and most visually

complex remnant forest patches are along these rivers (**Figure 6.2**). Large complex remnant patches (Krummel et al. 1987; Sharpe et al. 1987) often typify flood plains, which are 'protected' from development by seasonal flooding. The importance of flooding in preserving these fragments is may be inferred from the rapid loss of forest after the construction of the Shellmouth Dam on the Assiniboine river. Following its completion in the early 1970's (Welsted 1996), farming was extended onto the Assiniboine floodplain southwest of the park. The loss of habitat in these areas is particularly critical as they function both as corridors as well as in maintaining regional biodiversity (Naiman et al 1993; Franklin 1993; Lord and Norton 1993). The remaining riparian forest fragments surrounding RMNP are locally connected, but no longer provide corridors at the regional scale or within the Grandview valley.

The shape of the remaining forest fragments in the region reflect the geometry of the land survey system rather than landform. For instance, glacial striations with a ridge and swale topography predominates in the area east of RMNP, however many of the remaining forest patches are square. Similar trends were observed in Cadiz township Wisconsin, where nearly all remaining forest patches (approx. 10% of the total landbase) are square woodlots or linear shelterbelts despite marked changes in edaphics and landform (Sharpe et al 1987). In general physiography and landform rarely influence patch shape on the agricultural landscape (Turner 1990). In this study, an increasingly rectangular patch structure is evident, except along river systems and other drainage features (**Figure 6.1** and **6.2**).

Change in Dispersion of Forest Fragments

In this study, changes in the spatial dispersion of forest patches was quantified by implementing a random transect sampling method. While random transects are often used to obtain an 'unbiased' measure of pattern (e.g. Leduc et al. 1994; Shiyomi and Yamamura 1993), here sampling was constrained to 'radiate' outwards from RMNP providing a 'directional' component to the analysis. One of the consequences of this sampling strategy was that the proportion habitat observed along the transects is generally higher than estimates obtained for the entire region (**Table 6.1a&b.**). This is because the intensity of agricultural development generally increases with distance from the Park. This directionality in landscape pattern is important when assessing isolation from the perspective of wildlife movements. Most studies examining the influence of anthropogenic development on landscape pattern measure patch shape (e.g. Krummel et al 1987; Sharpe et al. 1987; Turner 1990; O'Neill et al 1996; Sachs et al. 1998), or connectivity over entire regions (e.g. With

and Crist 1995). However, moving organisms do not perceive the entire landscape or patch, as they "encounter" the environment "step-by-step or by the mouthful" (Milne 1992). The transects used here, are reflective of the directionality and spatial autocorrelation between habitat "encounters" for moving organisms. It is felt that this sampling approach gives insight into both habitat pattern as well as addresses the "perception" of landscape fragmentation experienced when moving outwards from RMNP.

The cluster fractal dimension was used as an 'index' of isolation (*sensu* Smalley et al. 1987) between RMNP and other forested areas in the region. Previous applications of the cluster dimension to study fragmentation processes have been in the geologic sciences, to examine fault and earthquake patterns (Turcotte 1997). However, this measure can be used to determine the scaling properties of many spatio-temporal 'event' sequences (Smalley et al. 1987). It was found that forest habitat along the transects became clustered over time as fragmentation increased. The implications of this from the perspective of wildlife movement can be addressed by considering the sequence of habitat intersections along the transects as analogous to habitat encounters of moving organisms. From this perspective, the greater the degree of scale invariant clustering on a transect (i.e. greater isolation as $D \rightarrow 0$), the greater the likelihood of fewer favorable habitat "encounters" across all spatial scales. Thus, quantifying the fractal scaling of these patterns can provide information about the constraints imposed by fragmentation.

A significant increase in the degree of habitat fragmentation around RMNP was observed over the forty years examined in the study. The long-term effects of this fragmentation on species dispersal and regional biodiversity are hard to predict. For dispersing small mammal populations, habitat availability along the dispersal route influences juvenile survival rates and genetic variability (Wauters et al. 1994; Diffendorfer et al. 1995). Under moderate levels of fragmentation where intervening patch sizes are large, dispersing organisms can adjust their behavior to maximize 'positive' habitat encounters while minimizing exposure to less favorable conditions (Haddad 1999). On highly fragmented landscapes, isolation tends to magnify the influence of habitat loss on dispersal success (Gustafson and Gardiner 1996; Keymer et al. 2000). Species that cannot cope with the conditions among patches will stop making dispersal movements. For instance in butterfly species, an increase in interpatch distances can result in an exponential decrease in the number of dispersing individuals (Haddad 1999). When movements between patches become too energetically costly, the long-term survival of the metapopulation can be threatened (Keymer et al. 2000).

Under this scenario, biodiversity in the RMNP region may ultimately suffer from loss of connectivity to other natural areas.

The changes observed in the cluster fractal dimension raise several important questions: what maintains self similar properties on the agricultural landscape and what mechanism drives the changes observed? The loss of fractal complexity in patch shape on the agricultural landscape has been attributed to land clearing that results in rectilinear remnant patches (Krummel et al. 1987; Sharpe et al. 1987). This interpretation works for patch geometry, but the cluster fractal dimension measures dispersion among patches and is not necessarily sensitive to patch shape (Leduc et al. 1994). Patch shape has also been shown to vary with scale, as smaller patches often have a simple geometry compared with larger patches (Krummel et al. 1987; Sharpe et al. 1987). In this study, it was found that clearing within the grid based agricultural system resulted in lower fractal dimension, however fragmentation pattern was scale invariant. The implication is that land clearing does maintain some degree of self-similarity on these landscapes. This fragmentation process can be explained by way of analogy using the Sierpinski Carpet, a regular fractal (**Fig. 6.7**). The generation 'steps' in the creation of this fractal form can be used in comparison with temporal fragmentation processes occurring on the agrolandscape. For both the Sierpinski carpet and the agroecosystem some "areas" (i.e. forest patches) are retained between "iterations" (i.e. time periods) while other "blocks" (e.g. sections or quarter sections) are removed. In generating the Sierpinski Carpet, the middle section of a block from the previous step is always removed, a self similar process occurring at increasingly finer scales. Similarly, when forest is cleared on the agricultural landscape, it is removed in blocks, often bisecting an existing patch. Indeed, throughout the agricultural land grid, clearing takes place in a 'block within a block' pattern as sections and quarter sections are carved out of larger patches. However unlike the Sierpinski Carpet where finer and finer scale pieces are removed, forest clearing on the agricultural landscape follows a euclidean prescription of development (i.e. the repeated imposition of a single land survey paradigm). Patch dispersion on a grid based agricultural landscape will therefore begin to increasingly reflect the geometric simplicity of human development patterns.

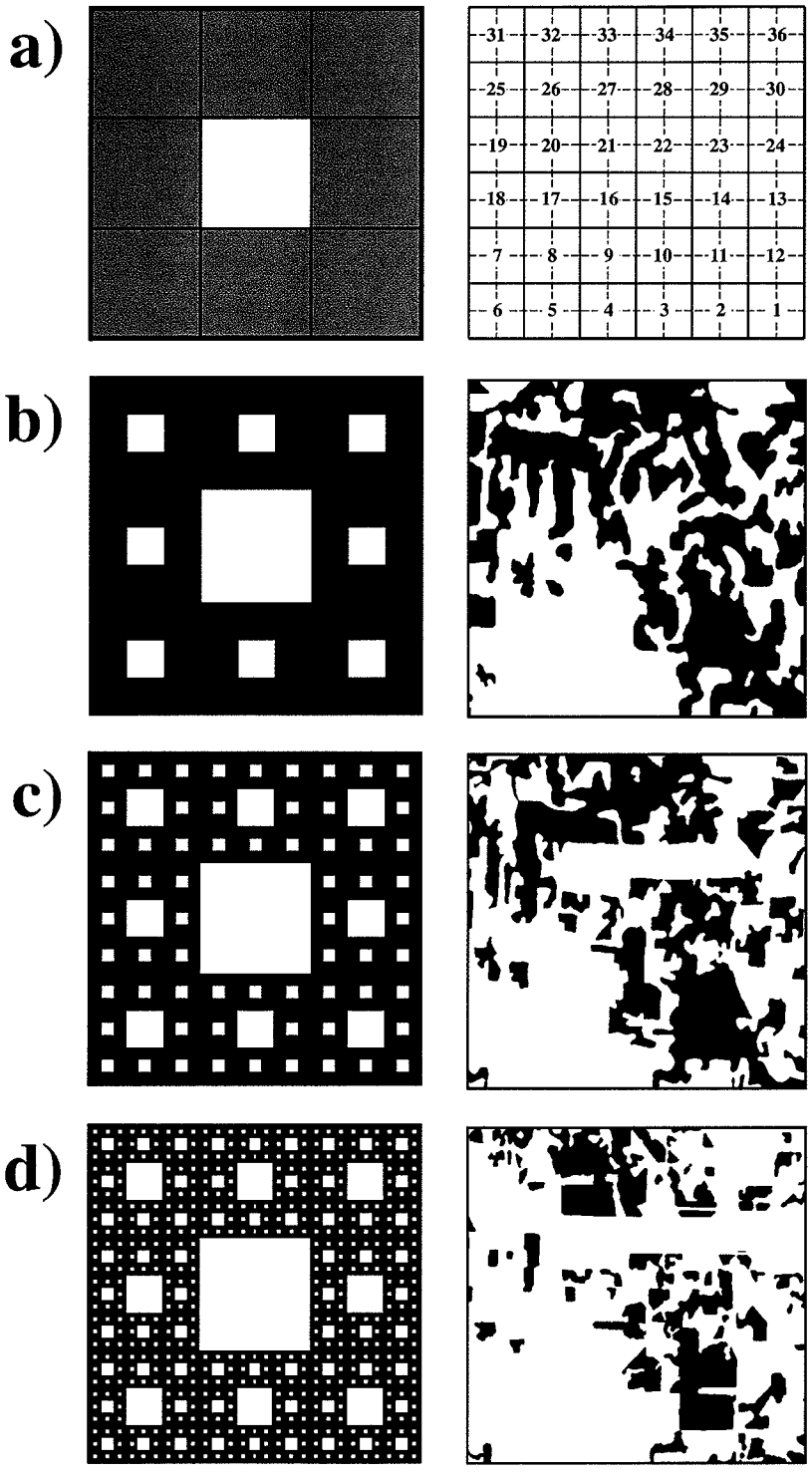

Figure 6.7: The geometric properties of fragmentation on the agrolandscape compared with the fractal Sierpinski carpet: a) the "generator" pattern for the Sierpinski carpet (left) and the standard range and township survey pattern for the agrolandscape (right); b to d) subsequent iterations of the "generator" pattern for the Sierpinski carpet compared with fragmentation pattern on the agrolandscape (b=1950's, c=1970's and d=1991).

6.7 Conclusion

Perhaps the greatest challenge in conservation is the loss of connectivity between remnant habitat patches and wildlife reserves at the regional scale (Shafer 1995; Lord and Norton 1990). Habitat loss was appreciable in the Riding Mountain region and completely severed the Park from other forested areas. Loss of connectivity at this scale can significantly change native species movements and behaviour (Kruess and Tscharntke 1994; Grashof-Bokdam 1997; Haddad 1999). The enhancement and creation of corridors has been suggested as a means to facilitate population persistence on these landscapes (Woodley 1991; Harrison 1992; Frankel et al 1995). However, research on the effective use of corridors by wildlife has produced conflicting results (Collingham and Huntley 2000; Debinski and Holt 2000). Although some species will avoid leaving preferred habitat within a corridor (Haddad 1999), most can cope with some degree of fragmentation and cross small gaps (Lord and Norton 1990). Indeed, species will often adopt larger dispersal movements on fragmented landscapes (Diffendorfer et al 1995). Management of wildlife on these landscapes must consider the scaling response of organisms to differing degrees of fragmentation. An optimal level of fragmentation should exist that provides the necessary degree of connectivity for wildlife without compromising crop productivity (Barrett and Peles 1994). In order to predict the influence of fragmentation on wildlife movements, it is essential that the scaling properties of habitat pattern be quantified.

Chapter 7

Optimizing vegetation maps of the boreal forest using multivariate approaches to Landsat image analysis

Abstract. Vegetation maps are spatially explicit models that must simplify floristic complexity on the landscape, while retaining ecologically meaningful information. In this study, a multivariate approach to mapping the mixedwood boreal forest in Riding Mountain National Park, Canada using multitemporal Landsat TM imagery is developed. Mapping the boreal forest is particularly challenging; canopy structure is spatially complex while often floristically simple. This study used species ground cover data collected from over nine hundred randomly located 10 x 10 m sample sites to determine floristic associations and their distribution in the Park. To ensure maximal correspondence between the spatial (geographic) distribution of vegetation associations in the Park and spectral reflectance classes, a rule based iterative strategy was applied. The rules had two component 'phases:' i) spectral assessments using multiple discriminant analysis (MDA) to test for class separation; and ii) spatial assessments that compared class distribution on the Landsat imagery with the known geographic distributions of the vegetation associations. Using these rules, the training sites and classes were adapted (modified, added or amalgamated) to improve accuracy of the final map. Accuracy was assessed using both a traditional confusion matrix, as well as a novel approach using MDA. In this application of MDA, the map was tested to determine if the mapped vegetation classes could discriminate among species cover values measured on the ground. It was found that spectral separation and the performance of individual classes often corresponded with canopy physiognomy and spatial structure. As these properties of the canopy often change with time, it is imperative that multivariate methods such as MDA be used in producing and assessing satellite classifications.

7.1 Introduction

Vegetation maps are spatially explicit landscape models (*sensu* Jeffers 1982) that summarize and simplify floristic complexity while retaining enough information to be ecologically meaningful (Franklin 1995; Treitz and Howarth 2000). Simplifying land cover complexity results in the loss of spatial information, but is necessary for the

practical application of vegetation maps in landscape management (Baskent and Jordan 1995). The critical step in this process is the creation of vegetation associations that can be linked to a spatial database to form discrete land cover types (Goodchild 1994; Mucina 1997). The number and kind of mapped cover types are limited by ecological knowledge of the study area and the technology available to adequately sample and classify large regions. In the past, high costs of implementing regional sampling programs resulted in 'static' vegetation maps that neglected the structure, function and change inherent in ecosystems (Franklin 1995; Goward and Williams 1997). With the development of modern satellite remote sensing technology, imagery covering large regions throughout the growing season is available for use in terrestrial mapping (Richards 1993; Goward and Williams 1997). A paradigm shift from mapping as a static exercise to a dynamic and adaptive modeling process is now possible, if statistically rigorous and methodological approaches to image analysis are adopted (Congalton 1991; Stehman 2001).

Image classification is primarily dependent on the availability of extensive ground data to provide information about the structural and floristic composition of a region. Vegetation in the boreal forest is spatially heterogeneous, reflecting the superimposition of multiscale disturbance events and complex physiographic gradients (Hall et al. 1991; Frelich and Reicht 1995). Floristic composition within this system varies along a continuum in both space and time (Bonan and Shugart 1989). Extensive ground sampling is required to ensure that the full range of vegetation diversity is represented in the classified map (Peddle et al. 1997). Once this reference data is collected, it must be divided into discrete, ecologically meaningful categories. While a variety of methods exist for this purpose (see Mucina 1997; Legendre and Legendre 1998), in many mapping efforts an independent analyses of the vegetation data is often overlooked (Franklin 1995). The relatively low accuracy of many map classifications may be attributable to the subjectively defined and relatively static 'landcover' classes used prior to spectral analysis (Congalton 1991; Peddle et al. 1997; Stehman 2001).

The production of regional maps from satellite imagery assumes that a relationship exists between the spectral reflectance from the land surface and the vegetation classes on the ground (Zhao and Maclean 2000). Establishing this relationship is challenging because satellite imagery does not detect vegetation composition directly, it measures the backscatter of solar radiation from the land surface (Goward and Williams 1997; Sampson et al. 2001). The amount of information obtained from a scene depends on the

number of bands sampled, the scale (pixel size) of measurement and the structural properties of the surface. In Landsat, only seven bands are available for spectral separation. To provide additional information, other time periods or ancillary data layers are required (Shen et al. 1985; Bolstad and Lillesand 1992). Class separation is also influenced by scale, since the typical sampling 'footprint' for remotely sensed imagery is usually larger than the scattering elements on the ground (Peddle et al. 1997). Pixel reflectance in each band is therefore a composite value of scattering from multiple canopy components (Sampson et al. 2001). The structural properties of these sub-pixel components such as leaf shape, size and arrangement, as well as shadows, slope effects and the orientation of sunlit surfaces all contribute to spectral reflectance measured (Colwell 1974; Myneni et al. 1992; Hall et al. 1995; Peddle et al. 1997). Because scale and structure of the canopy influence this scattering as much as floristic composition, it is essential that vegetation associations be evaluated to ensure adequate separation in spectral space (Treitz et al. 1992).

Significant overlap often exists in the spectral reflectance properties of vegetation classes (Zhao and Maclean 2000). When overlap is observed, a rule-based algorithm is required to determine the action to be taken (Treitz and Howarth 2000). Vegetation classes can be merged or added as necessary to represent the full range of spectral reflectance and biological variation (Markon 1992; Franklin 1995). Image classification is therefore a reciprocal training procedure where floristic classes are used to 'train' the spectral data. The spectral data in turn determines the number of mappable vegetation classes (Goodchild 1994). Traditionally, pairwise bivariate analyses have been used in evaluating the number of classes discriminated in spectral space (Richards 1993). Canonical multivariate approaches while less commonly used, are better suited to an iterative approach in image classification (Peddle 1993; Zhao and Maclean 2000). In combination with a rule-based algorithm, multivariate analysis can potentially increase classification accuracy as well as the number of vegetation classes recognized (Goodchild 1994; Treitz and Howarth 2000).

Evaluation of final map accuracy is generally performed using a confusion matrix approach. The confusion (error) matrix is a contingency table where class assignments on the map (rows) and class assignments in the reference test set (columns) are compared (Congalton 1991). A simplistic interpretation of this table would be that the diagonal elements represent correct classifications between the map and the reference sites and off-diagonals indicate misclassifications. In reality, each cell in the matrix has a

finite associated random error including the diagonal elements (Lark 1995). To correct for potential chance agreement between row and column values, the Kappa statistic (k-hat) is calculated (Hudson 1987; Congalton 1991). One of the fundamental disadvantages of this method is the necessity of a classification of the test set. This can lead to potential errors because of difficulty in making class assignments in the field (Stehman and Czaplewski 1998). An alternative approach would recognize that the ground data represents a continuous data-type and a canonical method suited to comparing the map classification to these data would be used instead. Such a method may be more appropriate to landscapes dominated by spatially complex land patterns, where *post hoc* ground classification may be difficult.

7.2 Objective

The spatial patterning of boreal forest communities reflects a complex continuum of floristic associations, successional processes (e.g. disturbance, differential growth), and canopy structure (Frelich and Reich 1995; Hall et al. 1995; Cihlar et al. 1997). Mapping strategies must be optimized to adequately characterize the structural and spatial complexity of the boreal forest. In this study, a statistically rigorous multivariate approach to the analysis of remote sensing imagery for mapping the boreal forest is presented. The objective is to provide a repeatable vegetation mapping strategy (algorithm) that maximizes the relationship between spectral information and vegetation distribution on the ground. The utility of the final map in distinguishing among vegetation on the ground was assessed using a multiple discriminant analysis (MDA) of ground cover data partitioned by map class.

7.3 Study Area – See Chapter 2

7.4 Materials and Methods

Landsat image preprocessing

The vegetation map of RMNP was based Landsat 5 TM bands 3 (0.63 - 0.69 μm), 4 (0.76 - 0.90 μm) and 5 (1.55 - 1.75 μm) from two scenes, acquired on August 13, 1991 and September 21, 1991. Image preprocessing was performed by Radarsat International (Vancouver) and included a standard radiometric correction to eliminate variability in sensor response. The scenes selected had high atmospheric transmittance and minimal

cloud cover. A dark order subtraction based on a path irradiance model of λ^{-4} (corresponding to a clear atmosphere dominated by Rayleigh scattering; Richards 1993) was performed to correct for residual atmospheric effects (following Chavez 1988). The final raster product conformed to the NAD27 grid system (Zone 14) at a pixel resolution of 30 x 30 m. Each of the LANDSAT bands was centred at 5631.3 km N by 403.4 km E. The scenes were coregistered to create a multitemporal 6 band scene (summer bands 3,4 and 5 and fall bands 3,4 and 5).

Landsat image "masking"

An initial principal component analysis (PCA) of the Landsat imagery identified water and agricultural land surrounding the Park as distinct spectral outliers. To improve classification performance these cover types were masked out during the image analysis phase (Zhao and Maclean 2000). Waterbodies were removed from the imagery by performing a supervised maximum likelihood classification on twenty-five training sites selected from lakes stratified into 5 groups by water depth. A binary mask (water/non-water) was generated from this classification by combining these five groups. A second mask was created to remove agricultural land from the Landsat scene. This was accomplished by hand-digitizing the border of RMNP using coordinates obtained from 1: 50,000 scale National Topographic (NTS) map sheets. The area within the digitized border of the Park was subsequently "filled" to create the binary mask layer (park/non-park). During the final map production phase, the forest habitat in the agricultural area was extracted to distinguish cropland from forested habitat patches. These forest patches were classified using maximum likelihood training data from the Park dataset.

Ground data collection

Three independent ground vegetation datasets were collected from within RMNP, reflecting the iterative approach taken in map classification. Exact site locations were obtained for all sites using a handheld Global Positioning System (GPS) and recorded as Universal Transverse Mercator (UTM) coordinates based on the North American datum 1927 (NAD27). Vegetation data collected at these sites were used to: a) objectively determine the vegetation associations and their distributions in the Park; b) "train" the Landsat image classification; c) "test" the final map classification.

1. Parks Canada dataset (vegetation classification and map verification)

Parks Canada located thirteen hundred ground sample sites along random transects within RMNP during the summers of 1992 and 1993. At each site, percent cover values for each canopy tree and total crown closure was estimated within 20 x 20 m plots. These plots were sub-sampled using randomly placed 1 x 1 m quadrats and the relative cover of species in the shrub and herb layers was recorded. A subset of these data (926 sites x 60 species) was selected to delineate the major terrestrial vegetation associations in RMNP. Species were stratified into 3 categories (trees, shrubs and herbs) and cover values for each strata were standardized and expressed as relative proportions. Cluster analysis was performed using Ward's method (SPSS Inc. 1995; Legendre and Legendre 1998) from an Euclidean distance matrix, resulting in the delineation of fourteen terrestrial vegetation associations. An aquatic "Emergent" association was added based on supplemental data (ground reconnaissance and aerial photographs). Some of these data were used to perform a preliminary classification of RMNP, while a second subset (250 sites x 60 species) was randomly selected from the dataset and used in final map verification. No sites were used for both the initial classification and map testing.

2. Landsat classification "training" dataset

Following preliminary analysis of the Parks Canada dataset, an independent classification "training" dataset was collected in the summer of 1995. One hundred and twenty sample sites were established in stands visually homogenous within a radius of 100 m from the sample location. At each site, percent cover values for each canopy species and total crown closure was estimated within 10 x 10 m plots. Shrub and herbaceous species with cover exceeding 10% were recorded. All "training" sites for the final Landsat classification were selected from these data.

3. Map verification (contingency matrix) dataset

These data were collected in the summer of 1997 to provide an assessment of map classification accuracy using a contingency (error) matrix approach (Congalton 1991). Two Hundred and fifteen sites were established using a stratified random sampling procedure to ensure that all vegetation classes in the Park were visited. For each site a

visual assessment of the vegetation was performed and an assignment to one of the map vegetation classes was made.

Mapping Algorithm

Map production requires an iterative sequence of optimization steps with the purpose of maximizing correspondence between ground cover data and remotely sensed imagery (**Figure 7.1**). The mapping algorithm was rule-based, where the decisions made at each step considered the spectral, spatial and floristic information in determining the final map classification. In some cases this required revisiting and redefining vegetation classes in light of the new knowledge, as part of an adaptive map production strategy.

1. Spatial assessment

Spatial assessment was performed to ensure that the distribution of vegetation associations on the ground (geographic distribution) matched with the class distribution on the Landsat map (image class distribution). This involved two stages: 1) determining the geographic distribution for each association and 2) generating a binary distribution for each vegetation class on the Landsat imagery. Geographic distributions for vegetation associations were determined by plotting the UTM coordinates for ground sites in each class (**Figure 7.2**). These data became the reference spatial dataset that was compared to binary class distributions on the Landsat imagery. The binary images were created by first performing a maximum likelihood classification on each class separately. From this analysis, the likelihood probability for each pixel in the image was saved. The "probability" maps were then converted to a binary representation by thresholding (i.e. excluding from a class) all pixels with a probability of belonging of < 1%. These binary images were used to determine:

- if the Landsat classification distribution matched the ground site distribution for an association;
- if rare or spatially isolated classes were adequately represented by the classification.

When either of these conditions were not met, the response was to either: (1) examine the spectral discrimination of the group and modify the training sites to ensure a better spatial distribution for the class, or (2) add training sites to provide better spatial representation if necessary.

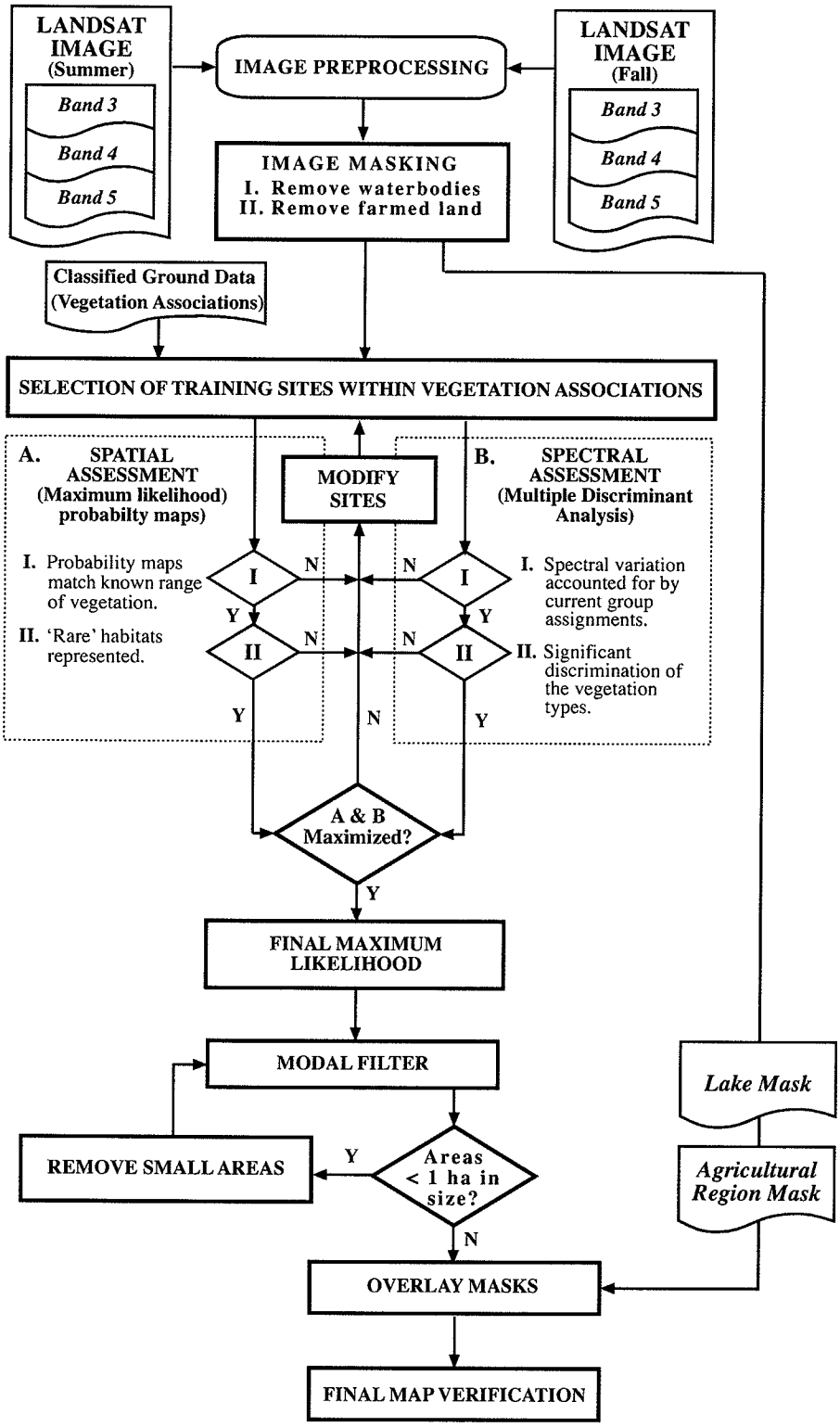

Figure 7.1: Map production flow diagram showing the major steps in image classification (square boxes). The analytical process is followed from initial data input layers (wavy boxes) through the rule based spatial-spectral optimization (dotted lines) to final map assessment. Decision rules for each iterative step (diamond box) determine the path followed through the flowchart.

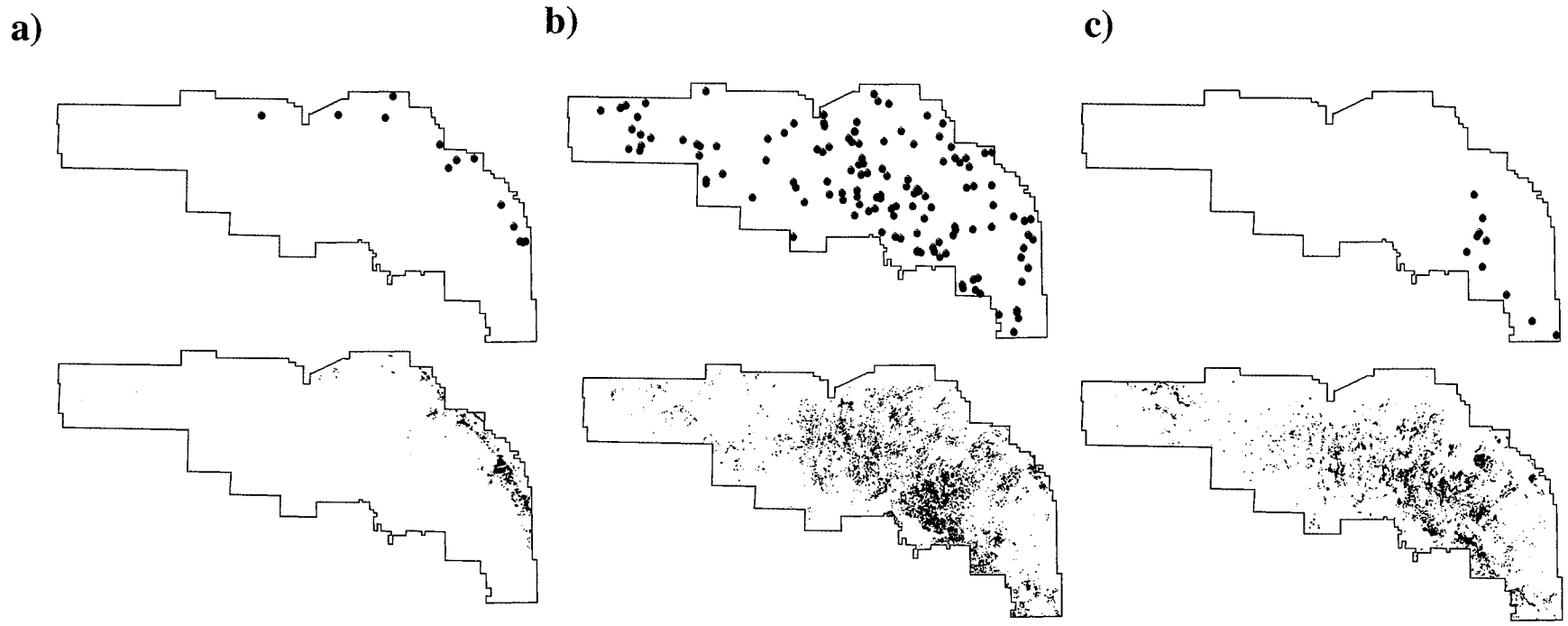

Figure 7.2: Geographic (top) and Landsat image (bottom) class distributions for selected vegetation associations within RMNP: a) bur oak; b) mixed coniferous-deciduous; c) jack pine.

2. Spectral Assessment (MDA)

The separation of the vegetation associations in Landsat spectral space was determined using multiple discriminant analysis (MDA) on spectral reflectance in bands 3,4 and 5 for the combined summer and fall imagery (ORDIN, Podani 1994). MDA is a multivariate method that finds linear combinations of the original variables that maximize the ratio of the between to within-group variance (Peddle 1993; Legendre and Legendre 1998). MDA was used to graphically assess the relative separation of classes by examining the dispersion of groups along the discriminant axes (Zhao and Maclean 2000) . Biplot scores (structure correlations) for the variables and the 95% confidence intervals for the group means were also plotted. During the spectral assessment phase of map production, MDA was used as an exploratory tool and to provide rule-based decision support. The discriminant axes were examined to determine:

- if spectral variation was adequately partitioned by the classes present;
- if the vegetation classes were non-overlapping in spectral space.

Classes that did not meet these requirements were carefully examined to determine the nature of their spectral properties. Failure to meet the first condition was often the result of poor partitioning of variation among existing classes or within an existing class. The response in these instances was to either: (1) reselect training sites that better partitioned spectral variance, or (2) split "multimodal" classes into two or more new classes if they formed recognizable groups on the ground. For overlapping classes, a decision was made to do one of the following: (1) determine whether sufficient floristic or structural differences existed in the vegetation classes to modify the "training" sites to better separate the groups spectrally, or (2) combine the classes and make note of the floristic variants within the class.

Map production

The final map was based on 13 vegetation classes with an equal number of training sites for each (9 per class; total 117). A maximum likelihood classification was performed with a probability of belonging threshold value set at .01. This created an "unclassified" category for pixels with a low probability of belonging to any of the existing classes. These pixels were removed during the map simplification step (see below). Training site performance was assessed using a resubstitution approach

(Richards 1993). The kappa statistic (k-hat) was calculated to correct for chance agreement between row and column categories in the confusion matrix (Congalton 1991).

To simplify the map, all patches less than 1 ha (13 contiguous Landsat pixels of the same class using a rook's adjacency rule) were removed and placed in the "unclassified" category. A spatial context filter was then used to assign these unclassified pixels to the value of the adjacent class. This step created a completely filled vegetation layer over which the agricultural and lake masks were draped to produce the final map product.

Map verification

Two map verification techniques were used to assess the accuracy of the final vegetation map. The first method involved the creation of a standard confusion matrix where the classification accuracy was determined for each class by comparing the ratio of the diagonal to the off diagonal elements in the matrix (Congalton 1991). Two measures of accuracy were calculated: "producers accuracy" (diagonal elements divided by each column total) and "users accuracy" (diagonal elements divided by the row totals). The 214 ground sites visited in 1997 were used to construct this matrix. The kappa statistic (k-hat) was calculated to assess the overall performance of the map classification.

In this study, a second map verification approach using multiple discriminant analysis was developed. Unlike the construction of a confusion matrix, this method does not require an independent user-based ground classification of the test sites. Instead, the actual cover of individual species are recorded at each "test" site. Test site vegetation is then partitioned according to the map class in which the site occurred. An MDA is then performed on the vegetation data. It is expected that if no relationship exists between species cover on the ground and the map classes, discriminant analysis of the partitioned vegetation data matrix would not be significant. For this analysis, 250 test sites representing 6 map categories were randomly selected (forest and shrub classes) from the Parks Canada dataset. Each test site was located on the Landsat map and coded by the map category in which it occurred. Because the number of recorded species greatly exceeded the number of test sites in some of the rarer cover types, a data reduction step was implemented prior to MDA (Green 1993). A variant of Correspondence Analysis

(Detrended Correspondence Analysis, DCA; Hill and Gauch 1980), was chosen for this purpose. The first four DCA axes were retained for subsequent discriminant analysis.

7.5 Results

Vegetation associations and spatial-spectral optimization

Cluster analysis of the Parks Canada dataset identified 14 terrestrial vegetation classes ranging from closed coniferous forest to open grassland. These were used to generate the reference distribution maps for each of the classes (**Figure 7.3**). During the spectral and spatial assessment phase, six of the vegetation associations were combined into two larger classes as follows:

1. "Closed coniferous forest" – the four closed-canopy conifer associations had significant overlap in spectral space (**Table 7.1**). Attempts at improving spectral separation were unsuccessful and the resultant probability maps from the Landsat classification were inconsistent with known ground distributions (e.g. **Figure 7.2c**). It was observed that within the Park, the geographical distribution of these associations overlapped (**Figure 7.3**). Indeed, canopy composition within these groups often included an admixture of conifer species (e.g. jack pine and black spruce are often codominant). The rule implemented was to pool the closed-canopy coniferous forests into a single class while recognizing the floristic variants.

2. "Shrubland" – significant spectral and spatial overlap was observed for regenerating alder shrubland, hazelnut and aspen in the 1980 burn (**Figure 2.5**). Because of the discrete spatial extent of the 1980 Rolling river fire, the alder and hazelnut classes were combined.

To better partition spectral variance, two new vegetation associations were added:

1. "Open canopy coniferous forest" – within conifer dominated systems it was found that as canopy closure decreased, band spectral reflectance increased significantly. This often corresponded with change in understory constituents (ericoids and graminoids). A class was added to ensure that these open canopy sites were represented on the final map.

2. "Low shrub grassland" – During preliminary MDA examination the grassland class appeared to have two discrete "subclasses." It was determined that these differences represented changes in the relative cover of shrub species in the grassland sites. The decision was to partition this class into high and low shrub "phases."

For the production of the final map, 13 vegetation associations were recognized as being spatially and spectrally distinct within RMNP (**Table 7.2; Table 7.3**).

Final map production

An MDA of the training sites used in the production of the final map shows the relationship between the 13 vegetation classes (117 sites, 6 bands) in spectral space (**Figure 7.4**). Discrimination was significant on both of the first two MDA axes (65.8% and 17.3%, respectively), and none of the 95% confidence ellipsoids overlapped. The relative separation of the classes varied by canopy type: deciduous forest classes were tightly clustered indicating greater spectral similarity, while coniferous, grassland and shrubland classes were spectrally distinct. Class dispersion along the first MDA axis appears to correspond with increasing albedo and decreasing canopy closure. Separation of vegetation classes on MDA axis 2 seem to follow trends in canopy structural development (multiple strata) and leaf shape (planar leaves versus linear conifer "needle" and grass "blades").

The time of year that the imagery was taken (summer vs. fall) had little influence on broad patterns in class discrimination. It was found that each summer band was highly correlated with its corresponding fall counterpart. The vegetation classes that benefited the most from the addition of fall imagery were the mixedwood classes (IX and X) and bur oak forest (V). Otherwise, the class trends along each band for both the summer and fall imagery were similar. In RMNP, band 3 appears to separate treed and grassland systems, band 4 among different forested canopy types (i.e. conifer, grassland, deciduous tree, and shrubland), and band 5 the degree of canopy closure related to albedo (i.e. conifer to open graminoid dominated classes).

The selected training sites resulted in a robust final maximum likelihood classification of RMNP. Classifier performance (using resubstitution) ranged between 93% (Low

Canopy Deciduous) to 100% (Oak and Shrubland) with few misclassified training site pixels (k-hat = 98.2%). Despite the removal of all patches less than 1 ha, the final map reflects the heterogeneity of the boreal mixedwood with high class interspersion and patchiness across spatial scales (**Figure 7.5**).

Final map assessment

The confusion matrix constructed for the 13 vegetation classes using the 1997 field reference dataset (n = 215; **Table 7.4**) had few misclassifications (k-hat = 85.32%). Individual class performance varied: producers accuracy ranged between 73% (for Aspen Parkland and Regenerating Conifer) to 100% (Grassland) and user accuracy from 74% (Deciduous Canopy–Conifer Subcanopy) to 100% (Grassland and Closed Canopy Conifer). In general, the classes most subject to producer and user error were closed to semi-open canopy forests, while misclassifications were rare for conifer and graminoid dominated associations.

The second method used to determine map accuracy utilized the DCA scores for test sites selected from the Parks Canada dataset (subsample of 250 sites, 60 species). Because the map-accuracy MDA was based on DCA site scores, the trends along these axes were examined. It was found that site dispersion along the first DCA axis corresponded with changes in the relative dominance of conifer and deciduous species in the canopy, while the second axis separated rich moist sites from xeric open canopy communities (**Figure 7.6**). These broad trends compare favorably with those observed for the spectral MDA (**Figure 7.4**). The relative dispersion of canopy dominants on the DCA (especially for the deciduous species) corresponds with the distribution of deciduous vegetation associations on the spectral MDA. However, the site scores for conifer dominated stands are more variable on the DCA than was observed on the spectral MDA, indicating that floristic variability does not necessarily result in spectral distinctiveness. Having established that the DCA produced interpretable vegetation trends, the first 4 axes representing 36% of the total variance of the test set were used in the subsequent map verification step.

Results from the map-accuracy MDA indicate that the map consistently discriminated among species cover on the ground (**Figure 7.7**). Three MDA axes (83%, 12 % and 3%) were required to provide adequate separation of the map classes within the DCA space. Class discrimination varied, with Oak (V), Closed Canopy Conifer (XII), Eastern

Deciduous (VIII) sites being consistently separated from other vegetation classes and Parkland (VII) sites often overlapping with other deciduous dominated canopies. In some cases discrimination was better than anticipated from the confusion matrix analysis. It was found that the Deciduous Canopy–Coniferous Subcanopy class (IX) was could be confused with the Mixed Canopy Deciduous-Coniferous class (X) when visited on the ground. However, these classes were well separated on the MDA.

Table 7.1: Conifer training class mean spectral reflectance (± std. err.) in digital numbers (DN) for summer and fall Landsat TM bands 3, 4, and 5; n=9 for each class.

Conifer Class	Summer Landsat Bands			Fall Landsat Bands		
	3	*4*	*5*	*3*	*4*	*5*
Black spruce	7.5 (±0.5)	44.3 (±2.3)	34.1 (±2.0)	6.5 (±0.5)	29.1 (±1.5)	23.3 (±1.5)
Jack pine	6.7 (±0.8)	43.9 (±2.9)	36.6 (±2.6)	6.1 (±0.5)	28.5 (±1.9)	24.7 (±1.6)
White spruce	7.6 (±0.5)	48.1 (±2.3)	36.9 (±2.1)	6.9 (±0.6)	30.7 (±1.5)	24.9 (±1.5)
Balsam fir	6.1 (±0.6)	46.7 (±1.8)	36.4 (±2.1)	5.6 (±0.5)	30.6 (±1.6)	25.2 (±1.5)

Table 7.2: Vegetation class mean spectral reflectance (± std. err.) in digital numbers for summer and fall Landsat TM bands 3, 4, and 5; n=9 for each class.

Veg. Type	*Name*	*Summer Band Reflectance*			*Fall Band Reflectance*		
		B3	**B4**	**B5**	**B3**	**B4**	**B5**
-	Open Water	-	-	-	-	-	-
-	Agricultural Land	-	-	-	-	-	-
-	Forested land (outside of RMNP)	-	-	-	-	-	-
I	Wetlands	17.7 (±0.5)	54.1 (±2.7)	83.1 (±1.9)	18.0 (±0.6)	40.8 (±2.1)	68.1 (±2.9)
II	Grassland	20.9 (±0.8)	74.2 (±2.6)	97.6 (±1.6)	21.8 (±0.5)	52.6 (±1.2)	83.7 (±0.6)
III	Low Shrub Grassland	16.0 (±0.3)	104.7 (±2.8)	92.9 (±1.0)	21.4 (±0.5)	69.0 (±2.7)	82.1 (±1.3)
IV	Shrubland	10.1 (±0.3)	102.6 (±0.8)	86.3 (±1.3)	12.7 (±0.3)	58.6 (±2.3)	66.3 (±1.3)
V	Bur Oak Forest	7.9 (±0.1)	85.4 (±0.4)	69.8 (±0.3)	8.7 (±0.2)	58.8 (±0.6)	51.9 (±0.3)
VI	Low Canopy Deciduous Forest	8.7 (±0.1)	91.1 (±0.8)	62.8 (±0.4)	15.0 (±0.3)	46.7 (±1.8)	55.5 (±0.4)
VII	Aspen Parkland	9.8 (±0.2)	76.9 (±0.7)	74.7 (±0.9)	11.6 (±0.3)	49.5 (±0.6)	51.6 (±0.4)
VIII	Eastern Deciduous Forest	8.0 (±0.2)	91.4 (±0.8)	57.9 (±0.6)	11.0 (±0.7)	61.5 (±1.4)	44.6 (±0.7)
IX	Deciduous Canopy-Coniferous Subcanopy	9.2 (±0.3)	62.8 (±0.8)	58.4 (±0.6)	8.5 (±0.2)	40.4 (±1.6)	39.6 (±0.5)
X	Mixed Canopy (Deciduous-Coniferous) Forest	7.7 (±0.3)	63.4 (±0.9)	44.8 (±0.5)	9.1 (±0.4)	41.5 (±1.3)	33.4 (±0.5)
XI	Open Canopy Coniferous Forest	11.7 (±0.4)	65.5 (±2.0)	55.9 (±1.0)	13.4 (±0.8)	42.0 (±0.8)	42.7 (±1.5)
XII	Closed Canopy Coniferous Forest	6.3 (±0.4)	43.2 (±1.0)	33.3 (±0.9)	5.5 (±0.2)	27.9 (±0.6)	22.8 (±0.7)
XIII	Regenerating Coniferous Forest	13.0 (±0.3)	59.6 (±2.4)	71.1 (±0.7)	12.2 (±0.3)	38.9 (±1.8)	50.7 (±1.3)

Table 7.3: Vegetation association descriptions of the thirteen classes used in producing the final map of RMNP. The main vegetation association and floristic variants (when present) are indicated. For each of the classes the species composition, canopy physiognomy (structure) and environment is given.

Class	Association Name Floristic Variants	Species	Canopy Structure	Environment
I	**Wetlands** (a) Meadow marsh (semi-permanently flooded) (b) Marsh (permanently flooded)	(a) Bluejoint grass (*Calamagrostis canadensis*) and/or sedges (*Carex spp.*). (b) Cattails (*Typha spp.*) or reeds (*Scirpus spp.*).	(a) Graminoid Meadows and Marshes. (b) Graminoid Marshes.	(a) Floodplains of small streams, beaver meadows, and lakeshores. (b) Wave-washed lake shores, sheltered bays and isolated basins.
II	**Grassland** (a) Plains Rough Fescue (b) Kentucky Bluegrass-Wheatgrass (c) Junegrass-Wheatgrass	(a) Plains rough fescue (*Festuca hallii*). (b) Kentucky bluegrass (*Poa spp.*). (c) June grass (*Koeleria gracilis*), wheat grass (*Agropyron trachycaulum*) and rose (*Rosa spp.*)	Low graminoid-forb vegetation with few low shrubs. Low 'bunchgrass hummocks' in plains rough fescue prairie.	Well to excessively drained sandy outwash material, or coarse glacial till.
III	**Low Shrub Grassland** (a) Low shrub (b) Low and tall shrub	(a) Western snowberry (*Symphoricarpos albus*) and/or shrubby cinquefoil (*Potentilla fruticosa*). (b) Hawthorn (*Crataegus spp.*) and chokecherry (*Prunus virginiana*).	(a) Grasslands with moderate or high cover of low (generally < 1m high) shrubs. (b) Grasslands with moderate cover of shrubs (approx. 1m tall).	Well-drained sandy outwash material, or coarse-textured glacial till.
IV	**Shrubland** (a) Beaked Hazel (b) Regenerating alder and aspen	(a) Beaked hazelnut (*Corylus cornuta*). (b) Regenerating alder (*Alnus spp.*) and aspen (*Populus tremuloides*).	Tall shrubland; subject to heavy browsing.	Moderately to well drained tills, often in exposed areas (higher elevations) or on steep slopes along the Escarpment.
V	**Bur Oak Forest** (a) Oak on sandy deposits (b) Oak on shale slopes (c) Oak on alluvial fan deposits	(a) Bur oak (*Quercus macrocarpa*), green ash (*Fraxinus pennsylvanica*), and Manitoba maple (*Acer negundo*). (b) Bur oak, with poison ivy (*Rhus radicans*), beaked hazel, and a graminoid-forb understory. (c) Bur oak, with an understory of low shrubs (e.g. rose, snowberry) and graminoids-forbs.	Open forest stands, with an understory of low shrubs, graminoids and forbs.	(a) Well drained sandy ancient beach ridges with low to moderate nutrient status. (b) Excessively drained south-facing shale slopes with low nutrient status. (c) Well drained alluvial fans with low to moderate nutrient status.
VI	**Low Canopy Deciduous Forest** (a) Lowland balsam/aspen (b) Upland low aspen (c) Regenerating 30 yr old aspen stands	(a) trembling aspen, balsam poplar (*Populus balsamifera*) or willow (*Salix spp.*) with a forb understory. (b) stunted trembling aspen with a forb understory. (c) regenerating trembling aspen with low shrub understory (esp. near Gunn lake).	Continuous low canopy trembling aspen forest with tall shrubs; includes younger (< 50 years) post-burn stands (e.g. 1961 Gunn Lake fire area).	Well-drained (sandy outwash) or poorly drained (clay deposits) nutrient-limited substrates.
VII	**Aspen Parkland**	Stands of trembling aspen alternating with shrubby grasslands. Balsam poplar stands and small wetlands occur in poorly-drained areas.	Mosaic of trembling aspen groves (often with a high shrub component), shrublands, shrubby grasslands, and wetlands.	Moderately-drained glacial till; gently rolling topography.
VIII	**Eastern Deciduous Forest** (a) Mature trembling aspen (b) Mixed eastern deciduous	(a) Tall trembling aspen with a shrub and herb-rich understory. Paper birch (*Betula papyrifera*) may also be present. (b) Rich deciduous forests with aspen, Manitoba maple, green ash, American elm (*Ulmus americana*) restricted to the base of the Escarpment . species show an eastern floristic affinity.	Stands with a high canopy, and several subcanopy and sapling layers of varying development; tall shrubs such as mountain ash (*Acer spicatum*) and beaked hazelnut are relatively common.	Moist, nutrient-rich loamy soils, often with a well-developed organic layer. Generally found at the base and lower slopes of the Escarpment, in the extreme eastern and north-eastern portions of the Park.
IX	**Deciduous Canopy-Coniferous Subcanopy** (a) Open deciduous canopy with tall hazel and low stature conifer (b) Semi-closed canopy deciduous with a conifer subcanopy.	(a) Tall degenerate trembling aspen, paper birch with hazelnut; low stature white spruce common. (a) Tall degenerate trembling aspen with hazelnut; low stature white spruce common.	(a) Discontinuous open canopy shrubland, with a low stature conifer 'subcanopy' of varying density. (b) Semi-closed canopy with a conifer subcanopy.	Moderately drained glacial till, often associated with undulating topography; largely restricted to areas of the Park that have not been burned for at least 100 years.
X	**Mixed Canopy (Deciduous-Coniferous) Forest**	Mixed canopy forests, typically with trembling aspen and white spruce as codominants; black spruce, paper birch, balsam poplar and jack pine are occasional.	Mixed deciduous-coniferous canopy, sometimes with a subcanopy dominated by conifers. Tall shrubs are sparse to relatively common. Understory is often herb-rich; feathermosses may be common.	Moderately drained glacial till; often undulating topography.
XI	**Open Canopy Coniferous Forest** (a) Semi-treed bog (b) Sparsely treed upland	(a) Black spruce (*Picea mariana*) and/or easterm larch (*Larix laricina*); low ericaceous shrubs are often abundant; peat moss and sedges are common. (b) White spruce growing on grasslands or sedge meadows.	Semi-treed stands, often associated with low shrubs (bogs, fens) or shrubby grassland (dry uplands).	Variable; poorly-drained organic substrates (bogs, fens), or well drained sandy outwash material or glacial till (dry uplands).
XII	**Closed Canopy Coniferous Forest** (a) White spruce (b) Balsam fir (c) Jack pine-black spruce (d) Black spruce	(a) Mature stands of white spruce, mostly in eastern portions of the park. (b) Mature stands of balsam fir (*Abies balsamea*) these stands are restricted to the north-eastern portion of the Park. (c) Jack pine (*Pinus banksiana*) and black spruce, restricted to the south-eastern portion of the Park. (d) Black spruce and eastern larch may be locally codominant in treed bogs.	Pure stands of moderate to complete canopy closure, or more commonly with a minor component of deciduous trees (esp. in white spruce stands) and a forb understory, mosses common (black spruce stands).	Moderately drained glacial till (white spruce, balsam fir, jack pine) or poorly drained organic material (black spruce).
XIII	**Regenerating Coniferous Forest**	Dense, regenerating coniferous forest stands. In the 1980 Rolling River fire, most of these stands are dominated by jack pine or black spruce. Presence of swamp birch (*Betula glandulosa*) common in the training sites.	Dense to sparse conifer canopy (generally < 3 m tall), with a sparse to moderate shrub cover (swamp birch) esp. in beaverflooded areas.	Generally moderately to well-drained glacial till and sandy soils; burned organic substrates occasional. Recent disturbance (fire or rarely beaverflood).

Table 7.4: Accuracy assessment comparing the vegetation classes determined for the ground test sites (post hoc field assignments) with their class on the Landsat map (n=215). Both producers and users accuracy is calculated given.

		Testing (reference) set														
	Class	**I**	**II**	**III**	**IV**	**V**	**VI**	**VII**	**VIII**	**IX**	**X**	**XI**	**XII**	**XIII**	***Row Total***	***Users Accur. %***
Training (classification) set	**I**	16	-	-	-	-	-	-	-	-	-	1	-	-	17	94.1
	II	-	16	-	-	-	-	-	-	-	-	-	-	-	16	100.0
	III	1	-	16	-	-	1	-	-	-	-	-	-	2	20	80.0
	IV	-	-	-	14	-	1	-	-	1	-	-	-	-	16	87.5
	V	-	-	-	1	13	-	2	1	-	-	-	-	-	17	76.5
	VI	-	-	-	-	-	13	2	-	-	-	-	-	-	15	86.7
	VII	-	-	-	1	-	1	14	-	-	-	-	-	-	16	87.5
	VIII	-	-	-	-	-	-	1	16	-	-	-	-	-	17	94.1
	IX	-	-	-	-	-	-	-	-	14	3	1	-	1	19	73.7
	X	-	-	-	-	-	-	-	-	2	14	-	1	-	17	82.4
	XI	1	-	-	-	-	1	-	-	-	-	12	1	1	16	75.0
	XII	-	-	-	-	-	-	-	-	-	-	-	16	-	16	100.0
	XIII	-	-	1	-	1	-	-	-	-	-	-	-	11	13	84.6
	Column Total	18	16	17	16	14	17	19	17	17	17	14	18	15	215	
	Producers Accur. %	88.9	100.0	94.1	87.5	92.9	76.5	73.7	94.1	82.4	82.4	85.7	88.9	73.3		

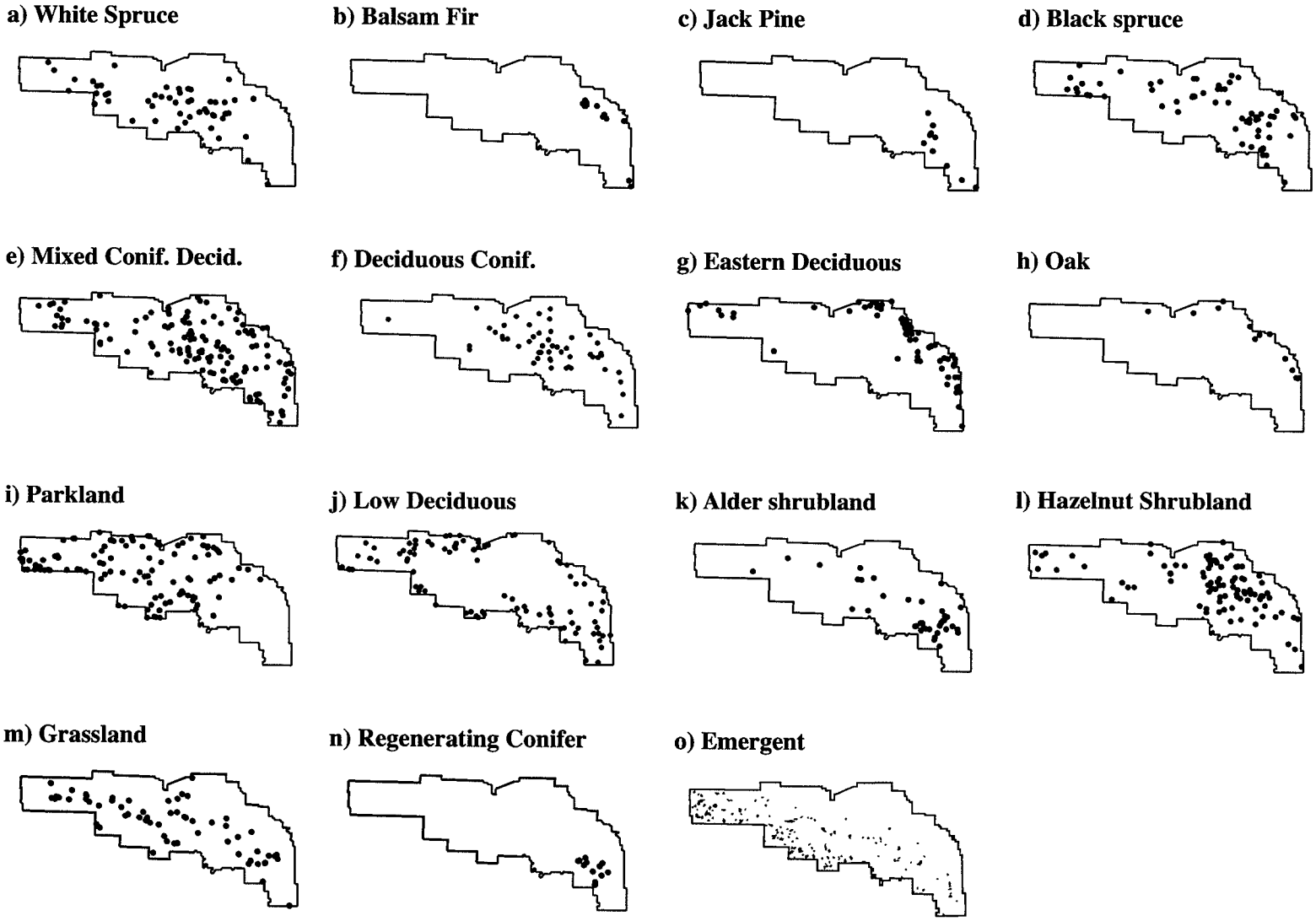

Figure 7.3: Geographic distributions of the vegetation associations in RMNP used during the spatial optimization phase of Landsat image classification. Some of these associations were amalgamated during the spectral-spatial optimization procedure (e.g. conifer classes)

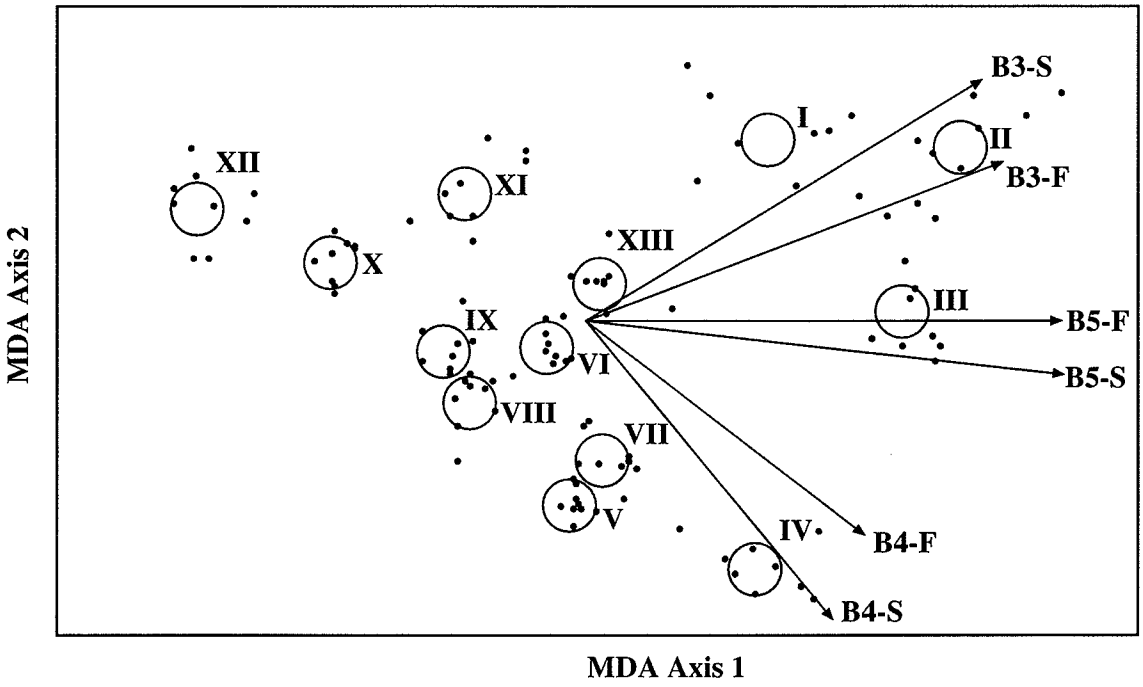

Figure 7.4: Multiple discriminant analysis of spectral reflectance in the summer and fall (S/F) Landsat TM bands 3, 4 and 5 for the final training sites used in map classification. The 95% confidence ellipses for means are shown; class labels follow **Table 7.2**. The first two MDA axes account for most of the spectral discrimination (65.8% and 17.3% respectively).

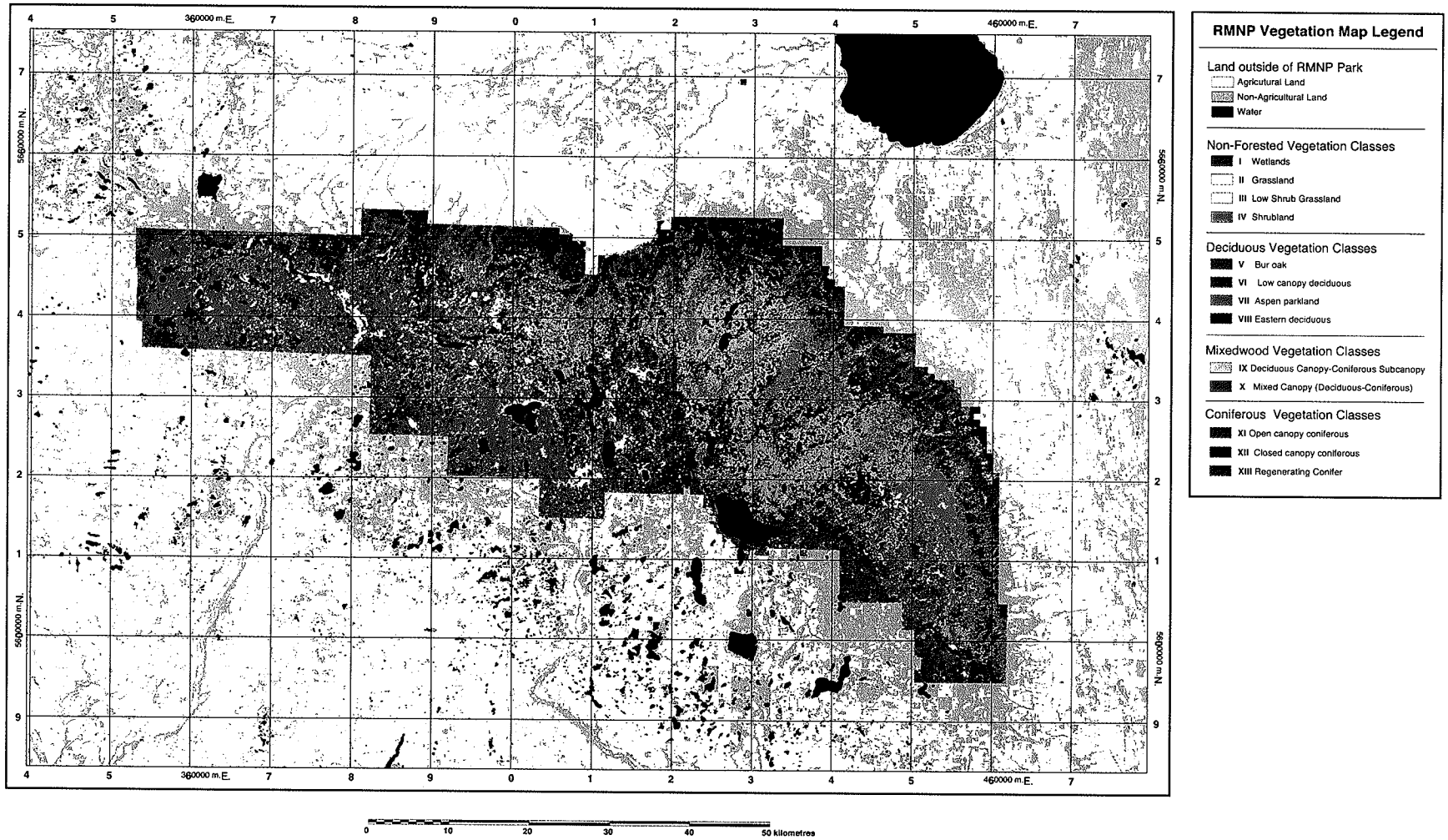

Figure 7.5: Final vegetation map of Riding Mountain National Park. The map projection is Universal Transverse Mercator (UTM) following North American Datum 1927 (NAD27, Zone 14). Class labels and class descriptions follow **Table 7.2**.

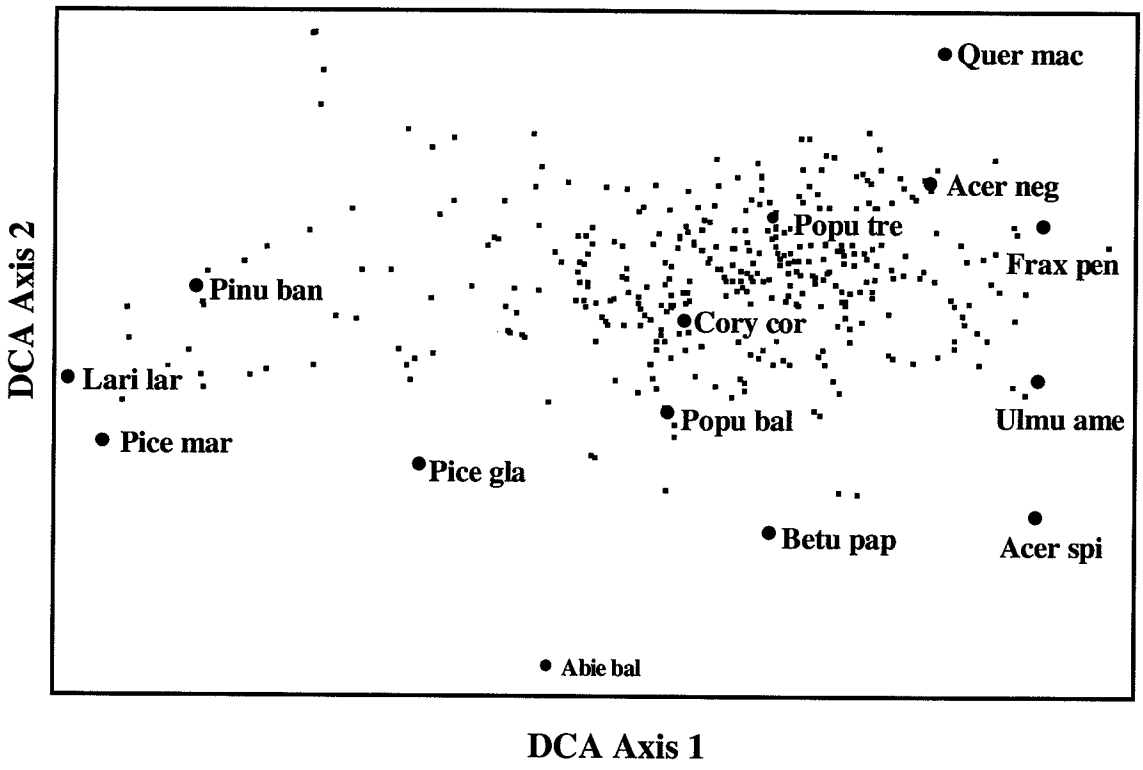

Figure 7.6: Detrended correspondence analysis of the sites used to assess accuracy of the map of RMNP. Scores for the dominant tree and shrub species are indicated (Abie bal=*Abies balsamea*; Acer neg=*Acer negundo*; Acer spi=*Acer spicatum*; Betu pap=*Betula papyrifera*; Cory cor=*Corylus cornuta*; Frax pen=*Fraxinus pennsylvanica*; Lari lar=*Larix laricina*; Pice gla=*Picea glauca*; Pice mar=*Picea mariana*; Popu bal=*Populus balsamifera*; Popu tre=*Populus tremuloides*; Quer mac=*Quercus macrocarpa*; Ulmu ame=*Ulmus americana*).

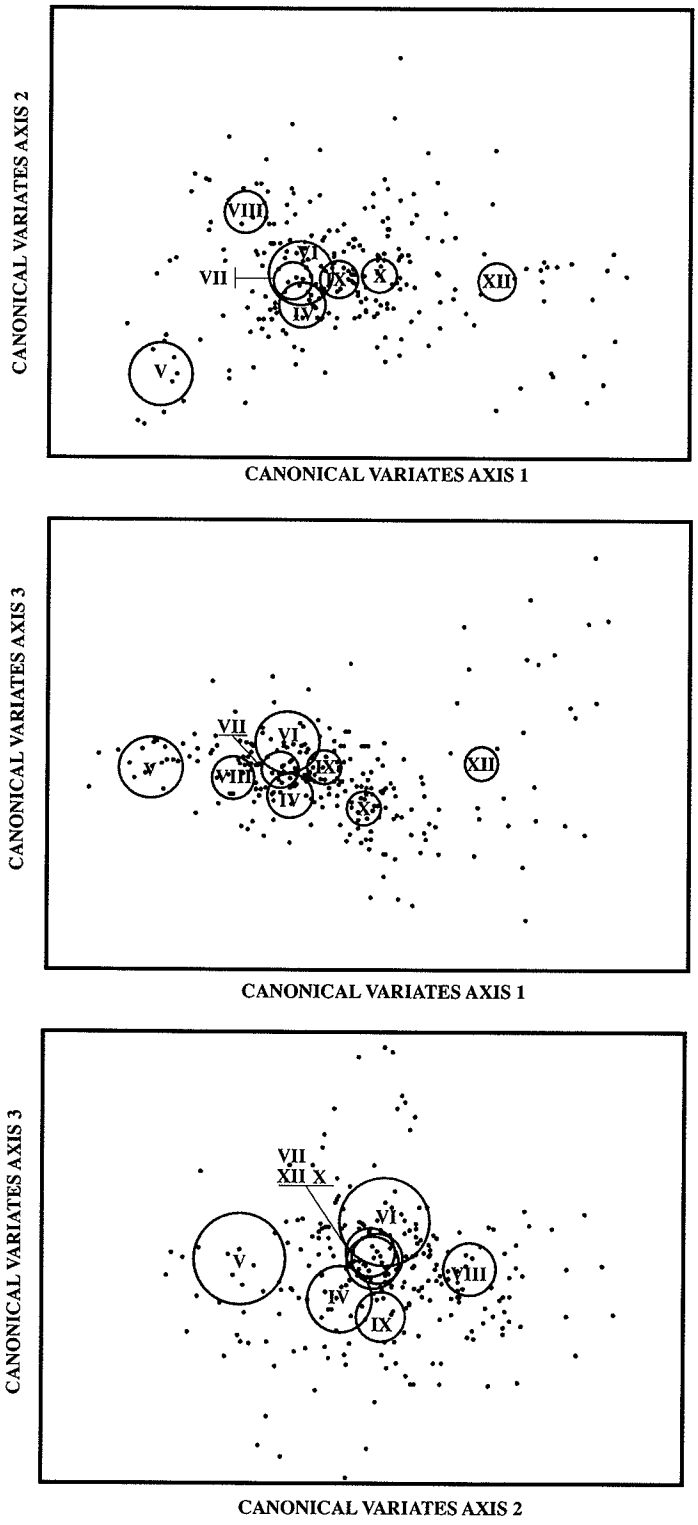

Figure 7.7: Pairwise combinations of the first three canonical discriminant axes for vegetation cover partitioned by map class. The 95% ellipsoids for the class distributions are shown; class labels follow **Table 7.2** (g=8; n=250).

7.6 Discussion

In this study an extensive ground dataset was used in the classification of vegetation associations within RMNP. The availability of ground data is important in landscape level mapping, as image classification is ultimately constrained by the floristic variation 'captured' in a ground sample (Goodchild 1994; Stehman 2001). This is especially true for the boreal forest where vegetation communities follow a complex continuum of floristic and structural variation (Peddle et al. 1997). It is therefore surprising that until recently image spectral classifications have been developed using limited vegetation data divided into subjectively defined categories (Congalton 1991; Franklin 1995). This approach provides little information about the relationships among the vegetation classes and ignores the variation within those classes. Without an independent means of analyzing these data, there is a tendency to treat the ground classification as absolute. Indeed, when aerial photograph interpretation is used to train classifications, it is often assumed that vegetation classes are identified and classified without error (Congalton 1991). An adaptive rule based approach to satellite image classification requires that decisions be based on a firm understanding of the surface being modeled (Stehman 2001). By recognizing the inherent variability within the vegetation associations, it was possible to revisit and redefine the classes to maximize the ecological information in the final map.

The classification of extensive ground sample data not only provides information about the floristic affinities among vegetation communities but can also be used to derive their spatial distributions. In this study, sample sites were established at random throughout the Park providing an unbiased estimate of overall vegetation patterns for the area (Edwards et al. 1998; Stehman 2001). This gave us the opportunity to verify whether the distribution of particular class on the vegetation map corresponded with the known geographic distribution for that association. Other spatial-spectral approaches to image classification such as ECHO (Extraction and Classification of Homogenous Objects) or semivariance use local autocorrelation in spectral reflectance values to improve patch classification (e.g. Treitz and Howarth 2000). While these methods tend to give larger more uniform classified patches, they do not necessarily recover the geographic distribution of those landcover types (Franklin 1995). It was found that knowing the geographic distribution of rare cover types such grassland, and those that tend to form stands in localized areas of the Park such as bur oak and eastern deciduous forests, aided in selecting better training sites. Ultimately, this improved separation these classes

in spectral space. Conversely, the overlapping spatial distribution of black spruce and jack pine in the eastern portion of the Park was an important consideration in merging the conifer classes.

The spectral optimization approach made use of multiple discriminanant analysis to provide a graphical representation of vegetation classes in band space. Graphical exploration is recommended during preliminary analysis in map classifications (Richards 1993), but usually this is undertaken by examining bivariate scatterplots of all possible band combinations. These plots often prove to be misleading as they neglect shared information that may provide additional discrimination. As well, spectral overlap in some band pair combinations may have little influence on map accuracy, because not all Landsat bands contribute equally to class discrimination (Moore and Bauer 1990; Lark 1995; Zhao and Maclean 2000). Indeed, while seven spectral bands are available for image classification, it has been established that a combination of TM band 3 (visible), band 4 (near infrared) and band 5 (short-wave infrared) provides 90% of total scene information and class discrimination (Bolstad and Lillesand 1992; Horler and Ahern 1986; Shen et al. 1985). Furthermore, restricting maximum likelihood classification to only these bands can produce more accurate results because of increased atmospheric noise when using all channels in the visible portion of the spectrum (Zhao and Maclean 2000). The subtleties of these relationships can only be examined by using a multivariate approach during image analysis.

Of the three bands used in this study, the results indicate that TM band 5 best discriminated among the broad range of vegetation conditions in RMNP. This band has been found to be correlated with changes in albedo related to canopy height, increasing leaf area and stem density (Horler and Ahern 1986; Jakubauskas 1996). These properties varied substantially from heavily treed classes (e.g. closed canopy conifer with low albedo) to open classes (e.g. grasslands with high albedo). Among the semi-closed to closed canopy classes separation was more pronounced on MDA axis 2. Although Bands 3 and 4 were correlated with MDA axis 1 they had the highest canonical loading on the second axis. It was found that MDA axis 2 split needle leafed conifers and linear bladed graminoids from broadleaf deciduous types. The near-infrared has been shown to be sensitive to the presence of conifers within the canopy, which when present often result in a substantial reduction in surface reflectance (Colwell 1974; Ranson and Williams 1992; Shen et al. 1985). Reflectance in this band is highest for broadleaf species, increasing with green biomass in the upper canopy and with

increasing cover of understory constituents (Horler and Ahern 1986; Jakubauskas 1996). The results of the discriminant analysis in this study differ somewhat from those of a Michigan study, where the canonical loading for bands 4 and 5 on the first and second MDA axes were reversed (Zhao and Maclean 2000). In that study only closed forest stands were examined, which suggests that the mid-infrared is an important band for mapping regions where canopy physiognomy is highly variable. Absorption in band 3 is almost exclusively the result of plant pigments that increase with green biomass (Myers 1983), resulting in a negative correlation between band 4 and 3 in discriminant space.

The spectral spatial-optimization used in this study was effective in improving the overall performance of the classification. The accuracy of Landsat map classifications of the northern boreal forest vary widely (40% to 95%), with a mean error > 15% (Bolstad and Lillesand 1992). Part of this variability is the result of the relative spectral similarity of many boreal canopy types (Shen et al. 1985). In many cases, it is impossible to discriminate between vegetation types based purely on spectral information, especially among the softwoods (Horler and Ahern 1986; Moore and Bauer 1990; Bolstad and Lillesand 1992; Zhao and Maclean 2000). The addition of supplementary data in rule-based GIS classification has been suggested as means to improving these classifications (Markon 1992; Goodchild 1994; Treitz and Howarth 2000). This approach works well where classes with similar spectral reflectance have different spatial distributions or responses to prevailing environmental conditions (Franklin 1995). For instance, in Wisconsin the discrimination between conifer species in boreal uplands and lowlands was improved through the incorporation of soils and terrain information (Bolstad and Lillesand 1992). Unfortunately these data sources are not independent, as soil maps are often based on inferences derived from the relationship between vegetation and soil. An alternative approach is to use multitemporal imagery to improve class discrimination. In previous studies, modest success has been achieved using spring and summer imagery (Moore and Bauer 1990). In this study, summer and fall imagery was used because of promising recent work examining seasonal changes in conifer leaf area index (LAI, Chen 1996b). However, there was little difference in reflectance among the five common arboreal softwood species in the study area even when fall imagery was included. Indeed, the multitemporal imagery was much better suited to the separation of several deciduous types (e.g. Oak - V and Shrubland - IV). To reduce the misclassification of softwoods, it became necessary to combine these divergent floristic groups into a single class.

The similar spectral properties of conifers on Landsat imagery is acknowledged but not discussed in the literature. Despite taxonomic differences among these species, it is felt that the nearly identical architectural properties of the canopy may be critical in determining their spectral reflectance. In most discussions regarding the interaction of light with vegetation, individual components of the canopy are often considered in isolation (but see Williams 1991). Real canopies are a mixture of different components: leaves, other plant structures, background and shadow that vary with scale (Colwell 1974; Myneni et al. 1992). These variations in crown closure, stand density and basal area may contribute as much to spectral reflectance as species composition and amount (Treitz et al. 1992; Zao and Maclean 2000). Measuring the signature spectrum at the scale of a single element neglects the emergent properties of the whole canopy. At needle-level scales jackpine and black spruce have different optical reflectance properties (Middleton et al. 1997) and the albedo for these needles is higher than that of deciduous leaves. However, at the stand level coniferous species have nearly identical optical reflectance properties and a lower albedo than broadleaf stands (Williams 1991). It has been long noted that conifers of similar stand density can rarely be identified to species (Horler and Ahern 1986) and even with supplimental information and hyperspectral data this is still the case (Trietz and Howarth 2000). This is almost certainly the result of the similari crown architecture and biophysical properties (Zhao and Maclean 2000; Walker and Kenkel 2000).

While biophysical parameters were not measured directly, vegetation cover values were weighted by canopy closure. Closure is often identified as a primary component of canopy structure influencing reflectance by altering the proportion of sunlit areas and shade within a pixel (Myneni et al. 1992; Hall et al. 1995; Sampson et al. 2001). It is perhaps not surprising then that many of the spectrally distinct vegetation classes identified in this study correspond to differing degrees of canopy closure. These classes occur along a structural continuum that can be modeled as spatial sequence (**Figure 7.8**):

- Parkland 'series': In western regions of RMNP tall aspen canopies (> 25m) with a well developed shrub understory on fresh soils are structurally similar to rich Eastern Deciduous forest (VIII) and are classified spectrally as such. On poor clay soils, aspen canopies with high canopy closure and low stature (10 –15 m) are spectrally distinct (Class VI). Interestingly, these low stature

aspen stands are spectrally indistinguishable from tall stature willow stands with the same overall physiognomy. As the aspen canopy becomes more open and uneven, reflectance changes to that of aspen Parkland (VII). As aspen density further declines, patches may be classified as shrubland (IV) or shrub grassland (III). Within the 'Parkland' series, the graminoid dominated canopies (e.g. dry Grassland II and Emergent I classes) share a similar physiognomy but are spectrally distinct because of differences in soil moisture.

- Mixed canopy conifer 'series': The presence of conifer species in the overstory or understory has a dramatic influence on stand reflectance. For instance, Open Canopy Conifer (XI) was distinctly different from Closed Canopy Conifer (XII) and mixedwood types (IX and X), the open canopy structure promoted higher albedo (largely resulting from increased reflectance from understory graminoids). However, within the Open Canopy Conifer class (XI), white spruce on grasslands was spectrally similar to black spruce on sedge dominated fens. Mixed Canopy Deciduous-Coniferous (X) typified by a tall stature trees (>25 m) and high crown closure differs spectrally from Deciduous Canopy-Coniferous Subcanopy (IX) stands which have a more open uneven structure. These two types are floristically identical, with class IX perhaps representing a later successional sere of X (following canopy break-up). Further break-up of the class IX canopy increases the spectral reflectance from tall shrubs resulting in the intergrading of this class with Shrubland (IV) in exposed sites. This sequence might also correspond with site age, as many of the upland shrub dominated areas have not burned in over 120 years (Sentar 1992).

- Burn 'series': Perhaps the most difficult area to classify using a training based approach was the 1980 Rolling River burn (**Figure 2.5**). Although post-fire patches were uniform in structure, the juxapositioning of unburned (e.g. Mixed Canopy Deciduous-Coniferous – X patches), partially burned and post-fire colonization patches made the establishment of training sites difficult. The spatial properties of this area differs from most in the Park, patch boundaries could be abrupt, sometimes accompanied by dramatic changes in floristic composition but not necessarily by changes in physiognomy. For instance, post-fire regenerating aspen patches were structurally similar to both

hazelnut and alder shrubland in the 11 year old stands. Although these patches were floristically distinct, they were all classified as Shrubland (IV). Similarly, post-fire regenerating conifer patches mixed with swamp birch were found to be structurally similar to vegetation establishing on post-disturbance beaver meadows. Many of the regenerating patches identified on the Landsat map outside of the Rolling River fire may be the latter.

The complex floristic and structural continua in the boreal forest require a different approach to accuracy assessment. Error matrices based on categorical data are problematic in a heterogeneous environment because of the requirement for a classification of the test set. This classification must either be performed at the same time as the training set (by randomly dividing the classified ground data into a 'training' and 'test' sets) or by the map user (tester) making *post hoc* class assignments of vegetation observed in the field into the map classes (Congalton 1991). The former method is problematic as statistical properties of the training and test sets often differ when sampled from a spatially heterogeneous population (Richards 1996; Stehman and Czaplewski 1998). *Post hoc* classification methods also have little to recommend because of error in field class assignments independent of map error (Congalton 1991). Error matrices also neglect the continuous nature of vegetation and the interrelationships among community types. This has important implications because some misclassifications may represent fundamental problems with the map (e.g. softwoods misidentified as hardwoods), while others are a matter of degree (e.g. confusion between two mixedwood types). Unfortunately, an error matrix makes no distinctions between these two cases (Gopal and Woodcock 1994). For instance, it was found that the Deciduous Canopy–Coniferous Subcanopy class (IX) shared off-diagonal elements with the Mixed Canopy Deciduous-Coniferous class (X), implying lower map accuracy (**Table 7.4**). These classes were adjacent but well separated in map discriminant space, indicating that species cover and composition could be partitioned between the groups. Both mixedwood forest types had similar floristic composition but were characterized by differences in the relative abundance of species in the overstory and understory. The lower accuracy on the error matrix approach was more likely the result of class confusion during *post hoc* assignment in the field because of the difficulty in assessing relative composition on the ground. In heterogeneous dynamic systems such as the boreal forest, this form of class confusion can be commonplace. A canonical approach to accuracy assessment eliminates any issues regarding the identification of 'classes' on

the ground while providing a means to assess the degree of similarity between categories.

7.7 Conclusion

The management of large natural areas requires affordable landscape-level cover data (Sachs et al. 1998). Satellite imagery is a practical source of information regarding ground cover composition, biophysical structure and landscape heterogeneity (Rey-Benayas and Pope 1995; Sampson et al. 2001). However, the measurement of these parameters from reflectance data is indirect, requiring a statistical relationship be established. Indeed, a map can only make a "statistical prediction about conditions on the ground and this must be interpreted in the light of estimates of the frequency and magnitude of errors" (Lark 1995). An iterative approach using extensive ground data and multivariate analysis is essential for understanding these relationships.

a)

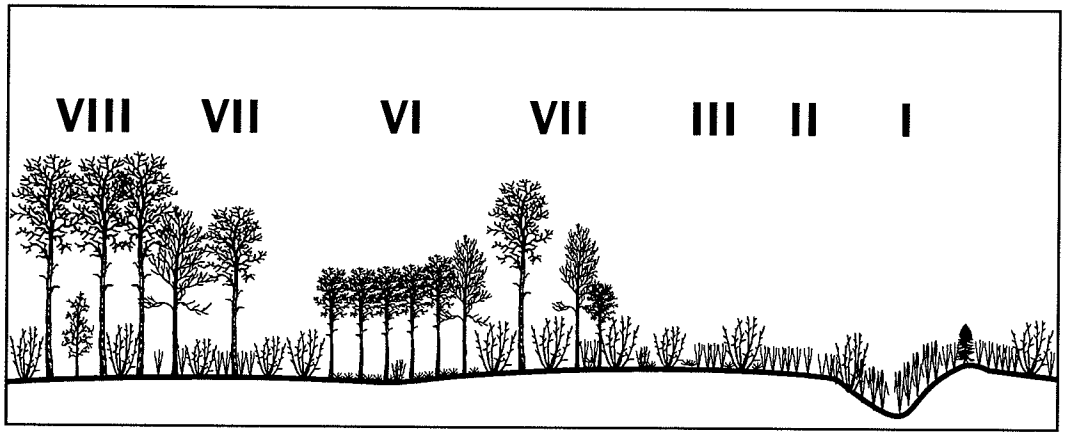

b)

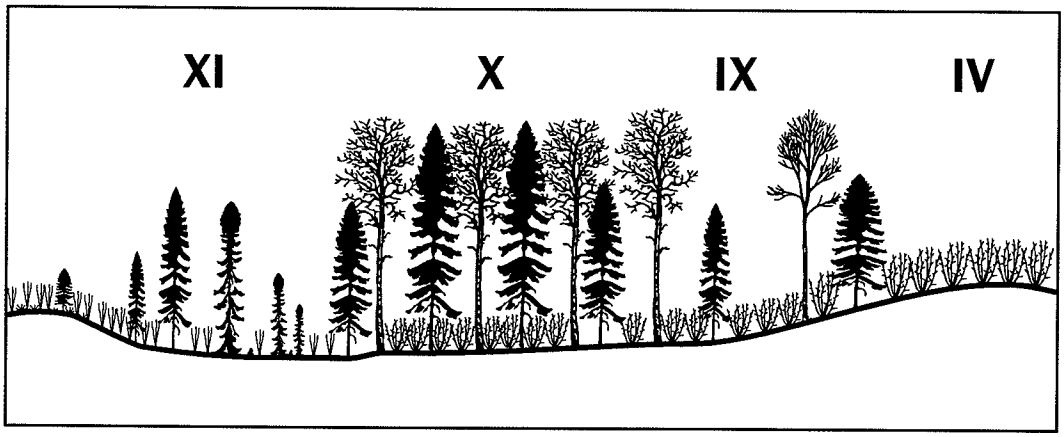

c)

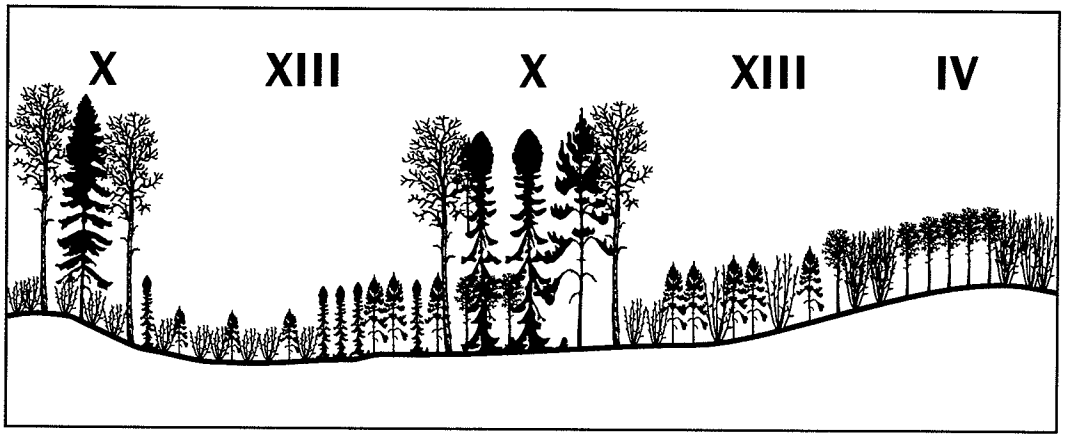

Figure 7.8: Canopy structural sequences corresponding with changes in spectral reflectance: a) Aspen Parkland series; b) Mixed canopy conifer series and c) Burn series.

Chapter 8

The Adaptive Geometry of Boreal Conifers

Abstract. Accurate and unbiased radiative energy transfer models are critical to our understanding of ecosystem primary productivity, carbon cycling, and climate change. Much of the current research in this area is based on models parameterized for grasslands and broadleaf forests. However, many temperate montane and boreal forests are dominated by conifers, which present unique challenges to modellers. It is proposed that two fundamentally different strategies by which plant canopies optimize solar radiation interception. Laminar canopies (e.g. grasslands, broadleaf trees) are 'solar panels' that directly intercept incoming radiant energy. By contrast, conifer canopies are conical anechoic ('without echo') surfaces that intercept radiant energy by scattering it through the canopy. The properties of anechoic surfaces are well known in acoustical and electrical engineering, but have not been applied in environmental biophysics. In this study, the physical principles of anechoic surfaces is discussed, and it is demonstrated how these principles apply to conifer trees and canopies. A key feature of anechoic interception is low radiance over all wavelengths, which is an emergent property of the system. Using empirical data from boreal forest stands in Riding Mountain National Park (Manitoba, Canada), it is demonstrated that conifer canopies have very low near-infrared radiance compared to laminar broadleaf canopies. Vegetation index values for conifers are thereby reduced, resulting in underestimates of primary productivity and other biophysical parameters. The adaptive significance of boreal conifer geometry is discussed, and the factors driving selection of laminar versus anechoic canopy architectures are considered.

8.1 Introduction

Over the past decade, the modelling of carbon flux has become a central focus of research in boreal ecosystems (Sellers et al. 1995; Brown et al. 2000). Such models require accurate and unbiased estimates of ecoregional photosynthetic rates (carbon-fixation), primary productivity, and phytomass (Middleton et al. 1997; Gholz et al. 1991). Boreal forests, which occupy about 20% of the world's landmass, are dominated by conifers (Sprugel 1989; Middleton et al. 1997; McDonald et al. 1998). However, forest canopy radiative transfer models are specific to broadleaf trees (Norman and

Jarvis 1975; Hall et al. 1995), and the derivation of biophysical productivity indices is based on empirical data from grasslands and broadleaf forests (Jordan 1969; Rouse et al. 1973). Broadleaf trees use a 'solar panel' approach to light capture, arranging their leaves in horizontal laminar layers within the canopy (Sprugel 1989; Norman and Welles 1983). This is a very efficient strategy for capturing direct solar radiation (Horn 1971; Hall et al. 1995). By contrast, conifers have conical crowns containing clusters of needle-shaped leaves, making them appear poorly adapted for optimal light capture (Bond 1989; Dalla-Tea and Jokela 1991). Given this fundamental difference in crown architecture, it is not unreasonable to suggest that existing biophysical models might produce biased results when applied to conifer forests (cf. Nelson 1997).

Numerous studies have demonstrated that conifer and broadleaf canopies 'behave' very differently. The optical properties of conifers vary with scale (Williams 1991), making phytomass estimation unreliable and subject to considerable error (Hall et al. 1995). Prediction of conifer canopy light extinction as a function of the leaf area index (LAI) is also problematic (Norman and Jarvis 1975; Gholz et al. 1991), as is the use of biophysical indices to estimate primary productivity (Ranson and Williams 1992; Chen 1996a; Liu et al. 1997). In satellite images (e.g. Landsat thematic mapper), closed conifer stands are characterized by low reflectance over all wavelengths (Ranson and Williams 1992), indicating a strongly absorptive canopy. Explanations for this observation are vague, and include 'canopy heterogeneity' (Gholz et al. 1991; Rowe 1993) and 'needle aggregation and angle' (Sprugel 1989; Sampson and Smith 1993). Another vague term, the 'shadowing' effect of conifer canopies, has been used to explain away errant estimates of biophysical parameters (Colwell 1974; Hall et al. 1995). These observations invite an important question: why do conifers cast such a deep shade, especially in portions of the spectrum where no pigments exist to absorb the incoming radiation? To our knowledge, no plausible mechanism has been forthcoming to explain the scale-related optical behaviour of conifers across the radiative spectrum.

Basic tree architecture is determined by fixed genetic rules (Tomlinson 1983; Bégin and Filion 1999). The conical crown and needle-like leaves of conifers are presumably evolutionarily adaptive, as otherwise they would not have been selected for (Horn 1971; Farnsworth and Niklas 1995). Indeed, the dominance of gymnosperms in many temperate ecosystems (e.g. the boreal and Pacific coast forests of North America) is testament to the adaptive significance of the conifer architecture (Bond 1989; Sprugel 1989).

In this paper, a mechanism for radiant energy capture based on wave physics is proposed to explain the scale-related optical properties of conifers. Specifically, it is postulated that:

- Conifers are anechoic (literally, 'without echo') surfaces that are strongly absorptive over all wavelengths of incident radiant energy.
- The anechoic structure of conifers is an emergent property that is reinforced by a 'cone-on-cone' self-similarity across scales, from stands to individual trees to component branches, shoots and needles.
- Boreal climates favour the anechoic canopy architecture as an efficient strategy for radiant energy capture.
- Biophysical productivity estimation assumes that the ratio of red to near infrared radiance declines as biomass increases. But because conifer canopies are strongly absorptive over all wavelengths, biophysical indices will generally underestimate boreal forest primary productivity.

8.2 Strategies for Light Capture

There are two fundamentally different strategies of light capture by plant canopies (**Figure 8.1**). Laminar canopies (e.g. grasslands, broadleaf tree canopies) optimize light capture through direct interception and absorption. By contrast, conical anechoic surfaces (e.g. conifer tree canopies) intercept light by scattering it through the canopy.

1. Laminar Interception

A flat laminar surface is an optimal strategy for the direct interception and absorption of radiant solar energy. This 'solar panel' approach is characteristic of broadleaf forests and grasslands. In laminar canopies, an efficient arrangement of photosynthetic pigment promotes absorption of photosynthetically active radiation (PAR) while minimizing backscattering (Myers 1983). Conversely, the lack of near-infrared (NIR) absorptive pigments renders laminar surfaces high reflective in these wavelengths (Ranson and Williams 1992). NIR reflectance therefore increases with phytomass, i.e. as a multi-layered laminar interception surface develops (Colwell 1974).

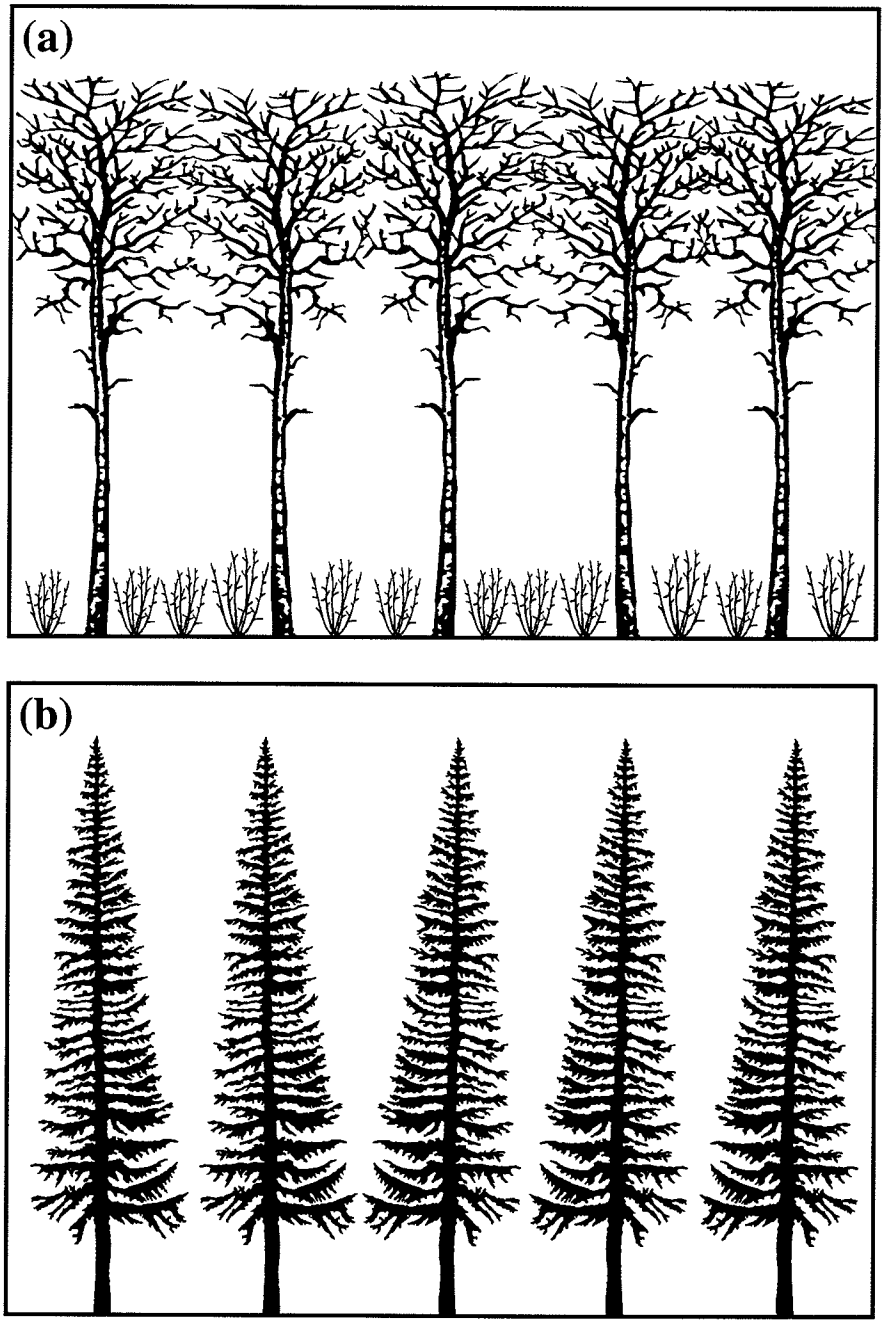

Figure 8.1: Contrasting canopy architectures for light interception. (a) Laminar interception: broadleaf forest, showing laminar canopy and understory layers; (b) Anechoic interception: conifer forest, showing conical tree crowns.

In broadleaf forests, light interception often occurs over several discrete laminar layers (Lieffers et al. 1999). Although vertical stratification of laminar canopies increases total absorption, self-shading restricts the number of layers present (Norman and Welles 1983). A typical laminar leaf layer casts a deep shadow (umbral shade) to a distance of about 100 leaf diameters from the point of interception. A partial shadow (penumbral shade) is cast at greater distances, allowing development of a second layer (Horn 1971). Maximal photosynthesis for an idealized multilayer laminar canopy occurs at a leaf area index (LAI) of 1.6. In typical broadleaf forests leaf angles are rarely perfectly horizontal and LAI values of 5 or higher are often observed (Horn 1971; Sprugel 1989).

In laminar canopies, a predictable relationship exists between LAI and the PAR extinction coefficient *k*. This relationship is commonly modelled using the Beer-Lambert negative power law:

$$I/I_o = e^{-k\,LAI} \qquad [1]$$

where I_o is the incident PAR. The equation is simply inverted to obtain an estimate of LAI from an empirically derived *k*-value (Lieffers et al. 1999). This model assumes that leaves are randomly located in the canopy, but empirical corrections are available to account for non-random or clustered distributions of leaves (Norman and Welles 1983; Gholz et al. 1991). In laminar canopies, leaf area and foliar biomass are tightly coupled to canopy transmittance and photosynthetic efficiency. It is this architecturally determined relationship that is exploited by the Beer-Lambert equation.

2. Anechoic Interception

It is proposed that light interception and capture by boreal conifers utilizes an anechoic ('without echo') strategy. In acoustics and electrical engineering, echo reflection occurs when a wave propagating in one medium encounters a second medium of greater impedance (Pierce 1981). The magnitude of reflection is proportional to differences in impedance between the two media (Van Heuvelen 1986). For waves propagated in a hollow tube, anechoic termination involves attenuating mechanisms that cause the amplitude of the generated wave to decrease exponentially with wave propagation distance *x*, following:

$$e^{-\alpha x} \qquad [2]$$

where α is a frequency-dependent quantity. A tube has anechoic properties if the length (L) through which the wave passes is sufficiently long:

$$e^{-\alpha L} << 1 \qquad [3]$$

In practical applications, anechoic termination for a tube of finite length is achieved when the attenuation per unit length increases slowly, following the relation:

$$\exp\left(-2\int_0^L \alpha \ dx\right) << 1 \qquad [4]$$

When L is sufficiently large, the amount of echo is minimal since slow attenuation (tapering) greatly reduces partial wave reflection.

The anechoic property of cones or tapers has been exploited in the design of sound chambers, transmission lines, and electromagnetic test facilities (Beranek and Sleeper 1946; Klopfenstein 1952; Holloway et al. 1997). To obtain an efficient anechoic surface, cones must be tightly packed and cone length must be many times greater than the wavelength of the energy to be absorbed (Holloway et al. 1997). Cone angle can vary from 8° to 22°, with a reported optimum of 12.5° (Bornkessel and Wiesbeck 1996; Koidan et al. 1972). To maximize absorption, cones should be constructed of a material dense enough to absorb the incident waves, but not so dense as to result in cone tip reflection (Holloway et al. 1997; Koidan et al. 1972). In engineering applications, density is manipulated by mixing materials of different dielectric properties.

Anechoic surfaces can also absorb or 'capture' radiant energy, as recently demonstrated for sheets of 'black' silicon (**Figure 8.2a**). This anechoic material, which consists of cones 10-12 μm in height, absorbs substantially more incident radiation than typical laminar silicon (Her et al. 1998). A light wave entering the cone interstices 'bounces' off the tapered surfaces and is reflected inward, resulting in multiple reflections. Each reflection results in partial absorption as the energy contacts the denser cone material. Because very little of the incident energy survives these numerous reflections, radiance from an anechoic surface is very low (Holloway et al. 1997). It is hypothesized that

boreal conifers use this light 'capture' strategy: note the striking resemblance between anechoic 'black' silicon and a dense white spruce canopy (**Figure 8.2b**). The tapered conical architecture of boreal conifers is thus highly adaptive, resulting in an anechoic canopy that efficiently scatters and absorbs radiant energy. Transmission within the interstices of tree crowns is high (cf. Canham et al. 1999), but once a radiant energy wave strikes the canopy it is scattered downward and ultimately absorbed. High absorption occurs over all wavelengths, including NIR. This light 'capture' strategy is fundamentally different from that used by broadleaf species, suggesting that laminar canopy transmission models (based on the Beer-Lambert law) are inappropriate for conifer canopies.

8.3 Scaling Properties of Conifer Canopies

Because an anechoic surface consists of a large number of cones, high absorption is an emergent property of the system (cf. Koidan et al. 1972). Scaling properties are also important in characterizing the absorptive properties of complex anechoic surfaces. Within the PAR spectrum, conifer and broadleaf trees have similar reflectance properties across the leaf, branch and canopy scales (Williams 1991). However, substantial differences occur in the NIR spectrum. NIR reflectance of typical laminar leaves (sugar maple) is 5-10% greater than that of conifer needles (Norway spruce, white and red pine; see also Middleton et al. 1997). At the branch and canopy scales, this difference increases to 20%. Irrespective of species, conifer canopies absorb much more NIR radiation than broadleaf canopies (Ranson and Williams 1992; Brown et al. 2000).

In conifers, radiant energy scattering is scale-dependent: measurements made at the canopy scale differ from those made at the leaf and branch scales (cf. Chen 1996b). For example, measured NIR radiance declines by 30-35% from the leaf to canopy scales (Williams 1991). Norman and Jarvis (1975) also noted the scale-dependent nature of conifer scattering, concluding "with the aid of hindsight, it is possible to suggest that the scattering properties of shoots should be measured as well as those of needles". Such findings are entirely consistent with anechoic termination.

Conceptually, a conifer stand can be viewed as a complex anechoic surface consisting of a cascading series of 'cones-on-cones' from the needle to stand scales (**Figure 8.3**).

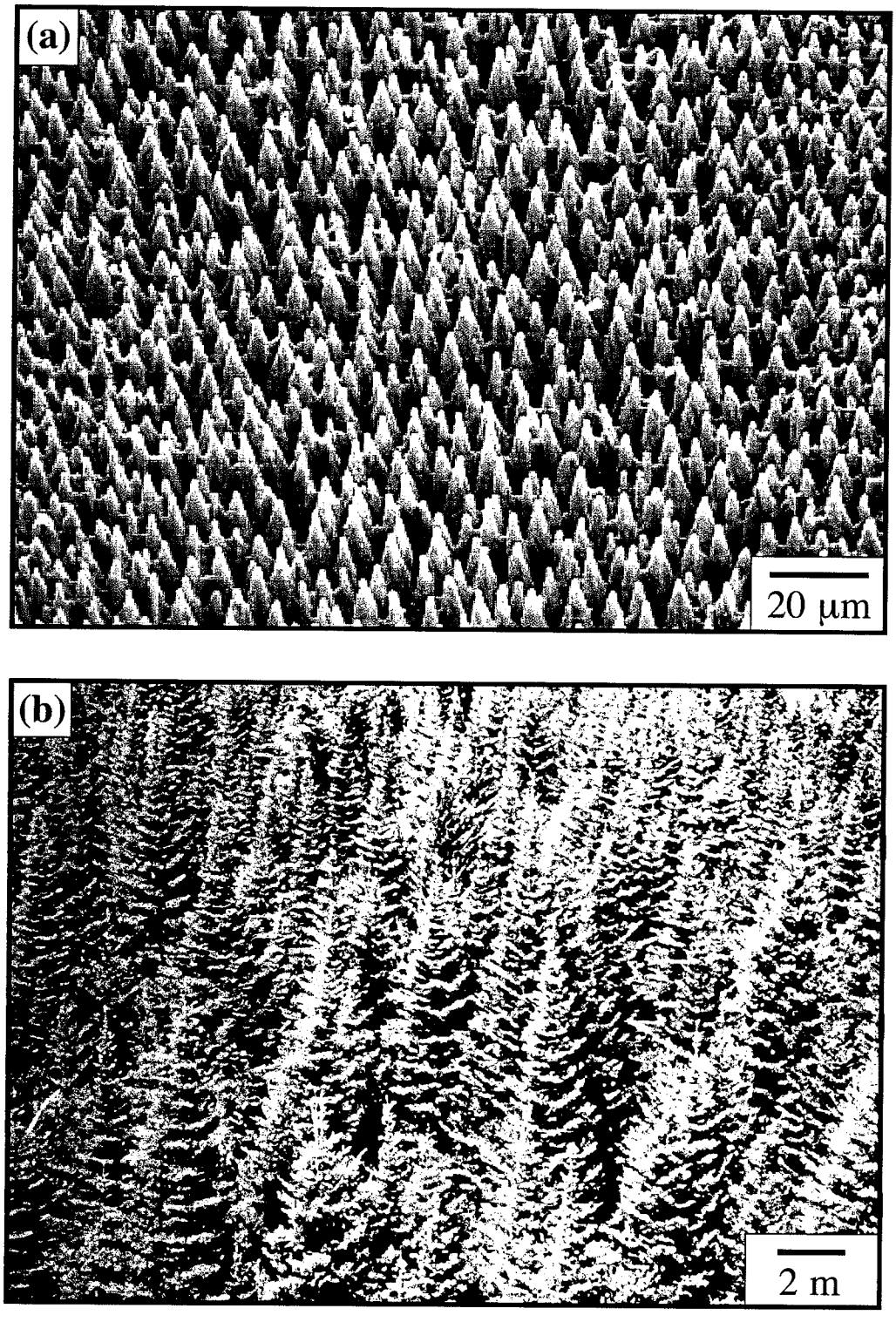

Figure 8.2: (a) 'Black' silicon, image courtesy of Eric Mazur; (b) Aerial view of a boreal white spruce stand.

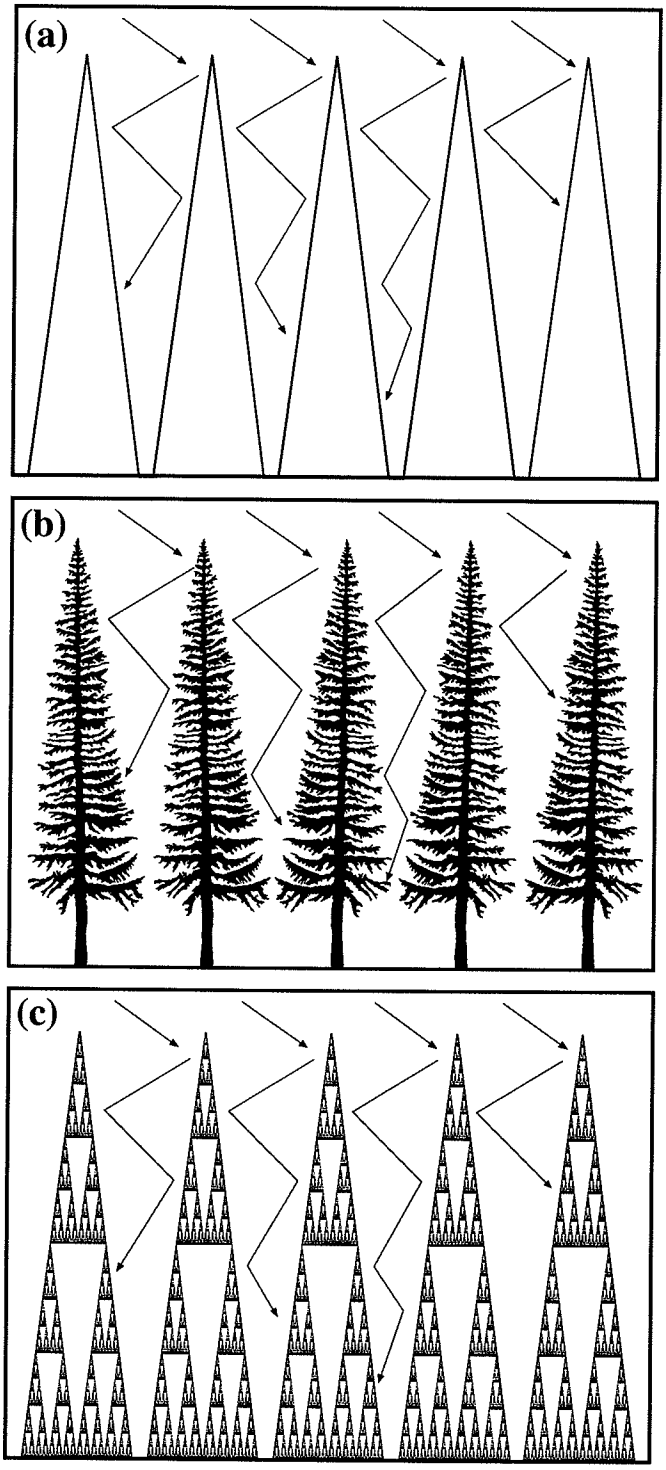

Figure 8.3: (a) Schematic of an idealized anechoic surface, showing multiple scattering and absorption of light (after Holloway et al. 1997); (b) A conifer stand as an anechoic surface. The conical crowns allow light to deeply penetrate the canopy, but light eventually contacts a branch/needle where it is either absorbed or scattered to another branch/needle; (c) Representation of a conifer stand as a self-similar fractal surface, illustrated using the Sierpinski gasket. Multiscale complexity ensures that most incident solar radiance is absorbed, not reflected.

In this sense, conifers are statistically self-similar and display fractal properties (*sensu* Mandelbrot 1983). It is suggested that fractal iteration of the basic conical form produce a maximally absorptive (anechoic) surface from which very little incident solar radiation 'escapes' (**Figure 8.4**). Fractal scaling has been observed in many biological systems, including conifer canopies (Zeide 1999), but specific hypotheses relating process to fractal form have not been forthcoming (Kenkel and Walker 1996). The development of a fractal surface in conifer canopies is an example of self-organization, where the conical structure is driven at all scales by the same underlying physical process of anechoic termination (Perry 1995; Parker 1999).

8.4 Evolutionary Implications

Laminar and anechoic surfaces are fundamentally different geometric strategies for optimizing light capture. While light interception is an important aspect of the arboreal habit (King 1990), structural support, nutrient and water supply, and propagule dissemination must also be considered (Farnsworth and Niklas 1995). Tradeoffs associated with light interception, foliar respiration and water balance result in the selection of arboreal habits that match specific environmental conditions (Horn 1971). In this section, the factors driving selection of laminar versus anechoic canopy architectures are considered.

1. Laminar Interception

Laminar leaf and canopy architectures are characteristic of broadleaf trees. This 'solar panel' strategy optimizes direct light interception, thus maximizing photosynthesis provided that other resources are not limiting (Bond 1989). Broadleaf trees in mesic environments typically form flat, umbrella-shaped crowns with few lower branches (Horn 1971). This results in relatively high photosynthetic efficiency and low respiration costs, since only a thin laminar canopy need be maintained (Sprugel 1989; Dalla-Tea and Jokela 1991). Thin laminar leaves are also efficient dissipaters of heat, which is of great adaptive significance in hot tropical environments (Whitmore 1990). However, a laminar architecture also results in high evapotranspiration rates, placing a strain on plants to maintain a positive water balance (Sprugel 1989). In angiosperms, advanced vessel elements and anastomosing leaf veins efficiently supply water to leaf tissue, but at a cost of increased rates of embolism under moisture stress and at low temperatures (Raven et al. 1987; Bond 1989).

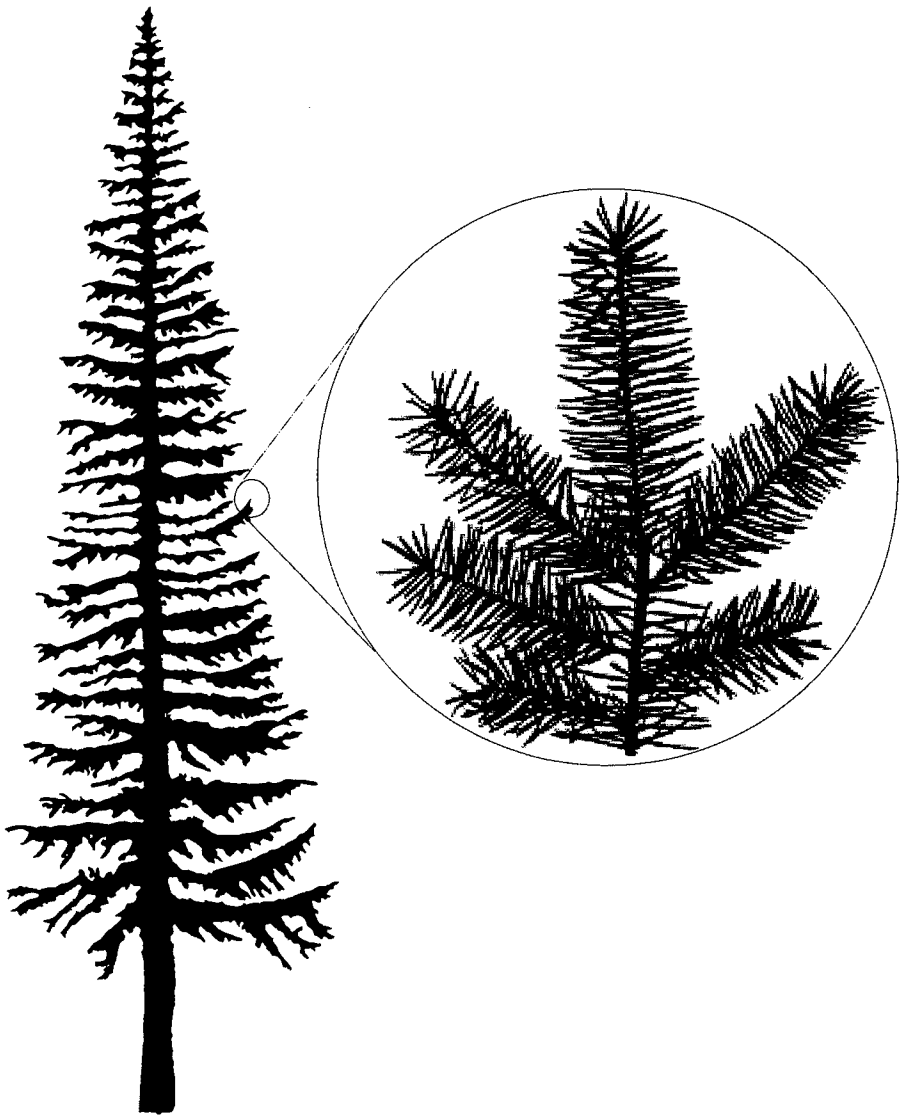

Figure 8.4: Self-similar scaling properties of a white spruce tree. The overall conical shape of the crown is repeated in the whorls of conical-shaped branches. The magnification illustrates similar scaling properties in the fine branches and needles.

Although laminar canopies are highly efficient interceptors of direct solar irradiance, light saturation in the sunleaves of temperate forest trees typically occurs at 25% of full sunlight (Horn 1971; Norman and Jarvis 1974; Sprugel 1989). Adding laminar layers increases stand photosynthetic efficiency, but shading effects may severely limit the development of a lower canopy (Horn 1971). Because laminar surfaces are highly reflective (Richards 1993), leaf transmissivity must be high enough to ensure efficient PAR absorption (Ranson and Williams 1992). Xeromorphic leaf adaptations (e.g. thick leaf cuticle), while reducing evapotranspirative water loss, also increase reflectance and so reduce light interception.

A laminar interception strategy is favoured in uneven-aged, mixed-canopy stands where interspecific competition for light is strong, water is in sufficient supply, and large-scale catastrophic disturbances (e.g. crown fires) are rare. Laminar leaves and canopies are also favoured in warm-temperate to tropical environments, where solar zenith angle is high, radiant energy is direct (maximizing 'solar panel' efficiency), and ambient temperatures are high (i.e. where dissipation of heat from leaves is important).

2. Anechoic Interception

Anechoic interception is characteristic of the gymnosperms. Conifers typically have a conical crown, maintain branches deep into the subcanopy (except in very dense stands), and have needle-like leaves. The anechoic strategy efficiently captures both direct and scattered radiant energy (cf. Sellers et al. 1995; cf. Parker 1999). Because light scatters internally within the canopy, individual needles do not need to photosynthesize or transpire at a maximal rate (Sprugel 1989). However, maintaining a high needle density in the canopy, while increasing light capture efficiency, also increases respiration costs (Sprugel 1989; King 1990). The photosynthetic efficiency of individual needles is also limited by xeromorphic traits such as thick epidermal-hypodermal layers and sunken stomata (Raven et al. 1987). Such adaptations are required in conifers because they lack efficient water conductive tissue (Raven et al. 1987; Sprugel 1989). The absence of large diameter vessel elements in conifers limits growth under mesic conditions, but at low temperatures and under high water stress xylem tracheids have a lower rate of embolism (Bond 1989).

The absorption of radiant energy in anechoic systems is structurally based, resulting in high interception of all wavelengths. Absorbed energy is ultimately emitted as heat

(Van Heuvelen 1986; Sellers et al. 1995), suggesting that anechoic architecture may also be an adaptive strategy to thermally warm conifers growing in cold environments. In closed conifer stands, inner canopy temperatures may be 5-10°C warmer than ambient, particularly when the sun angle is low (Smith and Carter 1988). In cool-temperate environments, such thermal warming extends the effective growing season (Sprugel 1989; Smith and Brewer 1994).

A dense packing of cones increases the overall efficiency of anechoic surfaces (Holloway et al. 1997). In conifer stands, a dense canopy has the added benefit of suppressing potential competitors that may be present in the advance regeneration layer (Messier et al. 1999). Development of an efficient anechoic canopy requires that individuals be of similar size and shape, such as occurs in monodominant, even-aged stands established following a catastrophic fire. Subsequent canopy breakup and/or invasion by broadleaf species will reduce the efficiency of the anechoic canopy.

It is expected that the anechoic interception strategy to be selected for in environments where recurrent catastrophic disturbances favour the perpetuation of monodominant, even-aged conifer stands. North-temperate cloudy environments (e.g. North America's north-west coast) and other regions where the majority of incident radiation is indirect (e.g. north-facing slopes), as well as northern boreal regions where the solar zenith angle is low, will also favour anechoic over laminar interception. Anechoic properties are also favoured in cold climates, since heat energy capture rather than dissipation is paramount. Finally, conifers may be favoured in temperate xeric environments where water rather than light is the limiting factor.

8.5 Implications for Biophysical Indices

Canopy Transmissivity, LAI and Productivity

Anechoic interception provides a ready explanation for conflicting data on conifer canopy transmissivity. While some studies have found that conifer canopy transmittance is < 1% of incident irradiance (Norman and Jarvis 1974; Ranson and Williams 1992), others have recorded deep penetration of diffuse irradiance into the canopy (Gholz et al. 1991; Rowe 1993; Sampson and Smith 1993). Conical branch and tree architecture in conifers ensures high transmittance between structural elements, with the result that light may penetrate well into the canopy (Sampson and Smith 1993; Canham et al. 1999).

However, once the incident radiant energy strikes a structural element of the canopy, it is scattered until completely absorbed. Needle packing and orientation are optimized to simultaneously increase transmissivity into, and absorption by, the canopy (Sprugel 1989). Given the structural complexity of conifers, it is clear that a single measure of transmissivity cannot quantify inherent heterogeneity of the anechoic surface (cf. Chen 1996b). The importance of this assertion cannot be understated, as LAI is often determined indirectly from canopy transmissivity data (Lieffers et al. 1999).

Indirect estimates of LAI are commonly used to model canopy radiative transfer (Norman and Jarvis 1975; Lieffers et al. 1999). Indirect methods for estimating LAI work well in broadleaf canopies, but they consistently underestimate leaf cover in conifer stands (Ranson and Williams 1992; Chen 1996a). Empirical corrections are therefore required to obtain reasonable estimates of conifer LAI (Sampson and Smith 1993). In addition, transmissivity models based on needle properties alone are biased unless needle aggregation is also considered (Norman and Jarvis 1975; Chen 1996b; Middleton et al. 1997).

Field measurements reveal that LAI values for conifers are often 2-4 times higher than for broadleaf trees (Sprugel 1989). Numerous authors have suggested that high needle density results in self-shading, reducing canopy photosynthetic efficiency (Gholz et al. 1991; Dalla-Tea and Jokela 1991; Sampson and Smith 1993). However, this assertion is inconsistent with empirical data: conifer productivity often equals or exceeds that of broadleaf trees under similar climatic conditions (Sprugel 1989). This paradox has been explained by 'shadowing' within the canopy: while conifers do indeed cast a deep shade, they also absorb virtually all incident radiation (Ranson and Williams 1992; Rowe 1993; Hall et al. 1995; Sellers et al. 1995). It is suggested that 'shadowing' is the product of an adaptively efficient anechoic surface consisting of densely-packed needles arranged so as to maximize radiant energy 'capture'.

NDVI:

Anechoic scattering by conifer canopies has important implications for the interpretation of vegetation indices derived from remotely sensed data. Commonly used indices express PAR and NIR spectral band values as a ratio (Myers 1983; Chen 1996a). Spectral band ratioing, which is often used to predict primary productivity, is based on two assumptions: that leaf pigments differentially absorb visible light (PAR),

and that NIR reflectance increases as phytomass increases (Ranson and Williams 1992; Chen 1996a). Thus, productive habitats are expected to have low PAR radiance but high NIR radiance (Tucker 1979; Myers 1983). The 'simple ratio' (SR) vegetation index, originally developed for tropical forests (Jordan 1969), uses this assumed relationship:

$$SR = NIR/PAR \qquad [5]$$

where the units of reflected PAR and NIR energy are in $W/m^2/ster/\mu m$. Higher SR values are assumed to indicate greater photosynthetic efficiency. Because it is a simple ratio, the SR index is unbounded. Furthermore, it is sensitive to non-selective atmospheric scattering (so-called Mie scattering), variations in aspect, and incidence angle (Colwell 1974; Tucker 1979; Richards 1993). Proportional differences in magnitude are thus assumed to reflect 'noise' that should be corrected for through normalization. The 'normalized difference vegetation index' (NDVI) was originally developed to measure phytomass/productivity in North America's Great Plains grasslands (Rouse et al. 1973):

$$NDVI = \frac{NIR - PAR}{NIR + PAR} \qquad [6]$$

NDVI is normalized to range between –1 and +1, but negative values are uncommon (Blair and Baumgardner 1977). Although developed to estimate grassland production (Rouse et al. 1973; Myers 1983), NDVI has been uncritically applied across various ecosystems, e.g. to estimate global primary productivity (Los et al. 1994; Prince and Goward 1995).

NDVI has been successfully used to quantify spatial and temporal changes in phytomass and/or productivity across broadly-defined vegetation classes: examples include changes in LAI along a moisture gradient from interior high desert to wet coastal forest (Peterson et al. 1987), grassland productivity along a gradient from bare ground to complete vegetation cover (Paruelo et al. 1997), and tree density over a range of 0-50% canopy closure (McDonald et al. 1998). However, there are some problems inherent in applying NDVI to boreal forest ecosystems (Chen 1996a). Indeed, the relationship between NDVI and phytomass/LAI is largely invariant once canopy closure exceeds a critical threshold (McDonald et al. 1998; Ranson and Williams 1992).

To further investigate the behaviour of NDVI, the reflectance properties of grassland, shrubland, and boreal broadleaf and conifer forest in Riding Mountain National Park (RMNP), Canada are examined. A Landsat-5 thematic mapper image of the region dated August 3, 1991 was used. This image was selected for its high atmospheric transmittance and minimal cloud cover. The spectral ranges used to calculate NDVI were PAR = 0.63-0.69 μm and NIR = 0.76-0.90 μm. Atmospheric effects were eliminated using a path irradiance model of λ^{-4}, which corresponds to a clear atmosphere dominated by Rayleigh scattering (Richards 1993). A dark order subtraction was then applied to correct for residual path irradiance effects (Chavez 1988). To calculate NDVI, Landsat-5 digital numbers were converted to absolute PAR and NIR radiance values following Markham and Barker (1986).

In the summer of 1999, $n = 57$ ground sites over six vegetation classes were located at RMNP. The classes are: *I* = grassland; *II* = grassland with shrubs; *III* = shrubland; *IV* = broadleaf (trembling aspen) forest; *V* = mixed broadleaf-conifer forest (trembling aspen-white spruce); *VI* = conifer forest, which included four canopy-types: white spruce, black spruce, balsam fir, and jack pine. Each ground site had a uniform cover and species composition over at least 1 ha. Nine ground sites were located for each of classes *I-V*. For class *VI*, three ground sites were located in each of the four canopy-types ($n = 12$). Ground site were positioned on the Landsat image using differentially-corrected GPS coordinates obtained in the field. PAR and NIR radiances were determined from a 3x3 grid of Landsat pixels (approx. 1 ha) centred on each ground site.

As expected, NDVI increases with phytomass along a gradient from grasslands, through mixed grass-shrublands and shrublands to closed broadleaf forests (**Figure 8.5a**). These four vegetation classes are characterized by laminar canopy interception. NDVI values for shrublands and broadleaf forests are very similar (0.83 vs. 0.85), despite the forests having much higher phytomass. This result is largely attributable to lower NIR backscattering from the forests, which is contrary to expectation: NDVI implicitly assumes that PAR radiance decreases, and NIR backscattering increases, with increasing phytomass (Myers 1983). The assumed positive relationship between NIR radiance and phytomass is particularly problematic in conifers (Peterson et al. 1987; Ranson and Williams 1992). Mixed conifer-broadleaf forests and pure broadleaf forests have similar PAR reflectances, but the much lower NIR radiance of mixed forests reduces NDVI to 0.79. Pure conifer forests reflect even less NIR, reducing NDVI to 0.73 (the

same value was obtained for much less productive grass-shrubland, **Fig. 5a**). In fact, these results indicate that NIR radiance from conifer forests is actually lower than from grasslands.

Why is NDVI such an ineffective statistic for estimating biophysical parameters of forested ecosystems? From these empirical results, a simple model of the relationship between PAR and NIR reflectance for both laminar and anechoic canopies is developed. In laminar canopy systems, the absolute magnitude of the PAR-NIR reflectance vector remains reasonably constant as a third-dimensional physiognomic structure develops (i.e. from grassland to broadleaf forest). At the same time, the relative proportion of PAR to NIR reflectance changes in a manner consistent with the NDVI model. PAR and NIR reflectance values thus trace out an arc on the plane that corresponds to increasing phytomass (**Figure 8.5b**). This relationship holds since laminar surface reflection is diffuse and isotropic (Richards 1993), and because laminar surfaces reflect NIR radiation in a predictable way (Myers 1983). Anechoic surfaces such as conifer canopies behave in an entirely different way: the structural arrangement of biomass scatters radiant energy (including NIR) deeper into the canopy, where it is eventually absorbed (cf. Rowe 1993). Spectral radiance (including NIR) from conifer stands is therefore very low over all wavelengths. Because NDVI isolines necessarily converge at zero, decreased NIR reflectance along a continuum from pure broadleaf to pure conifer forest results in a precipitous drop in NDVI (**Figure 8.5b**). This model is consistent with empirical results indicating that NDVI produces biased estimates of phytomass/productivity in closed forest ecosystems, particularly when conifers are present (Ranson and Williams 1992; Hall et al. 1995; McDonald et al. 1998).

Because anechoic conifer canopies have very low overall albedo, relatively small differences in NIR and/or PAR reflectance can dramatically alter spectral ratio values (cf. Myneni et al. 1992; Peterson et al. 1987). Obtained NDVI values ranged from 0.72-0.77 for different conifer canopies, despite very small changes in absolute PAR and NIR reflectance (**Fig. 5a**). Even within a single conifer stand, minor changes in directional reflection can dramatically affect NDVI values (Leblanc et al. 1997).

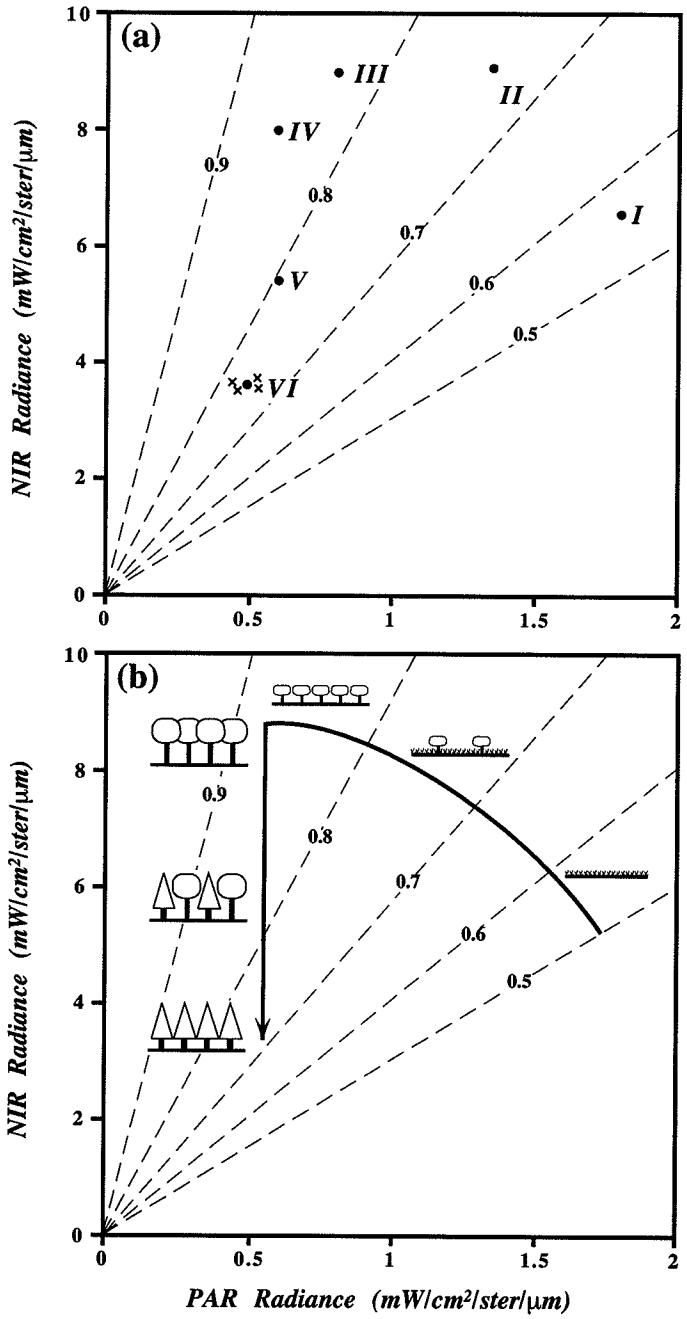

Figure 8.5: (a) PAR (0.63-0.69 μm) and NIR (0.76-0.90 μm) radiance for six vegetation classes, based on a Landsat TM image of Riding Mountain National Park: I = grassland; II = grassland with shrubs; III = shrubland; IV = broadleaf forest (trembling aspen); V = mixed broadleaf-conifer forest (trembling aspen-white spruce); VI = conifer forest (the four x symbols are separate values for white spruce, black spruce, balsam fir and jackpine stands). Dashed lines are NDVI isolines; (b) A simple model of the relationship between PAR and NIR reflectance for different vegetation classes. The relationship (dark line) has two distinct trends: an arc that represents increasing NDVI as phytomass increases (grassland to shrubland to broadleaf forest), and a considerable decline in NIR radiance when conifers enter the canopy.

8.6 Conclusion

Broadleaf and conifer trees have fundamentally different strategies for acquiring solar energy. Broadleaf trees employ a laminar or 'solar panel' strategy, in which flat leaves are oriented within a canopy to optimally intercept direct solar energy. By contrast, conifer trees develop a conical crown consisting of numerous overlapping branches that are densely packed with needle-like leaves. While the physiological efficiency of a laminar canopy is intuitive and widely recognized, the structural architecture of conifers seems enigmatic: a conifer canopy is nothing like a solar panel, yet the conifers as a group are highly successful and dominate many north-temperate regions. This paradox is resolved by viewing the conifer canopy as a highly absorptive anechoic surface. Such a surface absorbs radiant energy through repeated deflections from hierarchically arranged structural elements. Solar energy acquisition in conifers is therefore an emergent property: while an isolated needle-leaf may not be particularly efficient, the structural arrangement of needle-leaves within the canopy produces a highly effective energy-acquiring system. The architectural geometry of conifers, characterized by a 'cone-on-cone' self-similarity from the leaf to canopy scales, is therefore highly adaptive.

Chapter 9

Summary and the Contribution to New Knowledge

9.1 General Conclusions

This dissertation has contributed new information and ideas in several important areas in landscape ecology and conservation. These will be summarized in the following sections.

1. The first contribution was the adaptation of several fractal measures to examine spatial pattern in the boreal forest. In this thesis fractal density functions were used to examine contagion, multifractals to assess pattern complexity, persistence of reflectance to examine change in canopy structure and Cantor point processes to measure anthropogenic fragmentation. Some of these statistics have never been used in landscape ecology prior to this dissertation. These statistics are valuable, as many 'traditional' measures of spatial complexity are scale specific. Furthermore, fractal measures incorporated into 'canned' software packages (e.g. FRAGSTATS) are often not appropriate for the spatial data to which they are applied.

2. A major portion of the dissertation deals with the role of succession and physiographic complexity in determining landscape complexity. For the boreal forest, very little is known about the role of long-term spatial dynamics in determining ecosystem complexity. This knowledge is critical, active fire suppression and forest management policy is forcing a new disturbance 'paradigm' on the boreal forest. The influence of large-scale processes in shaping landscape structure is being replaced by a 'paradigm' dominated by small-scale asynchronous stochastic events. In this dissertation patch contagion, pattern complexity and persistence were used to examine different aspects of landscape complexity influenced by successional processes and physiographic complexity.

- In the first of three chapters dealing with landscape dynamics, it was found that the forest patch structure (using a fractal density function) of regenerating post-fire sites (11 and 30 years old) was more contagious than late-successional sites (> 95 years old). In the boreal forest landscape level patch structure becomes increasingly entropic during succession as small-scale disturbances begin to 'chip away' at post fire stands. It was found that physiography was also an important determinant of landscape pattern. Landscapes with simple physiographies (well-drained sites) were characterized by a few dominant, overdispersed land-cover classes, while less frequent classes showed high contagion. In contrast, sites with a complex physiography (impeded drainage, topographically complex) had greater equitability of land-cover classes, and all classes had similar (and higher) degrees of patch contagion.

- A second aspect of landscape complexity dealt with the role of disturbance and physiographic complexity in determining landscape pattern complexity (analysed using a multifractal statistic). It was found that the multifractal spectrum (D_q) for all landscapes was high ($D \rightarrow 2$) indicating highly complex landcover pattern in the boreal forest. Landscape pattern complexity was found to increase with site age; the multifractal profiles of young sites (11 yr old) were lower than adjacent stands. However, the multifractal profiles of 30 year old and adjacent older stands were almost indistinguishable, suggesting that change in landscape complexity occurs rapidly following fire. Physiographically "complex" sites had consistently greater landscape pattern complexity than adjacent "simple" sites. It is concluded that landscape complexity increases over time as successional proceeds, and in space along a gradient from "simple" to "complex" physiographies. It follows that landscape pattern complexity is lowest in early-succession on physiographically "simple" sites and highest in late-succession on physiographically "complex" sites.

- In the third chapter dealing with the role of disturbance dynamics in determining landscape complexity, Landsat TM scene reflectance data was analyzed directly. A method based on fractional brownian motion (using the Hurst exponent) was used to examine the spatial persistence. All sites examined had Hurst (H) exponents less

than 0.5, indicating anti-persistent spatial patterns. It was found that H declined from younger to older landscapes indicating that as sites age, they begin to loose landscape-level 'memory.' Small scale asynchronous changes to canopy biophysical structure are likely responsible for the observed trends.

These results indicate that natural landscapes are structurally complex, and that landscape patterning is highly dynamic in space and time. The recognition that physiographic complexity strongly influences forest landscape pattern complexity may have important implications for predicting trends in biodiversity. Complex fractal habitats have greater overall species richness than simple ones in the same way that complex physiographic surfaces promote the "coexistence" of a larger number of habitats. Complexity also increases as a function of multiscale disturbance in the boreal forest. Active fire suppression results in the accumulation of independent stochastic disturbances on the landscape and the loss of shared 'memory' at the landscape-level.

3. Another contribution to new knowledge was related to the role that human development plays in landscape fragmentation. Human-driven fragmentation of the landscape presents major challenges for conservation. Extensive fragmentation of the landscape reduces biodiversity through restricting movement of individuals to isolated patches. In this dissertation, data from a variety of sources was used to reconstruct land use patterns following World War II in the region surrounding RMNP. A transect sampling approach was developed and a novel application of the Cantor point process fractal was used to examine changes in the dispersion of fragmented forest habitat in the region. It was found that forest losses in the region were extensive during the 40 years examined. The areas most impacted were to the north and east of RMNP virtually eliminating natural corridors of vegetation in the region (e.g. the Grandview Corridor). Fractal analysis of the landscape pattern indicated that the park is becoming increasingly isolated. Human patterns of fragmentation in the region ultimately reflect the geometric simplicity of the land survey system, and not natural community patterns. Management of wildlife on these landscapes must consider the scaling response of organisms to differing degrees of

fragmentation. Land managers must determine whether an 'optimal' level of habitat fragmentation exists that provides the necessary degree of connectivity for wildlife without compromising crop productivity. The approach to studying habitat fragmentation presented in this dissertation could be used to work towards a restoration goal.

4. A contribution was also made in the area of vegetation mapping, Vegetation maps are somewhat paradoxical: they represent spatially explicit models that must both simplify floristic complexity while retaining ecologically meaningful information. This balance can only be achieved by a rigorous analysis of vegetation patterns on the ground. Maps developed from remotely sensed data are even more challenging to produce because imagery based on spectral reflectance samples vegetation indirectly. Thus it is essential that i) relationships within the vegetation data be examined; ii) relationships among elements within the remotely sensed scene be examined; iii) the joint (or canonical) relationship between the vegetation and spectral reflectance be optimized and iv) the optimized relationship must be tested ('verified'). In this dissertation a multivariate approach to image classification and optimization is presented. A novel use of multiple discriminant analysis (MDA) to examine accuracy of the final vegetation map was developed. In this application of MDA, it is tested whether vegetation classes on the map produce a significant discrimination among species cover values measured on the ground. Unlike traditional contingency matrix approaches to accuracy assessment, the metric properties of the vegetation dataset are retained, and relationships among the groups can be examined. Using this approach it was found that spectral separation and the performance of individual classes often corresponded with canopy physiognomy and spatial structure. As these properties of the canopy often change with time, it is imperative that multivariate methods such as MDA be used in producing and assessing satellite classifications.

5. As well, this dissertation discusses the scattering of light in boreal forest canopies and its adaptive significance for conifer species. While the unique light scattering properties of conifer canopies have been recognized in the remote sensing literature (e.g. forward scattering models), no one has ever addressed whether these properties

are adaptive. Two fundamentally different light interception strategies are suggested by which plant canopies optimize solar radiation capture. Laminar canopies (e.g. broadleaf trees) are 'solar panels' that directly intercept incoming radiant energy. By contrast, the regular conical structure of softwood canopies represents an anechoic (without echo) surface that optimally scatters light into the canopy. The properties of anechoic surfaces are well known in acoustical and electrical engineering, but have not been applied in environmental biophysics. An anechoic surface absorbs radiant energy through repeated deflections from hierarchically arranged structural elements. The structural arrangement of elements within a conifer stands is characterized by a 'cone-on-cone' self-similarity from the leaf to canopy scale, this produces a highly effective light interception system. A key feature of anechoic interception is low radiance over all wavelengths, which is an emergent property of the system. Using Landsat reflectance data from RMNP it is demonstrated that conifer canopies have very low near-infrared radiance compared to laminar broadleaf canopies. Vegetation index values for conifers are thereby reduced, resulting in underestimates of primary productivity and other biophysical parameters. This has important implications for global climate change models and the use of vegetation indices in monitoring the ecosystem.

9.2 Ecosystem Management Implications

This project contributes to our understanding of ecosystem management in the boreal forest. Indeed, the project was initiated to determine methods of measuring and assessing biodiversity and productivity using satellite data as part of a Park management strategy. However, during preliminary investigations it became clear that assessing biodiversity using 'standard' measures of species richness directly from satellite data, or using spectral indices of productivity such as NDVI was problematic in the boreal forest: stand structure influences reflectance as much or more than species composition (**Chapter 7**) and NDVI values are biased for conifer dominated stands (**Chapter 8**). A new approach using spatial variation in reflectance was chosen to provide a measure of landscape complexity (i.e. variation from changes in *habitat structure* and *overall composition*) as a surrogate for ecosystem diversity and hence species diversity. Furthermore, fractal spatial

statistics that consider pattern over a range of scales were selected. This allowed for the consideration of scale in the measurement of landscape complexity, a critical and often overlooked component of pattern. The important contributions of these spatial measures to conservation and management are briefly summarized here:

1. Vegetation dynamics in boreal forest: management and biodiversity implications

Disturbance is critical in the boreal forest, as landscape level crown fire results in the temporary reduction of spatial pattern complexity (**Chapter 4**) and greater equitability of patches on the landscape (**Chapter 3**). Over time, spatial complexity increases with the accumulation of small-scale disturbance events (**Chapter 5**). While this is commensurate with increased habitat structural complexity, on a uniform substrate one patch-type generally becomes dominant, likely lowering overall diversity. Where management practices favor the suppression of fire, it is suggested that overall diversity may decline, while stands simultaneously become structurally 'chaotic' because of accumulation of small-scale disturbances. Indeed, it is important to recognize that the control of fire at the landscape-level is not the control of disturbance; it simply increases the influence of smaller scale stochastic processes on forest structure and dynamics. If active fire control is to be practiced in the future, one area where further research is required is the influence of spatial persistence (or lack of) on the temporal persistence of wildlife species (i.e. does the development of a highly entropic canopy result in the loss of certain wildlife species). Alternative management practices such as controlled burns may be suggested where wildlife populations are threatened by fire control measures. However controlled burns, when implemented in the past, has been at a scale that is sub-landscape. 'Crownfire-scale' burns are likely essential to achieve 'natural' patterns on this landscape, although controlled prescriptions of this type are likely not attainable. Where controlled burns are implemented, it is suggested that areas of lower landscape complexity would likely benefit more so than complex sites. It should be noted that on complex landscapes, selectivity along environmental gradients preserves greater class equitability over time. Furthermore, these landscapes are typified by high species turnover and complex interdigitations among patches. These areas are important from a species conservation perspective, but may also promote greater diversity even where fire suppression policies

are enforced. Despite the implementation difficulties, it is felt that fire management that includes controlled burns, should be investigated as a means of preserving biodiversity in this ecosystem.

2. Corridor connectivity: management and biodiversity implications

While RMNP has been long recognized as isolated from other natural landscapes, little work has been done in quantifying the loss of habitat in the region over time. Initial investigations in this study, indicated that forest habitat patches are a reasonable indicator of fragmentation region (i.e. they often correspond with availability of other habitat types). What was discovered in this study is that while forest habitat fragmentation is severe, the losses have not been random. This has important implications for management, since nearly all fragmentation models have used a 'neutral' landscape approach (i.e. habitat loss as a random anisotropic process). Estimates of fragmentation and its influence on connectivity have thus been biased for these landscapes in past studies. The approach adopted in this thesis, considers the patterns created from habitat losses as well as changes in the total amount (**Chapter 6**). Results indicate that the loss of connectivity may be greater than previously thought, as patch isolation around RMNP has increased dramatically over the last half of the 1900's. The reliance on existing habitat patches as 'stepping stones' for the dispersal of most organisms, except for the largest species of 'megafauna,' should be reconsidered. A more aggressive approach should be taken to restore natural habitat corridors in the region. In undertaking such a project, the size and pattern of restored patches should be included in planning. Furthermore, a holistic approach that includes the agricultural 'matrix' needs to be adopted. Agricultural diversification in areas surrounding corridor patches may be of benefit to dispersing organisms that need to make extra-corridor movements. It is suggested that studies examining the influence of crop-type on matrix 'hostility' (i.e. the role of crop-type in functional connectivity – for definitions see **Chapter 1**) should be undertaken.

3. Mapping of boreal systems: management and biodiversity implications

In mapping landcover in boreal forest using remote sensing, this study found that structure of the canopy is as important as species composition. Thus, components of habitat structure should be considered when collecting data for use in satellite classification. The sensitivity to structure also has important implications for the estimation of map to ground vegetation agreement. In this study, a method of testing agreement using Multiple Discriminant analysis was presented (**Chapter 7**). With this approach, sites can be revisited and the analysis performed repeatedly, allowing for the examination of successional processes on class separation and discrimination over time. Important questions relating to management of these systems can be addressed, including those land classes that might be expected to decrease or increase in proportion over time under different fire suppression regimes. While the agreement measured in this study was relatively high (>85%), it should be noted that class accuracy is not uniform over all classes (e.g. greater error in agreement was found for regenerating conifer class) and that there is a spatial component in error estimation that is hard to quantify (homogenous 'polygons' were tested, not ecotonal sites). For example, the presence of swamp birch (*Betula glandulosa*) in many of the post-fire regenerating stands makes this class 'sensitive' to the presence of this species. This appears to be true for post disturbance stands where flooding not fire was an important factor and where colonization by swamp birch was high. Spatial arrangement also has an influence on map agreement; many of these post-disturbance areas can be heterogeneous resulting in mixed pixels and potentially misleading class assignments. Mixed pixels also play a role in the classification of ecotonal areas where several vegetation types are often interspersed. In testing for map agreement, ecotonal sites were not chosen because i) class boundaries along a continuum are by nature arbitrary; ii) GPS positional accuracy becomes an important component of error. In the application of the vegetation classification for Park management, additional GIS layers that include roadways, drainage and landform should be used in conjunction with the vegetation map for decision support.

4. Boreal conifer scattering properties: implications for productivity estimates

In this thesis it is suggested that broadleaf and conifer trees have fundamentally different strategies for acquiring solar energy. Broadleaf trees employ a laminar or 'solar panel' strategy, in which flat leaves are oriented within a canopy to optimally intercept direct solar energy. By contrast, conifer trees develop a conical crown consisting of numerous overlapping branches that are densely packed with needle-like leaves. Such a surface absorbs radiant energy through repeated deflections from hierarchically arranged structural elements. This form of light scattering within the canopy is highly effective at intercepting light, including those wavelengths not normally associated with photosynthesis. Thus NDVI and other band ratio approaches that were developed for broadleaf canopies are relatively ineffective for estimating biophysical parameters for forested ecosystems. A simple model of the relationship between PAR and NIR reflectance was discussed in this thesis (Chapter 8) that illustrates these differences. Because of scattering effects in conifer canopies, albedo is low resulting in highly variable spectral ratio values and an underestimate of canopy productivity. While Parks Canada has used NDVI for northern parks dominated by tundra vegetation, application of band ratio approaches to forested systems should be carefully considered. The use of biophysical inversion models should be investigated to provide necessary productivity estimates for the Canadian park system.

Appendix 1 Plant silouettes

Picea mariana

Pinus banksiana

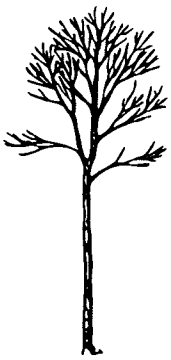

Betula papyrifera

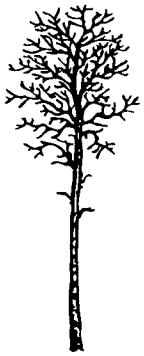

Populus tremuloides

Picea glauca

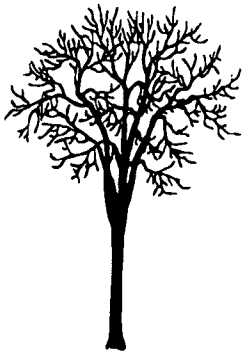

Ulmnus americana

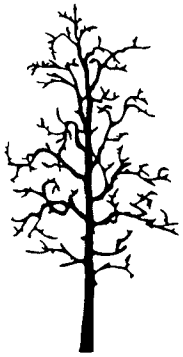

Quercus macrocarpa

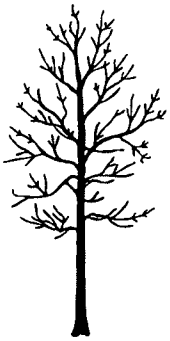

Fraxinus pennsylvanica

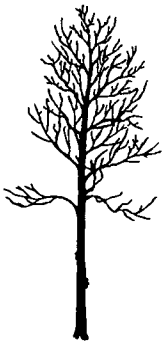

Populus balsamifera

Acer spicatum

Corylus cornuta

Festuca hallii

Solidago spp.

Typha spp.

Scirpus spp.

References

Anderson, H.G. and A.W. Bailey. 1980. Effects of annual burning on grassland in the aspen parkland of east-central Alberta. Can. J. Botany. 58: 985-996.

Andrén, H. 1994. Effects of habitat fragmentation on birds and mammals in landscapes with different proportions of suitable habitat: a review. Oikos. 71: 355-366.

Appleby, S. 1996. Multifractal characterization of the distribution pattern of the human population. *Geogr. Analysis* 28: 147-160.

Bailey, R.H. 1968. Notes on the vegetation of Riding Mountain National Park, Manitoba. National Parks Forest Survey No. 2. Dept. For. Rural Devel., Ottawa. 80 pp.

Baker, W.L. 1992a. Effects of settlement and fire suppression on landscape structure. Ecology 73: 1879-1887.

Baker, W.L. 1992b. The landscape ecology of large disturbances in the design and management of nature reserves. Landscape Ecology. 7: 181-194.

Banfield, A. W. F. 1974. The mammals of Canada. National Museum of Natural Sciences, National Museums of Canada. University of Toronto Press. Pp. 438.

Barber, D.G. and E.F. LeDrew. 1991. SAR sea ice discrimination using texture statistics: a multivariate approach. Photo. Eng. Rem. Sens. 57: 385-395.

Barrett, S.W. and J.D. Peles. 1994. Optimizing habitat fragmentation: an agrolandscape perspective. Landscape and urban plan. 28: 99-105.

Baskent, E.Z. and G.A. Jordan. 1995. Characterizing spatial structure of forest landscapes. Can. J. For. Res. 25: 1830-1849.

Bayne, E.M. and K.A. Hobson. 1998. The effects of habitat fragmentation by forestry and agriculture on the abundance of small mammals in the southern boreal mixedwood forest. Can. J Zool.. 76: 62-69.

Bégin, C. and L. Filion. 1999. Black spruce (*Picea mariana*) architecture. Can. J. Bot. 77: 665-672.

Beier, P., and R.F. Noss. 1998. Do habitat corridors provide connectivity? Cons. Biol. 12:1241-1252.

Beranek, L.L. and H.P. Sleeper. 1946. The design and construction of anechoic sound chambers. J. Acoust. Soc. Am. 18: 140-150.

Bergeron, Y. and M. Dubuc. 1989. Succession in the southern part of the Canadian boreal forest. Vegetatio 79: 51-63.

Bergeron, Y., A. Leduc, H. Morin, and C. Joyal. 1995. Balsam fir mortality following the last spruce budworm outbreak in northwestern Quebec. Can. J. For. Res. 25: 1375-1384.

Bergeron, Y.A. 2000. Species and stand dynamics in the mixedwoods of Quebec's southern boreal forest. Ecology. 81: 1500-1516.

Bettinger, P., G.A. Bradshaw and G.W. Weaver. 1996. Effects of geographic information system vector-raster-vector data conversion on landscape indices. Can. J. For. Res. 26:1416-1425.

Bird, R.D. 1961. Ecology of the Aspen parkland of western Canada. Dept. of Agric. Ottawa.

Blair, B.O. and M.F. Baumgardner. 1977. Detection of the green and brown wave in hardwood canopy covers using multidate multispectral data from Landsat-1. Agronomy J. 69: 808-811.

Blood, D.A. 1966. Range relationships of Elk and Cattle in Riding Mountain National Park, Manitoba. *Wildlife Management Bulletin*. Series 1. No. 19. pp. 62.

Bolstad, P.V. and T.M. Lillesand. 1992. Improved classification of forest vegetation in northern Wisconsin through a rule-based combination of soils, terrain, and LANDSAT Thematic Mapper data. For. Sci. 38: 5-20.

Bonan, G.B. and H.H. Shugart. 1989. Environmental factors and ecological processes in boreal forests. Ann. Rev. Ecol. Syst. 20: 1-28.

Bond, W.J. 1989. The tortoise and the hare: ecology of angiosperm dominance and gymnosperm persistence. Biol. J. Linnean Soc. 36: 227-249.

Bornkessel, C. and W. Wiesbeck. 1996. Numerical analysis and optimization of anechoic chambers for EMC testing. IEEE Trans. Electromag. Compat. 38: 499-506.

Brown, L., J.M. Chen, S.G. Leblanc and J. Cihlar. 2000. A shortwave infrared modification to the simple ratio for LAI retrieval in boreal forests: an image and model analysis. Rem. Sens. Environ. 71: 16-25

Bunnell, F.L. and D.J. Huggard. 1999. Biodiversity across spatial and temporal scales: problems and opportunities. For. Ecol. Mgmt. 115:113-126.

Canada 1979. Riding Mountain National Park resource description and analysis. Parks Canada, Winnipeg.

Caners, R.T. and N.C. Kenkel. 1998. Modeling landscape-level vegetation dynamics in Riding Mountain National Park. Final Report to Parks Canada, Ottawa. University of Manitoba. pp.156.

Canham, C.D., K.D. Coates, P. Bartemucci and S. Quaglia. 1999. Measurement and modeling of spatially explicit variation in light transmission through interior cedar-hemlock forests of British Columbia. Can. J. For. Res. 29: 1775-1783.

Carleton, T.J. and P.F. Maycock. 1978. Dynamics of the boreal forest south of James Bay. Can. J. Bot. 56: 1157-1173.

Carlyle, W.J. 1996. Agriculture in Manitoba. In: J. Welsted, J. Everitt and C. Stadel. The geography of Manitoba. University of Manitoba Press. Winnipeg. Pages: 219-236.

Chavez, P.S. 1988. An improved dark-order subtraction technique for atmospheric scattering correction of mulispectral data. Remote Sens. Environ. 24: 459-479.

Chen J. M. 1996a. Evaluation of vegetation indices and a modified simple ratio for boreal applications. Can. J. Remote Sens. 22: 229-242.

Chen J. M. 1996b. Optically-based methods for measuring seasonal variation of leaf area index in boreal conifer stands. Agric. For. Meteorol. 80: 135-163.

Cihlar, J., J. Chen and Z. Li. 1997. On the validation of satellite-derived products for land applications. Can. J. Rem. Sens. 23: 381-389.

Clark, F.S. and R.B. Slusher. 2000. Using spatial analysis to drive reserve design: a case study of a national wildlife refuge in Indiana and Illinois (USA). Landscape Ecol. 15: 75-84.

Clements, F.E. 1936. Nature and structure of the climax. J. Ecol. 24: 252-284.

Cody, W.J. 1988. Plants of Riding Mountain National Park, Manitoba. Agric. Canada, Ottawa. Pub. No. 1818/E.

Cogbill, C.V. 1985. Dynamics of the boreal forests of the Laurentian Highlands, Canada. Can. J. For. Res. 15: 252-261.

Cohen, W.B., T.A. Spies and G.A. Bradshaw. 1990. Semivariograms of digital imagery for analysis of conifer canopy structure. Remote Sensing of Environment. 34:167-178.

Collingham, Y.C. and B. Huntley. 2000. Impacts of habitat fragmentation and patch size upon migration rates. Ecol. App. 10: 131-144.

Collins, S.L., S.M. Glenn and D.W. Roberts. 1993. The hierarchical continuum concept. J. Veg. Sci. 4: 149-156.

Colwell, J.E. 1974. Vegetation canopy reflectance. Remote Sens. Environ. 3: 175-183.

Congalton, R.G. 1991. A review of assessing the accuracy of classifications of remotely sensed data. Rem. Sens. Environ. 37:35-46.

Conroy, M.J. and B.R. Noon. 1996. Mapping of species richness for conservation of biological diversity: conceptual and methodological issues. Ecological Applications. 6: 763-773.

Cumming, S.G., P.J. Burton and B. Klinkenberg. 1996. Boreal mixedwood forests may have no "representative" areas: some implications for reserve design. Ecography. 19: 162-180.

Curran, P.J. 1988. The semivariogram in remote sensing. Remote Sensing of Environment. 24:493-507.

Czaran, T. 1989. Coexistence of competing populations along an environmental gradient: a simulation study. Coenoses 4: 113-120.

Dale, M.R.T. 2000. Lacunarity analysis of spatial pattern: a comparison. Land. Ecol. 15:467-478.

Dalla-Tea, F. and E.J. Jokela. 1991. Needlefall, canopy light interception, and productivity of young intensively managed slash pine stands. For. Sci. 37: 1298-1313.

De Cola, L. 1989. Fractal analysis of a classified Landsat scene. Photo. Eng. Remote Sens. 55: 601-611.

De Cola, L. 1994. Simulating and mapping spatial complexity using multi-scale techniques. Int. J. Geog. Inf. Syst. 8: 411-427.

De Grandpré, L.D. and Y. Bergeron. 1997. Diversity and stability of understory communities following disturbance in the southern boreal forest. J. of Ecol. 85: 777-784.

De Grandpré, L.D. Gagnon and Y. Bergeron. 1993. Changes in the understory of Canadian southern boreal forest after fire. J. Veg. Sci. 5: 803-810.

Dearden, P. and R. Rollins. 1993. Parks and protected areas in Canada: Planning and management. Oxford Univ. Press, Toronto.

Debinski, D.M. and R.D. Holt. 2000. A Survey and Overview of Habitat Fragmentation Experiments. Cons. Biol. 14: 342-355.

Dickson, J.R. 1909. The Riding Mountain Forest Reserve. Bulletin No. 6, Dept. Interior, Forestry Branch, Ottawa.

Diffendorfer, J.E., M.S. Gaines and R.D. Holt. 1995.Habitat fragmentation and movements of three small mammals (*Sigmodon, Microtus* and *Peromyscus*). Ecology 76:827-839.

Dix, R.L. and J.M.A. Swan. 1971. The roles of disturbance and succession in upland forest at Candle Lake, Saskatchewan. Can. J. Bot. 49: 657-676.

Dixon, J.R. 1909. The Riding Mountain Forest Reserve. Bulletin No. 6, Dept. Interior, Forestry Branch, Ottawa.

Donkor, N.T. and J.M. Fryxell. 1999. Impact of beaver on structure of lowland boreal forests of Algonquin Provincial Park, Ontario. For. Ecol. and Managmt. 118: 83-92.

Dyer, J.M. and P.R. Baird. 1997. Wind disturbance in remnant forest stands along the prairie-forest ecotone, Minnesota, USA. Plant Ecol. 129: 121-134.

Dytham, C. 1995. The effect of habitat destruction pattern on species persistence: a cellular model. Oikos 74: 340-344.

Edwards, T.C.,Jr., G.G. Moisen and D.R. Cutler.1998. Assessing map accuracy in a remotely sensed, ecoregion-scale cover map. Rem. Sens. Environ. 63: 73-83.

Egler, F.E. 1954. Vegetation science concepts I. Initial floristic composition, a factor in old-field vegetation development. Vegetatio 4: 412-417.

Emerson, C.W., N. N-S. Lam and D. Quattrochi. 1999. Multiscale fractal analysis of image texture and pattern. Rem. Sens. Environ. 65: 51-61.

Environment Canada. 1993. Canadian climate normals 1961-1990. Atmospheric Environment Service, Ottawa.

Evans, S.L. 1923. Report of land classification surveys in part of Riding Mountain Forest Reserve. Dept. of Interior, Ottawa.

Evans, S.L. 1923. Report of land classification surveys in part of Riding Mountain Forest Reserve. Dept. Interior, Ottawa.

Farnsworth, K.D. and K.J. Niklas. 1995. Theories of optimization, form and function in branching architecture in plants. Funct. Ecol. 9: 355-363.

Fiorella, M. and W.J. Ripple. 1993. Determining successional stage of temperate coniferous forest with LANDSAT satellite data. Photogramm. Eng. Remote Sens. 59: 239-246.

Fisher, P. 1997. The pixel: a snare and delusion. Int. J. Remote Sensing. 18:679-685.

Forman, R. T. T., and M. Godron. 1986. Landscape ecology. Wiley, New York.

Forman, R.T.T. 1995. Some general principles of landscape regional ecology. Landscape Ecol. 10: 133-142.

Foster, D.R. 1992. Land-use history (1730-1990) and vegetation dynamics in central New England, USA. J. of Ecol. 80:753-772.

Foster, D.R. and G.A. King. 1986. Vegetation pattern and diversity in S.E. Labrador, Canada: *Betula papyrifera* (birch) forest development in relation to fire history and physiography. *J. Ecol.* 74: 465-483.

Frankel, O.H., H.D. Brown and J.J. Burdon. 1995. The conservation of plant biodiversity. Cambridge Univ. Press, New York.

Franklin, J. 1986. Thematic mapper analysis of coniferous structure and composition. Int. J. of Rem. Sens. 7: 1287-1301.

Franklin, J. 1995. Predictive vegetation mapping: geographic modeling of biospatial patterns in relation to environmental gradients. Prog. Phys. Geogr. 19:474-499.

Franklin, J.F. 1993. Preserving biodiversity: species, ecosystems, or landscapes? Ecol. App. 3: 202-205.

Frelich, L.E. and P.B. Reich. 1995. Spatial patterns and succession in a Minnesota southern-boreal forest. Ecol. Monogr. 65: 325-346.

Frelich, L.E. and P.B. Reich. 1995. Spatial patterns and succession in a Minnesota southern-boreal forest. *Ecol. Monogr.* 65: 325-346.

Frelich, L.E. and P.B. Reich. 1999. Neighborhood effects, disturbance severity, and community stability in forests. *Ecosystems* 2: 151-166.

Frelich, L.E. and Reich, P.B. 1995. Spatial patterns and succession in a Minnesota southern-boreal forest. Ecol. Mongr. 65: 325-346.

Frelich, L.E. and Reich, P.B. 1995a. Neighborhood effects, disturbance, and succession in forests of the western Great Lakes region. Écoscience 2: 148-158.

Frelich, L.E. and Reich, P.B. 1995b. Spatial patterns and succession in a Minnesota southern-boreal forest. Ecol. Mongr. 65: 325-346.

Frelich, L.E. and Reich, P.B. 1999. Neighborhood effects, disturbance severity, and community stability in forests. Ecosystems. 2: 151-166.

Frelich, L.E. S. Sugita, P.B. Reich, M.B. Davis and S.K. Friedman. 1998. Neighborhood effects in forests: implications for within-stand patch structure. *J. of Ecol.* 86: 149-161.

Fritz R. and G. Merriam. 1994. Fencerow and forest edge vegetation structure in eastern Ontario farmland. Ecoscience. 1: 160-172.

Galipeau, C., D. Kneeshaw and Y. Bergeron. 1997. White spruce and balsam fir colonization of a site in the southeastern boreal forest as observed 68 years after fire. Can. J. For. Res. 27: 139-147.

Gautestad, A.O. and I. Mysterud. 1994. Fractal analysis of population ranges: methodological problems and challenges. Oikos 69: 154-157.

Gholz, H.L., S.A. Vogel, W.P. Cropper, K. McKelvey, K.C. Ewel, R.O. Teskey and P.J. Curran. 1991. Dynamics of canopy structure and light interception in *Pinus elliottii* stands, North Florida. Ecol. Monogr. 6: 33-51.

Gleason, H.A. 1926. The individualistic concept of the plant association. Bull. Torr. Bot. Club 53: 7-26.

Glenn, S.M. and T.D. Nudds. 1989. Insular biogeography of mammals in Canadian parks. J. Biogeogr. 16: 261-268.

Goldrup, C. 1992. An historic overview and analysis of consumptive uses of resources in Duck Mountain Provincial Park. Practicum. University of Manitoba, Winnipeg. 133 pages.

Goodchild, M.F. 1994. Integrating GIS and remote sensing for vegetation analysis and modeling: methodological isssues. J. Veg. Sci. 5: 615-626.

Gopal, S. and C. Woodcock. 1994. Theory and methods for accuracy assessment of thematic maps using fuzzy sets. Photo. Eng. Rem. Sens. 52:839-846.

Gosz, J.R. 1993. Ecotone hierarchies. Ecol. Appl. 3: 369-376.

Gould, W. 2000. Remote sensing of vegetation, plant species richness and regional biodiversity hotspots. Ecol. Appl. 10: 1861-1870.

Goward, S.N. and D.L. Williams. 1997. Landsat and Earth systems science: development of terrestrial monitoring. Photo. Eng. Rem. Sens. 63: 887-900.

Granström, A. 1993. Spatial and temporal variation in lightning ignitions in Sweden. J. Veg. Sci. 4: 737-744.

Grashof-Bokdam, C. 1997. Forest species in an agricultural landscape in the Netherlands: Effects of habitat fragmentation. J. Vegetation Sci. 8: 21-28.

GRASS 4.0. Geographic Resources Analysis and Support System (GRASS). Baylor University.

Green, R.H. 1993. Relating two sets of variables in environmental studies. Pages 149-163 in Patil, G.P. and C.R. Rao (eds.). Multivariate environmental statistics. Elsevier, Amsterdam.

Gustafson, E. J. and R. H. Gardner. 1996. The effect of landscape heterogeneity on the probability of patch colonization. Ecology. 77: 94-107.

Gustafson, E.J. and Parker, G.R., 1992. Relationships between landcover proportion and indices of landscape spatial pattern. Lands. Ecol. 7:101-110.

Haddad, N.M. 1999. Corridor use predicted from behaviors at habitat boundaries. Am. Nat. 153: 215-227.

Haig, A.R., U. Matthes and D.W. Larson. 2000. Effects of natural habitat fragmentation on the species richness, diversity, and composition of cliff vegetation. Can. J. Bot. 78: 786-797.

Hall, F.G., D.B. Botkin, D.E. Strebel, K.D. Woods and S.J. Goetz. 1991. Large-scale patterns of forest succession as determined by remote sensing. Ecology 72: 628-640.

Hall, F.G., Y.E. Shimabukuro and K.F. Huemmrich. 1995. Remote sensing of forest biophysical structure using mixture decomposition and geometric reflectance models. Ecol. Appl. 5: 993-1013.

Hamazaki, T. 1996. Effects of patch shape on number of organisms. Lands. Ecol. 11: 299-306.

Hansen, M.J., S.E. Franklin, C. Woudsma and M. Peterson. 2001. Forest structure classification using the Landsat TM tasseled cap wetness component. Can. J. Rem. Sens. 27: 20-32.

Hansson, L. 1992. Landscape ecology of boreal forests. Trends Ecol. Evol. 7: 299-302.

Hargis, CD, JA Bissonette and JL David. 1998. The behavior of landscape metrics commonly used in the study of habitat fragmentation. Land. Ecol. 13: 167 - 186.

Harrison, J.D.B. 1934. The forests of Manitoba. Forest Service Bulletin 85. Dept. of Interior, Canada. Pages: 68-72.

Harvey, P.H., R.K. Colwell, J.W. Silvertown and R.M. May.1983. Null models in ecology. Ann. Rev. Ecol. Syst. 14: 189-211.

Hastings, H.M. and G. Sugihara. 1993. Fractals: a user's guide for the natural sciences. Oxford Univ. Press, Oxford.

Hastings, H.M., R. Pekelney, R. Monticciolo, D. vun Kannon and D. del Monte. 1982. Time scales, persistence and patchiness. Biosyst. 15: 281-289.

He, H.S. and D.J. Mladenoff. 1999. Spatially explicit and stochastic simulation of forest landscape fire disturbance and succession. Ecology. 80: 81 - 99.

Heinselman, M.L. 1973. Fire in the virgin forests of the Boundary Waters Canoe Area, Minnesota. Quat. Res. 3: 329-362.

Helm, D.J. and W.B. Collins. 1997. Vegetation succession and disturbance on a boreal forest floodplain, Susitna River, Alaska. Can. Field Nat. 111: 553-566.

Hentschel, H.G.E. and I. Procaccia. 1983. The infininte number of generalized dimensions of fractals and strange attractors. *Physica D* 8: 435-444.

Her, T.-H., R.J. Finlay, C. Wu, S. Deliwala and E. Mazur. 1998. Microstructuring of silicon with femtosecond laser pulses. Appl. Phys. Lett. 73:1673-1675.

Hill, M.O. 1973. Diversity and evenness: a unifying notation and its consequences. Ecology 54: 427-432.

Hirsch, K.G. 1991. A chronological overview of the 1989 fire season in Manitoba. For. Chron. 67: 358-365.

Holling, C.S. 1992. The role of forest insects in structuring the boreal landscape. In: Shugart, H.H., R. Leemans and G.B. Bonan (eds.). A systems analysis of the global boreal forest. pp. 170-191. Cambridge Univ. Press, New York.

Holloway, C.L., R.R. DeLyser, R.F. German and P. McKenna. 1997. Comparison of electromagnetic absorber used in anechoic and semi-anechoic chambers for emissions and immunity testing of digital devices. IEEE Trans. Electromag. Compat. 39: 33-46.

Holt, R.D., G.R. Robinson and M.S. Gaines. 1995. Vegetation dynamics in an experimentally fragmented landscape. Ecology 76: 1610-1624.

Horler, D.N.H. and F.J. Ahern. 1986. Forestry information content of Thematic Mapper data. Int. J. of Rem.Sens. 7:405-428.

Horn, H.S. 1971. The Adaptive Geometry of Trees. Princeton Univ. Press, Princeton.

Horn, H.S. 1976. Succession. In: May, R.M. (ed.). Theoretical ecology. pp. 187-204. Saunders, Philadelphia.

Host, G.E., K.S. Pregitzer, C.W. Ramm, J.B. Hart and D.T. Cleland. 1987. Landform-mediated differences in successional pathways among upland forest ecosystems in northwestern Lower Michigan. For. Sci. 33:445-457.

Hudson, W.D. 1987. Correct formulation of the Kappa coefficient of agreement. Photogr. Eng. Rem. Sens. 53:421-422.

Hurst, H.E. 1951. Long-term storage capacity of reservoirs. Trans. Am. Soc. Civil Eng. 116: 770-808.

Hurtt, G.C. and S.W. Pacala. 1995. The consequences of recruitment limitation: reconciling chance, history and competitive differences between plants. J. Theor. Biol. 176: 1-12.

Jaeger, J.A.G. 2000. Landscape division, splitting index, and effective mesh size: new measures of landscape fragmentation. Landscape Ecol. 15: 115-130.

Jakubauskas, M.E. 1996a. Canonical correlation analysis of coniferous forest spectral and biotic relations. Int. J. Remote Sensing. 17: 2323-2332.

Jakubauskas, M.E. 1996b. Thematic mapper characterization of lodgepole pine seral stages in Yellowstone National Park, USA. Remote Sens. Environ. 56: 118-132.

Jakubauskas, M.E. 1997. Effects of forest succession on texture in LANDSAT thematic mapper imagery. Can. J. Remote Sens. 23: 257-263.

Jean, M. A. Bouchard. 1993. Riverine wetland vegetation: importance of small-scale and large-scale environmental variation. J. Veg. Sci. 4: 609-618.

Jeffers, J.N.R. 1982. Modelling. Chapman and Hall, London.

Jelinski, D.E. and J.G. Wu. 1996. The modifiable areal unit problem and implications for landscape ecology. Lands. Ecol. 11: 129-140.

Johnson, A.R., B.T. Milne and J.A. Weins. 1992. Diffusion in fractal landscapes: simulations and experimental studies of tenebrionid beetle movements. Ecology. 73: 1968-1983.

Johnson, E.A. 1992. Fire and vegetation dynamics: studies from the North American boreal forest. Cambridge University Press, Cambridge.

Johnson, E.A. K. Miyanishi and N. O'Brien. 1999. Long-term reconstruction of the fire season in the mixedwood boreal forest of western Canada. Can. J. Bot. 77: 1185-1188.

Johnson, E.A. K. Miyanishi and J.M.H. Weir. 1995. Old-growth, disturbance and ecosystem management. Can. J. Bot. 73: 918-926.

Jordan, C.F. 1969. Derivation of leaf-area index from quality of light on the forest floor. Ecology 50: 663–666.

Jorge, L.A.B. and G.J. Garcia. 1997. A study of habitat fragmentation in Southeastern Brazil using remote sensing and geographic information systems (GIS). For. Ecol. Mgmt. 98:35-47.

Keitt, T.H., D.L. Urban, and B.T. Milne. 1997. Detecting critical scales in fragmented landscapes. Conservation Ecology [online]1(1): 4. Available from the Internet. URL: http://www.consecol.org/vol1/iss1/art4

Kenkel, N.C. 1986. Structure and dynamics of jack pine stands near Elk Lake, Ontario: a multivariate approach. *Can. J. Bot.* 64: 486-497.

Kenkel, N.C. and D.J. Walker. 1996. Fractals in the biological sciences. Coenoses 11: 77-100.

Kenkel, N.C., D.J. Walker, P.R. Watson, R.T. Caners and R.A. Lastra. 1997. Vegetation dynamics in boreal forest ecosystems. Coenoses 12: 97-108.

Kent, C. & J. Wong. 1982. An index of littoral zone complexity and its measurement. Can. J. Fish. Aquat. Sci. 39: 847-853.

Keymer J.E., P.A. Marquet, J.X. Velasco-Hernandez and S.A. Levin. 2000. Extinction thresholds and metapopulation persistence in dynamic landscapes. Am. Nat. 156:478-494

King, D.A. 1990. The adaptive significance of tree height. Am. Nat. 135: 809-828.

Klopfenstein, R.W. 1956. A transmission line taper of improved design. Proc. IRE 44: 31-35.

Kneeshaw, D.D. and Y. Bergeron. 1998. Canopy gap characteristics and tree replacement in the southeastern boreal forest. Ecology 79: 783-794.

Koidan, W. G.R. Hruska and M.A. Pickett. 1972. Wedge design for National Bureau of Standards anechoic chamber. J. Acoust. Soc. Amer. 52: 1071-1076.

Kruess, A. and T. Tscharntke. 1994. Habitat Fragmentation, Species Loss, and Biological Control. Science. 264: 1581-1584.

Krummel, J.R., R.H. Gardner, G. Sugihara, R.V. O'Neill and P.R. Coleman. 1987. Landscape patterns in a disturbed environment. Oikos 48: 321-324.

Kushla, J.D. and W.J. Ripple. 1997. The role of terrain in a fire mosaic of a temperate coniferous forest. For. Ecol. Manag. 95: 97-107.

Kymer, J.E. , P.A. Marquet, J.X. Velasco-Hernández and S.A. Levin. 2000. Extinction thresholds and metapopulation persistence in dynamic landscapes. Am. Nat. 156: 478-494.

Lam, N.S-N. Description and measurement of LANDSAT TM images using fractals. Photogramm. Eng. Remote Sens. 56: 187-195.

Lang, A.H. 1974. Guide to the geology of Riding Mountain National Park and its vicinity - history of its upland and other scenery. Miscellaneous report 20. Geological Survey of Canada, Department of Energy, Mines, and Resources, Ottawa. 68 pp.

Lark, R.M. 1995. Components of accuracy of maps with special reference to discriminant analysis on remote sensor data. Int. J. Rem. Sens. 16: 1461-1480.

Lavorel, S., R.H. Gardner and R.V. O'Neill. 1993. Analysis of patterns in hierarchically structured landscapes. Oikos 67: 521-528.

Leblanc, S.G., J.M. Chen and J. Cihlar. 1997. NDVI Directionality in boreal forests: a model interpretation of measurements. Can. J. Remote Sens. 23: 369-380.

Leduc, A., Y.T. Prairie and Y. Bergeron. 1994. Fractal dimension estimates of a fragmented landscape: sources of variability. Lands. Ecol. 9: 279-286.

Legendre, P. and L. Legendre. 1998. Numerical Ecology. 2nd edition. Elsevier, Amsterdam.

Lehr, J.C. 1996. Settlement: the making of a landscape. In: J. Welsted, J. Everitt and C. Stadel. The geography of Manitoba. University of Manitoba Press. Winnipeg. Pages: 92-107.

Lieffers, V.J., C. Messier, K.J. Stadt, F. Gendron and P.G. Comeau. 1999. Predicting and managing light in the understory of boreal forests. Can. J. For. Res. 29: 796-811.

Liu, J., J.M. Chen, J. Cihlar and W.M. Park. 1997. A process-based boreal ecosystem productivity simulator using remote sensing inputs. Remote Sens. Environ. 62: 158-175.

Loehle, C. and G. Wein. 1994. Landscape habitat diversity: a multiscale information theory approach. Ecol. Modell. 73: 311-329.

Lord J.M. and D.A. Norton. 1990. Scale and the spatial concept of fragmentation. Cons. Biol. 4: 197-202.

Los, S.O., C.O. Justice and C.J. Tucker. 1994. A global 1° x 1° NDVI data set for climate studies derived from the GIMMS continental NDVI data. Int. J. Remote Sens. 15: 3493-3518.

Mandelbrot, B.B. 1967. How long is the coastline of Britain? Statistical self-similarity and fractional dimension. Science 156: 636-638.

Mandelbrot, B.B. 1975. Stochastic models for the Earth's relief, the shape and the fractal dimension of the coastlines, and the number-area rule for islands. Proc. Nat. Acad. Sci. U.S.A. 72: 3825-3828.

Mandelbrot, B.B. 1977. *Fractals form, chance and dimension.* Freeman, San Francisco. pp. 363.

Mandelbrot, B.B. 1983. The fractal geometry of nature. Freeman, San Francisco.

Manly, B.F.J. 1991. Randomization and Monte Carlo methods in

Markham, B.L. and J.L. Barker. 1986. Landsat MSS and TM post-calibration dynamic ranges, exoatmospheric reflectances and at-satellite temperatures. EOSAT LANDSAT Technical Notes 1: 3-8.

Markon, C. 1992. Land cover mapping of the upper Kuskokwim resource management area, Alaska, using LANDSAT and a digital data base approach. Can. J. Remote Sens. 18: 62-71.

May, R.M. 1975. Island biogeography and the design of wildlife preserves. Nature 254: 177-178.

McDonald, A.J., F.M. Gemmell and P.E. Lewis. 1998. Investigation of the utility of spectral vegetation indices for determining information on coniferous forests. Remote Sens. Environ. 66: 250 - 272.

Messier, C, R. Doucet, J-C Ruel, Y Claveau, C Kelly and MJ Lechowicz. 1999. Functional ecology of advance regeneration in relation to light in boreal forests. Can. J. For. Res. 29: 812-823.

Middleton, E.M., S.S. Chan, R.J. Rusin and S.K. Mitchell. 1997. Optical properties of black spruce and jack pine needles at BOREAS sites in Saskatchewan, Canada. Can. J. Remote Sens. 23: 108–119.

Miller, J.R., L.A .Joyce, R.L. Knight and R.M. King. 1996. Forest roads and landscape structure in the southern Rocky Mountains. Land. Ecol. 11: 115-127.

Milne, B.T. 1988. Measuring the fractal geometry of landscapes. Appl. Math. Comp. 27: 67-79.

Milne, B.T. 1991. Lessons from applying fractal models to landscape patterns. In: Turner, M.G. and R.H. Godron (eds.). Quantitative methods in landscape ecology: the analysis and interpretation of landscape heterogeneity. pp. 199-235. Springer-Verlag, New York.

Milne, B.T. 1992. Spatial aggregation and neutral models in fractal landscapes. Am. Nat. 139: 32-57.

Milne, B.T., M.G. Turner, J.A. Wiens and A.R. Johnson. 1992. Interactions between the fractal geometry of landscapes and allometric herbivory. Theor. Pop. Biol. 41: 337-353.

Mitsch, W.J. and J.G. Gosselink. 1993. Wetlands. van Nostrand Reinhold, New York.

Mladenoff, D.J., M.A. White, J. Pastor and T.R. Crow. 1993. Comparing spatial pattern in unaltered old-growth and disturbed forest landscapes. *Ecol. Appl.* 3:294-306.

Moore, M.M. and M.E. Bauer. 1990. Classification of forest vegetation in north-central Minnesota using Landsat Multispectral Scanner and Thematic Mapper data. For. Sci. 36: 330-342.

Morin, H. 1994. Dynamics of balsam fir forests in relation to spruce budworm outbreaks in the boreal zone of Québec. Can. J. For. Res. 24: 730-741.

Morrison, D.F. 1990. *Multivariate Statistical Methods. 3rd Ed.* McGraw-Hill. Toronto. pp 495.

Mucina, L. 1997. Classification of vegetation: past, present and future. J. of Veg. Sci. 8: 751-760.

Musick, H.B. and H.D. Grover. 1990. Image textural measures as indices of landscape pattern. In: Quantitative Methods in Landscape Ecology. M.G. Turner and R.H. Gardner (Eds.). Springer-Verlag, New York. pp. 77-103.

Myers, V.I. 1983. Remote sensing applications in agriculture. In: Colwell, R.N. (ed.). Manual of Remote Sensing, Vol. II. 2nd ed. American Society of Photogrammetry, Falls Church, VA. pp. 2111-2228.

Myneni, R.B., G. Asrar, D. Tanre and B.J. Choudhury. 1992. Remote sensing of solar radiation absorbed and reflected by vegetated land surfaces. IEEE Trans. Geosci. Remote Sens. 30: 302-314.

Naiman, R.J. 1988. Animal influences on ecosystem dynamics. *Biosci.* 38: 750-752.

Naiman, R.J., H. Décamps and M. Pollock. 1993. The role of riparian corridors in maintaining regional biodiversity. *Ecol. Appl.* 3: 209-212.

Nelson, R. 1997. Modeling forest canopy heights: the effects of canopy shape. Remote Sens. Environ. 60: 327-334.

Nienstaedt, H. and J.C. Zasada. 1990. *Picea glauca. In*: Burns, R.M. and B.H. Honkala (eds.). 1990. Silvics of North America: 1. Conifers. Agricultural Handbook 654. USDA, Forest Service, Washington D.C. Vol. 1. 675 pp.

Noble, I.R. and R.O. Slatyer. 1980. The use of vital attributes to predict successional changes in plant communities subject to recurrent disturbances. Vegetatio 43: 5-21.

Norman, J.M. and J.M. Welles. 1983. Radiative transfer in an array of canopies. Agronomy J. 75: 481-488.

Norman, J.M. and P.G. Jarvis. 1974. Photosynthesis in sitka spruce (*Picea sitchensis* (Bong.) Carr.): III. Measurements of canopy structure and interception of radiation. J. Applied Ecol. 11: 375-398.

Norman, J.M. and P.G. Jarvis. 1975. Photosynthesis in sitka spruce (*Picea sitchensis* (Bong.) Carr.): V. Radiation penetration theory and a test case. J. Appl. Ecol. 12: 839-878.

Normant, F. and C. Tricot. 1993. Fractal simplification of lines using convex hulls. Geogr. Anal. 25: 118-129.

Noss, R.F. 1999. Assessing and monitoring forest biodiversity: a suggested framework and indicators. For. Ecol. and Managmt. 115: 135-146.

Ohmann, J.L. and T.A. Spies. 1998. Regional gradient analysis and spatial pattern of woody plant communities of Oregon forests. Ecol. Monographs. 68: 151-164.

O'Neill, R.V., C.T. Hunsaker, S.P. Timmins, B.L. Jackson, K.B. Jones, K.H. Riitters and J.D. Wickham. 1996. Scale problems in reporting landscape pattern at the regional scale. Landscape Ecology. 11: 169-180.

Palmer, M.W. 1992. The coexistence of species in fractal landscapes. *Am. Nat.* 139: 375-397.

Palmer, M.W. and P.M. Dixon. 1990. Small-scale environmental heterogeneity and the analysis of species distributions along gradients. J. Veg. Sci. 1: 57-65.

Parker, A.R. 1999. Light-reflection strategies. Am. Sci. 87: 248-255.

Parks Canada. 1977. A master plan for Riding Mountain National Park. Parks Canada, Ottawa. 46 pp.

Paruelo, J.M., H.E. Epstein, W.K. Lauenroth and I.C. Burke. 1997. ANPP estimates from NDVI for the central grassland region of the United States. Ecology 78: 953-958.

Payette, S. 1992. Fire as a controlling process in the North American boreal forest. In: Shugart, H.H., R. Leemans and G.B. Bonan (eds.). A systems analysis of the global boreal forest. pp. 144-169. Cambridge Univ. Press, New York.

Peddle, D.R. 1993. An empirical comparison of evidential reasoning, linear discriminant analysis, and maximum likelihood algorithms for alpine land cover classification. Can. J. Rem. Sens. 19: 31-44.

Peddle, D.R. and S.E. Franklin. 1991. Image texture processing and data integration for surface pattern discrimination. Photo. Eng. and Rem. Sens. 57: 413-420.

Peddle, D.R., E.G. Hall, E.F. LeDrew and D.E. Knapp. 1997. Classification of forest land cover in BOREAS. II: comparison of results from a sub-pixel scale physical modeling approach and a training based method. Can. J. Rem. Sens. 23: 131-143.

Peitgen, H.-O., H. Jürgens and D. Saupe. 1992. Fractals for the classroom. Springer, New York.

Perry, C.R. & L.F. Lautenschlager. 1984. Functional equivalence of spectral vegetation indices. Remote Sensing of Environment 14: 169-182.

Perry, D.A. 1995. Self-organizing systems across scales. Trends Ecol. Evol. 10: 241-244.

Peters, E.E. 1994. Fractal market analysis. Applying chaos theory to investment and economics. J. Wiley and Sons, New York.

Peterson, D.L., M.A. Spanner, S.W. Running and K.B. Teuber. 1987. Relationship of thematic mapper simulator data to leaf area index of temperate coniferous forests. Remote Sens. Environ. 22: 323-341.

Pickett, S.T.A., S.L. Collins and J.J. Armesto. 1987. Models, mechanisms and pathways of succession. Bot. Rev. 53: 335-371.

Pierce, A.D. 1981. Acoustics: An Introduction to its Physical Principles and Applications. McGraw-Hill, New York. 642 pages.

Podani, J. 1994. Multivariate data analysis in ecology and systematics. SPB Academic Publishing, The Hague.

Polidori, L., J.J. Chorowicz and R. Guillande. 1991. Description of terrain as a fractal surface, and application to digital elevation model quality assessment. *Photo. Eng. Remote Sens.* 57: 1329-1332.

Prince, S.D. and S.N. Goward. 1995. Global primary production: a remote sensing approach. J. Biogeogr. 22: 815-835.

Pruess, S.A. 1995. Some remarks on the numerical estimation of fractal dimension. In: C.C. Barton and P.R. La Pointe (eds.). Fractals in the earth sciences. pp. 65-75. Plenum Press, New York.

Pulliam, H.R., J.B. Dunning and J. Liu. 1992. Population dynamics in complex landscapes: a case study. Ecol. Appl. 2: 165-177.

Ranson, K.J. and D.L. Williams. 1992. Remote sensing technology for forest ecosystem analysis. In: Shugart, H.H., R. Leemans and G.B. Bonan (eds.). A Systems Analysis of the Global Boreal Forest. Cambridge U. Press, Cambridge. pp. 267-290.

Ravan, S.A. and P.S. Roy. 1997. Satellite remote sensing for ecological analysis of forested landscapes. Plant Ecol. 131: 129-141.

Raven, P.H., R.F. Evert and S.E. Eichhorn. 1987. Biology of Plants. 4th ed. Worth, New York.

Rencz, A.N. 1985. Multitemporal analysis of LANDSAT imagery for monitoring forest cutovers in Nova Scotia. Can. J. Remote Sens. 11: 188-191.

Renyi, A. 1970. *Probability theory.* North-Holland, Amsterdam.

Rey-Benayas, J.M. and K.O. Pope. 1995. Landscape ecology and diversity patterns in the seasonal tropics from Landsat TM imagery. *Ecol. Appl.* 5: 386-394.

Richards, J.A. 1993. Remote Sensing Digital Image Analysis: An Introduction. 2nd ed. Springer-Verlag, New York.

Richards, J.A. 1996. Classifier performance and map accuracy. Rem. Sens. Environ. 57: 161-166.

Rignot, E., W.A. Salas and D.L. Skole. 1997. Mapping deforestation and secondary growth in Rondonia, Brazil, using imaging radar and Thematic Mapper data. Rem. Sens. Env. 59: 167-179.

Ringstrom, E. 1981. Riding Mountain yesterday and today. Prairie Publishing, Winnipeg. 111 pages.

Ritchie, J.C. 1956. The vegetation of northern Manitoba: I. Studies in the southern spruce forest zone. Can. J. Bot. 34: 523-561.

Ritchie, J.C. 1964. Contributions to the Holocene paleoecology of westcentral Canada. I. The Riding Mountain Area. Can. J. Bot. 42:181-197.

Ritchie, J.C. 1969. Absolute pollen frequencies and carbon-14 age of a section of Holocene Lake sediment from the Riding Mountain area of Manitoba. Can. J. Bot. 47:1345-1349.

Ritchie, J.C. 1985. Quaternary pollen records from the Western Interior and the Arctic of Canada. *In*: Bryant, V.M. Jr. and R.G. Holloway (eds.). 1985. Pollen records of late-Quaternary North American sediments. American Association of Stratigraphic Palynologists Foundation, Dallas, Texas. 426 pp.

Ritchie, J.C. and G.A. Yarranton. 1978. The late-Quaternary history of the boreal forest of central Canada, based on standard pollen stratigraphy and principal components analysis. J. Ecol. 66:199-212.

Rouse, J.W., R.H. Haas, J.A. Schell and D.W. Deering. 1973. Monitoring vegetation systems in the Great Plains with ERTS. Third ERTS Symposium, NASA SP-315 I: 309-317.

Rowe, C.M. 1993. Incorporating landscape heterogeneity in land surface albedo models. J. Geophys. Res. 98: 5037-5043.

Rowe, J.S. 1955. Factors influencing white spruce reproduction in Manitoba and Saskatchewan. Technical note no. 3. Department of Northern Affairs and National Resources, Forestry Branch. Ottawa, Canada. 27 pp.

Rowe, J.S. 1956. Vegetation of the southern boreal forest in Saskatchewan and Manitoba. Ph.D. thesis, University of Manitoba, Winnipeg.

Rowe, J.S. 1961. Critique of some vegetational concepts as applied to forests in northwestern Alberta. Can. J. Bot. 39: 1007-1017.

Rowe, J.S. 1972. Forest regions of Canada. Can. For. Ser., Ottawa, Publ. No. 1300.

Sachs, D.L., P. Sollins and W.B. Cohen. 1998. Detecting landscape changes in the interior of British Columbia from 1975 to 1992 using satellite Imagery. Can. J. For. Res. 28: 23-36.

Sampson, D.A. and F.W. Smith. 1993. Influence of canopy architecture on light penetration in lodgepole pine (*Pinus contorta* var. *latifolia*) forests. Agric. For. Meterol. 64: 63-79.

Sampson, P.H., P.M. Treitz and G.H. Mohammed. 2001. Remote sensing of forest condition in tolerant hardwoods: an examination of spatial scale, structure and function. Can. J. Rem. Sens. 27: 232-246.

Scheuring, I. 1991. The fractal nature of vegetation and the species-area relation. *Theor. Popul. Biol.* 39: 170-177.

Scheuring, I. and R.H. Riedi. 1994. Application of multifractals to the analysis of vegetation pattern. *J. Veg. Sci.* 5: 489-496.

Schroeder, M. 1991. Fractals, chaos, power laws: minutes from an infinite paradise. Freeman, New York.

Scoggan, H.J. 1957. Flora of Manitoba. Bulletin No. 140, Biological Series No. 47. Department of Northern Affairs and National Resources, Ottawa. 619 pp.

Sellers, P., F. Hall, H. Margolis, B. Kelly, D. Baldocchi, J. den Hartog, J. Cihlar, M. Ryan, B. Goodison, P. Crill, J. Ranson, D. Lettenmaier and D. Wickland. 1995. The Boreal Ecosystem-Atmosphere Study (BOREAS): an overview and early results from the 1994 field year. Bull. Am. Meteorol. Soc. 76: 1549-1577.

Sentar Consultants Ltd. 1992. Riding Mountain National Park: A literature review of historic timber harvesting and forest fire activity. Parks Canada 21 pp.

Shafer, C.L. 1995. Values and shortcomings of small reserves. Bioscience. 45: 80-88.

Shafi, M.I. and G.A. Yarranton. 1973. Vegetational heterogeneity during a secondary (postfire) succession. Can. J. Bot. 51: 73-90.

Sharpe. D.M. G.R. Gutenspergen, C.P. Dunn, L.A. Leitner and F. Stearns. 1987. Vegetation dynamics in a southern Wisconsin agricultural landscape. In: Landscape heterogeneity and disturbance. M.G. Turner (ed.). Springer-Verlag, New York.

Shaw, M.P. 1993. Spatio-temporal dynamics of the vegetation and seed bank of beaver meadows in Riding Mountain National Park, Manitoba. Department of Botany, University of Manitoba. Winnipeg, Manitoba.

Shen, S.S., G.D. Badhwar and J.G. Carnes. 1985. Seperability of boreal forest species in the Lake Jennette area, Minnesota. Photogr. Eng. Rem. Sens. 51: 1775-1783.

Shiyomi, M. and K. Yamamura. 1993. Spatial pattern indices based on distances between individuals on a line segment with finite length. Res. Popul. Ecol. 34:321-330.

Shorrocks, B., J. Marsters, I. Ward & P.J. Evennett. 1991. The fractal dimension of lichens and the distribution of arthropod body lengths. Funct. Ecol. 5: 457-460.

Simberloff, D. 1994. Habitat fragmentation and population extinction of birds. Ibis. 137: 105-111.

Sjörs, H. 1980. An arrangement of changes along gradients, with examples from successions in boreal peatland. Vegetatio 43: 1-4.

Skole, D. and C. Tucker. 1993. Tropical deforestation and habitat fragmentation in the Amazon: satellite data from 1978 to 1988. Science. 260: 1905-1909.

SLOGAN 1997

Smalley, R.F., J.L. Chatelain, D.L. Turcotte and R. Prevot. 1987. A fractal approach to the clustering of earthquakes: applications to the seismicity of the New Hebrides. Seis. Soc. Am. Bull. 77: 1368-1381.

Smith, T. and M. Huston. 1989. A theory of the spatial and temporal dynamics of plant communities. Vegetatio 83: 49-69.

Smith, W.K. and C.A. Brewer. 1994. The adaptive importance of shoot and crown architecture in conifer trees. Am. Nat. 143: 528-532.

Smith, W.K. and G.A. Carter. 1988. Shoot structural effects on needle temperatures and photosynthesis in conifers. Am. J. Bot. 75: 496-500.

Sousa, W.P. 1984. The role of disturbance in natural communities. Ann. Rev. Ecol. Syst. 15: 353-391.

Sprugel, D.G. 1989. The relationship of evergreenness, crown architecture, and leaf size. Am. Nat. 133: 465-479.

SPSS Inc. 1995. SPSS 6.1 for Macintosh. SPSS Inc. Chicago, Illinois.

Stadel, C. 1996. The non-metropolitan settlements of southern Manitoba. In: J. Welsted, J. Everitt and C. Stadel. The geography of Manitoba. University of Manitoba Press. Winnipeg. Pages: 152-166.

Stehman, S.V. 2001. Statistical rigor and practical utility in Thematic map accuracy assessment. Photo. Eng. Rem. Sens. 67: 727-734.

Stehman, S.V. and R.L. Czaplewski. 1998. Design and analysis for Thematic map accuracy assessment: fundamental principles. Rem. Sens. Environ. 64: 331-344.

Strahler, A.H., C.E. Woodcock and J.A. Smith. 1986. On the nature of models in remote sensing. Rem. Sens. Environ. 20: 121-139.

Sugihara, G. and R.M. May. 1990. Applications of fractals in ecology. Trends Ecol. Evol. 5: 79-86.

Tang, S.M., J.F. Franklin and D.R. Montgomery. 1997. Forest harvest patterns and landscape disturbance processes. Land. Ecol. 12: 349-363.

Taylor, P. D., L. Fahrig, K. Henein and G. Merriam. 1993. Connectivity is a vital element of landscape structure. Oikos 68: 571-573.

Thomson, K.P.B., C. Grosselin, B.W. Adams and I. Sutherland. 1985. Thematic mapper data used for rangeland management in rough fescue grasslands in western Canada. Can. J. Remote Sens. 11: 162-175.

Tinker, D.B., C.A.C. Resor, G.P. Beauvais, K.F. Kipfmueller, C.I. Fernandes and W.L. Baker. 1998. Watershed analysis of forest fragmentation by clearcuts and roads in a Wyoming forest. Land. Ecol. 13: 149-165.

Tischendorf, L. and L. Fahrig. 2000. On the usage and measurement of landscape connectivity. Oikos. 90: 7-19.

Tomlinson, P.B. 1983. Tree architecture. Am. Sci. 71: 141-149.

Treitz, P.M, P.J. Howarth, R.C. Suffling and P. Smith. 1992. Applications of detailed ground information to vegetation mapping with high spatial resolution and digital imagery. Remote Sens. Envir. 42: 65-82.

Treitz, P.M. and P.J. Howarth. 1999. Hypersectral remote sensing for estimating biophysical parameters of forest ecosystems. Prog. in Phys. Geog. 23:359-390.

Treitz, P.M. and P.J. Howarth. 2000. Integrating spectral, spatial, and terrain variables for forest ecosystem classification. Photo. Eng. Rem. Sens. 66: 305- 317.

Trottier, G.C. 1981. Beaked hazelnut - a key browse species for moose in the boreal forest region of western Canada. Alces 17:257-281.

Trottier, G.C. 1986. Disruption of rough fescue, Festuca halli, grassland by livestock grazing in Riding Mountain National Park, Manitoba. Can. Field-Nat. 100:488-495.

Tsonis, A.A. and P.A. Tsonis. 1987. Fractals: a new look at biological shape and patterning. Persp. Biol. Med. 30: 355-361.

Tucker, C.J. 1979. Red and photographic infrared linear combinations for monitoring vegetation. Remote Sens. Envir. 8: 127-150.

Tunstell, G. 1940. Forest working plan, Riding Mountain National Park. Can. Dept. Mines Res., Winnipeg.

Turchin, P. 1998. Quantitative analysis of movement : measuring and modeling population redistribution in animals and plants. Sinauer Associates, Mass. pp.396.

Turcotte, D.L. 1997. Fractals and chaos in geology and geophysics. 2nd Ed. Cambridge University Press, Cambridge, England.

Turner, M.G. 1989. Landscape ecology: the effect of pattern on process. *Annu. Rev. Ecol. Syst.* 20: 171-197.

Turner, M.G. 1990. Landscape changes in nine rural counties in Georgia. Photo. Eng. and Rem. Sens. 56:379-386.

Turner, M.G. and W.H. Romme. 1994. Landscape dynamics in crown fire ecosystems. Land. Ecol. 9: 59-77.

Tyre A.J., H.P. Possingham and D.B. Lindenmayer. 1998. Modelling dispersal behaviour on a fractal landscape. Environmental Modelling and Software. 14: 103-113.

van der Meer, P.J. and F. Bongers. 1996. Patterns of tree-fall and branch-fall in a tropical rain forest in French Guiana. J. of Ecol. 84: 19-29.

Van Heuvelen, A. 1986. Physics: A General Introduction. Little, Brown and Co., Toronto.

Voss, R.F. 1988. Fractals in nature: from characterization to simulation. In: Peitgen, H.-O. and D. Saupe (eds.). The science of fractal images. pp. 21-70. Springer, New York.

Voss, R.F. 1988. Fractals in nature: from characterization to simulation. In: Peitgen, H.-O. and D. Saupe (eds.). The science of fractal images. pp. 21-70. Springer, New York.

Waldron, R.M. 1966. Factors affecting natural white spruce regeneration on prepared seedbeds at the Riding Mountain forest experimental area, Manitoba. Dept. Forestry and Rural Devel, Ottawa. Publ. No. 1169.

Walker, D.J. 1994. A model for predicting boreal vegetation dynamics and management requirements on electric transmission right of ways, Interlake region, Manitoba. MSc. Thesis, University of Manitoba, Winnipeg.

Walker, D.J. and N.C. Kenkel. 1998. Fractal analysis of spatio-temporal dynamics in boreal forest landscapes. Abstracta Botanica. 22: 13-28.

Walker, D.J. and N.C. Kenkel. 2000. The adaptive geometry of boreal conifers. Community Ecology. 1: 13-24.

Walker, D.J. and N.C. Kenkel. 2001. Landscape complexity in space and time. Community Ecology. 2: 109-119.

Watt, A.S. 1947. Pattern and process in the plant community. J. Ecol. 35: 1-22.

Wauters, L.A, Y. Hutchinson, D.T. Parkin and A.A. Dhondt. 1994. The effects of habitat fragmentation on demography and on the loss of genetic variation in the red squirrel. Proc. Royal Soc. London Ser. B. 255: 107-111.

Weir, J.M.H. and E.A. Johnson. 1998. Effects of escaped settlement fires and logging on forest composition in the mixedwood boreal forest. Can. J. For. Res. 28:459-467.

Weir, J.M.H., E.A. Johnson and K. Miyanishi. 2000. Fire frequency and the spatial age mosaic of the mixed-wood boreal forest in western Canada. Ecol. Appl. 10: 1162-1177.

Weir, T.R. 1983. Atlas of Manitoba. Dept. Nat. Res., Winnipeg.

Welsted, J. 1996. Manitoba's water resources. In: J. Welsted, J. Everitt and C. Stadel. The geography of Manitoba. University of Manitoba Press. Winnipeg. Pages: 266-286.

Whitmore, T.C. 1990. An Introduction to Tropical Rain Forests. Oxford Univ. Press, Oxford.

Whittaker, R.H. 1953. A consideration of climax theory: the climax as a population and pattern. Ecol. Monogr. 23: 41-78.

Wickland, D.E. 1991. Mission to planet earth: the ecological perspective. Ecology 72: 1923-1933.

Wiens, J.A. 1995. Landscape mosaics and ecological theory. In: Lennart, H., L. Fahrig and G. Merriam (eds.). Mosaic and landscapes and ecological processes. pp. 1-26. Chapman and Hall, London.

Wiens, J.A. 1997. The emerging role of patchiness in conservation biology. In: Pickett, S.T.A. ...[et al.]. The ecological basis of conservation : heterogeneity, ecosystems, and biodiversity. Chapman & Hall, New York. Pp. 466.

Wiens, J.A., C.S. Crawford and J.R. Gosz. 1985. Boundary dynamics: a conceptual framework for studying landscape ecosystems. Oikos 45: 421-427.

Williams, D.L. 1991. A comparison of spectral reflectance properties at the needle, branch, and canopy level for selected conifer species. Remote Sens. Environ. 35: 79-93.

With K.A. and A.W. King. 2001. Analysis of landscape sources and sinks: the effect of spatial pattern on avian demography. Biological Conservation. 100: 75-88.

With, K.A. 1994a. Ontogenetic shifts in how grasshoppers interact with landscape structure: an analysis of movement patterns. Funct. Ecol. 8: 477- 485

With, K.A. 1994b. Using fractal analysis to assess how species percieve landscape structure. Landscape Ecology. 9:25-36.

With, K.A. and T.O. Crist. 1995. Critical thresholds in species' responses to landscape structure. Ecology 76: 2446-2459.

With, K.A., and A.W. King. 1999. Extinction thresholds for species in fractal landscapes. Cons. Biol. 13: 314-326.

With, K.A., R.H. Gardner and M.G. Turner. 1997. Landscape connectivity and population distribution in heterogeneous environments. Oikos. 78:151-169.

Woodley, S. 1991. Monitoring for ecosystem integrity in Canadian national parks. Canadian Parks Service. pp. 132.

Wright, S.J. and S.P. Hubble. 1983. Stochastic extinction and reserve size: a focal species approach. Oikos. 41: 466 - 476.

Zeide, B. 1991. Fractal geometry in forestry applications. For. Ecol. Manag. 46: 179-188.

Zhao, G. and A.L. Maclean. 2000. A comparison of canonical discriminant analysis and principal component analysis for spectral transformation. Photo. Eng. Rem. Sens. 66: 841-847.

Zobel, K., M. Zobel and R.K. Peet. 1993. Change in pattern diversity during secondary succession in Estonian forests. *J Veg. Sci.* 4: 489 - 498.

Zoladeski, C.A. and P.F. Maycock. 1990. Dynamics of the boreal forest in northwestern Ontario. Am. Midl. Nat. 124: 289-300.